U. S. NAVY

OFFICE OF NAVAL RESEARCH

Research Contract N7onr-32913

Project NR 051-056

A STUDY OF FAST REACTIONS IN FUEL-OXIDANT SYSTEMS

Technical Report No. 7

IGNITION DELAY WITH RAPIDLY MIXED LIQUID REACTANTS

by

Louis Baker, Jr.

submitted by

Martin Kilpatrick

August 1954

Department of Chemistry
Illinois Institute of Technology
3300 South Federal Street
Chicago 16, Illinois

U. S. NAVY

OFFICE OF NAVAL RESEARCH

Research Contract N7onr-32913

Project NR 051-056

A STUDY OF FAST REACTIONS IN FUEL-OXIDANT SYSTEMS

Technical Report No. 7

IGNITION DELAY WITH RAPIDLY MIXED LIQUID REACTANTS

by

Louis Baker, Jr.

submitted by

Martin Kilpatrick

August 1954

Department of Chemistry
Illinois Institute of Technology
3300 South Federal Street
Chicago 16, Illinois

TABLE OF CONTENTS

TABLE OF CONTENTS (continued)

P R E F A C E

This report, comprising the doctoral thesis of Louis Baker, Jr., represents a study of ignition delay when fuels and oxidants are contacted, with special emphasis on mixing. The report includes the design of an apparatus to contact the reactants rapidly, to mix efficiently, and to record ignition as a function of time. As mixing cannot be studied solely as a function of ignition, the apparatus also permits measurement of the injection rate and the change in pressure with time.

The systems studied were hydrazine and nitric acid; hydrazine, ammonia and nitric acid; aniline and nitric acid; and hydrazine and hydrogen peroxide.

In the event that the design details of the reactor are of interest to other workers in this field, copies of the detailed working drawings may be obtained at a nominal cost from the Department of Chemistry of Illinois Institute of Technology, upon request to the Office of Naval Research, Chicago Branch Office.

ABSTRACT

A constant volume reactor was designed in which it was possible to contact and mix nearly equal quantities of two liquid reactants in a few milliseconds. The apparatus was suited for the study of self-igniting fuel-oxidant mixtures. It was possible to vary the reactant ratio, the mixing pattern, and the ambient temperature.

The reactions were studied by four techniques: (1) simultaneous measurement of the transient pressure and the light emitted by the reacting mixture, (2) simultaneous measurement of the transient pressure and the injection rate, (3) measurement of the final pressure of the product gases, and (4) chemical analysis of the reaction products. The transient pressure measurements were made by means of a strain gage, the output of which was amplified electronically by a method due to McKinney. The light emission measurements were made by means of three photoelectric circuits; each employed a vacuum phototube as the sensing device. The injection rate was measured by a photoelectric timer. The data from the electronic measurements were recorded on film by photographing the screens of two oscilloscopes simultaneously.

The transient pressure was found to oscillate about a mean value during the early stages of a reaction. It was found necessary to attenuate the vibrations by placing obstructions in the piping connecting the strain gage with the reactor. It was suggested that the phenomenon might set an upper limit to the speed with which chemical reactions may be followed by measuring their pressure.

The reactions studied were: (1) the reaction of sodium-potassium alloy with water and ethanol, (2) the reaction of hydrazine with nitric

acid, (3) the reaction of aniline with nitric acid, (4) the reaction of hydrazine with hydrogen peroxide, and (5) the reaction of hydrazine, liquid ammonia mixtures with nitric acid.

The two pressure peaks observed by McKinney for the reaction of sodium-potassium alloy with excess water in McKinney's reactor were explained in terms of inefficient mixing and an explosion occurring between the hydrogen produced by the reaction and oxygen originally present in the reactor atmosphere. The reaction of equal quantities of the reactants showed only a single pressure peak corresponding to the simultaneous evolution of hydrogen and the hydrogen, oxygen explosion.

The ignition delays of the fuel-oxidant systems were measured and found to be less than three milliseconds for every reaction studied. The delays were lower than those reported by other investigators who employed mixing methods where the efficiency of mixing was most uncertain. The short delays were attributed to (1) the rapid rate of mixing in the apparatus and (2) the impact and turbulence associated with the mixing process.

There was a negligible effect of the reaction temperature or of the hydrazine concentration on the ignition delay of the reaction of nitric acid with liquid ammonia, hydrazine mixtures. This result was more indicative of ignition by impact than it was of ignition controlled by the rate of a homogeneous chemical reaction.

An analysis of the products of several reactant ratios of the hydrazine, nitric acid reaction was made. The results were compared to the products expected from thermodynamic considerations. It was shown that the reaction had been quenched short of completion. The observed products have been discussed in terms of the possible intermediate stages of the reaction.

LIST OF TABLES

LIST OF TABLES (continued)

LIST OF TABLES (continued)

LIST OF ILLUSTRATIONS

LIST OF ILLUSTRATIONS (continued)

LIST OF ILLUSTRATIONS (continued)

LIST OF ILLUSTRATIONS (continued)

CHAPTER I
INTRODUCTION

Certain liquid fuels when brought into contact with strong oxidising agents will ignite spontaneously. The ignition of such systems may take place instantaneously when the liquids are first brought into contact or there may be a time delay. Most of the studies of the ignition delay in such systems have employed methods designed to simulate conditions met in a rocket motor. In a typical rocket motor the two reactants are contacted by the impingement of a number of fuel and oxidant streams in a relatively unconfined area. By such measurements it does not seem possible to differentiate between the delay created by the time required to achieve efficient mixing and the delay caused by an actual chemical induction period.

Methods have been devised to achieve the complete mixing of useful amounts of two liquids in a very short time. The work of Roughton,[1*] Chance[2] and McKinney[3] has proven conclusively that it is possible to effect the complete intermixing of two liquids and begin observation of the resulting mixture only a few msec. (milliseconds) after the initial contact. These methods have never been applied to the study of the ignition of fuel-oxidant mixtures. The present research is an attempt to apply the mixing methods of Roughton, Chance and McKinney to the problem of the self-ignition of fuel-oxidant systems and to study the associated explosive reactions.

The system, nitric acid - hydrazine, is of particular interest. This reaction was chosen as the main subject of the present research.

---

*For all numbered references, see bibliography.

It was believed that the use of an inorganic fuel would be more suitable for an exploratory study of this nature.

Reactions of Hydrazine and Nitric Acid

There appears to be very little information in the literature regarding the reaction between concentrated solutions of hydrazine and nitric acid. Dilute solutions of the two will react to form the salt hydrazine nitrate which can be crystallized from the aqueous solution. Both a mononitrate and a dinitrate exist. The mononitrate is quite stable. It has been heated to 300°C without decomposition.[4] The stoichiometry of the thermal decomposition of the mononitrate is not fully understood. Hodgkinson[5] found decomposition to nitrogen, nitric oxide and water in a vacuum at 200°; Keenan[6] found nitrous oxide to be one of the principal products. Hydrazine nitrate has been found to be much more susceptible to explosion than ammonium nitrate. When hydrazine nitrate is heated with dilute sulfuric acid some hydrogen azide is formed.[4] The oxidation of hydrazine sulfate with strong nitric acid has also been shown to yield some hydrogen azide.[4]

The oxidation of hydrazine in dilute aqueous solutions has been the subject of many investigations. The oxidation by hydrogen peroxide has been shown to yield hydrogen azide under certain conditions along with nitrogen and water. Gordon[7] in a recent kinetic study has proposed the following mechanism for the oxidation in dilute alkaline solution:

(1) a. $N_2H_5OH + H_2O_2 \rightleftharpoons N_2H_5OOH + H_2O$

b. $N_2H_5OOH \xrightarrow{k} N_2H_2 + 2\,H_2O$

c. $N_2H_2 + H_2O_2 \xrightarrow{\text{rapid}} N_2 + H_2O$

The salt N_2H_5OOH is an unstable intermediate, the decomposition of which is the rate determining step. The subsequent oxidation of the diimide is supposed to be very rapid. In this study Gordon found no hydrogen azide or ammonia in the reaction mixture.

Oxidizing agents which can react with acidic solutions of hydrazine can be grouped into three categories:[8,9] (1) those that accept only one electron, (2) those that accept two electrons, and (3) those involving a stepwise oxidation through several intermediates in which both one and two electrons are transferred. It has been found that hydrogen azide is formed only in reactions involving group (2) or (3) oxidizing agents. Both nitric acid and hydrogen peroxide are in one of these two groups because of their known tendency to form hydrogen azide. Oxidizing agents of group (1) such as cupric ion or ferric ion are supposed to react according to the following scheme:

(2) a. $N_2H_5^+ \longrightarrow N_2H_3 + 2\,H^+ + e^-$

b. $2\,N_2H_3 \longrightarrow N_4H_6$

c. $N_4H_6 \longrightarrow N_2 + 2\,NH_3$

In the actual reaction studies the ratio of nitrogen to ammonia may deviate considerably from that indicated by Eq. 2c because of side reactions characteristic of the particular oxidizing agent. Oxidizing agents of group (2) are thought to react through the diimide radical according to Eq. 3:

(3) $N_2H_5^+ \longrightarrow N_2H_2 + 3\,H^+ + 2\,e^-$

The diimide radicals can condense with each other or with hydrazine to form higher hydronitrogens some of which can decompose to yield hydrogen azide as well as ammonia and nitrogen. Tetrazene is the most logical

hydronitrogen to be formed from diimide radicals. Triazene could conceivably be formed from one diimide radical and an imide radical resulting from the possible dissociation of diimide. The only known organic hydronitrogen that can decompose to yield derivatives of hydrogen azide are the isotetrazenes. It is therefore reasonable to assume that isotetrazenes are also intermediates in oxidations involving two electron steps.

A great number of studies have been made of the decomposition of gaseous hydrazine. Hydrazine has been found to decompose into varying amounts of nitrogen, hydrogen and ammonia. The only study of the thermal decomposition of hydrazine in which the decomposition was claimed to be homogeneous was one due to Szwarc.[10] The primary step is represented by Eq. 4:

(4) $$N_2H_4 \longrightarrow 2\ NH_2$$

The resulting amino radicals were removed by reaction with toluene. The decomposition, however, was carried to a very slight extent to avoid side reactions. The catalytic decomposition on silica was shown to follow Eq. 5:[11]

(5) $$3\ N_2H_4 \longrightarrow 4\ NH_3 + N_2$$

Decomposition on a hot platinum or tungsten wire was shown to yield hydrogen, nitrogen and ammonia according to Eq. 6.[11]

(6) $$2\ N_2H_4 \longrightarrow 2\ NH_3 + N_2 + H_2$$

A recent study of the thermal decomposition of nitric acid vapor was made by Johnston.[12] In this study rapid flow techniques were used to determine the kinetics of the decomposition reaction. The proposed mechanism is as follows:

(7) a. $HNO_3 \xrightarrow{a} NO_2 + OH$

b. $OH + NO_2 \xrightarrow{b} HNO_3$

c. $OH + HNO_3 \xrightarrow{c} H_2O + NO_3$

d. $NO_3 + NO_2 \longrightarrow NO_2 + O_2 + NO$

e. $NO_3 + NO \longrightarrow 2\ NO_2$

The observed kinetics are in agreement with this scheme and can be represented by Eq. 8:

$$(8) \qquad -\frac{d(HNO_3)}{dt} = 2a(HNO_3)\left[\frac{1}{1 + \frac{b(NO_2)}{c(HNO_3)}}\right]$$

The net reaction is given by Eq. 9:

$$(9) \qquad 4\ HNO_3 \longrightarrow 4\ NO_2 + 2\ H_2O + O_2$$

Eq. 9 also described the decomposition that occurs when liquid, anhydrous nitric acid is allowed to stand for long periods of time at room temperature or higher. Reaction 9 is known to be readily reversible; the equilibrium constants of Reaction 9 have been calculated by Forsythe and Giauque.[13]

A great deal of work has been done to determine the nature of nitric acid solutions[14] particularly with regard to aromatic nitration.[15] It is generally conceded that the nitronium ion NO_2^+ is the nitrating agent in a large number of nitration reactions. In a recent cryoscopic study of pure liquid nitric acid, Dunning and Nutt[16] have estimated that there is about 8% of dissociation products present in equilibrium at room temperature. The known dissociation equilibria are given in Eq. 10:

(10) a. $2\ HNO_3 \rightleftharpoons H_2O + N_2O_5$

b. $N_2O_5 \rightleftharpoons NO_2^+ + NO_3^-$

c. $HNO_3 + H_2O \rightleftharpoons H_3O^+ + NO_3^-$

d. $2\ HNO_3 \rightleftharpoons H_2NO_3^+ + NO_3^-$

Flames and Explosions of Hydrazine

The decomposition of hydrazine can give rise to a flame even in the absence of an oxidizer. The explosive decomposition of gaseous hydrazine was studied by Bamford.[17] He found decomposition to take place according to Eq. 11:

(11) $5\ N_2H_4 \longrightarrow 4\ NH_3 + 3\ N_2 + 4\ H_2$

The first successful attempt to stabilize a hydrazine decomposition flame was made by Murray and Hall.[18] They found the decomposition to proceed according to Eq. 12:

(12) $2\ N_2H_4 \longrightarrow 2\ NH_3 + N_2 + H_2$

They studied the flame velocity of the hydrazine decomposition flame for gaseous hydrazine, water mixtures. They also studied the flame velocity of the hydrazine, oxygen flame; the ammonia, oxygen flame; and the flame produced when a 2:1:1 mixture of ammonia, nitrogen and hydrogen burns in oxygen. They proposed that in the case of oxygenated flames the hydrazine is decomposed according to Eq. 12 before it reaches the flame front; the resulting ammonia and hydrogen then react with oxygen in the flame front. The authors hoped to prove this hypothesis by studying the combustion of the ammonia, nitrogen and hydrogen mixture. The results, however, were inconclusive. The authors calculated the adiabatic flame temperature

for the hydrazine decomposition flame according to Eq. 12 and found a value of 1660°C. They also calculated it on the basis that decomposition produced only nitrogen and hydrogen and found a value of 1100°C. They measured the flame temperature crudely with a thermocouple and found a value intermediate to those calculated. However they expected a measured temperature of several hundred degrees below the true value because of the large size of the thermocouple.

It is interesting that ammonia should persist at these temperatures because of its high temperature instability. Tanner[19] found ammonia to decompose only 45% per sec. at 900°C in a tube which certainly had a catalytic surface. Wolfhard and Parker[20] found ammonia as such in diffusion flames up to 2400°C by a spectroscopic method. The persistence of ammonia at such high temperatures indicates that the homogeneous rate of the thermal decomposition of ammonia may be very low since reaction conditions in a carbon free flame are essentially homogeneous.

Ordinarily the final products of a high temperature decomposition such as the hydrazine decomposition or of a combustion reaction such as that between hydrazine and nitric acid would be expected to be those predictable from thermodynamic considerations alone. By a simple thermodynamic argument it can be shown that temperatures as high as 3000°K can be expected from the reaction of nearly equimolar amounts of anhydrous hydrazine and anhydrous nitric acid.* It must be assumed that the reaction is carried out under adiabatic conditions. At such high temperatures the rates of almost any possible gas reaction would be expected to be very high so that a condition of complete thermodynamic equilibrium should

---

*Sample calculations are given in Appendix IV for certain cases of the hydrazine, nitric acid reaction.

result unless the gases are cooled very rapidly. The temperature that is expected to result from the adiabatic reaction of two combustibles leading to complete chemical equilibrium is usually referred to as the adiabatic flame temperature.

The practical calculation of the adiabatic flame temperature can be very complicated. One first calculates the relative atomic composition of the reactant mixture. By a trial and error procedure one can then determine the equilibrium composition of the mixture at any assumed high temperature. It remains to calculate the heat evolved by an assumed reaction between the starting materials leading to the trial composition, the entire reaction taking place at the original temperature of the starting materials. The heat required to bring the reaction products to the assumed high temperature is then calculated using specific heat data. When the correct high temperature has been assumed, the heat evolved by the reaction will just equal the heat required to bring the products up to the high temperature. The calculation is somewhat more complicated when the total pressure of the final products is also unknown.

It is obvious that in the case of nitric acid vs. hydrazine only simple compounds such as water, nitric oxide, the elements and certain radicals are thermodynamically stable at such high temperatures. When the final products of such a reaction are cooled to permit analysis, the composition will in general be changed somewhat because of radical recombinations, etc.

The adiabatic condition can be very nearly realized in the laboratory in the case of the explosions of gases. This is usually accomplished by igniting the gas mixture in a spherical, constant volume bomb. If the gases are ignited at the center of the spherical chamber, the explosion front will move radially toward the chamber walls. It is obvious that

no heat losses can occur until the hot front reaches the chamber wall; at this point, however, the reaction is complete. By using a rapid pressure recording method it is possible to measure accurately the pressure maximum corresponding to this condition. Since the maximum pressure is calculable with thermodynamic data it is possible to obtain thermodynamic information from the study of such explosions.[21]

Ignition Delay Studies

Most of the impetus for the study of the ignition delay time of liquid fuel-oxidant systems is due to the potential use of such systems in rocket motors. Systems which do not ignite spontaneously can be used successfully in rocket motors if some external means of ignition can be found. From a practical standpoint, however, it is preferable to employ a system that will ignite spontaneously. In such a rocket motor it is imperative that ignition takes place in a very short time after the contact of the reactants. An excessive delay will cause the unreacted materials to accumulate in the motor chamber; ignition could then cause a destructive explosion. For this reason the study of hypergolic ignition (self-ignition) is of great practical importance in the field of rocket technology.

Some of the experimental variables which must be controlled for the precise measurement of ignition delay time include: (1) the reactant ratio, (2) the time required to effect complete mixing, (3) the chemical composition of the reactants, (4) the ambient temperature, and (5) the ambient pressure. It is of interest to see how these variables have been controlled in the previous investigations of ignition delay.

A method which has been widely used to measure ignition delay

times is usually referred to as the "drop test" or the "open cup test".[22] In this test the fuel is usually contained in a metal cup; one drop of the oxidizer is allowed to fall into the cup. Various methods are employed to measure the time delay between the first contact of the fuel with the oxidizer and the onset of luminosity. Methods ranging in complexity from an observer with a stop watch to an elaborate system of photoelectric cells have been used to record the delay time. High speed motion pictures are also commonly used in this connection. In a test of this type there is no way of determining the effective reactant ratio at the time of ignition or to ascertain the completeness of mixing. The method is of value for the rough screening of bipropellant pairs.

A highly refined open-cup testing apparatus has recently been described by Gunn.[23] In this apparatus the oxidizer is contained in a thermostatted reaction dish. The fuel is originally contained in a weir-lipped cup located above the reaction dish. The weir-lipped cup can be rotated, pouring the fuel out of it in the form of a thin sheet into the reaction dish. The thin sheet of fuel then contacts and slowly mixes with the oxidizer and chemical reaction ensues. The ignition delay is defined as the time interval between the first contact of the reactants and the instant that visible light emission begins. The delay time is measured by an ingenious electronic timer. The weir-lipped cup and the reaction dish form the plates of a condenser, the capacity of which is abruptly altered when the fuel contacts the oxidizer. This capacity change is converted into a small voltage pulse that triggers a single sweep generator. The output of the single sweep generator is fed to the horizontal plates of a cathode-ray oscilloscope. The beginning of visible light emission is sensed by a phototube, amplifier combination the output of which is fed to the vertical plates of

the oscilloscope. The intensity modulation electrode of the oscilloscope is connected to a sinusoidal oscillator of accurately known frequency. The oscilloscope trace is then a series of dots, the recording of which is accomplished by photographing the screen of the cathode-ray tube. Counting the number of dots from the start of the trace to the point at which it is vertically deflected gives the ignition delay.

The data obtained with the refined open-cup apparatus were found to be accurately reproducible. The systems nitric acid vs. aniline, nitric acid vs. furfuryl alcohol and nitric acid vs. aniline, furfuryl alcohol mixtures were studied. The system aniline vs. anhydrous nitric acid showed that the longest ignition delay was 0.41 second at room temperature. The system red fuming nitric acid* vs. aniline was found to have an ignition delay of about 90 msec. in the temperature range 15 to 40°C; however, the delay rose sharply below 15°C reaching 200 msec. at 0°C. There was a similar sharp increase of the ignition delay of the system white fuming nitric acid* vs. furfuryl alcohol as the temperature was decreased. At 25°C the delay was about 36 msec., but at -15°C the ignition delay was found to be about 180 msec. The author suggested that the sharp increase of the ignition delay was due to decreased mixing efficiency at the lower temperatures due to the rapid increase in the viscosity of the fuels as the temperature approached their freezing points.

It is apparent from the description of this method that there is no experimental control exercised over the reactant ratio or the mixing efficiency so that any effect of a change of the chemical reaction rate is masked by the mixing effect.

---

*The compositions of red and white fuming nitric acid are given in Appendix III.

A study of the ignition delay of the systems hydrazine vs. nitric acid, furfuryl alcohol vs. nitric acid and liquid ammonia hydrazine mixtures vs. nitric acid was made by the M. W. Kellogg Co.[22] The reactions were carried out in a small rocket motor. In this motor the reactants were contacted by the impingement of a single fuel stream with a single oxidant stream. The jets were located at one end of a cylindrical combustion chamber; at the other end was a simple convergent nozzle. In one of the motors used by Kellogg the combustion chamber was made of glass; the time from propellant entry to ignition was determined by means of high speed motion pictures. In another apparatus the chamber was made of metal; the start of ignition was determined by a pressure rise method. The moment of impingement was recorded by oscilloscope photography, advantage being taken of the electrical conductivity of the reactants. The moment of ignition was recorded by means of a capacitance type pressure gage and associated electronic apparatus. A capacitance gage employs a pressure sensitive diaphragm; motion of the diaphragm causes a capacity change between the diaphragm and stationary gage elements. This capacity change can be converted electronically into a voltage change. Provisions were made to cool the entire apparatus to temperatures as low as -50°C. The reactant ratio could be varied by changing the diameters of the injection jets, allowing more or less of one reactant to stream into the motor chamber.

The results obtained with the small rocket motor were not entirely reproducible. The nominal values obtained for the ignition delay for optimum test conditions are given in Table 1. Ignition tests were also made for the system white fuming nitric acid vs. liquid ammonia, hydrazine mixtures. These tests were made in a larger rocket motor at room temperature and only qualitative observations were made. Smooth

Table 1. Ignition Delay in a Small Rocket Motor[22]

Reactants			Temperature, in °C	Ignition Delay, in msec.
Hydrazine, 96%	-	RFNA*	21	3.1 ± 1.4
Hydrazine, 96%	-	WFNA**	21	5.0 ± 1.7
Furfuryl alcohol	-	WFNA	21	16.6 ± 2.4
Furfuryl alcohol	-	WFNA	-29	22 to 40
Hydrazine, 71.5%	-	WFNA	25	ca. 37
Hydrazine, 71.5%	-	RFNA	-48	ca. 37
Ammonia, 14.1% hydrazine	-	RFNA	-36	6 to 10
Ammonia, 9.5% hydrazine	-	RFNA	-35 to -40	ca. 14
Ammonia, 5.0% hydrazine	-	RFNA	-37 to -47	37#

* RFNA, red fuming nitric acid, 24% NO_2.
** WFNA, white fuming nitric acid, 96% HNO_3.
# Sporadic ignition.

ignition was found for hydrazine contents as low as 4.3%. When the hydrazine content was reduced to 2.2%, there was a noticeable ignition delay which resulted in damage to the motor. Although somewhat different delay values were obtained for differing reactant ratios, the poor reproducibility of the data appeared to mask the effect of this variable.

An ignition delay tester which was very similar to a rocket motor was described by Broatch.[24] In this apparatus contact was also made by the impingement of two streams; however, the combustion chamber was cut away to allow visual observation. The delay time again was considered to be the time difference between first contact and the moment of visible light emission.

In a given rocket motor the reactant ratio uniquely determines the conditions in the steady state, i.e., the flame temperature, the chamber pressure, reaction products, thrust, etc. The effect of the reactant ratio on the ignition delay time, however, is not clear when the conditions of mixing are unknown as they appear to be in a method involving the impingement of streams in an unconfined area. If the complete intermixing of a fuel-oxidant combination could be effected in a time very short compared to the ignition delay time of the mixture then the measured delay would be the true "chemical delay" or induction period. One would expect a change of the reactant ratio to lead to a different chemical delay time. When ignition takes place before the mixing is completed, it cannot be known what the local reactant concentrations were in the fluid element which first exploded, igniting the remainder of the mixture.

An example of the delay due to incomplete mixing is found by comparing the results obtained by Gunn with the refined open-cup apparatus

with those of the Kellog Co. using the impingement method. The ignition delay of the system furfuryl alcohol vs. white fuming nitric acid was found to be 36 msec. at room temperature with the open-cup apparatus and 16.6 msec. by the impingement method. At -15°C the open-cup apparatus gave a value of 180 msec. while at -29°C the impingement method gave a value of only 22 to 40 msec. The impingement method would be expected to yield more efficient mixing than the open-cup method because of the greater turbulence and impact associated with impinging streams so that a lowered ignition delay should result.

It was believed at the beginning of the present study that a fundamental approach to the phenomena of ignition delay was possible only if a mixing method could be found in which complete mixing is accomplished in a time short compared to the ignition delay values. Such a method is that devised by Roughton, Chance and McKinney.

Rapid Mixing Studies

The first comprehensive study of the efficiency of the rapid mixing of two aqueous solutions was made by Hartridge and Roughton.[1] They were interested in mixing in order to study the kinetics of rapid reactions in solution. The basic scheme of the method was to contact two reactant streams in a confined area. Several mixing patterns were tested. The most efficient one was found to be a "T" shaped mixer; the reactants each entered one leg of the "T" and the mixed solution emerged from the third leg. The passages through which the solutions entered the mixer were called jets while the passage through which the mixed solution flowed was called the observation tube. Two arrangements of the jets were found to perform about equally well at high flow rates. In one of these the jets were directly opposed to each other while in the other the jets were

directed tangentially into the observation tube. The tangential arrangement was found to be better at low flow rates. Some of the methods used by Hartridge and Roughton to test the mixing efficiency of such a mixer will be briefly reviewed in the following paragraphs.

In one mixing test 0.01 N HCl was reacted with 0.01 N NaOH containing phenolphthalein. The solution in the observation tube was slightly colored; however, when some was collected and allowed to stand the color disappeared. The flow rate of the alkaline solution was then diminished until the color in the observation tube just disappeared. A sample of the outflow in this case had a final pH of 5.6. Assuming that the chemical reactions are infinitely fast in this case, it is possible to calculate the mixing error. It is necessary to assume that some color still remains in the observation tube. The authors estimated that at the worst 1% of the phenolphthalein was colored in the original stream. Since phenolphthalein is colorless below a pH of 9.6, they assumed that the colored portion of the stream was made up of 1% unmixed alkali having a pH of 9.6; the bulk of the solution had a pH of 5.6 so that the efficiency of mixing in the observation tube was

$$E = 100 \times \frac{49.97}{50.03} \times \frac{49.988}{50.013} = 99.8\%$$

where 49.97/50.03 is the mixing ratio necessary to produce a pH of 9.6 and 49.988/50.013 is the ratio necessary to produce a pH of 5.6. Under these unfavorable assumptions the fluid at the exit from the mixer had the following composition:

1% is mixed 99.8% (pH 9.6)
1% is mixed 99.8% (acid predominating)
98% is mixed 100.0%

In a later study by Roughton[25] and in one by Roughton and Millikan[26] another mixing test was employed. This method depends upon the fact that the amount of heat liberated by a chemical reaction is a measure of the amount of reaction. In this test a very fine thermocouple is inserted into the observation tube so that temperature measurement is possible at any point in the tube. The reaction of NaOH with HCl, which was considered to be infinitely rapid, was run in the apparatus. The temperature rise was measured during steady-state flow conditions at a number of points at varying distances from the mixer. At a sufficient distance downstream the temperature rise reached a constant value corresponding to complete mixing. The percentage of this total temperature rise measured at some point near the mixer was then equal to the percentage completion of the mixing at this point. The quantitative results obtained by this method will be discussed in a later paragraph.

A great number of successful kinetic studies of reactions in solution were made by the method of Hartridge and Roughton. A number of different methods were used to determine the extent of reaction at points in the observation tube. The results obtained by various investigators for the velocity constant of the carbonic acid decomposition are shown in Table 2 in order to illustrate some of the analytical methods that can be used.

Table 2. Values of k, the Velocity Constant of the Reaction[26]
$H_2CO_3 \longrightarrow CO_2 + H_2O$

Method	Value at 18°C in $sec.^{-1}$
Thermal	12.1
Conductivity	12.7
H_2 electrode	10.2
Colorimetric	12.9

A thorough analysis of the flow method for use in kinetic studies was made by Chance.[2] His analysis included a study of the power necessary to drive solutions through "T" type mixers as well as the mixing efficiencies obtainable by the method. Chance used the photoelectric recording method exclusively, studying reactions accompanied by a color change. In this method a light beam is passed through the observation tube; the amount of light absorbed by the mixed solution is a measure of the extent of reaction. Chance found that at high flow velocities a phenomenon known as cavitation made photoelectric measurements impossible. Cavitation is a separation of the fluid elements of the stream caused by extreme turbulence resulting in optical inhomogeneity. Chance found that the angle the jets made with the observation tube had an important effect on this factor. By using a compromise between the tangential arrangement and directly opposed jets, flow rates up to 2300 cm. per sec. could be used before cavitation interfered with the recording method. A study of numerous mixer and observation tube combinations was made. An empirical equation, Eq. 13, was developed from which the expected flow rate could be calculated knowing the dimensions of the mixer and the pressure drop across the mixer:

$$V^2 = \frac{\Delta P \, A_o^2}{K_1} \qquad (13)$$

where V is the total volume flow rate, in cc. per sec.,

ΔP is the pressure drop in lb. per sq. in.,

A_o is the area of the observation tube, in sq. mm.,

K_1 varies from 0.3 to 0.8.

The mixers were studied only for the case where equal volumes of reactant solutions were contacted. The effect of the jet diameters and number of

jets on the flow rate is not clear from the data. In general jet diameters from 0.5 to 1.4 mm. and observation tube diameters of 0.5 to 1.8 mm. were used with no apparent regard for the observation tube diameter, jet diameter ratio.

The efficiency of mixing was verified by Chance by running reactions known to be very fast. This was accomplished by using reactions showing bimolecular characteristics. The rate of the reactions were determined in very dilute solutions; the concentrations were increased until the system could no longer follow the reaction rate. At these concentrations it was the mixing rate then that was measured. The reaction between iodine and thiosulfate, the concentration of each reagent being 5×10^{-4} N, is about 96% complete in 0.3 msec. (the shortest measurable time with Chance's apparatus). The mixing was shown to be at least 98% complete at the observation point (10 mm. from the mixer) at all flow velocities by increasing the thiosulfate concentration. The reaction between ceric sulfate and hydrogen peroxide was similarly shown to be immeasurably rapid at sufficiently high concentrations. The mixing efficiency was again shown to be better than 98% in all cases. Since the photoelectric error was of the order of 2%, the estimate of 98% mixing may be conservative.

A very recent rapid kinetic study was made by Trowse.[27] A unique method was used to verify the mixing efficiency. In this method two solutions having different optical properties were mixed. The approach to optical homogeneity was taken as the criterion of the extent of mixing. During mixing there is an appearance of turbidity due to multiple refractions of the illuminating light; eventually the solution clears. The light transmission changes that occurred during the mixing of water

and a 20% aqueous ammonium sulfate solution were followed by a photoelectric recording method.

The quantitative results obtained for the mixing efficiency in "T" type mixers was reported in great detail in a recent comprehensive review of the subject of rapid reactions in solution by Roughton and Chance.[28] The data are summarized in Tables 3 and 4. In Table 3 the apparatus and method are indicated and in Table 4 the results are shown. The final column of Table 4 is the product of the linear velocity of flow through the observation tube and the time required to achieve 97% mixing. This distance is clearly the distance that the solution had to flow from the point of initial contact to the point at which mixing was 97% complete. It was pointed out by Roughton that the data of Millikan shows that this distance decreased as the flow velocity was increased for a given mixer. It is thus apparent that mixing complete to within a few per cent can be obtained in a rapidly flowing stream in a distance of less than a centimeter. The data shown in the tables refer only to the mixing of aqueous solutions. Only one reference was made to the mixing of physically different liquids. Roughton[1] brought together a paraffin oil and water in a "T" type mixer and found that a very fine emulsion was formed.

It is instructive to consider what concentration gradients exist in a solution that is 97% mixed. The distribution of concentration must certainly be statistical. It is very unlikely that 3% of the original reactants remain together at their original concentration, rather the range of concentrations must all be very close to that corresponding to complete intermixing.

In all of the rapid reaction studies made by Roughton, Chance and their followers the pressure drop across the mixers never exceeded one

Table 3. Tests of Mixing Efficiency, "T" Type Mixers[28]

Author	Apparatus	Test
Hartridge and Roughton	8 jet metal mixer	HCl, NaOH, Colorimetric
	8 jet ebonite mixer	HCl, NaOH, Thermal
Roughton	3 way glass T-taps bore 1.5 mm.	HCl, NaOH, Thermal
Millikan	4 jet Bakelite tap mixer, jets 0.5 mm.	HCl, NaOH, Thermal
Chance	8 jet polystrene, jets 0.4 mm., tube bore 1.0 mm.	I_2, $S_2O_3^=$, Colorimetric
Dalziel	2 jet glass mixer,	
	0.5 mm. bore	H_2SO_4, NaOH, Thermal
	1.0 mm. bore	H_2SO_4, NaOH, Thermal
	1.0 mm. bore	H_2SO_4, NaOH, Thermal
Trowse	2 jet glass mixer,	
	0.7 mm. bore	Light Transmission
	0.5 mm. bore	Light Transmission
Chance	4 jet all glass mixer, 0.5 mm. jets, 1.0 mm. bore	H_2O_2, Peroxidase, Colorimetric

Table 4. Results of Mixing Efficiency Tests[28]

Author	Flow rate in the observation tube, in cm. per sec.	Maximum time, in msec., for mixing 95%	97%	99%	Distance, in mm. 97%
Hartridge and Roughton	345	-	0.3	-	1.0
	1000	-	0.4	-	4.0
Roughton	400	10	-	-	-
Millikan	268	-	0.5	2	1.3
	175	-	1.5	7	2.6
	100	-	4.0	10	4.0
Chance	2300	-	0.4	-	9.2
Dalziel	140	-	-	5	-
	280	-	-	5	-
	140	-	-	8	-
Trowse	440	0.9	1.3	3.0	5.7
	995	0.5	0.6	0.8	6.0
Chance	1000	-	1.0	-	10

or two atmospheres. The first attempt to extend the range of the method using high pressures was made by Kilpatrick and McKinney.[3,29,30,31] They wanted to study rapid reactions in solution in which a gas is evolved. The steady flow method of Chance was clearly not suited for this type of reaction. It was necessary to mix a useful quantity of reactants, stop the mixing and begin static measurements of the gas evolution. This was accomplished through the use of a constant volume bomb reactor made entirely of stainless steel. In this apparatus the reactants were driven through a conventional "T" mixer by means of floating pistons which in turn were driven by high pressure nitrogen gas. The entire quantity of reactants, 25 ml. of one solution and 1.0 ml. of a second solution, was injected into a closed volume in about 10 msec.; static pressure rise measurements were then made. The efficiency of mixing was determined by running the reaction represented by Eq. 14:

(14) $Ca(MnO_4)_2 + 5H_2O_2 + 3H_2SO_4 \longrightarrow CaSO_4 + 2MnSO_4 + 5O_2 + 8H_2O$

Using concentrations of the order of 10^{-4} M, Chance[2] found the velocity constant of the reaction to be 2900 liters per mole second. With this value of the velocity constant, and with concentrated solutions (1 ml. of 50% $Ca(MnO_4)_2$ and 25 ml. of 15% H_2O_2 which was also 3M in H_2SO_4), the half time of the reaction was estimated to be 55 microseconds. Under these conditions, the reaction was assumed to be essentially instantaneous. The mixing time was evaluated by measuring the pressure rise due to oxygen evolution. Oxygen evolution was found to be complete in about 10 msec. The efficiency of mixing was further verified by noting that the permanganate color was completely discharged at the end of a run.

The principel difficulty experienced by Kilpatrick and McKinney with the bomb reactor resulted from the possibility that the two floating

pistons might not descend at the same time. The two pistons are not connected mechanically so that any excessive static friction could delay the start of motion of one of the pistons and severely affect the mixing efficiency. The bomb reactor of Kilpatrick and McKinney will be discussed in detail in a later chapter since it was used in connection with the present research.

Reactions of Sodium-Potassium Alloy

The reaction of sodium-potassium eutectic alloy with water and ethanol was studied by McKinney and Kilpatrick.[30] The composition of the liquid alloy corresponded roughly to the formula NaK_2. The reaction with ethanol is represented by Eq. 15:

(15) $$NaK_2 + 3\ C_2H_5OH \longrightarrow 1.5\ H_2 + 2\ C_2H_5OK + C_2H_5ONa$$

and the reaction with water is represented by Eq. 16:

(16) $$NaK_2 + 3\ H_2O \longrightarrow 1.5\ H_2 + 2\ KOH + NaOH$$

The pressure rise in the reaction with excess ethanol was found to follow an approximately first order law. The half-time of the reaction was found to be about 6.2 msec. The authors point out, however, that the reaction is probably heterogeneous and that the first order characteristic might be a fortuitous combination of effects since the injection time is comparable to the observed half-time.

The pressure, time curve obtained in the case of the reaction of the liquid alloy with excess water showed two large maxima. The first maximum occurred about 5 msec. after the beginning of injection. The pressure then decreased to about that expected from the theoretical yield of hydrogen according to Eq. 16 in about 30 msec. A second sharp maximum occurred about 40 msec. after injection. The first maximum

could be attributed to the heat evolved by the reaction; it was unlikely, however, that the second maximum was also due to the heat of the simple reaction represented by Eq. 16.

At the outset of the present research, it was considered likely that the second pressure peak might be due to an explosion of the hydrogen evolved by the reaction with the oxygen of the air present initially in the reactor. If true, this would present an interesting example of a delayed ignition. In view of this it was decided to begin the present research with a further study of the alloy, water reaction.

CHAPTER II
REACTOR DESIGN

Two different constant volume reactors were used during the course of this study. One of these was designed and built by Dr. C. D. McKinney, Jr. and described by him.[3] This reactor will be referred to as Reactor I. Another reactor, which is specifically suited for the study of ignition delay, was designed and built during the course of this research. This reactor will be referred to as Reactor II.

Reactor I

Although Reactor I is adequately described in the thesis by McKinney,[3] the basic features of it will be reviewed. A cross-sectional assembly drawing of Reactor I and the pneumatic injector is shown in Fig. 1. The pneumatic injector is mounted above the reactor; it functions as a quick opening valve discharging high pressure nitrogen gas into the area behind the two pistons. The injector is identical to one described by Neas, Raymond and Ewing.[32] The driving gas, nitrogen at pressures up to 2000 lb. per sq. in., is charged into the storage reservoir A. To start a run, the cocking block B is rotated clockwise by means of a solenoid (not shown in the drawing) or by hand. This shows the toggle C off-center, allowing the gas in the storage reservoir to move the valve D outward, rotating the toggle until it strikes the brass impact pad shown in the drawing as a small upward projection in the center of the cocking block. When the valve opens, the pressure of the driving gas is communicated to both floating pistons. It is important to note that any leakage of gas through the valve gaskets could not drive the pistons down prematurely because of the presence of a small pressure release duct. The motion of the valve seals off this duct preventing leakage

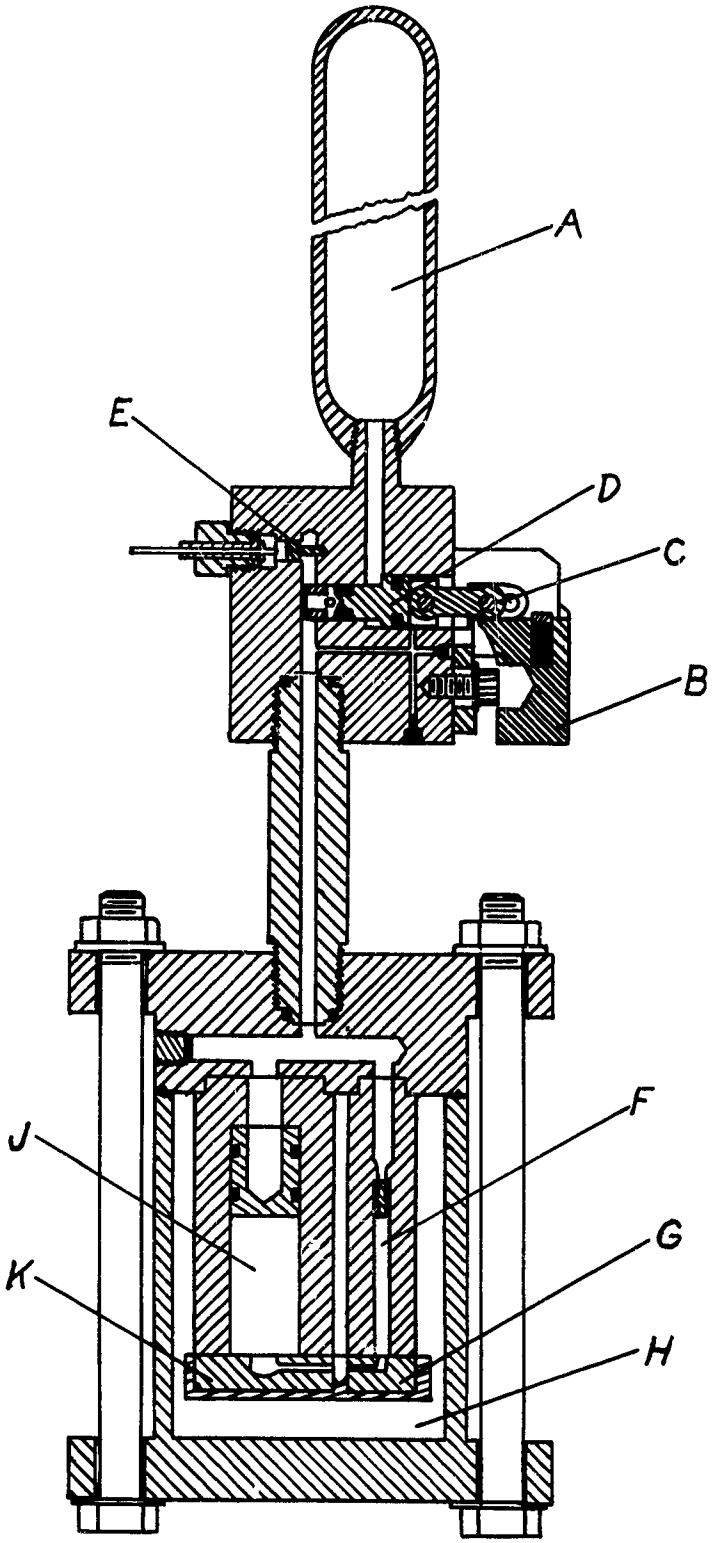

Fig. 1. Cross-sectional Assembly Drawing of Pneumatic Injector and Bomb Reactor I.

during the normal operation of the pneumatic injector. The expanding gas also forces the movable contact E to the left, causing it to strike the fixed contact which is insulated from the body of the injector. The closing of the contact initiates the time base of the recording system.

The two solutions to be mixed are contained in the cylinders at J and F. The cylinder J contains 25 ml. of one reactant solution and the cylinder F contains 1 ml. of the other reactant solution. The pressure of the driving gas on the floating pistons forces them downward, driving the reactants through the jets located in the small and large injection plates G and K into the mixing chamber and out into the body of the bomb H where they react to completion. The two jets are directly opposed.

The gaskets used to seal the valve in the pneumatic injector are neoprene rings which are closely ground to fit the valve cylinders. The gaskets are lubricated with powdered graphite. The gaskets on the floating pistons are also neoprene rings lubricated by powdered graphite. They serve to prevent the driving gas from directly entering the interior of the reactor. They must also prevent leakage of the product gases from the interior of the reactor to the atmosphere once the driving gas pressure has been released. If the piston gaskets are too tight, the start of motion of one or both of the pistons may be seriously delayed. The piston gaskets must therefore be ground to a very exacting tolerance.

During the present study it was found necessary to add a window to Reactor I so that the presence of an ignition could be verified photoelectrically or visually. The window is made of Plexiglass (one-quarter inch thick) and provides a direct view of the area immediately surrounding the mixing chamber. The important parts of Reactor I, including the window assembly, are shown in Fig. 2.

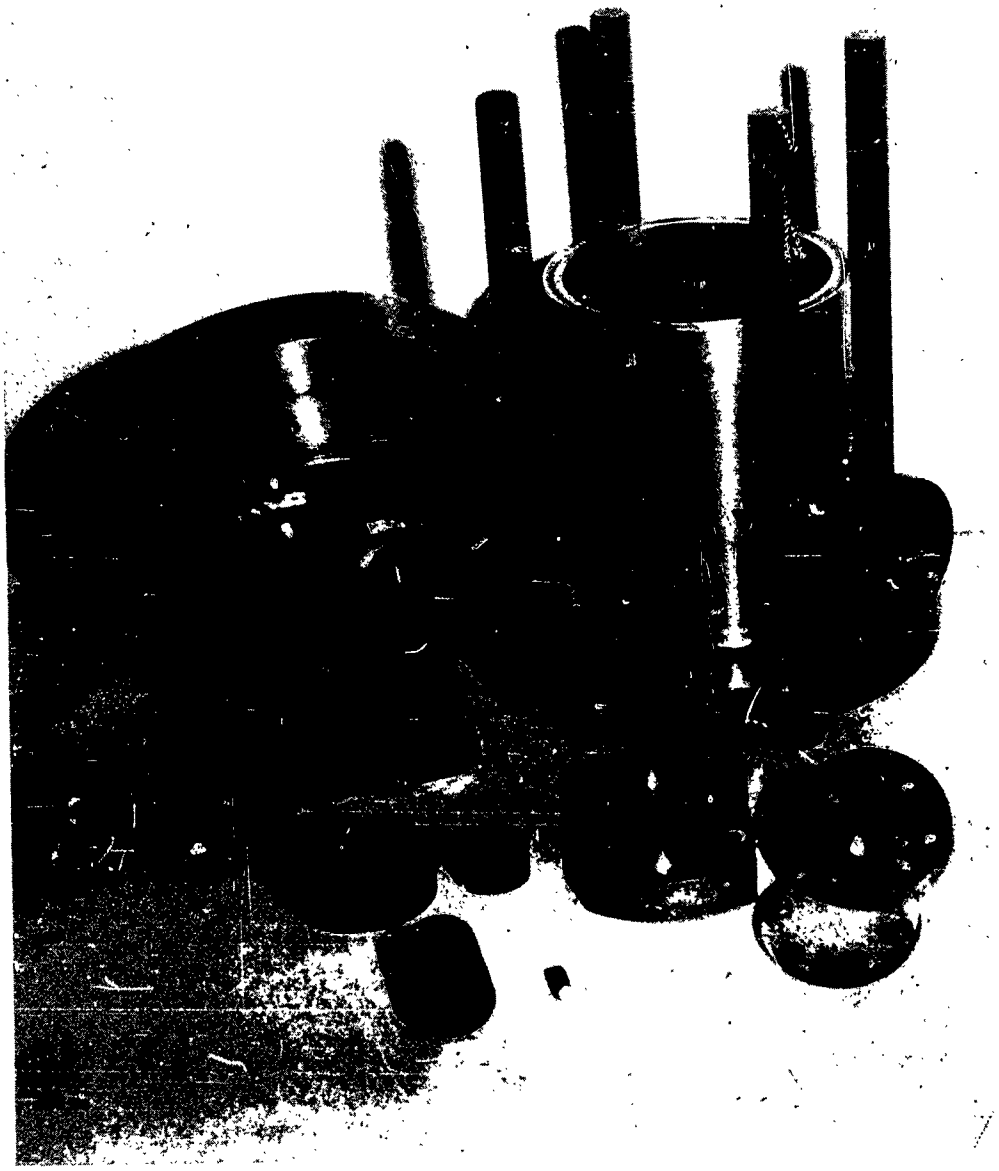

Fig. 2. Reactor I, Showing Injection Plates, Pistons and Window Assembly.

Reactor II

Reactor II was designed specifically for the study of self-igniting fuel, oxidant systems. For this purpose it is necessary to contact more nearly equal volumes of reactants than in the case of Reactor I. A cross-sectional assembly drawing of Reactor II is shown in Fig. 3. The same pneumatic injector that was described in conjunction with Reactor I is used with Reactor II. The reactant solutions are contained in the cylinders at A and B. During injection the driving gas is communicated to the driving piston C. The driving piston in turn forces both of the smaller pistons D and E to descend. The reactant solutions are then forced to flow into the jets in the mixing plate F and into the mixing chamber or exit tube G where they enter the body of the reactor H and react to completion. The baffle plate J can be attached to the mixing plate or it can be dispensed with. If it is used, it serves to ensure complete mixing by breaking up the effluent stream immediately as it leaves the mixing chamber G. It also serves to reflect any emitted light directly into the observation arms M. One observation arm of the reactor is closed with a plexiglass window and the other joins with the piping leading to the strain gage. Two valve blocks, each attached to a stainless steel needle valve, can be interposed between each observation arm and the measuring apparatus, if needed.

Reactor II was designed to allow for immersion in a low temperature bath. For this purpose the reactor is as compact and as light in weight as possible. The outside diameter of the main cylinder block L is only five inches. The observation arms are directed almost vertically so that the apparatus to be used to follow the changes of pressure and light emission can be located well above any thermostatic bath.

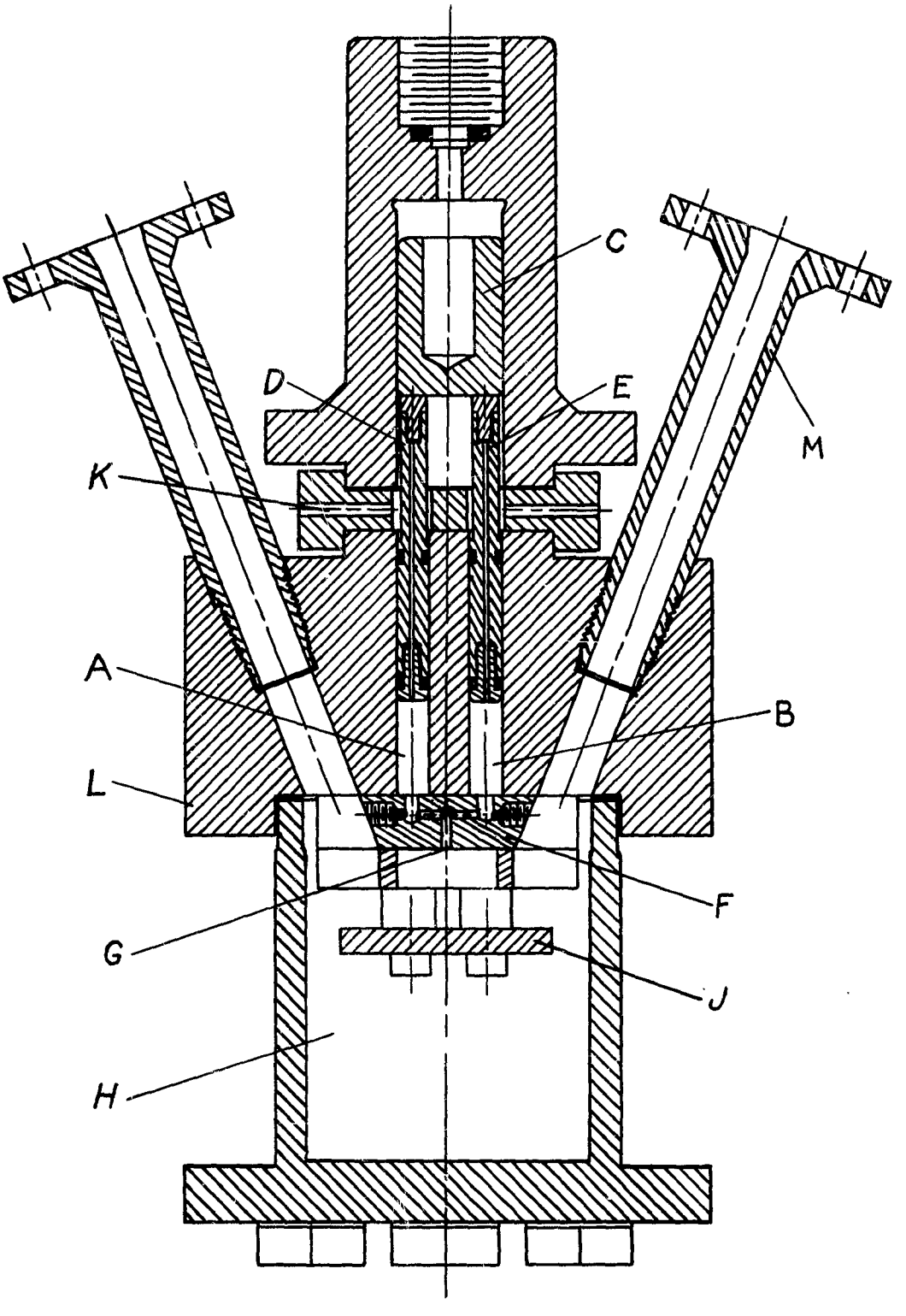

Fig. 3. Cross-sectional Assembly Drawing of **Reactor II.**

Reactor II, just as in the case of Reactor I, is constructed entirely of stainless steel. The driving piston was machined to a close fit with the large cylinder so that no gasket or lubrication is required. A slight leakage of driving gas past the driving piston could not affect the measured pressure in the reactor because this gas is vented to the atmosphere through the air escape ports K. The gaskets on the smaller pistons must withstand the pressure of the product gases from within the reactor and must prevent any back-flow of the liquid reactants during injection. A number of different gasket arrangements were used on the smaller pistons. These will be discussed in a later chapter. It should be pointed out, however, that the pistons are constructed in several parts, so that it is possible to remove the lower part of the pistons and attach a gasket material such as Teflon that could not be stretched over a one-piece piston and attached in that way. The upper gasket must, however, be of neoprene or another rubber because it must be stretched over the steel piston and set into place.

The important parts of Reactor II are shown in Fig. 4. The mixing plate F shown in Fig. 3 and in Fig. 4 and used throughout this research was designed according to the principles established by Roughton and Chance. It is apparent from Fig. 4 that other mixing plates having entirely different mixing patterns could be substituted for mixing plate F without requiring a change in any of the other reactor parts. In a similar way another cylinder block could be substituted for cylinder block L. This would allow the selection of more than a single reactant ratio without requiring the design of an entirely new reactor.

Another cylinder block was designed and built to provide a range of possible reactant ratios. The original cylinder block shown in

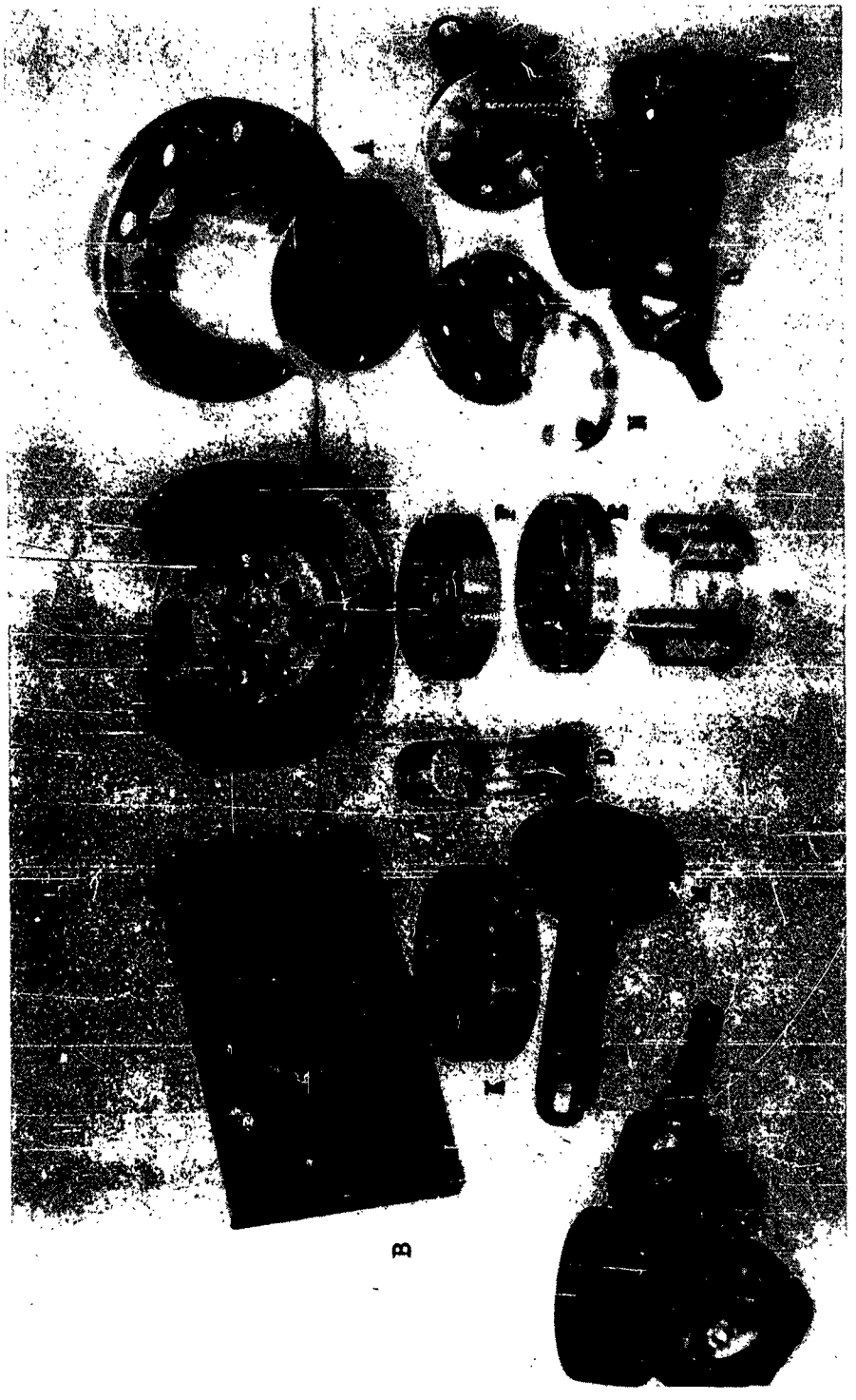

Fig. 4. Reactor II Disassembled. (See Key to Figure)

Key to Fig. 4

A Reaction bomb

B Driving cylinder

C Driving piston

D Small pistons

E Subplate

F Mixing plate

G Valve blocks

J Baffle plate

K Spacer plate

L Cylinder block

M Observation arms

N Window assembly

Fig. 4 has two cylinders of equal diameter providing a single ratio of one to one. The new block has cylinders of unequal diameter providing a reactant ratio of approximately four to one. Fittings were constructed which made it possible to decrease the diameter of the larger cylinder so that two more reactant ratios could be realized: a two to one ratio and a one and one-half to one ratio. Several additional pistons had to be constructed to fit the new cylinders. The two cylinder blocks, the fittings and the pistons are shown in Fig. 5. The measured cylinder diameters and the exact values of the volume ratios obtainable with Reactor II are given in Table 5.

Table 5. Dimensions of Reactant Cylinders, Reactor II

Nominal reactant ratio	Diameter of larger cylinder, inches	Diameter of smaller cylinder, inches	Reactant ratio
1 : 1	0.3135	0.3135	1.00
1.5 : 1	0.3135	0.257	1.49
2 : 1	0.376	0.257	2.14
4 : 1	0.502	0.257	3.82

Several additional mixing plates were designed and built to provide a number of possible mixing patterns. The mixing pattern provided by the original plate has the form of a "T". The other basic pattern that can be obtained with the new plates has the form of a "Y". Several subplates were constructed to fit beneath either main mixing plate. These plates have single holes in them so that the mixed solution emerging from the main mixing plate could be made to flow through additional lengths of a confined passage.

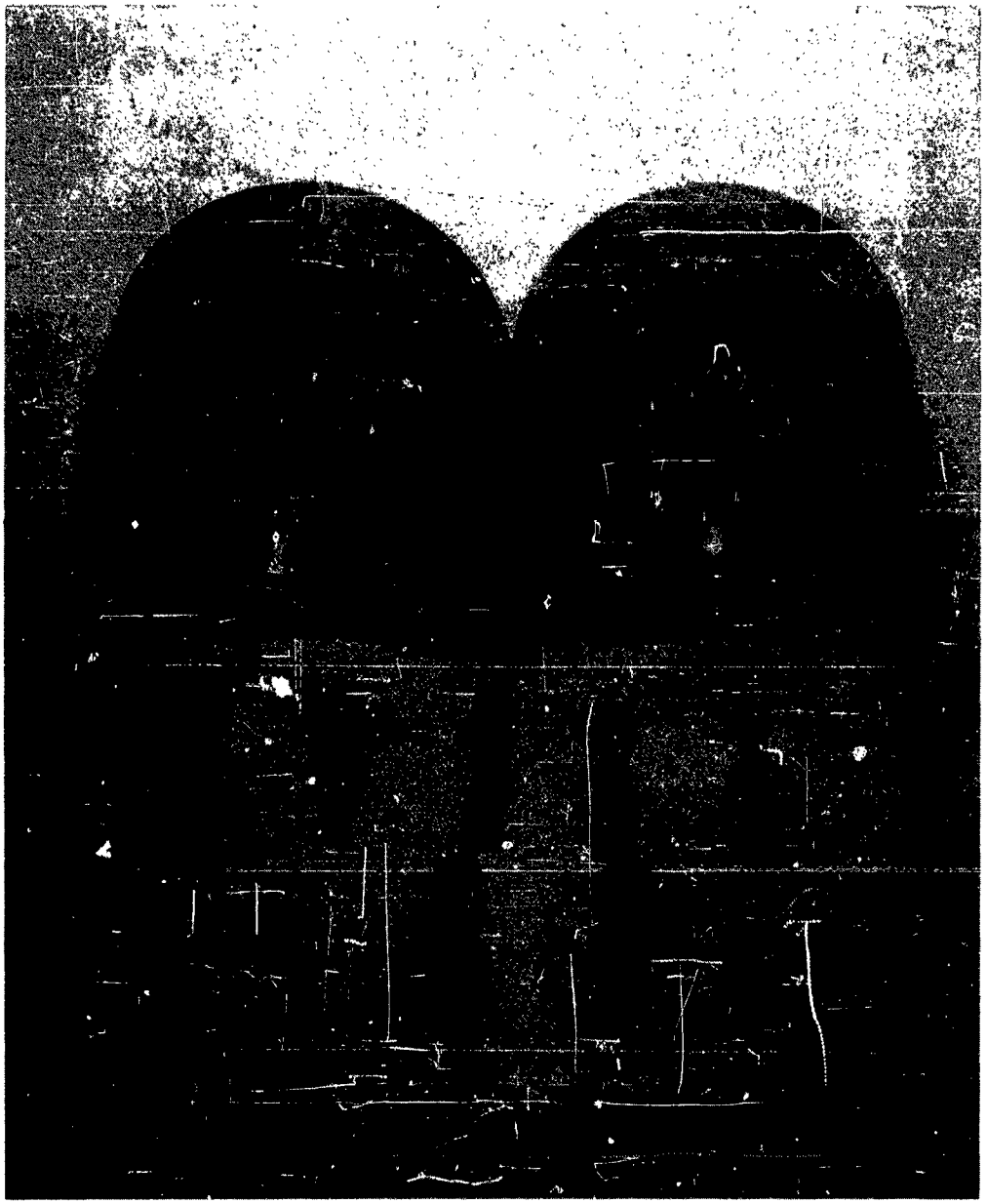

Fig. 5. Cylinder Blocks, Fittings and Pistons, Reactor II.

Reactor II has several design advantages over Reactor I. The fact that the two pistons must begin descent at the same instant and must travel at the same rate ensures uniformity of the mixed solution. Reactor II is much more powerful than its precursor. A substantial hydraulic advantage is achieved by having a single large piston drive two smaller ones. The piston gaskets do not have to withstand the pressure of the driving gas. Reactor II is suited for immersion in a thermostatic bath and is lighter in weight than its precursor. Reactor II is easily adapted to a change of the mixing pattern or a change of the reactant ratio.

Measurement of Transient Pressure

The measurement of the transient pressure of gases in either reactor is the principal means of following the course of the reactions under study. The pressure measuring system to be used must have a very rapid response. The methods used by McKinney appeared to fulfill this requirement adequately. The recording apparatus designed and built by him was used with only a few minor changes. Although the method is described in detail by McKinney, the essential features of the method will be reviewed here.

The pressure sensitive element is a diaphragm type strain gage manufactured by the Statham Laboratories, Inc., Los Angeles, California. In this instrument the gas pressure is applied to a metal diaphragm which is thereby deformed. The motion produced is transmitted to a series of strain wires whose electrical resistance depend upon the degree of strain. The wires are arranged in the form of a balanced bridge within the pressure gage itself. The unbalance of the bridge is then a measure of the gas pressure acting on the diaphragm. The

gage elements are stated to have a natural frequency in excess of 2000 cycles per second so that the gage should faithfully reproduce pressure events occurring at frequencies up to this value. The output of the strain gages is stated to be strictly proportional to the applied pressure. Originally two such gages were available: one having a range 0 to 50 lb. per sq. in. and the other 0 to 150 lb. per sq. in. The range of these gages was not high enough for the proposed study involving high energy fuel-oxidant systems. Two other gages, one having a range 0 to 100 lb. per sq. in. and the other 0 to 500 lb. per sq. in., were purchased. The new gages have a special overrange feature: the smaller one will withstand a pressure of 750 lb. per sq. in. and the larger one 1750 lb. per sq. in. without damage.

The bridge of the strain gage is supplied with A C current of variable frequency. This is accomplished by means of a variable frequency audio oscillator in combination with a power amplifier. The A C voltage applied to the gage is about 10 volts RMS; the output of the strain gages is about 20 millivolts RMS at full rated pressure. An A C voltage amplifier is used to increase this voltage to an amount suitable to deflect the beam of a cathode ray tube. The amplified unbalance of the strain gage is applied to the vertical plates of a cathode ray tube. In order to record the transient pressure during a reaction, a time base generator is used to sweep the cathode-ray beam across the tube screen. An accurately timed pulse generator is employed to make timing marks on the cathode-ray trace.

The components of the pressure measuring system are shown in a block diagram in Fig. 6. The oscilloscope is a Du Mont, Type 274. The output of the time base generator is applied to the horizontal plates of the oscilloscope. The time base generator supplies an

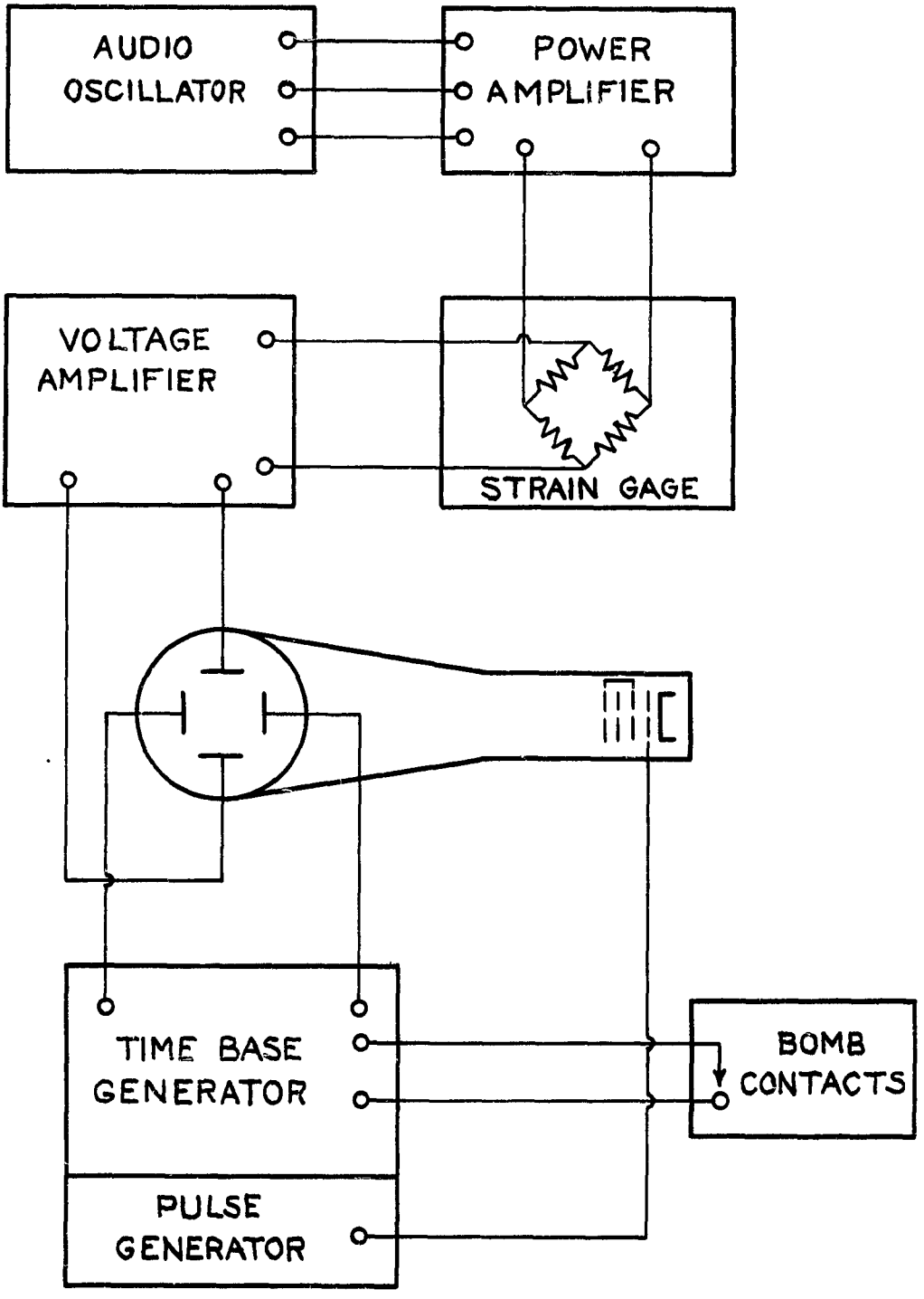

Fig. 6. Block Diagram of Transient Pressure Measuring System.

approximately linear sweep to the cathode-ray beam. The sweep is triggered by the closing of the bomb contacts located in the pneumatic injector. The pulse generator supplies sharp pulses occurring at an accurately known frequency to the intensity modulation electrode of the cathode-ray tube. This has the effect of blanking the cathode-ray beam at regular intervals. The ultimate pressure record is obtained by photographing the screen of the cathode-ray tube.

The audio oscillator has a range of 24 to 17,000 cycles per sec. in five overlapping ranges. Excellent amplitude stability is obtained because of the thermistor control network that is incorporated into the oscillator.

The power amplifier employs two 6V6 tubes in a conventional class AB_1 push-pull circuit capable of delivering about 10 watts of audio power. This is an ample reserve of power to avoid distortion since the Statham gages require a power input of only 0.6 watt. The amplifier is terminated in a 500 ohm line to match the input resistance of the Statham gages. The amplifier output is permanently connected to a panel voltmeter, the dial of which has 25 arbitrary voltage units. The meter is set to read 20 units when the voltage output of the amplifier is the correct value (ca. 10 volts) to supply the strain gage. Before each experiment the output voltage is adjusted to twenty units to ensure the reproducibility of the pressure calibration. The power amplifier circuit also has provision for the external balancing of the bridge contained within the strain gage. The bridge must be balanced both resistively and capacitively.

The voltage amplifier is stabilized by large amounts of negative feed-back. The gain of such amplifiers is almost completely unchanged by small fluctuations of the power supply voltage and by changes in

tube characteristics. The amplifier has five gain ranges varying from 1800 to 12000. The full scale output of the strain gages was estimated to be 20 millivolts RMS. At a gain of 1800, this provided 36 volts RMS with which to deflect the cathode-ray beam. The amplitude of the oscilloscope trace depends not upon the RMS voltage but upon the peak to peak voltage. Thirty-six volts RMS is equivalent to 102 volts peak to peak. The deflection sensitivity of the cathode-ray tube used in the Du Mont instrument is about 30 volts per inch so that the full scale amplitude was expected to be almost 3.5 inches.

The time base generator and the pulse generator have also been described by McKinney; however, it was found necessary to make several changes in these circuits. A schematic diagram of the revised time base generator, pulse generator and some of the switching circuits are shown in Fig. 7. A discussion of the revised switching circuits will be given in a later section.

For the normal operation of the time base generator and the pulse generator switch SW-1 must be in position III and switch SW-2 in position B or C. The closing of the bomb contacts provides a sharp positive pulse to the condenser C5. This causes the thyratron V3 to fire decreasing the plate voltage to a low value in a few microseconds. A sudden deflection of the cathode-ray beam across the tube screen results. The original plate voltage of V3 is gradually restored. The rate of rise of the plate voltage is determined by the RC product selected by switches SW-3 and SW-4. The rise of the plate voltage causes the cathode-ray beam to return to its original position at a predetermined rate. The time range with C11 is about 0.01 to 0.30 second, with C6 it is about 0.09 to 0.8 second, and with C7 it is about 0.6 to 11 seconds.

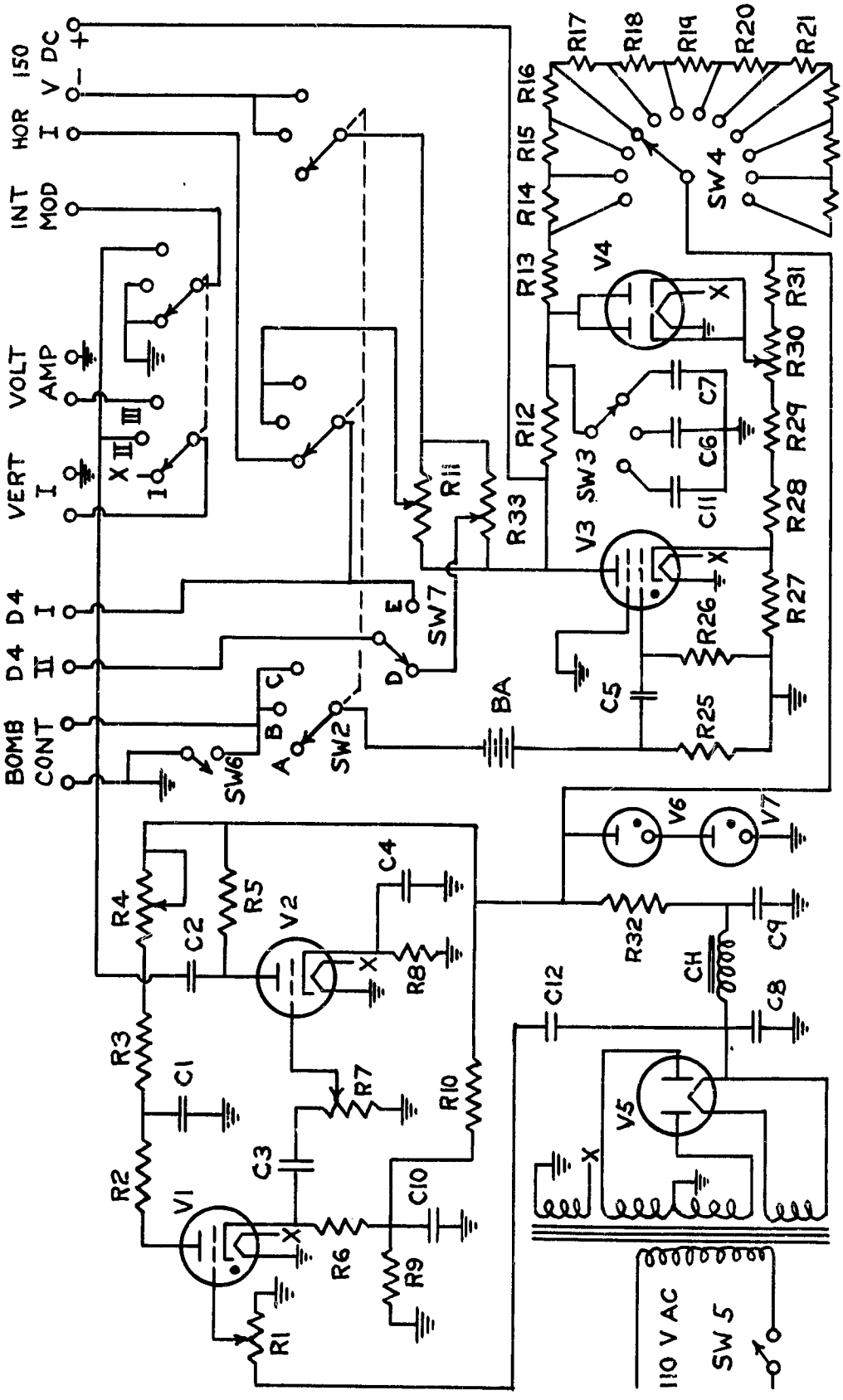

Fig. 7. Schematic Diagram of Time Base Generator, Pulse Generator and Switching Circuits.
(See Table 6)

Table 6. Circuit Constants for Time Base Generator, Pulse Generator and Switching Circuits (See Fig. 7)

Component	Circuit constant
R1, R11, R33	100K potentiometer
R2	500 ohms
R3	900K
R4	3M potentiometer
R5	50K
R6	1500 ohms
R7	500K potentiometer
R8	2K
R9	600 ohms
R10	30K
R12	1800 ohms
R13-R24	1M
R25	4M
R26	100K
R27	1100 ohms
R28	5K
R29	10K
R30	5K potentiometer, wire wound
R31	10K
R32	5K
BA	90 V
T	Power transformer, 110 V primary, secondaries: 700 V ct, 5 V, 6.3 V

Component	Circuit constant
C1, C2, C3, C6, C12	0.1 mfd, 400 V
C4	10 mfd, 25 V, electrolytic
C5	0.2 mfd, 400 V
C7	1.0 mfd, 400 V
C8, C9	8-8 mfd, 400 V, dual electrolytic
C10	25 mfd, 25 V, electrolytic
C11	0.01 mfd, 400 V
V1	Type 884
V2	Type 605 GT
V3	Type 2050
V4	Type 6H6
V5	Type 5U4 G
V6, V7	Type OD3/VR 150
SW1, SW2	Lever action switch, 4 circuits, 3 positions
SW3	Selector switch, 1 circuit, 3 positions
SW4	Selector switch, 1 circuit, 12 positions
SW5	SPST Toggle switch
SW6	DPST Push button switch
SW7	SPDT Toggle switch
CH	Chokes, 15 henries

The length of the trace on the screen is controlled by R30. A 150 volt power supply located on a separate chassis and shown schematically in Fig. 8 supplies the voltage necessary to control the position of the time base on the tube screen by means of the position control R11. It will be pointed out in a later section that it is necessary to provide two oscilloscopes with an identical time base. This could be done by simply connecting the plate of V3 through R11 to the horizontal deflection plates D4 of two oscilloscopes; however, it is desirable to control the position of the time base on the oscilloscopes independently. This is accomplished through the use of a separate position control R33.

The original circuit described by McKinney employed a different network to provide the positive pulse to C5 to initiate the time base. With the original circuit the frame of the pneumatic injector and hence the entire reactor had a positive potential of 50 volts with respect to the chassis ground during the course of a run. With the present circuit so long as bomb contact A is connected to the injector frame, the entire reactor is electrically grounded at all times. It was believed that this would contribute toward decreasing the pick-up of random electrical disturbances. The original circuit had only two time base ranges; the third and most rapid one was found to be necessary for the present study. In the original circuit a 135 volt battery pack was used to provide the positioning voltage. The batteries became rapidly exhausted in this application so that a more convenient line operated power supply was built.

The pulse generator, shown in the upper left hand corner of Fig. 7, serves to provide accurate timing of the pressure trace by blanking the cathode-ray beam at regular intervals. The unit is essentially a relaxation oscillator producing sharp negative pulses. The frequency

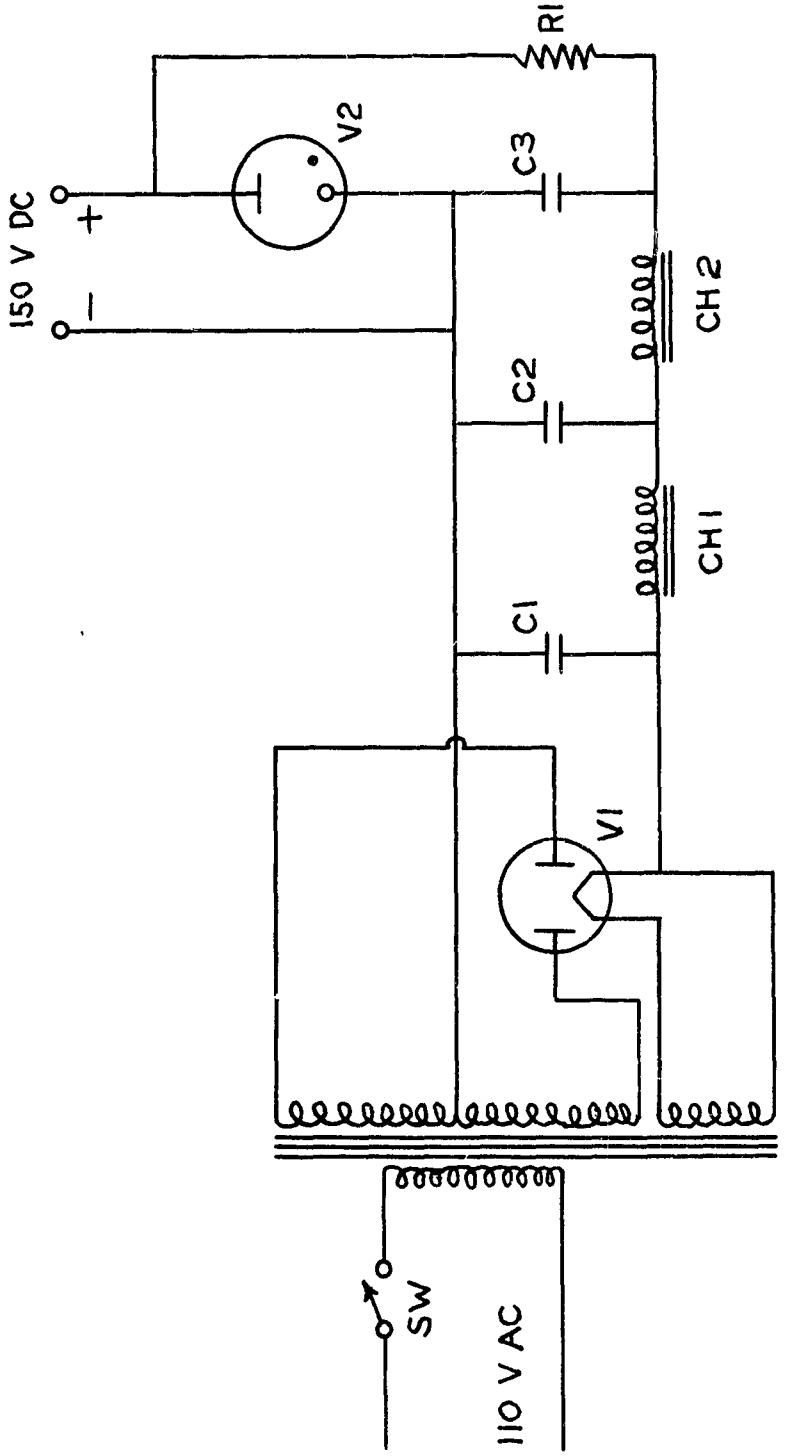

Fig. 8. Schematic Diagram of Auxiliary Power Supply. (See Table 7)

Table 7. Circuit Constants for Auxiliary Power Supply
(See Fig. 8)

Component	Circuit constant
R1	12 K, 4 watt
C1, C2, C3	8-8-8 mfd, triple electrolytic
V1	Type 5Y3 GT
V2	Type OD3/VR 150
T	Power transformer, 110 V primary, secondaries: 480 V ct, 5 V, 6.3 V
CH1, CH2	Filter choke, 35 henries
SW	SPST toggle switch

of repetition of the pulses is accurately controlled at a value of 120/n cycles per second, where n is a small integer, by synchronization with the 120 cycle component of the rectified line voltage. With the synchronization control R1 turned off, the oscillation frequency can be controlled with R4. Setting R4 to produce approximately the desired frequency, the synchronization control R1 may be adjusted to "lock in" the desired frequency. The amplitude of the pulses is controlled by R7. The frequency values that can be obtained with the unit are 120, 60 and 30 cycles per second. The output of the pulse generator is supplied directly to the intensity modulation electrode of the cathode-ray tube. The sharp negative pulses then cause the cathode-ray beam to be blanked at the synchronized frequency. Immediately following each negative pulse, there is a slight positive voltage swing which causes a slight intensification of the cathode-ray beam, making the timing marks even more pronounced.

In the original circuit, described by McKinney, the oscillator was synchronized directly with the 60 cycle line. Frequency values of 60, 30 and 20 cycles could be obtained. Because of the faster time base to be used in this study, it was imperative to have a timing frequency of at least 120 cycles.

The final record of the oscilloscope trace is obtained by photographing the screen of the oscilloscope. The camera is a Burke and James 4 x 5 inch view camera equipped with an f4.5 lens. A shield surrounding the camera lens and the oscilloscope screen prevents stray light from entering the camera. In normal operation, the camera shutter was opened before a run and remained open until after the run. The cathode-ray tube employed for this purpose is a 5 BP11A having a blue

fluorescence that is particularly suited for photographic purposes. Eastman Kodak Super Panchro-Press, Type B film was used.

Measurement of the Final Pressure of the Product Gases

It was believed that important information might result from accurate knowledge of the final pressure of a reaction carried out in the reactors. The pressure at infinite time cannot usually be obtained from the transient pressure trace for two reasons: (1) The transient pressure can be followed only for a short time if it is desired to secure good time resolution during the early stages of a reaction. This is particularly true in the case of an explosion where the reaction products may not cool to room temperature for some time. (2) The transient pressure during the early stages of a reaction is usually quite a bit higher than the final pressure. The resulting final amplitude may be too small to allow accurate measurements. Four different methods were used to obtain final pressure data during this research.

In some of the early runs with Reactor I the final pressure was measured by a metal Bourdon gage that was permanently connected to the reactor. The gage has a range 0 to 160 lb. per sq. in. and was manufactured by the Marsh Co. In many runs, however, the final pressure was less than 10 lb. per sq. in. The Bourdon gage can give only a crude estimate of the pressure in this low range.

In later runs a mercury manometer was connected to one of the valves leading to the reactor by means of rubber tubing. The valve was opened a few seconds after reactant injection, expanding the product gases into the tubing leading to the manometer. The final pressure can then be read from the manometer; a slight correction has to be made for the increase of the gas volume.

The manometer method was not suitable for measuring the final pressures of the high energy fuel, oxidant reactions carried out in Reactor II. The final pressures were well above two atmospheres in this case. The Bourdon gage could not be used either because of the very high transient pressures incurred in the early stages of reaction. It was decided to use, instead, another strain gage. For these high energy systems, the 500 lb. strain gage had to be used for the transient pressure measurements, so that the 100 lb. gage was available. It was considered likely that a Model 555 Oscillograph manufactured by the Midwestern Geophysical Laboratory would be very suitable as the recording instrument inasmuch as that instrument was available in the laboratory. The Midwestern instrument employs a rapid response mirror galvanometer. A light beam is reflected from the galvanometer mirror and focused on a photographic strip chart. The chart moves with a continuously variable speed up to 9 inches per second. The galvanometer used in the oscillograph is a Type 102A-100; it has a current sensitivity of 0.009 milliamperes per inch and a resistance of 30 ohms. The response is stated to be flat up to 60 cycles per second. With the oscillograph, strain gage combination, it should be possible to follow pressure events in the reactor from the time that the pressure first falls into the range of the strain gage for as long a time thereafter as is desired.

The associated circuits used with the oscillograph, strain gage combination are shown in Fig. 9. The oscillograph requires 24 volts DC at 2.5 amperes in order to operate it. At first the voltage was obtained from a voltage divider across the 125 volt DC line. It was found necessary, however, to supply the current needed to run the chart drive separately from that needed to operate the other components.

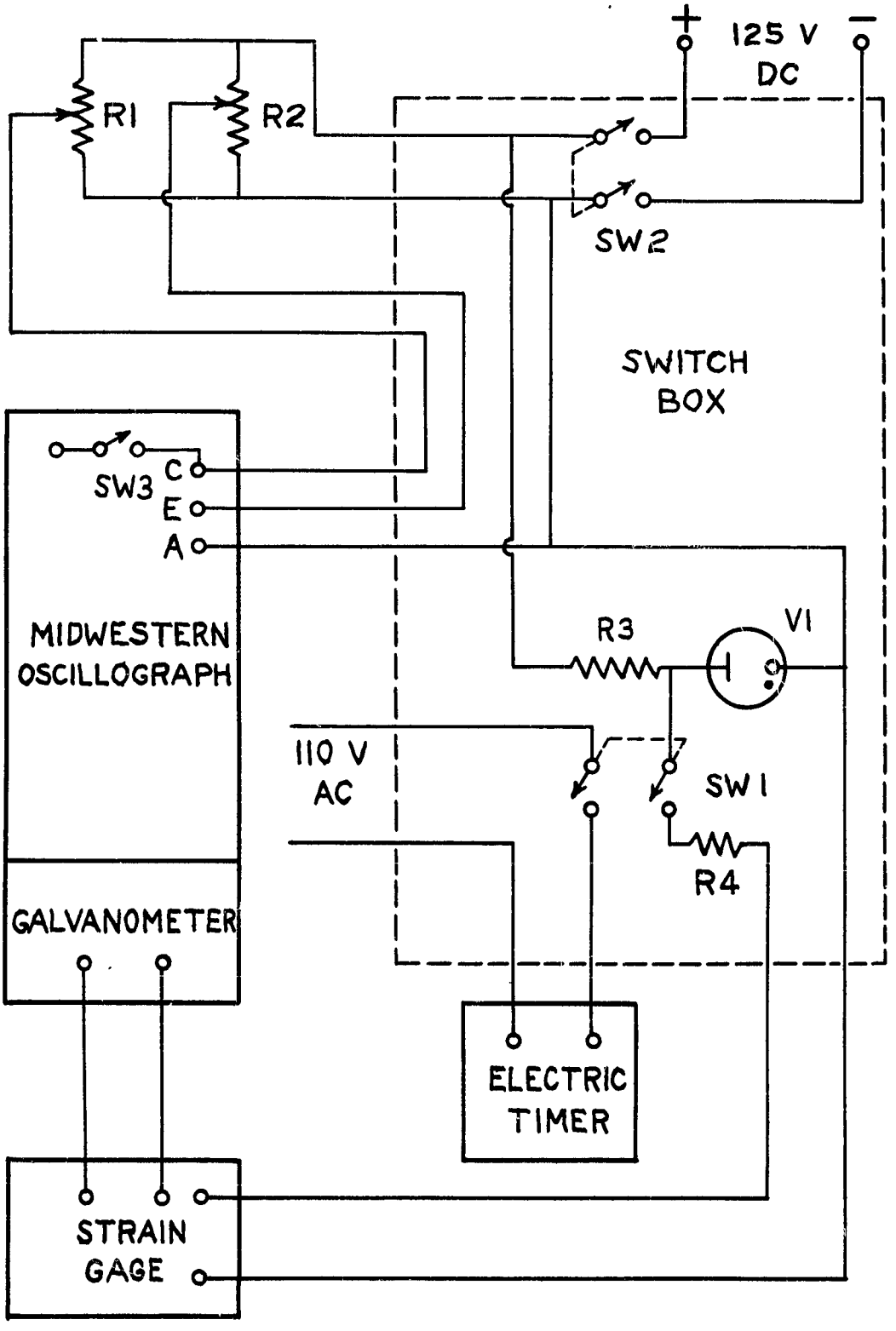

Fig. 9. Schematic Diagram of Circuits Associated with the Midwestern Oscillograph, Strain Gage Combination. (See Table 8)

Table 8. Circuit Constants for Midwestern Oscillograph, Strain Gage Combination (See Fig. 9)

Component	Circuit constant
R1	48 ohms, 2.9 A
R2	175 ohms, 1.6 A
R3	2500 ohms
R4	9300 ohms
V1	Type OA3/VR 75
SW1, SW2	DPST Toggle switches

The rheostat R1 was adjusted to supply 24 volts to the chart drive motor when it was operating, and R2 was set to supply 24 volts to the other components. In order to supply the bridge of the strain gage with a constant current, a VR-75 voltage regulator tube was connected across the DC line through R3. The voltage across the VR-75 tube is constant to within a few per cent in spite of normal line voltage variations.

The oscillograph contains a timing circuit capable of placing evenly spaced timing lines across the entire width of the strip chart. The circuit may be adjusted to a frequency of 10 lines per second or 100 lines per second. The lines represent equal time intervals; however, the day to day stability of the circuit was not satisfactory. In order to provide a time calibration, an electric timer was included in the circuit. By closing SW-1 the bridge of the strain gage was energized simultaneously with the starting of the electric timer. The amplitude of the pressure trace was set at approximately three inches on the strip chart for the full scale output of the strain gage by adjusting R4. With this setting, the voltage across the bridge of the strain gage was about 5 volts. The maximum allowable voltage for the strain gage is 17 volts so that a wide safety factor was obtained.

The procedure to obtain a pressure vs. time record is as follows: The unit is turned on by means of SW-2 and allowed to warm up. The strip chart motor is then started by means of SW-3 located on the panel of the Midwestern Instrument. After allowing a few seconds for the chart motor to reach a constant speed, SW-1 is closed actuating the electric timer and causing a slight break of the galvanometer trace as the bridge of the strain gage is energized. The pneumatic injector is then fired causing the reaction to occur. After a suitable time SW-1

is opened, the timer stops, and the trace returns to its original position. Counting the number of lines corresponding to the time read on the electric timer gives a calibration of the frequency of the timing lines for every run. The length of time of the record is controlled essentially by the length of strip chart one wants to handle. The chart is Kodak Linagraph Paper, #809, Spec. #1 and must be removed from the oscillograph cartridge in complete darkness. The paper is developed 4 minutes in a 1:1 solution of Kodak Dektol Developer.

If pressure measurements are required to extend for more than a minute, it is preferable to simply restart the chart drive and close SW-1 recording for a few seconds only. Timing in this case may be effected with a stopwatch or another electric timer.

In many of the fuel-oxidant reactions studied by means of the Midwestern instrument, the final pressure was observed to decrease with time indefinitely indicating the presence of a leak in the reactor (Reactor II). The leak was undoubtedly through the piston gaskets. It was found to be very difficult to seal the reactant cylinders against the rather high final pressures encountered in the hydrazine-nitric acid reaction. It was believed that far less product gas would be lost if the gases were expanded into a very large volume one or two seconds after injection. This was accomplished through the use of a large glass bulb system, the volume of which totalled about 5 liters. The bulb system was connected to a mercury manometer and to the valve leading to the reactor. Immediately after injection the valve was opened and the product gases expanded by a factor of about seventeen. This lowered the pressure so that it could easily be read on the manometer once the pressure fell to its final value. The pressure that the piston gaskets

had to withstand for extended periods of time was thereby reduced from up to 5 atmospheres to at most 25 cm. Hg. It is very likely that no leak occurs through the piston gaskets before about 10 seconds after injection because of the fact that the driving gas pressure is normally not released until about this time. The force exerted by the driving gas on the pistons should hold them tightly seated for this period of time.

Although the leakage problem was eventually solved through the use of more efficient gaskets, the expansion final pressure method was used to obtain most of the final pressure data reported in this study.

Measurement of Light Emission

The presence and time of occurrence of an ignition can be determined reliably by light emission measurements as well as by pressure rise measurements. Most of the previous ignition delay studies have employed light emission measurements exclusively in order to sense an ignition. It was believed, therefore, that provisions had to be made to include light emission measurements in the present study.

Many circuits are described in the literature for the rapid recording of light intensity changes. In most of these the oscilloscope is used as the recording instrument, the final record being obtained by photographing the screen of the oscilloscope. In all of these circuits, the oscilloscope trace consists of a continuous line. The vertical deflection of the line from its original position is the measure of light intensity. It was pointed out by McKinney[2] in connection with the design of the pressure recording system that single line traces are very susceptible to random electrical disturbances; however, if the signal to be recorded can be caused to modulate a

high frequency carrier wave, the effect of many of the disturbances can be removed. This point is demonstrated by the pressure traces obtained by McKinney. In many of the traces, the envelope was found to drift randomly about the x-axis of the tube screen. The pressure is, however, proportional to the amplitude of the envelope so that this drifting has no effect on the measurements. No entirely suitable circuit could be found in the literature in which the photoelectric signal is made to modulate an audio frequency carrier wave.

Since a rather bright flash was expected to result from the ignitions under study, it was believed that a phototube rather than a photomultiplyer tube could be used as the sensing device. In the usual application of a vacuum phototube, a rather high resistance is placed in series with it. A DC potential of anywhere from ten to several hundred volts is placed across the phototube, resistor combination. On illumination, current can pass through the phototube and hence through the resistor. This current develops a voltage drop according to Ohm's law. A larger value of resistance leads to a larger voltage drop and thus to a more sensitive circuit. There is, however, an upper limit to the resistance that can be used because of the need for rapid response. The resistance in combination with any stray capacitance that might exist between the two leads to the resistance forms a low pass filter section. There is necessarily a large stray capacitance in the present case because of the fact that the actual phototube cannot be located on the chassis with the remainder of the circuit elements. The time constant of such a filter section is equal to RC. It was considered likely that the stray capacitance did not exceed 0.001 microfarad. A phototube load resistor as high as 3 megohms

would then yield a time constant of about 3 msec. This means that for an instantaneous rise of the light intensity to a definite value, the voltage drop would rise to only about two-thirds of the final value in 3 msec. The start of the rise would, however, coincide with the increase in light intensity.

Three different circuits were used in the present study in order to amplify the photocurrent to a value suitable to deflect the beam of a cathode-ray tube. The first one to be used is shown schematically in Fig. 10 and will be referred to as Photocircuit I. The power supply to operate the circuit is located on a separate chassis along with a voltmeter to be used in connection with the circuit. The power supply and meter circuits are shown in Fig. 11. V1 is a 1P39 vacuum phototube. It is apparent from Fig. 10 that several different phototube load resistors can be chosen by means of SW1, the highest of which has a value of 3.3 megohms. An AC voltage is applied to the phototube, load resistor combination instead of a DC potential. The AC signal is taken from the output of the power amplifier and isolated from it by transformer T. The AC signal from the phototube load resistor is then amplified by one section of V2 and supplied to the vertical plates of the cathode-ray tube. When the phototube is not illuminated there should be no signal at the phototube cathode and the cathode-ray tube trace should be a line. It was found, however, that there was sufficient stray capacitance, shunting the phototube, to give a large signal even when the phototube was not illuminated. In order to avoid a large "dark signal", provisions were made to increase the bias of V2 so that the capacitance current would not be amplified. This is effected by means of R8 and R10. During illumination current flows through the load

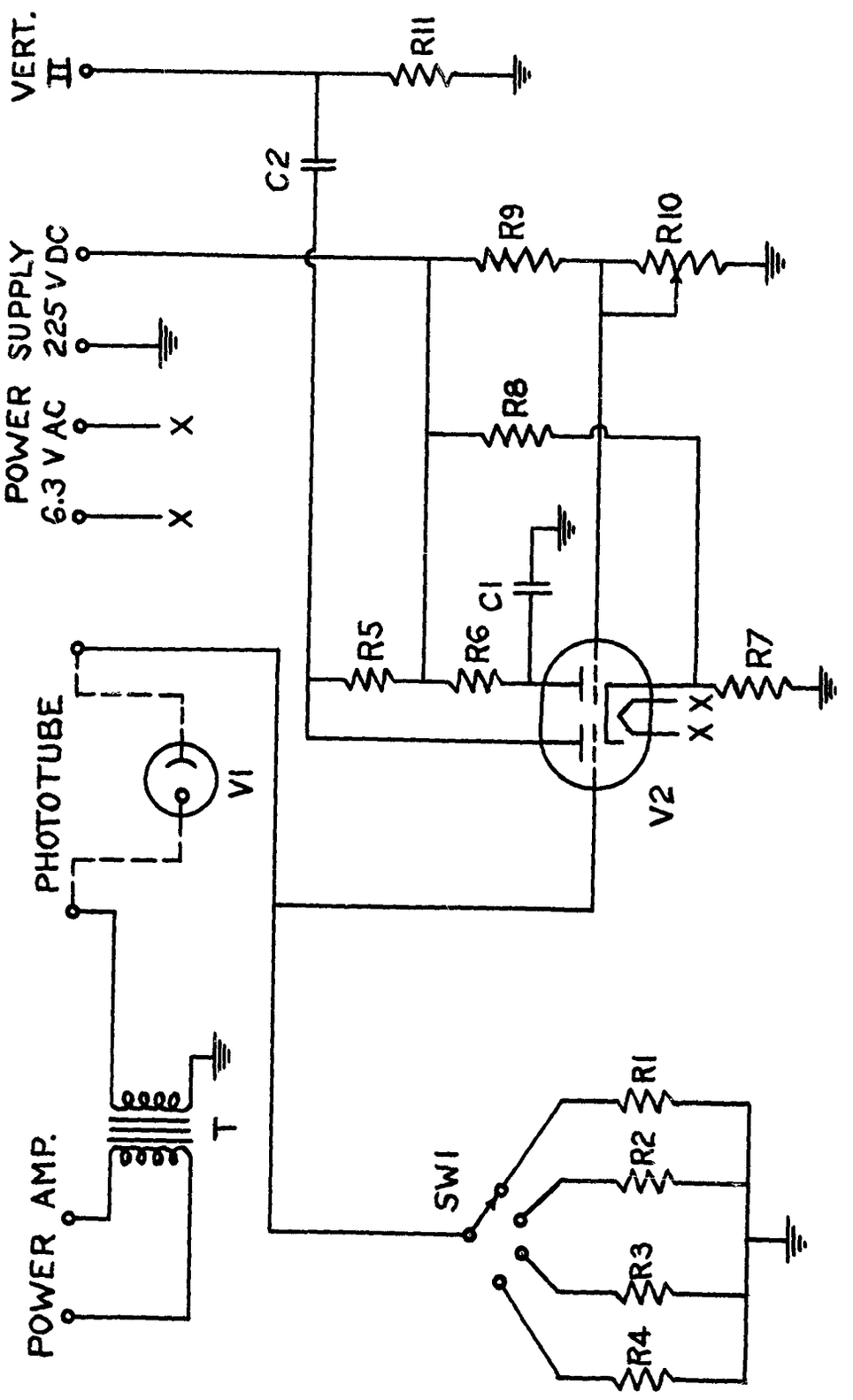

Fig. 10. Schematic Diagram of Photocircuit I. (See Table 9)

Table 9. Circuit Constants for Photocircuit I (See Fig. 10)

Component	Circuit constant
R1	3.3M
R2	1M
R3	470K
R4	270K
R5, R6	120K
R7	950 ohms
R8	60K
R9	300K
R10	10K potentiometer
R11	100K
C1	0.04 mfd, 400 V
C2	0.002 mfd, 400 V
V1	Type 1P39
V2	Type 6SC7
T	Audio interstage transformer, ratio 3:1, primary impedance 10,000 ohms
SW1	Selector switch, 1 circuit, 8 positions

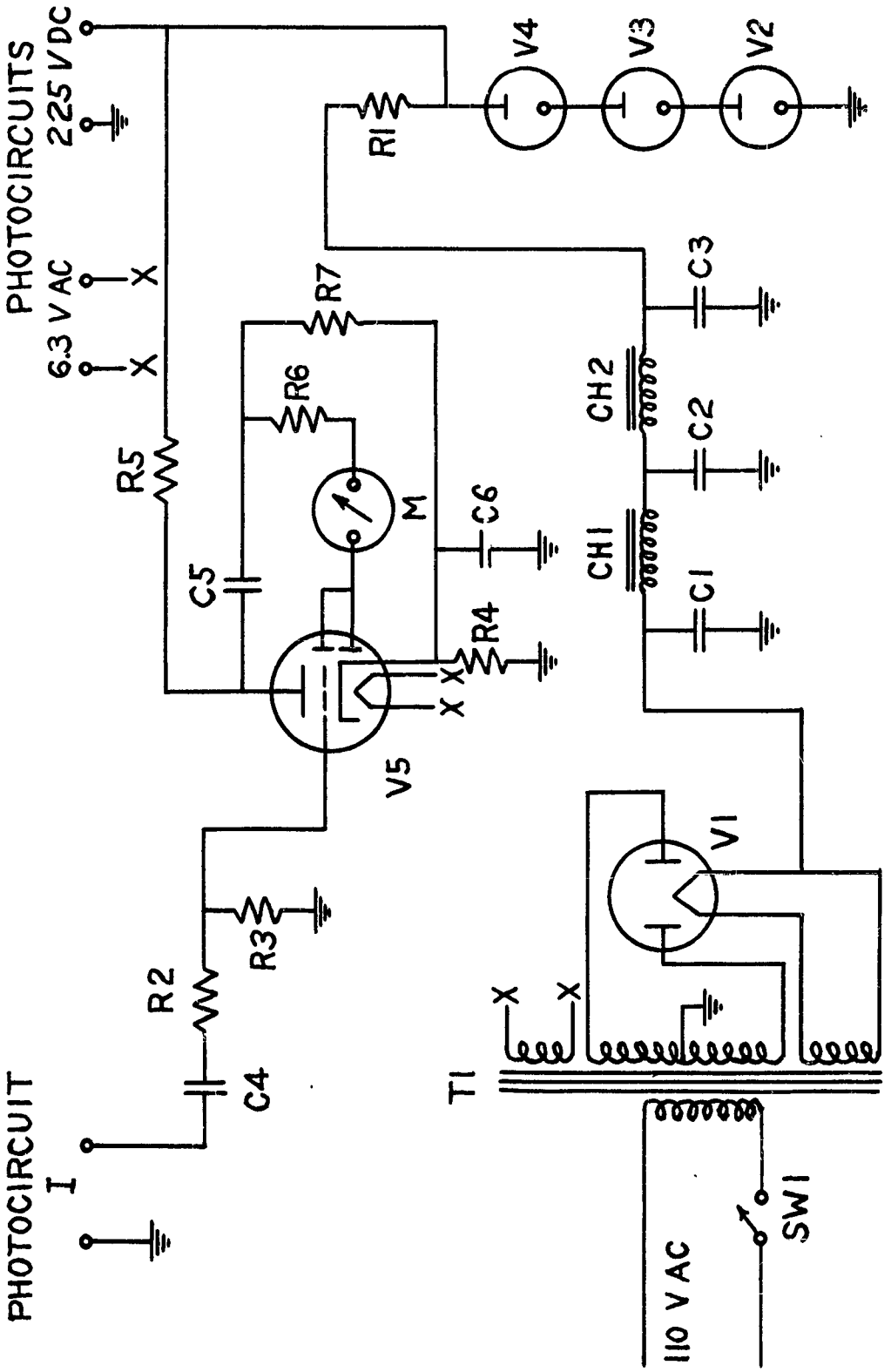

Fig. 11. Schematic Diagram of Power Supply and Meter Circuit. (See Table 10)

Table 10. Circuit Constants for Power Supply and Output Meter (See Fig. 11)

Component	Circuit constant
R1	6300 ohms, 20 watts
R2, R3	1M
R4	1900 ohms
R5	150K
R6	75K
R7	200K
C1, C2	8-8 mfd, 475 V, dual electrolytic
C3	15 mfd, 400 V, electrolytic
C4, C5	0.1 mfd, 600 V
C6	40 mfd, 25 V, electrolytic
V1	Type 5Y3 GT
V2, V3, V4	Type 0A3/VR 75
V5	Type 6Q7
T1	Power transformer, primary: 110 V, secondaries: 480 V ct, 5 V, 6.3 V
CH1, CH2	Filter chokes, 30 henries
M	2 inch panel meter, 0 - 200 microamperes
SW1	SPST, Toggle switch

resistor during the positive half-cycle of the voltage at the phototube anode. The amplitude of the output from V2 is then a measure of the light intensity.

The amplitude of the signal is not linear with the photocurrent because the amplification by tube V2 decreases only gradually near the cut-off point. In order to avoid biasing the tube too much, the output signal is fed to the meter circuit shown in Fig. 11 as well as to the oscilloscope. The meter is essentially an AC voltmeter having a range 0-10 volts RMS. Ten volts will cause a deflection of about one-half scale. Above 10 volts the meter circuit becomes very insensitive, 100 volts causing a deflection of only about three-fourths scale so that the meter cannot be overloaded. Before each measurement the "dark signal" is set at 20 units on the meter (ca. 0.9 volts) by adjusting R10 so that a reproducible bias is obtained.

It was found that Photocircuit I did not respond to low levels of illumination. At higher levels, the linear operating region of the amplifier tube was reached and a linear response was obtained. At very high levels, the grid of the amplifier was overloaded and a constant amplitude resulted.

A second photocircuit was built in order to secure linear response at all levels of light intensity. Photocircuit II is shown schematically in Fig. 12; it is also powered by the power supply shown in Fig. 11. In this circuit a square wave signal instead of a sine wave signal is supplied to the phototube anode. The sine wave signal from the power amplifier is greatly amplified by V1. The positive and negative peaks are clipped by the diode V2 resulting in a square wave signal having an amplitude of 45 volts peak to peak. The phototube load resistor R8

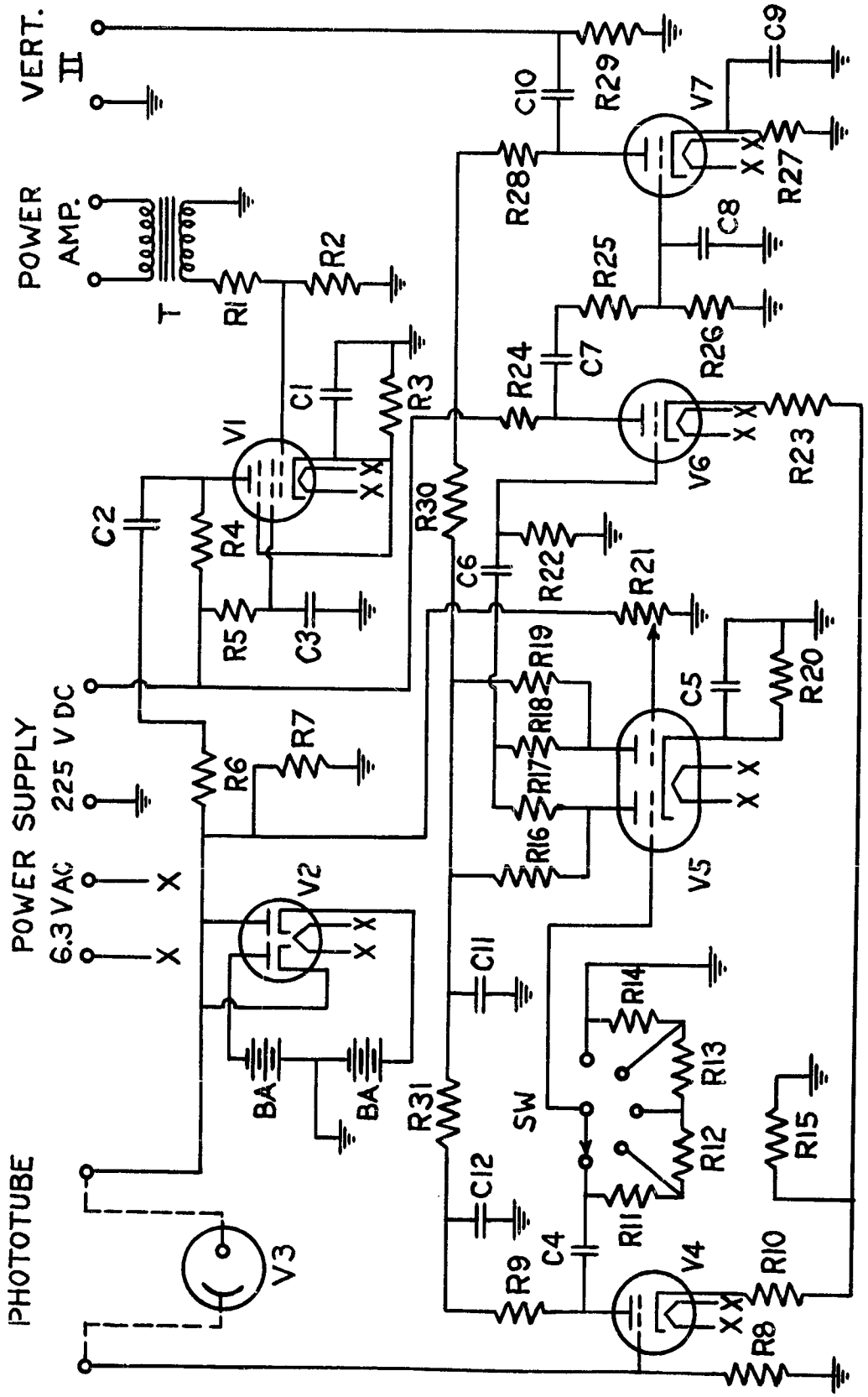

Fig. 12. Schematic Diagram of Photocircuit II. (See Table 11)

Table 11. Circuit Constants for Photocircuit II (See Fig. 12)

Component	Circuit constant
R1, R5, R7, R17, R18, R22, R26	1M
R2	4.7M
R3, R27	1K
R4, R16, R19	270K
R6, R24	100K
R8	15K
R9	330K
R10	1500 ohms
R11	820K
R12	150K
R13	27K
R14	6.8K
R15	150 ohms
R20	2200 ohms
R21	1M potentiometer
R23	3300 ohms
R25	220K
R28	47K
R29	470K

Component	Circuit constant
C1, C5, C9	40 mfd, 25 V, electrolytic
C2, C4, C6, C7	0.1 mfd, 600 V
C3, C10	0.25 mfd, 600 V
C8	100 mmfd
C11	10 mfd, 600 V, electrolytic
C12	40 mfd, 250 V, electrolytic
V1	Type 6SJ7
V2	Type 6H6
V3	Type 1P39
V4	Type 12AX7
V5	Type 6SC7
V6, V7	Type 6J5
T	Audio inter-stage transformer, ratio 3:1, primary impedance 10,000 ohms
SW	Selector switch, 1 circuit, 8 positions
BA	22½ V batteries

has a value of only 15,000 ohms so that the response should be essentially instantaneous. The capacitance current flowing through R8 is in the form of sharp pulses occurring during the reversal of polarity of the square wave signal. Tubes V4, V5 and V6 serve to amplify the signal appearing at the phototube cathode. The amplifier circuit has large amounts of negative feed-back and is similar in design to the voltage amplifier used in connection with the pressure measuring system. The amplification is limited by the interference of the sharp pulses with the normal operation of the tubes. The maximum gain was determined experimentally; it was found to be preferable to add a final triode stage V7 to the three stages V4, V5 and V6.

Because of the pulses, the light intensity is no longer proportional to the amplitude of the output signal from Photocircuit II. The "dark signal" appearing on the screen of the cathode-ray tube is essentially a line having sharp vertical pulses. During illumination, the signal appears to be two parallel lines, each line is broken into a series of dots by the pulses. The vertical distance between the two lines should be exactly proportional to the photocurrent and hence to the light intensity since each amplifier tube is biased to operate on the linear portion of the tube characteristic. The two lines correspond to the peaks of the square wave signal developed across the phototube load resistor. The appearance of a square wave is not obtained for two reasons: (1) The peaks are distorted because of the shunting capacitance across the phototube. (2) The vertical motion of the cathode-ray beam is so rapid during the reversal of polarity that the vertical retrace lines cannot be seen, giving the impression that the two horizontal lines are not connected.

Tube V5 can be used to mix the signal from the phototube cathode with the original square wave signal from diode V2. This allows any steady photocurrent to be balanced out. The initial condition of the phototube corresponded to complete darkness in all experiments carried out in the reactors so that no photocurrent had to be balanced out (R21 was adjusted so that the one grid of V5 was always grounded). The circuit could, however, be used for the static measurement of light intensity by calibrating the position of R21; the oscilloscope could then be used as a null detector.

The sensitivity of Photocircuit II can be reduced by adjusting switch SW. There are four gain ranges available. The feedback feature of the amplifier is lost when SW is not in the position of highest gain; however, no other satisfactory method could be found to provide separate gain ranges. The light emission in some of the reactions studied was so great that even the lowest gain range of Photocircuit II gave a signal that was too large. In order to decrease the intensity of light impinging on the phototube, a brass orifice was constructed to fit over the Plexiglass window. The diameter of the effective window area was thereby reduced from about 0.5 inch to about 0.3 inch.

The power amplifier, described in an earlier section, supplies the carrier wave to both Photocircuit I and II as well as to the pressure measuring system. This simplifies the problem of relative timing between a simultaneous pressure and light emission measurement.

Photocircuit II has a slight practical disadvantage because of the fact that the amplitude of the oscilloscope trace is strictly linear with the intensity of illumination of the phototube. It is often necessary to make several runs of the same reaction before the

correct gain range of the amplifier is chosen so that neither too small nor too large a deflection is obtained. Photocircuit III was designed and built to use with reactions where only the first moment of luminoscity is to be recorded. Photocircuit III is shown schematically in Fig. 13. It is also powered by the power supply shown in Fig. 11. The phototube anode is supplied by a 45 volt battery. The phototube load resistor R9 has a value of 100,000 ohms insuring both rapid response and good sensitivity. The signal from the phototube cathode is amplified by a three stage AC amplifier having large amounts of negative feedback. The circuit is almost identical in design to the voltage amplifier used in the pressure measuring system. The sensitivity of the amplifier circuit is controlled by the selection of the feedback resistor by means of switch SW. The output of the circuit is applied to the vertical plates of the oscilloscope just as in the case of other photocircuits. The circuit provides only a single line trace. The gain, however, is very high (when SW is in positions 1, 2 or 3) compared to Photocircuits I and II. At the moment of light emission, the amplifier is immediately overloaded and the cathode-ray beam is violently deflected. Because of the overloaded condition of the circuit, the output may show several low frequency oscillations and require some time to return to its original position once the light emission has ceased. The circuit is thus useful when only the first moment of luminoscity is of interest.

In order to allow the simultaneous recording of both pressure and light emission, it is clearly necessary to employ two oscilloscopes and two cameras. The oscilloscope described in connection with the pressure measuring system will be referred to as Oscilloscope I. The oscilloscope that was used to record light emission measurements was

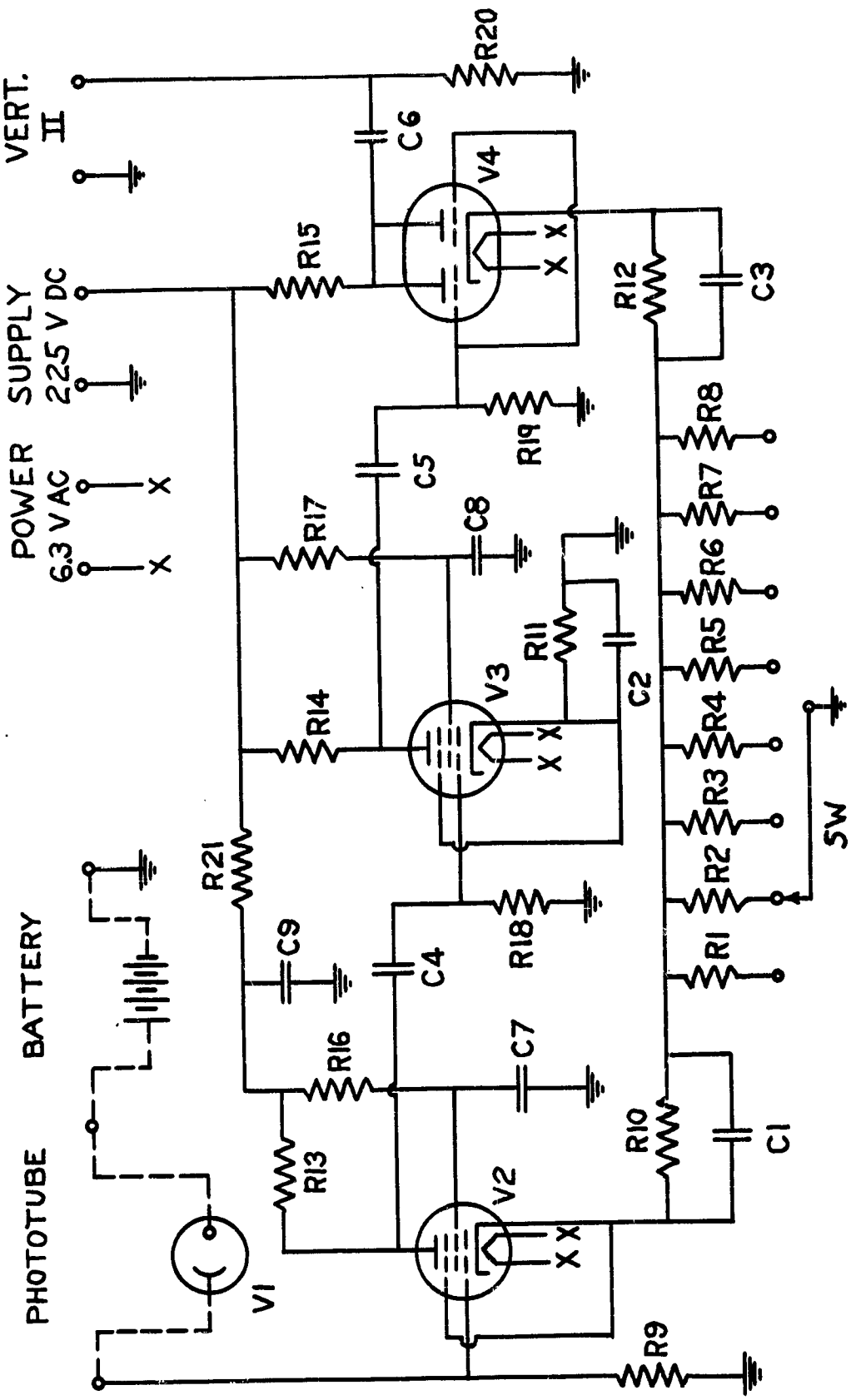

Fig. 13. Schematic Diagram of Photocircuit III. (See Table 12)

Table 12. Circuit Constants for Photocircuit III (See Fig. 13)

Component	Circuit constant	Component	Circuit constant
R1	1K	C1, C2, C3	25 mfd, 25 V, electrolytic
R2	220 ohms	C4, C5, C6	0.1 mfd, 400 V
R3	68 ohms	C7	0.2 mfd, 600 V
R4	22 ohms	C8	0.1 mfd, 600 V
R5	10 ohms	C9	8 mfd, 450 V, electrolytic
R6	3.3 ohms	V1	Type 1P39
R7	1 ohm	V2	Type 6SJ7
R8	0 ohms	V3	Type 6SK7
R9	100K	V4	Type 6SC7
R10, R11, R12	1K	SW	Selector switch, 1 circuit, 8 positions
R13, R14	220K		
R15	100K		
R16	1.5M		
R17, R18	1M		
R19	1M		
R20	650K		
R21	10K		

built during the course of the study. A schematic diagram of Oscilloscope II is shown in Fig. 14. The circuit is of conventional design; R11 controls the vertical position of the beam, R8 is the focus control, and R10 is the intensity control. The horizontal deflection plate D4 is connected to the time base generator in the manner described previously. The intensity modulation electrode of both oscilloscopes are permanently connected to each other so that the timing marks produced by the pulse generator register simultaneously on both oscilloscopes. Another camera identical to the one described previously was purchased and used in conjunction with Oscilloscope II.

Measurement of Injection Rate

The methods used to measure the injection rate in the case of Reactor I were described by McKinney.[3] In the case of Reactor II it was considered imperative to devise a method that would be capable of measuring the exact time of the start and finish of injection. The time at which the injection begins must be accurately known in order to measure the ignition delay time. The time at which the injection is completed must be known in order to verify the mixing efficiency. The method finally employed gives the time corresponding to a number of positions of the piston system during the period of descent.

The method involves the use of a serrated brass rod. The rod is three-sixteenths inch in diameter and fits freely into a hole in the top of either cylinder block. The rod is attached loosely to the top of the two smaller pistons so that the rod descends at the same rate as the piston system during injection. A strong light beam is passed through a hole perpendicular to the rod. The light transmitted through the rod shines on a phototube. As the rod descends the light

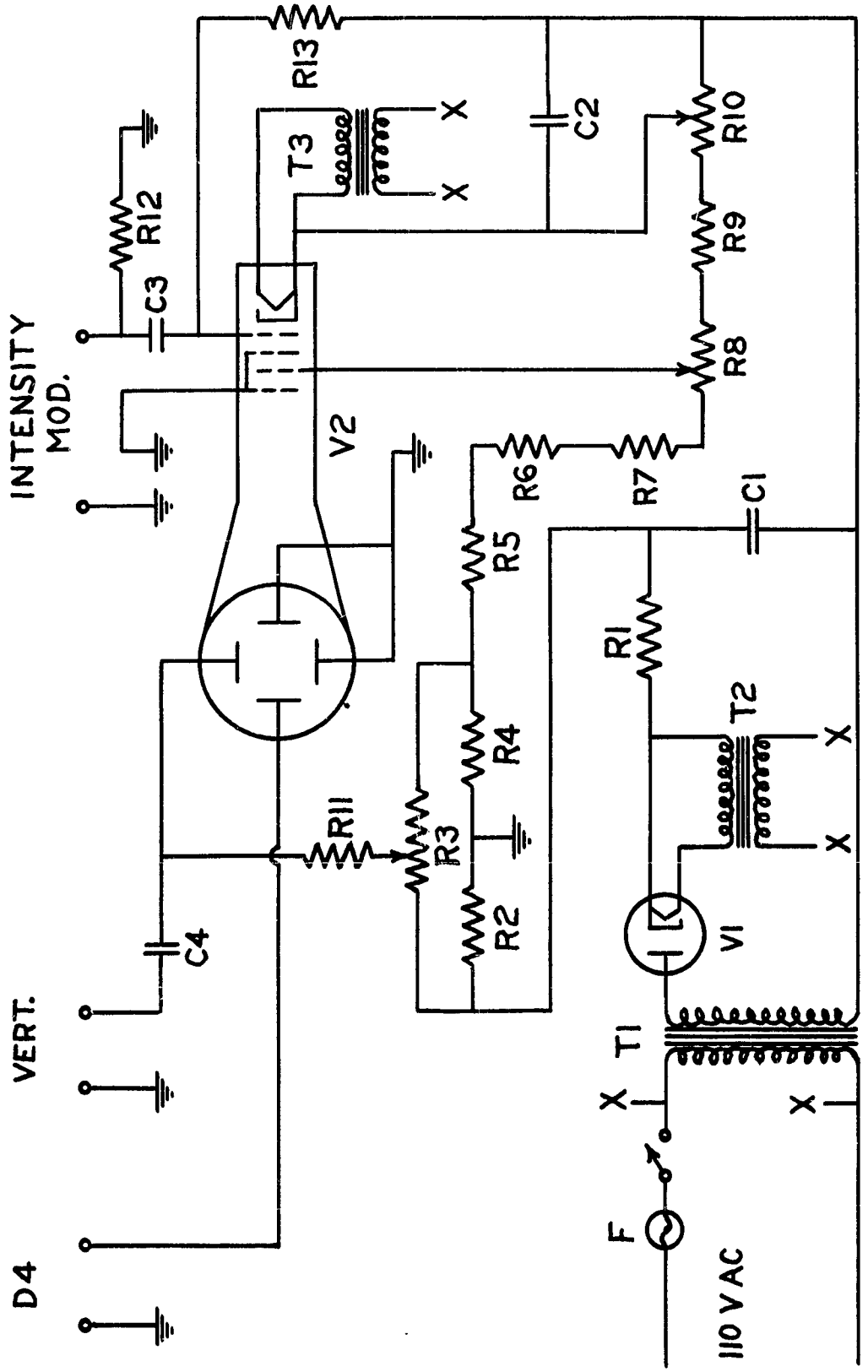

Fig. 14. Schematic Diagram of Oscilloscope II. (See Table 13)

Table 13. Circuit Constants for Oscilloscope II (See Fig. 14)

Component	Circuit constant	Component	Circuit constant
R1, R2	120K	C1	1 mfd, 3000 V
R3	1M potentiometer	C2	0.5 mfd, 600 V
R4, R7, R12	470K	C3	0.01 mfd, 3000 V
		C4	0.1 mfd, 600 V
R5, R6, R9	220K	V1	Type 2X2 A
R8	250K potentiometer	V2	Type 5BP11A
R10	100K potentiometer	T1	Power transformer, primary 110 V, secondary 1000 V
R11	5M		
R13	1M	T2	Filament transformer primary 110 V, secondary 2.5 V
		T3	Filament transformer primary 110 V, secondary 6.3 V

beam is chopped by the serrations on the rod giving rise to a rapidly alternating light intensity at the phototube.

A typical experimental arrangement for the measurement of the injection rate is shown in Fig. 15. The light source A is a 150 watt reflector spot bulb. The light is collected just ahead of the serrated rod B by a ground glass screen in the form of a glass tube C tapered to about 0.10 inch diameter and ground flat. The transmitted light shines through a wooden adaptor D into the brass container E in which the phototube is mounted. The rod B is loosely attached to a brass plate F. During injection, the plate is secured between the driving piston and the two smaller pistons so that the rod cannot descend ahead of the pistons.

The rod pictured in Fig. 15 has five serrations per inch. Rods having four per inch and five per seven-eighths inch were also used. The rods were prepared on a metal working lathe. The pitch of the serrations were cut to the desired dimensions accurately to within a few thousandths of an inch. Rods made of Plexiglass and painted with black stripes were also used to measure the injection rate. These rods were also prepared accurately on the lathe. They were found to be very susceptible to damage although they transmit a much higher fraction of the incident light intensity.

Photocircuit III shown in Fig. 13 was used for the measurement of injection rate. The intensity of the light transmitted by the descending rod was much smaller than that emitted by the explosions under study so that the circuit was at no time overloaded. The oscilloscope trace is a single line showing oscillations corresponding to the changing light intensity. Some of the preliminary measurements were

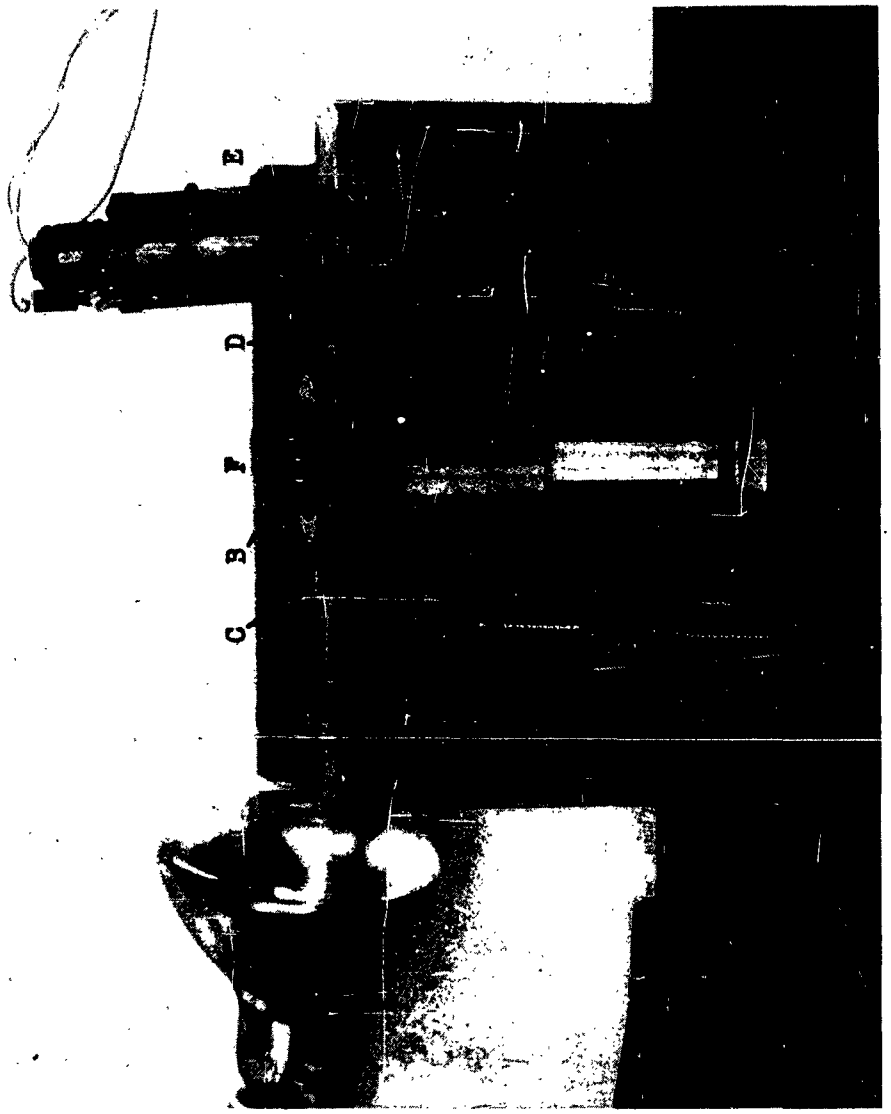

Fig. 15. Apparatus for Measurement of Injection Rate.

made with a single tube, battery operated preamplifier connected between the phototube and Photocircuit III. In other preliminary experiments other trial amplifier circuits were employed. The success of a given measurement can, however, be evaluated by the resulting trace. If the observed oscillation pattern agrees with that expected from the known pitch of the serrations, the stroke of the piston system, and the initial position of the rod relative to the light beam; there can be little doubt that the oscillations are actually due to the changing light intensity. All of the important data, however, were obtained with Photocircuit III just as it is shown in Fig. 13.

The time corresponding to each peak on the oscilloscope trace can be obtained by comparing the trace to a pressure trace recorded simultaneously. The method will be described in detail in a later chapter.

Low Temperature Operation

A thermostatic bath was constructed to enable the study of ignitions occurring at low temperatures. The bath was constructed from an obsolete waterless cooker. The cooker is a well insulated metal tank about 10 inches in diameter and 12 inches deep. A wooden frame was built to fit entirely around the tank. An angle iron support attached to the wooden frame made it possible to mount Reactor II in the bath. The reactor is normally immersed to about the top of the cylinder block. Attached to the support is a coil made of about 20 feet of one-quarter inch copper tubing. The tubing leads to an American Instrument Co. one-thirtieth horsepower pump which is immersed in a large Dewar flask containing a mixture of trichloroethylene and dry ice chunks. The large tank is also filled with trichloroethylene.

A stirring motor is mounted over the large tank to facilitate heat transfer between the cooling coil and the reactor.

In operation, the pump circulates trichloroethylene from the trichloroethylene, dry ice mixture through the cooling coils in the bath. Temperatures as low as -60°C can be easily obtained in the bath by this method. Because of the extremely short duration of the reactions to be studied, it is necessary only to bring the reactor to the desired temperature, to maintain it manually for some time to minimize temperature gradients in the reactor parts, and to initiate the reaction.

The reactor temperature is measured by a copper-constantan thermocouple located in a hole in the cylinder block. The thermocouple is located within three-eights inch of the cylinders containing the reactants so that it should indicate accurately the initial temperature of the reactants. The metal parts of the reactor located above the cylinder block could not be immersed in the bath. Because of this, there was an unavoidable vertical temperature gradient. The temperature difference between the reactant solutions and the bath itself seldom exceeded 5°C. In effect, then, the reactants contact and mix at a temperature very nearly equal to that indicated by the thermocouple. The walls of the interior of the reactor, however, may be at a slightly lower temperature.

CHAPTER III
REACTOR OPERATION

During the course of this study, numerous tests of the performance of the apparatus were made. These tests were intended (1) to check the linearity of the transient pressure measuring system and to calibrate the strain gages, (2) to calibrate the methods used to measure the final pressure of the product gases, (3) to check the linearity of Photocircuit II, (4) to measure the injection rate, (5) to measure the rate of mixing of the reactants, and (6) to determine the response of the transient pressure measuring system.

Calibration of the Transient Pressure Measuring System

The transient pressure measuring system is composed of the power amplifier output meter, the strain gage, the voltage amplifier, the cathode-ray oscilloscope and the camera. The design of the system is such that the amplitude of the oscilloscope trace is a function of the pressure applied to the gage. For the amplitude to be directly proportional to the applied pressure, each component must have a linear response. Instead of checking the linearity of each portion of the system, the entire system was calibrated at the same time.

To make static calibrations of the transient pressure measuring system, two Bourdon-type pressure gages were used. One of these has a range of 0 to 160 lb. per sq. in. and the other has a range of 0 to 1000 lb. per sq. in. The smaller gage was calibrated on a dead-weight tester by McKinney and found to be accurate to within 2%. Both gages were recalibrated using the triple point pressure of carbon dioxide. The absolute triple point pressure of carbon dioxide is 75.2 lb. per sq. in.[33] The larger gage was also checked against the vapor pressure

of carbon dioxide at 0°C which is 505.6 lb. per sq. in.[33] Both gages were found to be within 2% accuracy as guaranteed by the manufacturer.

An apparatus was constructed to facilitate the calibration procedure. It consisted of a small steel tank connected by means of steel piping to one of the Bourdon gages, a strain gage, and a steel valve. The tank was filled with dry ice before being attached to the apparatus. For the absolute calibration of the Bourdon gages, the air had to be removed. This was done by alternately allowing some of the dry ice to vaporize and then applying a vacuum to the system. The pressure gradually rose, once the valve was finally closed. The pressure remained constant for some time when the triple point was reached. After all of the dry ice liquefied, the pressure again began to rise slowly. Calibrations of the transient pressure measuring system were also carried out directly in the reactors. In this case either dry ice or liquid nitrogen was used to generate the static pressure.

The pressure record was obtained by firing the time base and photographing the screen of the oscilloscope. Several cardboard masks were made to fit over the film in the film holders of the camera so that only a small segment of the film could be exposed at a time. A typical pressure calibration trace is shown in Fig. 16. There are eight positions on the film, each corresponding to a particular value of the static pressure. The frequency of the carrier wave was 1080 cycles per second for the trace shown in the figure. Frequencies between 1000 and 1200 cycles per second were used for all of the transient pressure measurements so that the calibration traces simulated the actual conditions of a run very closely. The amplitude of the traces were measured on the photographic negative with an accurate centimeter scale.

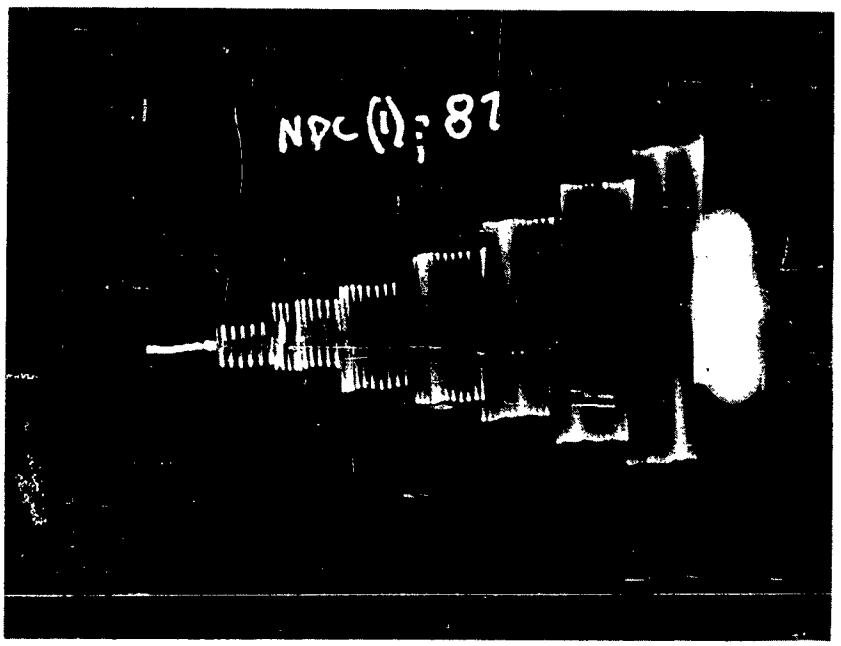

Fig. 16. Calibration Trace, Transient Pressure Measuring System.

Plots of amplitude vs. pressure are shown in Fig. 17 and Fig. 18 for the four strain gages. The data shown in the figures were obtained using the least sensitive of the five gain ranges of the voltage amplifier. The plots show that the measured amplitude is accurately proportional to the applied pressure, except for the small zero pressure amplitude. The zero pressure amplitude was not zero because of the finite size of the cathode-ray beam. The pressure measuring system was calibrated frequently. The sensitivities of the system for the important strain gage, amplifier range combinations are given in Table 14.

Table 14. Sensitivities of the Transient Pressure Measuring System

Range of strain gage, in lb. per sq. in.	Amplifier output	Sensitivity, in atm. per cm.
0 - 500	1	7.68
0 - 150	1	2.11
0 - 150	2	1.16
0 - 100	1	0.980
0 - 100	2	0.524
0 - 100	4	0.226
0 - 50	1	0.629
0 - 50	3	0.183
0 - 50	4	0.133

Transient pressures slightly higher than 500 lb. per sq. in. were obtained for certain of the fuel-oxidant systems under study. It was likely, however, that the 0 to 500 lb. per sq. in. gage had a linear response well above its stated range. This is evidenced by the fact that the rated full-scale millivolt output was not reached at a pressure

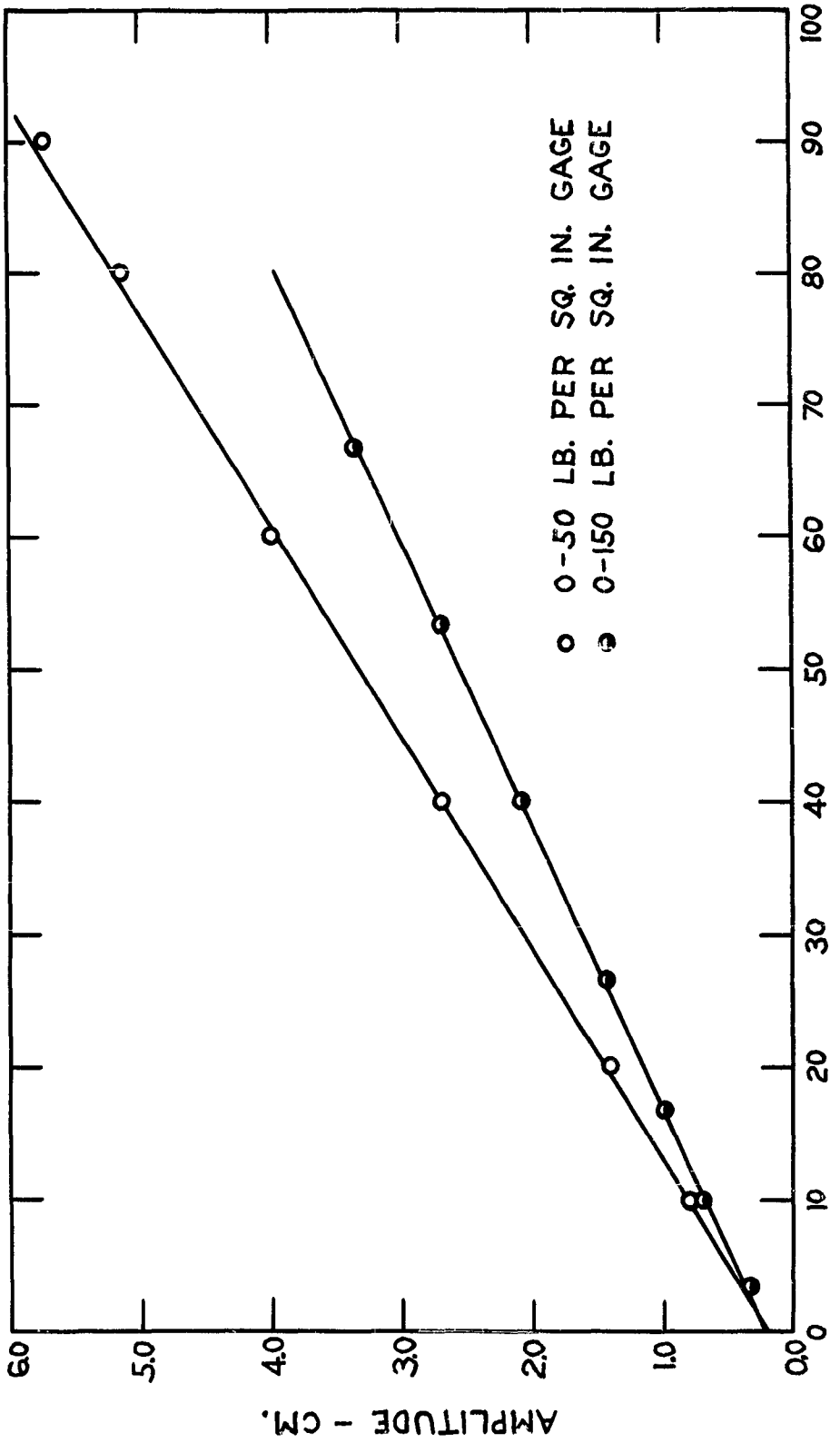

Fig. 17. Calibration of Transient Pressure Measuring System, 0 to 50 and 0 to 150 lb. per sq. in. Gages.

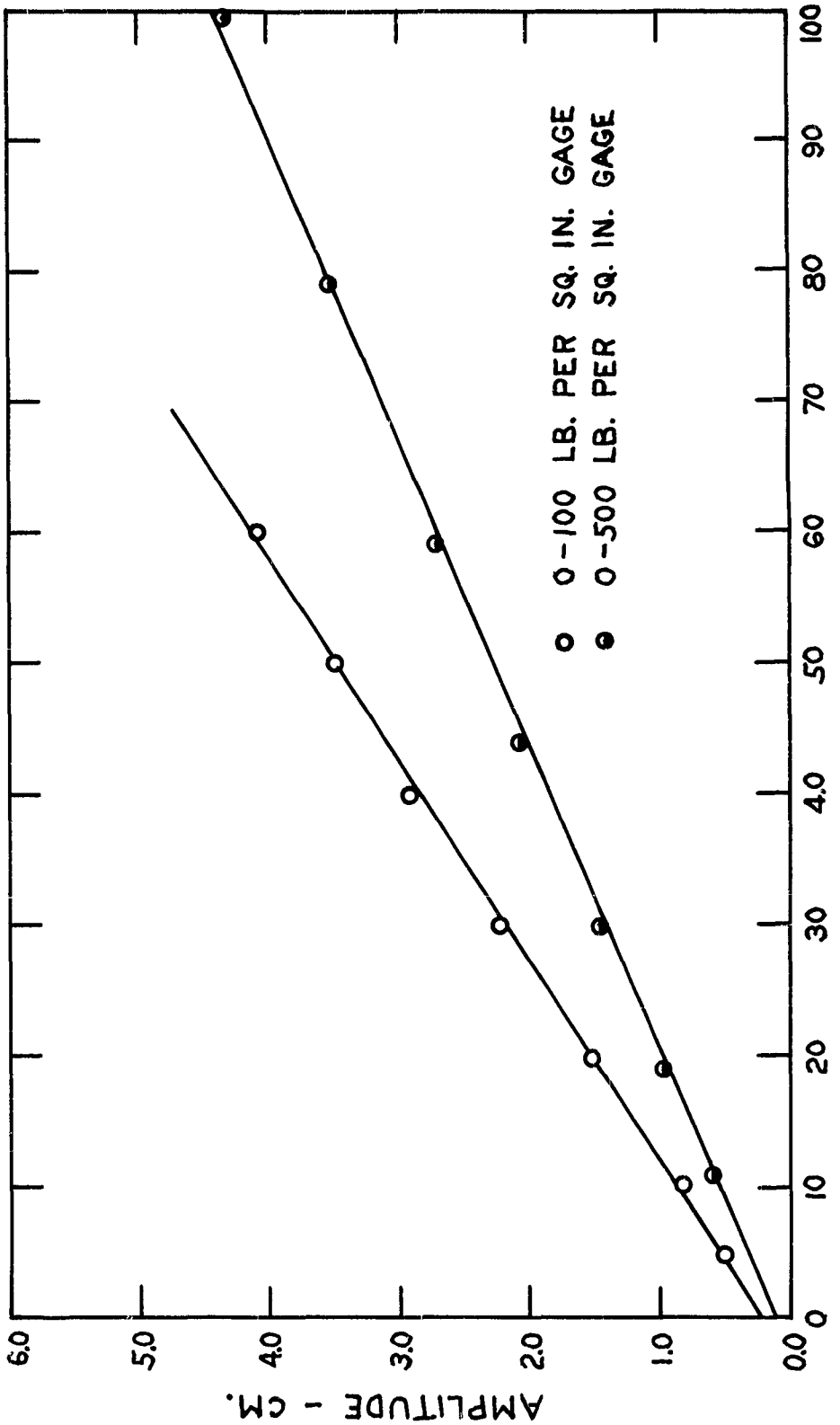

Fig. 18. Calibration of Transient Pressure Measuring System, 0 to 100 and 0 to 500 lb. per sq. in. Gages.

of 500 lb. per sq. in. It is apparent from Fig. 18 that the gage was calibrated up to 500 lb. per sq. in. It was not considered a safe procedure to apply any more pressure to the calibration apparatus. Several abrupt changes of calibration were noted for the 0 to 50 lb. per sq. in. gage. The runs in which the gage was used were sufficiently bracketed by calibrations so that the sensitivity changes did not affect the pressure data. The calibration changes were found to be due to a poor contact in the voltage amplifier. No further changes occurred once the contact had been repaired.

A voltage divider was built that could replace the strain gage in the circuitry. Periodic measurements of the amplitude of the oscilloscope trace using the same voltage divider were employed to ascertain the stability of the circuit elements other than the strain gage. Amplitude measurements made over a period of two and one-half years showed a maximum deviation of 6% from the mean value.

Calibration of the Final Pressure Measuring Systems

The calibration of the 0 to 160 lb. per sq. in. Bourdon gage has already been described. The mercury manometer method was used to measure final pressures for some of the reactions studied in Reactor II. The volume of the reactor varied during these measurements because of the fact that different piping arrangements were used to connect the reactor to the strain gage. The total volume of Reactor II and the manometer connections for a particular piping arrangement was found to be 387 ± 3 cc. by an air expansion method using a calibrated gas buret for reference. The volume of the manometer and connections was estimated from their dimensions to be 62 cc. The volume of the reactor was thus found to be 325 cc. The volume of the reactor with different piping

arrangements was estimated by measuring the volumes of the individual pipe fittings and correcting the total reactor volume. In this way the manometer readings could be corrected for the expansion of the product gases into the manometer.

The calibration of the 0 to 100 lb. per sq. in. strain gage in combination with the Midwestern oscillograph was made by applying static pressures of carbon dioxide to the gage by the method described previously. The pressure record was obtained by running the chart drive of the oscillograph for a few seconds for each pressure value. The distance between the trace line and a reference line was measured with an accurate centimeter scale. The result of the calibration is shown in Fig. 19.

The expansion final pressure method that was used extensively with Reactor II required the calibration of the large bulb system. To accomplish this a large vacuum dessicator was filled with exactly 5000 cc. of water. The remainder of the volume of the dessicator was measured by an air expansion method, comparing it to a calibrated gas buret having a volume of 445.6 cc. The volume of the bulb system including connections was found to be 5,660 ± 30 cc. by comparing it to the empty dessicator. For these runs the reactor piping arrangement was the same except for the number of valves attached to the reactor. Most of the runs were made with a single valve. The reactor volume was found to be 339 ± 2.5 cc. for this case. The volume added by each valve was estimated to be 6 cc. so that the reactor volume was 333 cc., 339 cc., or 345 cc., depending upon whether no valves, one valve or two valves, respectively, were used. For the one valve case, the pressure of the product gases was reduced by a factor of 17.7.

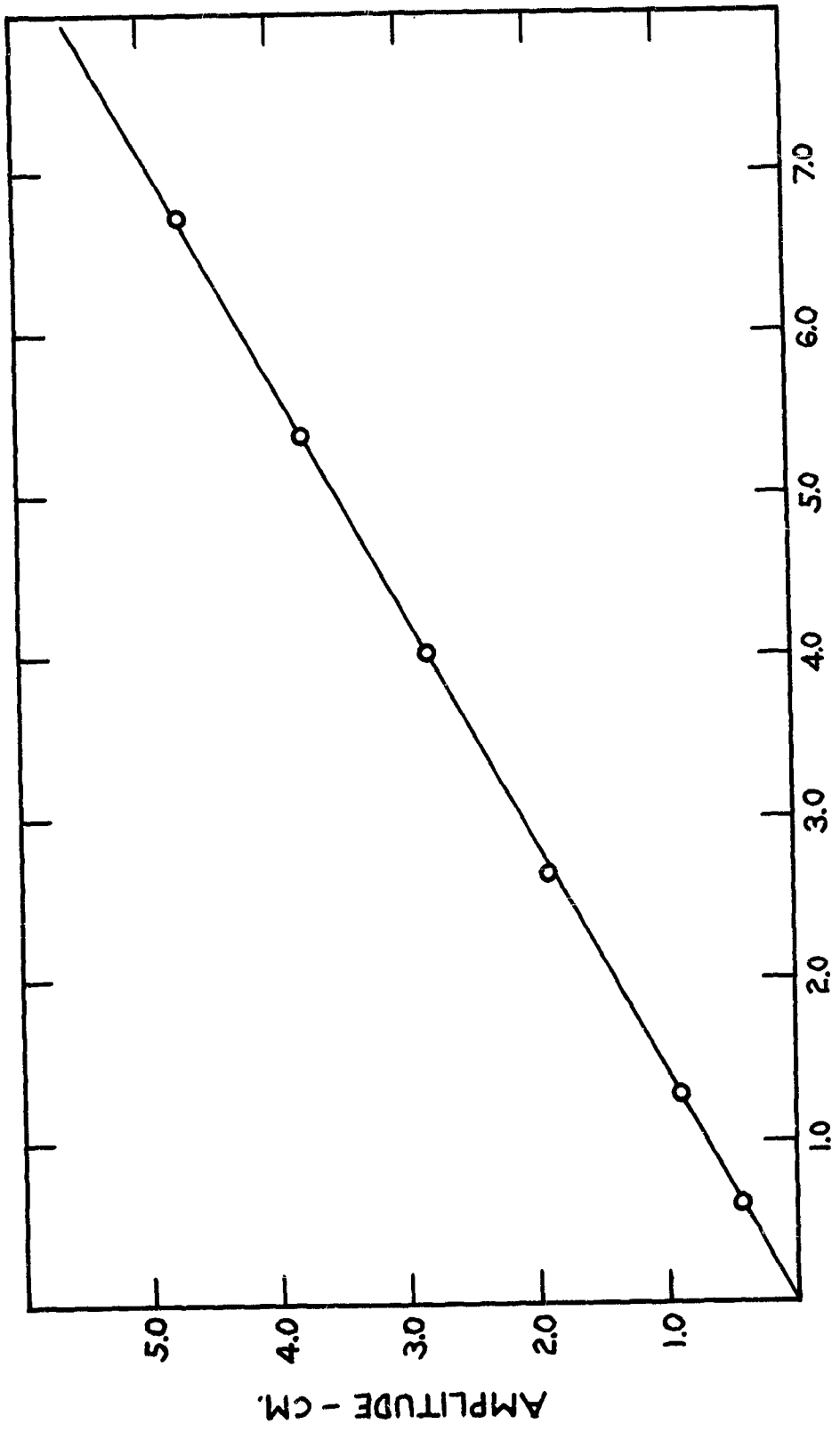

Fig. 19. Calibration of Midwestern Oscillograph, Strain Gage Combination.

Calibration of Photocircuit II

Photocircuit II was stated to have a nearly linear response. A simple test of this based upon the inverse square law was made. The filament of a 200 watt unfrosted light bulb served to approximate a point source of light. The bulb was connected to the 125 V DC line so that steady illumination was obtained. One of the observation arms of Reactor II was detached from the remainder of the reactor. The Plexiglass window was secured to one end of the observation arm in the usual way. The brass phototube container was then attached to the window assembly in the manner used in making a run. A ground glass screen was temporarily glued to the other end of the observation arm. Measurements of the amplitude of the oscilloscope trace were made as a function of the distance between the filament of the light bulb and the ground glass screen. The amplitude was recorded by photographing the screen of the oscilloscope using the same technique that was described in connection with the calibration of the transient pressure measuring system. A typical photoelectric calibration trace is shown in Fig. 20. The distance between the parallel dotted lines is the measure of the light intensity. The linearity of the circuit can be judged from the constancy of the product of the measured amplitude and the square of the distance. The data are shown in Table 15.

The relative sensitivity of the gain ranges of Photocircuit II was determined. This was accomplished by measuring the ratio of the amplitudes produced by adjacent gain ranges using identical illumination. The relative sensitivities are given in Table 16. The intensity of the light emitted by different reactions, however, cannot be compared accurately. Much of the light reaches the phototube by reflection from

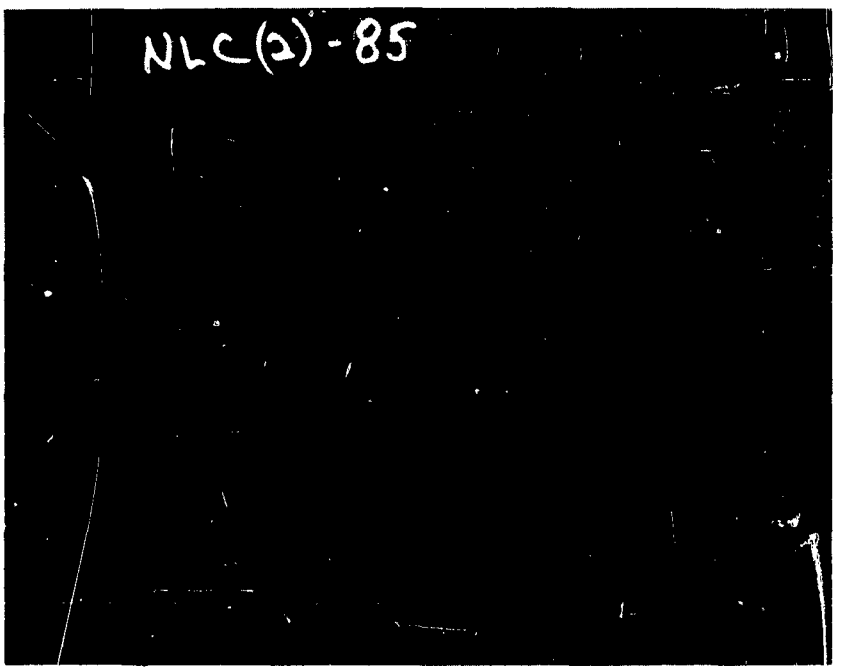

Fig. 20. Calibration Trace, Photocircuit II.

Table 15. Test of Linearity of Photocircuit II

Distance from source to screen, in inches	Amplitude, in cm.	Product of amplitude and the square of distance, in cm. $in.^2$
27	0.43	314
19	0.80	289
12	1.91	275
9	3.28	266
8	4.03	258
5.5	6.80	206

Table 16. Relative Sensitivity of Photocircuit II Ranges

Amplifier setting	Aperture, in inches	Relative sensitivity
1	*0.5	100
3	*0.5	45.4
1	**0.3	29.9
3	**0.3	13.6
4	**0.3	3.91

* Without brass orifice
** With brass orifice

various metal surfaces within the reactor. The reflectivity of these surfaces could not be considered constant from one run to another. The Plexiglass window was found to corrode gradually through contact with corrosive reaction products. The Plexiglass window was frequently polished to minimize the effect of the corrosion. In the later phases of the research, a window made of one-eighth inch Kel-F was used to

shield the heavier Plexiglass window from corrosive agents. No further corrosion of the window was noted.

Rate of Injection

The injection rates obtainable with Reactor I were measured by McKinney. His method will be briefly reviewed. The cylinders were filled 80% full with chloroform; the remaining space was filled with salt solution. Contacts were set up at the outlet from the jets. Initially, a small drop of salt solution closed the contact. When injection began, the chloroform opened the contact. When injection was 80% complete, the contact was again closed by the salt solution. A 1000 cycle signal was impressed upon the vertical plates of the oscilloscope through the contacts so that the time between the start of injection and 80% of complete injection could be recorded. McKinney found that the large piston descended in 9 msec. and the small piston in 5 msec. under a driving pressure of 1700 lb. per sq. in. The pistons were operated separately during these tests. The descent of the small piston would probably be slowed by the back pressure created by the stream issuing from the large jet. The time required to obtain the complete evolution of oxygen in the reaction between acidic hydrogen peroxide and concentrated calcium permanganate was indeed found to be about 9 msec.

Several measurements of the injection rate with Reactor I were made in the present research. The method involved the use of fine copper wires. Two of the wires were attached in the form of a cross by means of a small bead of DeKhotinsky wax. The wax prevented the wires from contacting each other. The bead was placed on one of the injection plates so that the piston would land directly on the bead at the completion of injection. The bead was crushed by the force of the piston

so that the wires were brought into contact, at least momentarily. A 1000 cycle signal was impressed on the vertical plates of the oscilloscope in such a way that the signal would be short circuited when the contacts closed. By counting the number of cycles recorded on the oscilloscope, the time interval between the closing of the bomb contacts in the pneumatic injector and the completion of injection was obtained. McKinney found that piston descent normally began about one msec. after the bomb contacts closed. The method had the advantage that both pistons were operating in the usual fashion during the measurement. One measurement using water in both cylinders, showed that the large piston completed its descent 10.5 msec. after the bomb contacts closed. The measurement clearly agrees with the result obtained by McKinney.

Several attempts had to be made before the contacts could be properly placed under the small piston. One successful measurement was made of the injection of water. The trace is shown in Fig. 21. In this run, the small piston did not complete its descent until 14 msec. after the bomb contacts closed. This result demonstrates that the small piston would not have completed its descent until 3.5 msec. after the large one, assuming that the large piston again required 10.5 msec. to descend.

The descent of both pistons in Reactor II must begin and end at precisely the same instant. The injection is followed by noting the time between pulses of light transmitted by either a serrated brass rod or a striped Plexiglass rod that descends with the piston system. A number of measurements were made of the injection rate for the injection of water from both cylinders of Reactor II. A typical trace is shown at the top of Fig. 22. The rod used in run 116 was made of Plexiglass. It was initially positioned so that the phototube was fully illuminated.

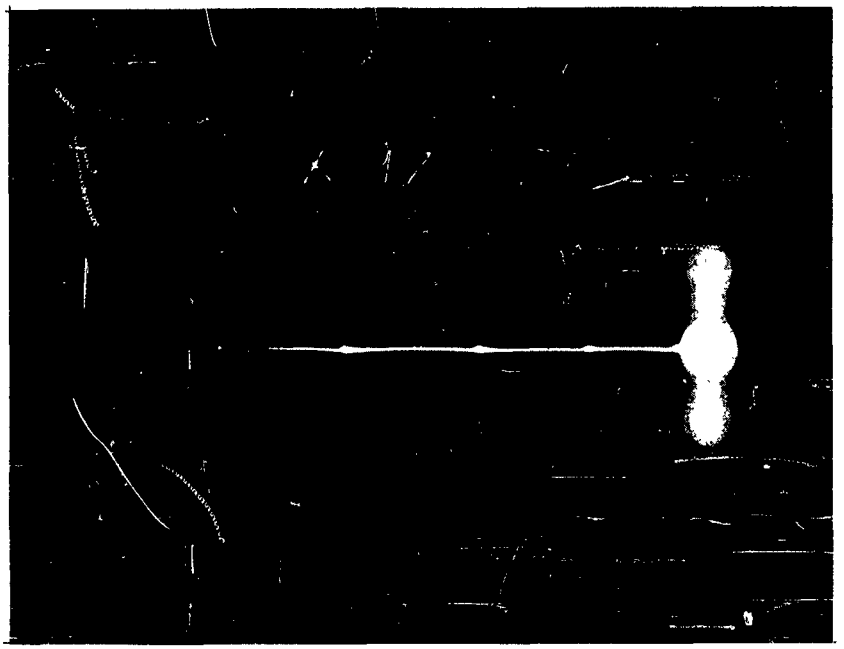

Time ⟶

Fig. 21. Timing Trace for Small Piston, Reactor I, Time Base: 70 msec.

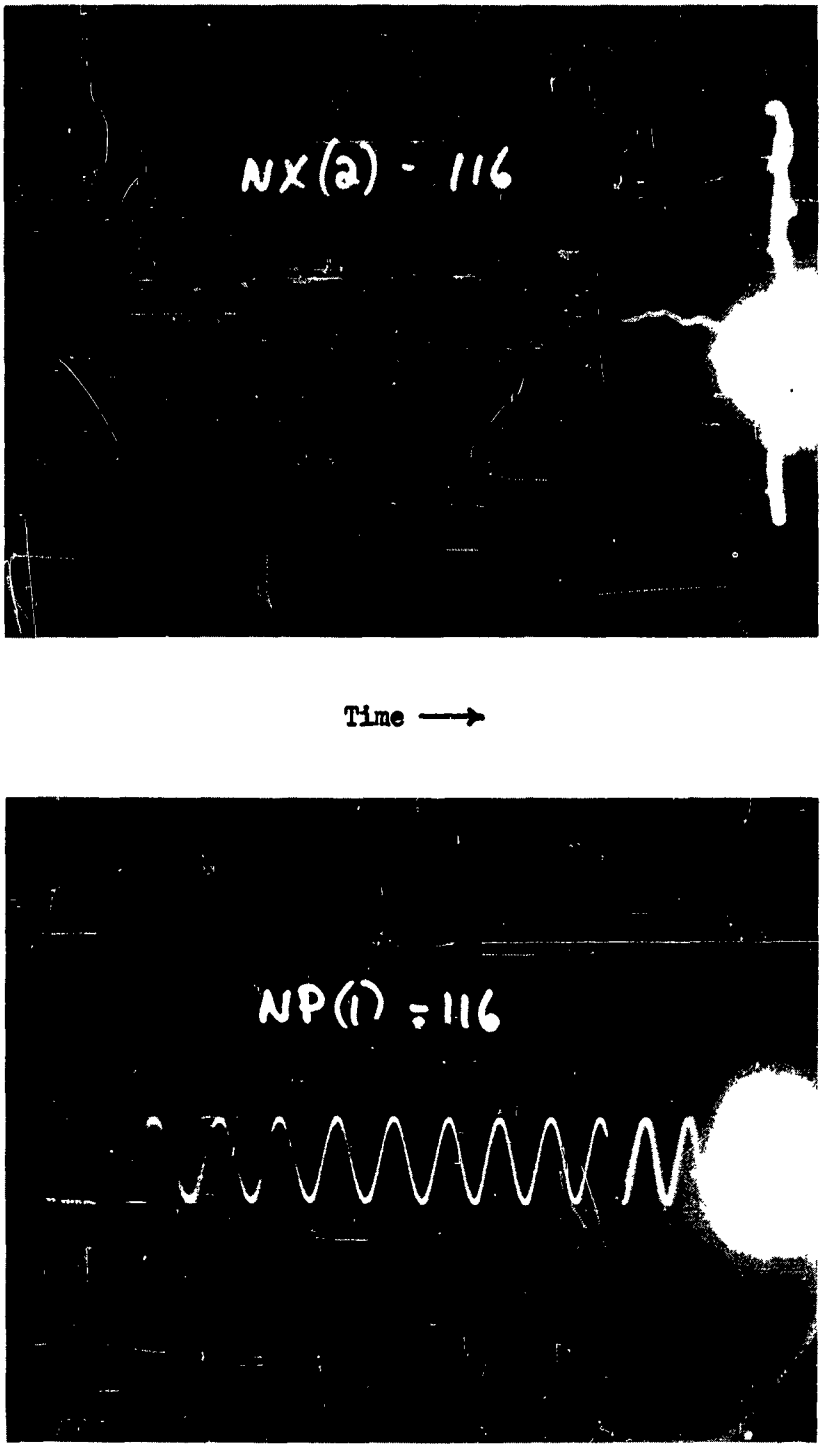

Fig. 22. Injection Rate Traces, Injection of Water, Reactor II, Time Base: 11 msec.

The stripes were evenly spaced so that there were four opaque and four clear positions per inch of rod. The stroke of the piston system was set at seven-eighths inch so that three and one-half cycles were expected. The final condition would correspond to complete darkness. The oscillation pattern on the photoelectric trace agrees with that expected from the conditions of the experiment. A sine wave having a frequency of 1080 cycles per second was recorded simultaneously on Oscilloscope I and is shown at the bottom of Fig. 22. The wave was produced by unbalancing the bridge of the strain gage, recording a signal of constant amplitude.

The rate of injection was calculated from the trace in the following manner: The distance from the start of the trace (at left of figure) to each peak was measured with an accurate centimeter scale. The length of the trace from the start to the timing mark (located about three-fourths of the way across the trace) was also measured. Only one 120 cycle timing mark appeared on this particular trace. The pulse generator that was responsible for the timing mark was connected to the intensity electrode of both oscilloscopes so that the break in both traces occurred at the same instant. The distance to each peak and to the timing mark was also measured on the sine wave trace. The same time base drives the horizontal plates of both oscilloscopes. The deflection sensitivity of the oscilloscopes were not identical, however, so that the distance measured on one of the traces must be divided by the sensitivity ratio. The sensitivity ratio is equal to the ratio of the measured distances from the start of each trace to the timing mark on each trace. The distances to each peak on the photoelectric trace were reduced accordingly. The sine wave has a frequency of 1080 cycles per

sec. This frequency was pre-set accurately since it is an even multiple of 120 cycles per sec. The distance between each peak on the sine wave trace then corresponds to 0.926 msec. A plot is made of the distance from the start of the sine wave trace to each peak vs. the time corresponding to each peak. The time corresponding to each peak on the photoelectric trace can then be found from the plot.

Each peak on the photoelectric trace corresponds to either a condition of maximum light transmittancy or minimum light transmittancy. The time between each peak must then correspond to one-eighth inch of descent of the piston system. A plot of the piston position vs. time can then be made. The position vs. time plots for the injection of water in Reactor II were found to be accurately linear. The slopes of the plots were obtained by a least squares method. Some of the plots obtained are shown in Fig. 23. The origin was arbitrarily placed so that the least squares line would pass through it. The exact time of the start and the finish of injection cannot be measured as accurately as the rate of injection because the pitch of the markings on the rod is known more accurately than either the initial or final positions of the rod with respect to the light beam. The time of the start and finish of injection, however, could not be in error by more than 0.2 msec.

The data shown in Fig. 23 were obtained with Reactor II using the one-to-one reactant ratio. Both cylinders initially contained water. The runs were made as a function of the pressure of the driving gas. The fact that the rate of descent of the piston system is constant throughout injection indicates that the moving parts must accelerate very rapidly to the equilibrium velocity. All of the data obtained for the injection of water are shown in Table 17. The rate of injection

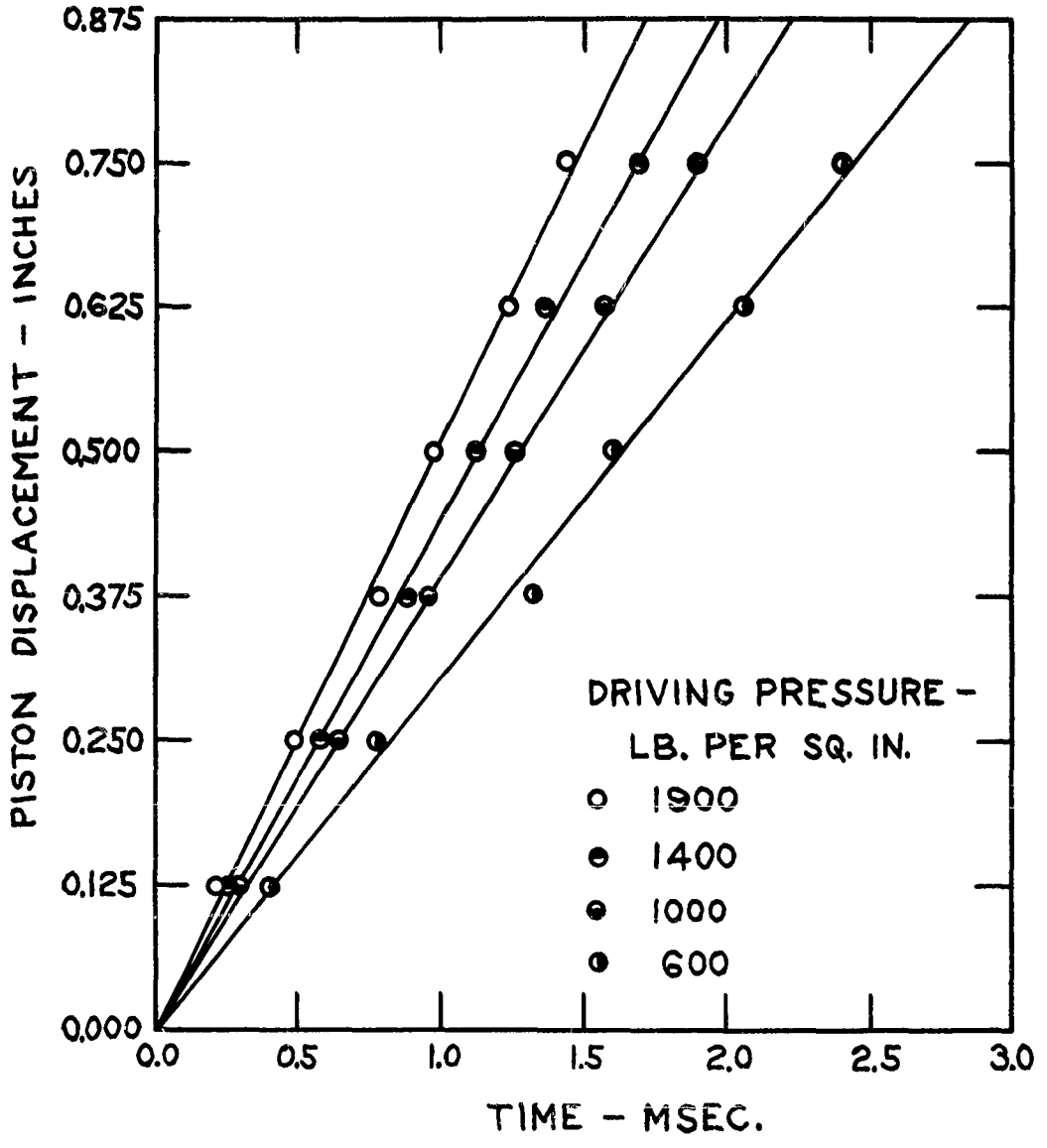

Fig. 23. Injection Rate Measurements, Reactor II.

Table 17. Injection Rate Measurements, Reactor II

Run	Reactant ratio	Pressure of driving gas, in lb. per sq. in.	Injection time, in msec.
73	4 : 1	1800	4.27
98	4 : 1	1700	4.31
114	1 : 1	1950	1.79
119	1 : 1	1900	1.71
117	1 : 1	1400	1.96
116	1 : 1	1000	2.21
120	1 : 1	600	2.84
123	1 : 1	1700	1.91
124	1 : 1	1700	1.91
10	1 : 1	1900	2.65
12	1 : 1	1800	2.83

is expressed as the time required for the pistons to descend seven-eighths inch. Two runs 73 and 98 were made using the four-to-one injection ratio. Runs 114 to 120, inclusive, were made with very loose piston gaskets in order to avoid the effect of gasket resistance. Runs 123 and 124 were made with very tight gaskets. It can be seen that the gasket resistance has only a small effect on the measured injection rate. This conclusion was also reached by McKinney during his studies of Reactor I. Run 124 was made with the large driving piston initially glued to the top of the driving cylinder rather than resting on the top of the smaller pistons. The large piston would then strike the smaller ones with considerable impact once the pneumatic injector was fired. This violent start had no effect on the injection rate. Two runs 10 and 12 made early during the research showed an abnormally slow injection rate compared to the more recent data. This effect may have been due to the fact that a large number of runs of explosive reactions had been carried out in the reactor between these series of injection measurements. The intersection of the jets with the exit tube and the intersection of the exit tube with the interior of the reactor were gradually rounded and enlarged by the force of the explosive reactions. The geometry of the mixing pattern seemed to be conditioned by the reactions themselves to give a more rapid injection rate.

No explosive reactions were studied during the series of runs 114 to 124. The data for these runs are shown in Fig. 24 where the linear flow rate of the water through the exit tube is plotted against the square root of the pressure of the driving gas. For the one-to-one ratio with Reactor II the linear flow rate is related to the injection or contact time according to Eq. 17:

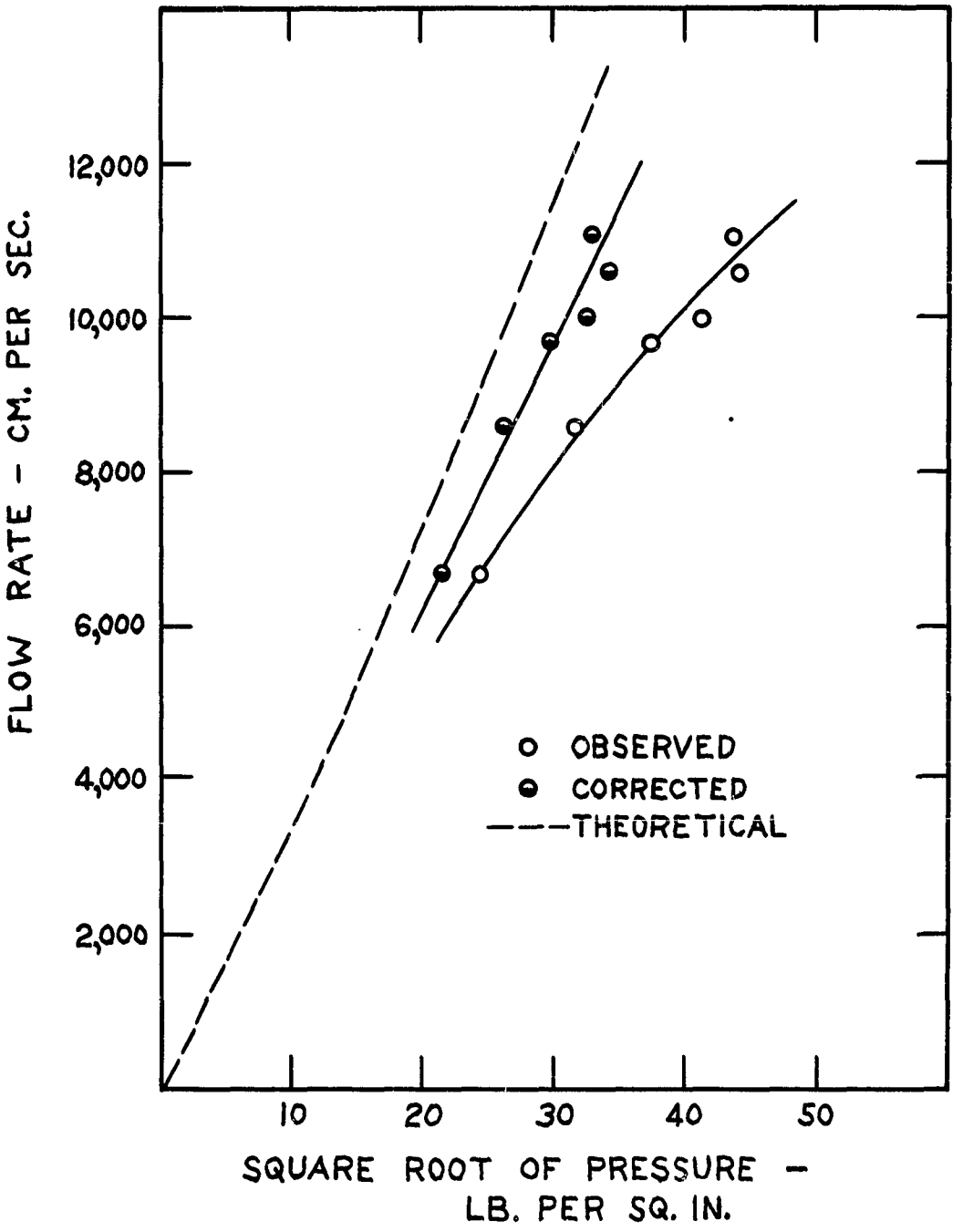

Fig. 24. Linear Flow Rate in the Exit Tube of Reactor II as a Function of the Square Root of the Driving Gas Pressure.

(17) $$u = \frac{18{,}920}{t}$$

where u is the linear flow velocity in the exit tube in cm. per sec.,

t is the contact time in msec.

Since the injection rate seems to be determined wholly by the resistance to fluid flow and not by the gasket resistance, it should be possible to calculate the expected injection rates. Such a calculation is made in Appendix I. The treatment is an empirical calculation based upon well established correlations described in standard engineering treatises.[34,35] Calculations were made for Reactor II for certain reactant ratios both for the water injection and for the injection of anhydrous hydrazine and anhydrous nitric acid. To derive an injection rate one must know only the properties of the fluid, the pressure of the driving gas, and the pertinent dimensions of the reactor. The values calculated for the one-to-one ratio for the water injection are shown in Fig. 24 as the dotted line. It is evident that the calculations predict a much more rapid injection rate than that observed.

The calculations show that the flow rate should be roughly proportional to the square root of the pressure. Chance[2] obtained injection rates that were precisely proportional to the square root of the pressure drop using identical mixing systems but at much lower pressure drops. It seemed likely, in view of the curvature of the observed plot that the resistance to gas flow in the pneumatic injector might be slowing the injection. If this were the case, there would be a pressure drop due to the nitrogen flow from the gas storage reservoir of the pneumatic injector to the driving cylinder. The pressure actually driving the large piston would then be less than the value read from the Bourdon gage located at the gas storage reservoir.

A calculation of the pressure drop due to gas flow in the pneumatic injector is given in Appendix II. The assumption is made that the driving gas pressure in the storage reservoir does not change during the period of injection because of the large size of the reservoir compared to the volume displacement of the driving piston. It is also assumed that the pressure acting on the driving piston is constant during the injection period. This is evidenced by the observed linear character of the injection process. The gas expansion process can then be treated approximately as a Joule-Thompson expansion. Such expansions are very nearly isothermal so long as the pressure drop is not too great.[36] The calculations in Appendix II are made by the isothermal method outlined in a paper by Beale and Docksey.[37] To calculate the pressure drop, it is necessary to know the rate of linear descent of the driving piston, the properties of the gas, and the pertinent dimensions of the pneumatic injector and driving cylinder.

The result of the calculation is shown in Fig. 25. The pressure drop is expressed as the ratio of the effective driving gas pressure to the pressure actually applied to the pneumatic injector. The pressure ratio is plotted against the injection rate expressed as the time required for the piston system to descend seven-eighths inch. The effect of the turbulent friction created by the gas flow through certain parts of the valve mechanism of the injector could not be evaluated because of their complexity. This effect was ignored in the calculation so that the results shown in Fig. 25 may be very conservative.

The results shown in Fig. 25 indicate that a large pressure drop did occur in the injector for some of the rapid injections reported in Table 17. The calculation is not valid for pressure ratios approaching

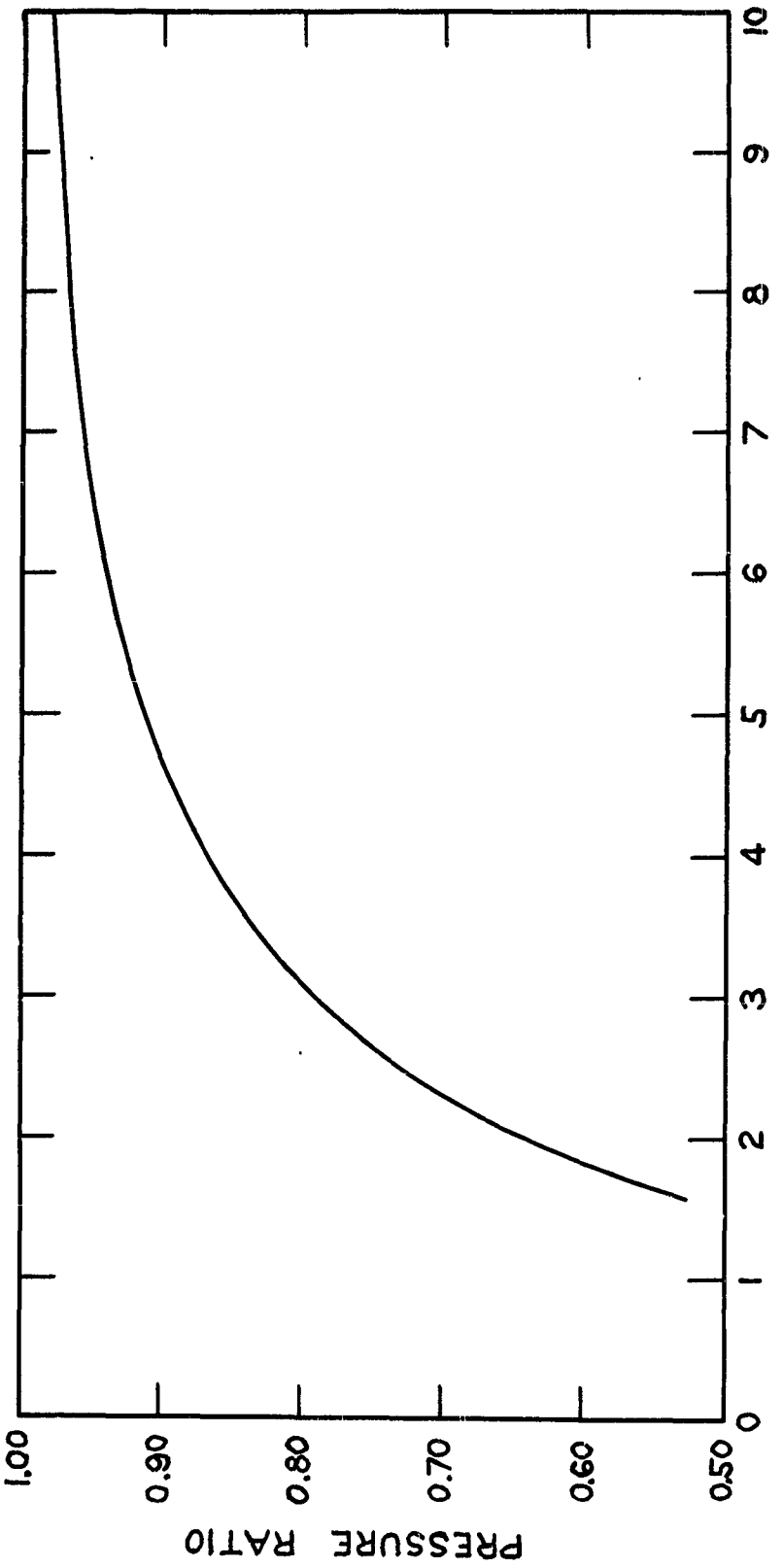

Fig. 25. Calculated Pressure Drop Due to Nitrogen Flow in the Pneumatic Injector.

the critical value. The critical pressure ratio for nitrogen gas is 0.528. At this ratio the gas flow in the injector reaches the velocity of sound and numerous uncertainties are added to the problem.

The runs plotted in Fig. 24 were corrected for the calculated pressure drop in the pneumatic injector by selecting the proper pressure ratio from the graph shown in Fig. 25. The corrected data were plotted in Fig. 24 and a solid line drawn through the points. The calculated injection rates (the dotted line in the figure) are still about 18% higher than the corrected values; however, the corrected data show much better agreement to the predicted proportionality between the flow rate and the square root of the pressure.

It is of interest to compare the observed injection rates to those predictable by the simple formula given by Chance and discussed in an earlier chapter. Chance's formula is given by Eq. 13:

$$V^2 = \frac{\Delta P \, A_o^2}{K_1} \tag{13}$$

where V is the total volume flow rate in cc. per sec.,

ΔP is the pressure drop in lb. per sq. in.,

A_o is the area of the observation tube in sq. mm.,

K_1 is an empirical constant having a value 0.3 to 0.8.

The effective pressure drop across the mixing plate of Reactor II is much higher than the actual gas pressure in the pneumatic injector because of the hydraulic advantage of the piston system. For the one-to-one ratio, the power gain of the mechanical system is equal to the ratio of the area of the driving cylinder to the combined areas of the smaller cylinders. This ratio was calculated from the measured dimensions to be 5.09. The area of the exit tube (Chance's observation tube)

in the mixing plate was found to be 11.7 sq. mm. A mean value of K_1 was taken as 0.5. Introducing these values, Eq. 13 reduces to:

$$P = \frac{3,870}{t^2} \tag{18}$$

where P is the effective driving pressure in lb. per sq. in.,

t is the contact time in msec.

The injection rate data are summarized in Table 18, along with the effective driving pressure calculated by means of the fluid dynamic analysis given in Appendix I and by means of the Chance formula.

Rate of Mixing

The rate of mixing obtainable with Reactor I was measured by McKinney.[3] He showed that the entire contents of the cylinders could be injected and mixed in a period of less than 10 msec. by measuring the extent of a reaction known to be very rapid.

A similar method was used to evaluate the mixing time for Reactor II. The pressure rise for the reaction between sodium-potassium alloy and water was found to reach a maximum in a time equal to the known injection time. This was demonstrated by making a simultaneous measurement of the injection rate and the pressure rise for the sodium-potassium alloy vs. water reaction in Reactor II. The result is shown in Fig. 26. The pressure maximum occurred 2.1 msec. after the start of the pressure rise whereas the injection required 2.3 msec. The time corresponding to the maximum pressure can be measured within an accuracy of only about 0.3 msec. because of the scatter of the pressure points and because only one point is obtained every 0.8 to 1.0 msec. depending upon the frequency of the carrier wave. The start of the pressure rise came about 1.5 msec. after the injection began. This effect was noted

Table 18. Correlation of Injection Rate Data

Run	Reactant ratio	Measured pressure, in lb. per sq. in.	Contact time, in msec.	Corrected pressure, in lb. per sq. in.	Calculated pressure, Appendix I	Calculated pressure, Chance formula
73	4 : 1	1800	4.27	1590	1090	-
98	4 : 1	1700	4.31	1510	1120	-
114	1 : 1	1950	1.79	1160	773	1210
119	1 : 1	1900	1.71	1090	840	1320
123	1 : 1	1700	1.91	1050	703	1060
124	1 : 1	1700	1.91	1050	703	1060
117	1 : 1	1400	1.96	890	670	1010
116	1 : 1	1000	2.21	685	543	794
120	1 : 1	600	2.84	465	346	480

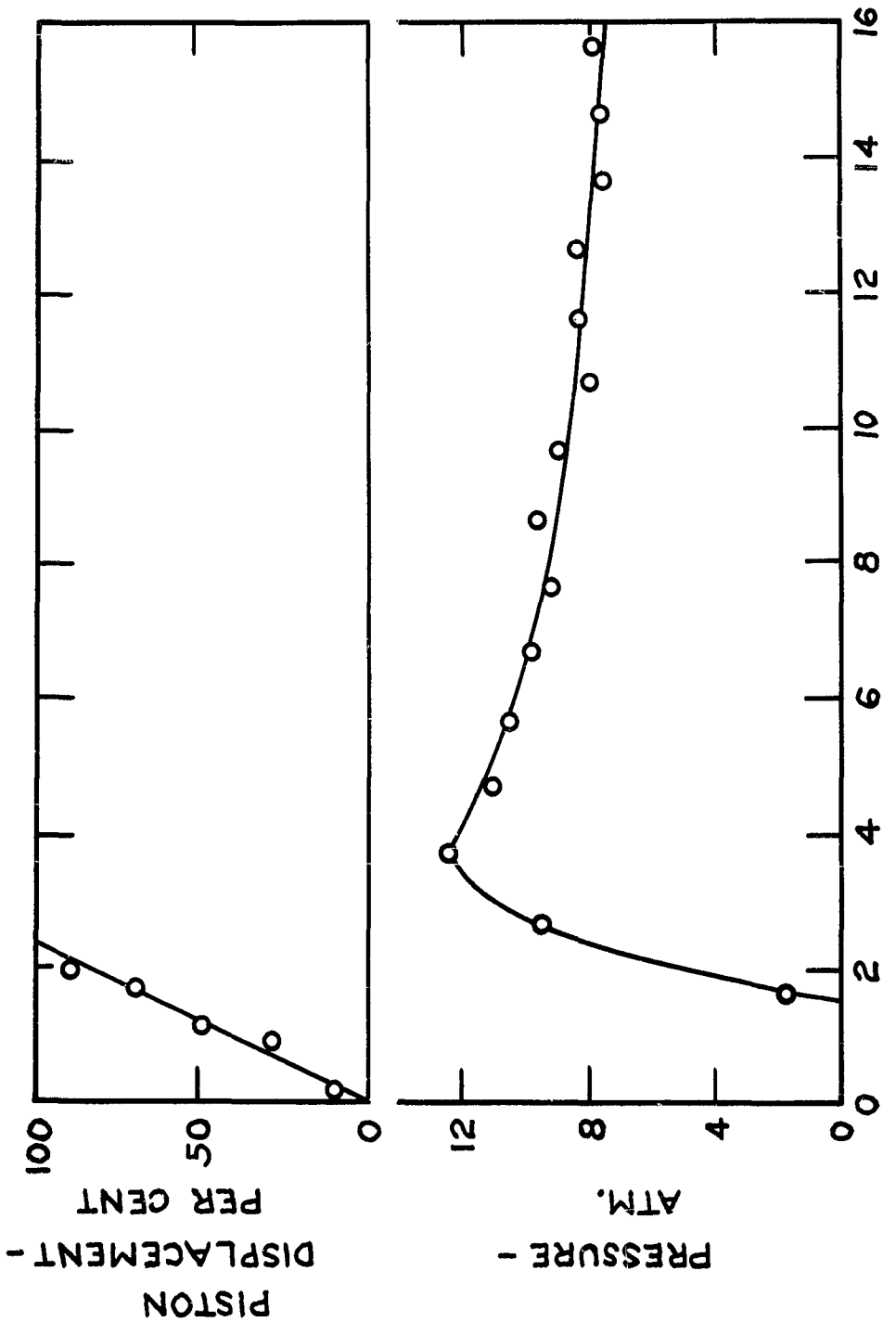

Fig. 26. Simultaneous Measurement of Injection Rate and Pressure Rise in the Reaction of Sodium-potassium Alloy with Water, Run 12, Reactor II.

in every run carried out in Reactor II. The delay is thought due to the time required for the first pressure pulse to travel the distance from the exit tube of the mixing plate to the diaphragm of the strain gage. A large number of runs of the system sodium-potassium alloy vs. water were made in which the time to the maximum pressure was about equal to the injection time expected from the data reported in the previous section.

The rate of the sodium-potassium alloy, water reaction was found to be too rapid to measure in Reactor I. The agreement between the time required to reach a maximum pressure and the injection time in Reactor II indicates that the reaction rate is also too rapid to measure in Reactor II. This agreement also indicates that the reactants were mixed essentially at the same rate that they were injected. It is likely that very little of the reaction heat was transferred to the walls of the reactor in the time required for injection. Indeed, the observed maximum pressures for the reaction in Reactor II were considerably higher than that expected from the stoichiometric yield of hydrogen. If a significant quantity of the reaction heat were transferred to the reactor walls during injection, it would have been possible to observe a pressure maximum before the completion of mixing. The slow decrease of the pressure during the period beyond about 5 msec. after injection suggests, however, that the reaction products did cool very slowly.

A number of previous investigations have been made of the mixing efficiency obtainable for the mixing of equal volumes of reactant solutions in "T" type mixers. The results of these studies* indicate that the mixing of reactants in Reactor II should be very thorough.

---

* Shown in Tables 3 and 4, Chapter I.

The results of these studies are not directly related to the mixing of reactants in Reactor I because of the very unequal amounts of reactants contacted in Reactor I. The mixing plate used in Reactor II has two jets discharging into an exit tube. The diameters of the jets are 2.5 mm.; the diameter of the exit tube or mixing chamber is 3.9 mm. A "T" type mixer described by Trowse also employs two jets. The diameter of the jets and the observation tube (exit tube) was 0.7 mm. Trowse found that reactant solutions were mixed 97%, 5.7 mm. downstream from the jets. His measurements were made at a linear flow velocity of 440 cm. per sec. referred to the exit tube. Millikan studied the extent of mixing in another "T" type mixer as a function of the flow velocity. He found that the distance downstream to the point of 97% mixing rapidly moved toward the point of first contact of the reactants as the flow velocities were increased. The linear flow velocities in the exit tube of Reactor II for all runs varied between 3,000 and 11,000 cm. per sec. so that mixing should be completed in a very short distance. The exit tube of Reactor II is 8 mm. long. The stream emerging from the exit tube travels about 25 mm. through an unconfined area and then strikes a baffle plate to further complete the mixing of the reactants.

The time of residence of the stream in the exit tube of Reactor II varies between 0.07 and 0.27 msec. for the range of flow velocities employed. The stream requires in all from 0.3 to 1.1 msec. to travel from point of first contact to the baffle plate. Under an unfavorable assumption, then, it would require only 1.1 msec. at the slowest flow rate to complete the mixing in addition to the time required to inject the reactants. For the study of ignition delay, the injection time is of no interest except as it affects the mixing efficiency. It is only

the time between the contact and the completion of mixing of a given fluid element that is of importance, since presumably the first element of fluid to be injected is the one that will first ignite.

Response of the Transient Pressure Measuring System

During the early phases of the research, a great deal of difficulty was encountered due to the presence of noise in the pressure traces. It was found necessary to connect the strain gages to the reactors in such a way that there was no metal-to-metal contact between them. This eliminated most of the random disturbances present in the early traces; however, a periodic vibration of the amplitude of the pressure traces remained. An example of the noise present in some of the traces from Reactor II is shown in Fig. 27 and Fig. 28. Fig. 27 shows the appearance of the traces. The pressure data for one of them is plotted in Fig. 28. The points represent the measured amplitude for each cycle of the 1200 cycle carrier wave. The dotted line was drawn through the points indicating the periodic nature of the disturbance while the solid line represents a time average value of the pressure.

It was very unlikely that the source of the noise was in the strain gage since the natural frequency of vibration of the strain gage diaphragm is stated by the manufacturer to be above 2000 cycles per sec. The characteristics of the noise were unchanged by using a different strain gage. It was thought possible that some part of the reactor was set into vibration during the injection process and was causing the noise. A number of runs were made in Reactor II in which the gaskets used to seal the various connections were drastically altered. In some cases, the parts were rigidly bolted together without gaskets. The general nature of the noise was unaffected by these variations. Several

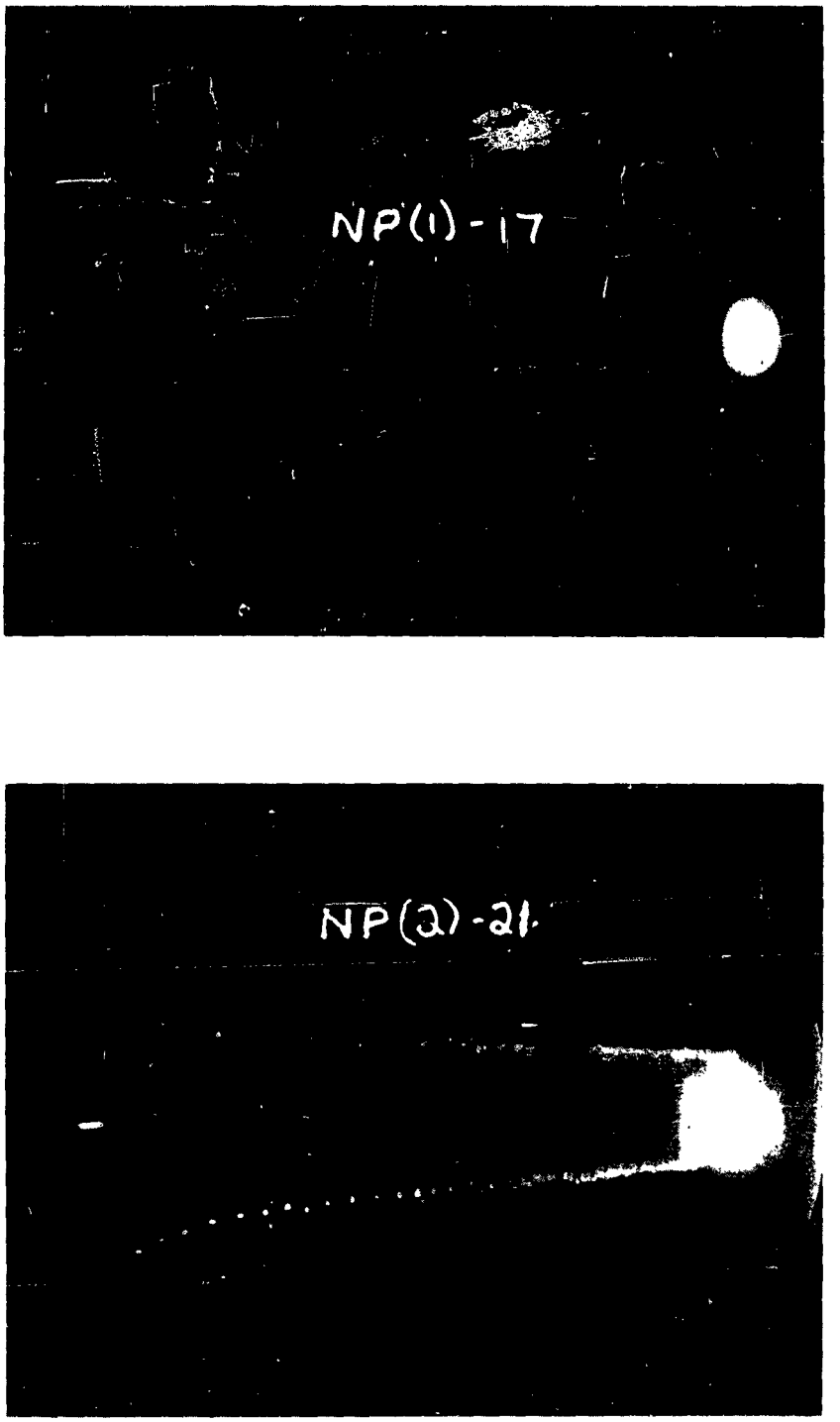

Fig. 27. Transient Pressure Traces of the Alloy, Water Reaction, Runs 17 and 21, Reactor II, Time Base: 100 msec.

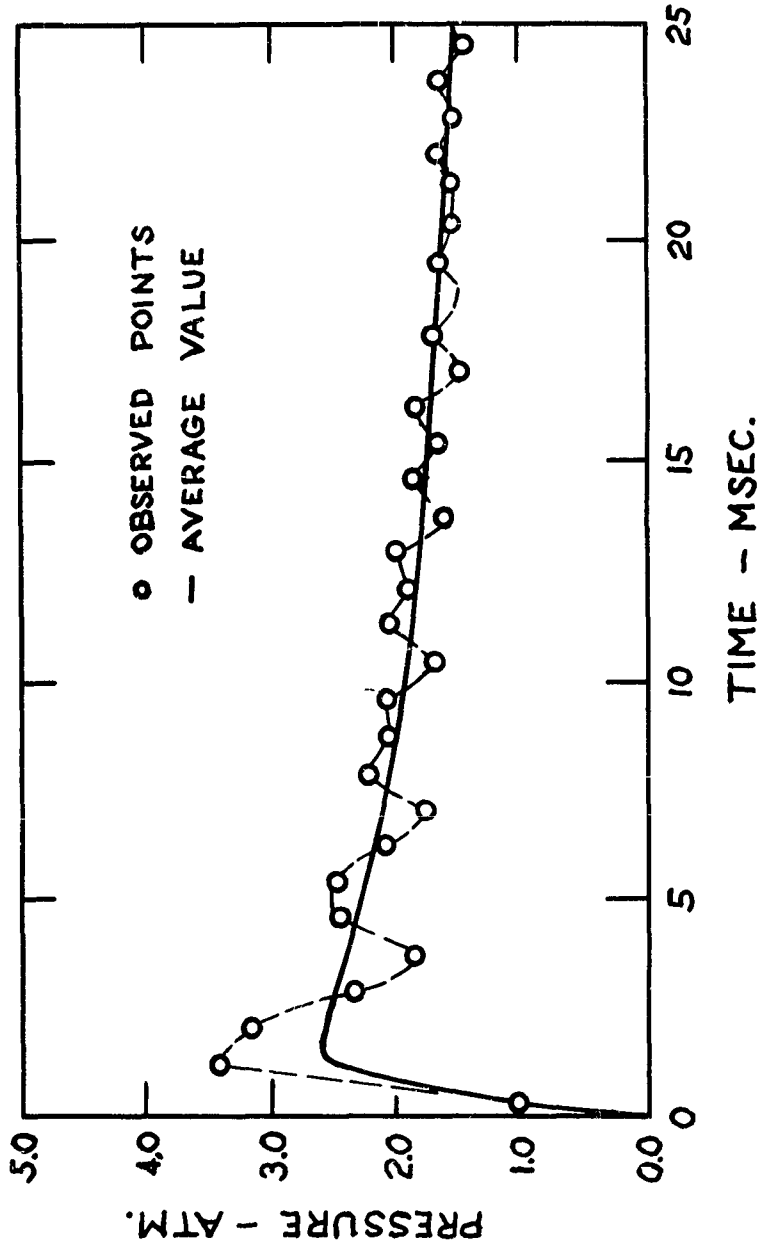

Fig. 28. Pressure Rise in Reaction of Sodium-potassium Alloy with Water, Run 17, Reactor II.

runs were made in which a high frequency carrier wave was used to supply the bridge of the strain gage. Again no change was observed in the noise present in the pressure trace, indicating that the difficulty was not electrical in nature.

Since the source of the noise could not be identified with any part of the apparatus, it was tentatively assumed that the noise was a real manifestation of the reaction process. An attempt was then made to attenuate the vibration in the coupling between the reactor and the strain gage. To compare the traces obtained during this study, a noise index was defined. The noise index is defined as the per cent deviation of the worst single point on the pressure vs. time plot from the time average value. The noise index for the run plotted in Fig. 28 is 30%. A run was made with a cork obstruction in the piping connecting the reactor to the strain gage. The trace is shown in Fig. 29. For this run the time required for the pressure to reach a maximum was 5.9 msec., but the noise index was only 8%. It was apparent that the noise had been largely removed but at great expense to the time response of the pressure measuring system. The fact that the disturbances could be removed by placing obstructions in the connecting arm between the reactor and the strain gage indicated that the pressure in the reactor was actually varying periodically as the traces indicated.

In order to secure interpretable pressure traces, it was necessary to seek a compromise between the response of the pressure measuring system and the amplitude of the noise. A series of runs was made of the sodium-potassium alloy vs. water reaction in which the number of 90° pipe elbows on the piping between the reactor and the strain gage was varied. The data obtained from the series of runs is summarized in Table 19.

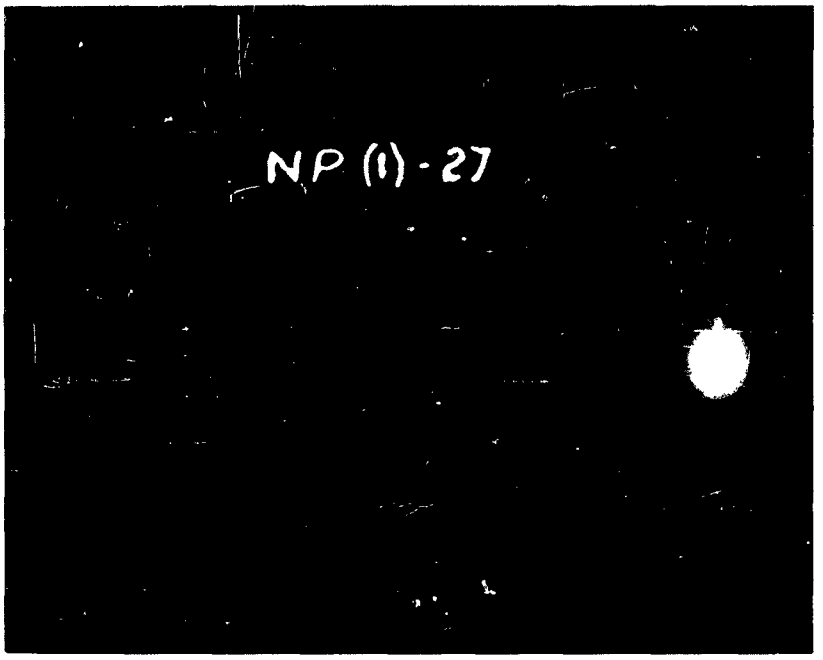

Fig. 29. Transient Pressure Trace of Alloy, Water Reaction, Showing Delayed Response, Run 27, Reactor II, Time Base: 100 msec.

Table 19. Response of the Pressure Measuring System

Run No.	Number of 90° pipe elbows*	Time to maximum pressure, in msec.	Noise index, in per cent
30	0	-	ca. 100
37	2	2.1	39
39	4	1.6	24
43	5	1.8	19
40	5	2.2	12
44	5	2.2	9
47	10	4.0	8

* One-quarter inch steel pipe, actual inside diameter 0.36 inch.

There was no apparent delay in response on increasing the number of pipe elbows from 0 to 5; however, a substantial attenuation of the noise was obtained. When 10 pipe elbows were employed, the response was seriously delayed. The final apparatus was arranged so that there were five 90° bends in the piping between the strain gage and the reactor to give the best possible compromise between the response and the noise.

An attempt was made to further decrease the noise level by adding a sharp edged orifice to the piping. An orifice having a diameter of 0.22 inch increased the time required to record the pressure rise to 5.5 msec. The traces obtained using Reactor I had a noise index of only a few per cent. This was thought due to the fact that the connecting arm had a one-inch long channel having a diameter of only 0.19 inch. It would appear that this channel would attenuate the noise quite thoroughly. A somewhat slower response time would not affect the data obtained with Reactor I because of the much slower injection rate.

CHAPTER IV
EXPERIMENTAL METHOD

Before beginning a discussion of the various reactions which were studied, a detailed description of the technique of operating the reactors and the electronic apparatus will be given. In this section, the discussion will be limited to the handling of chemicals that can be exposed to the air. Certain reactants required special handling techniques; the discussion of these will be deferred until the reactions themselves are discussed.

Experiments with Reactor I

The experimental procedure that was used to secure pressure vs. time data with Reactor I is as follows: The neoprene piston gaskets were first polished by rubbing them with powdered graphite. The pistons were then inserted into the cylinders. The cylinder block was inverted and supported on a wooden support so that the reactant solutions could be poured into the cylinders. When the cylinders were full, the injection plates were bolted on to the cylinders. A thin film of either polyethylene or Teflon was placed between the cylinders and the injection plates so that the solutions could not flow through the jets prematurely. The remainder of the reactor parts were then assembled and secured.

The electronic apparatus was turned on and allowed to warm up. Most of the adjustments were made by means of the switching circuits shown in Fig. 7. At first, switch SW1 was set in position I and SW2 in position A. In this position the vertical plates of Oscilloscope I were connected to a 60 cycle signal taken from the AC line. The horizontal plates were connected to the saw-tooth oscillator built into the Du Mont

instrument. The saw-tooth oscillator was then synchronized with the 60 cycle line using the controls on the panel of the Du Mont instrument. Switch SW1 was then turned to position II. In this position the vertical plates of Oscilloscope I were connected to the output from the pulse generator. The pulse generator was adjusted to the desired frequency, either 60 or 120 cycles, and synchronized to the saw-tooth oscillator. Switch SW1 was then turned to position III. In this position, the vertical plates of Oscilloscope I were connected to the output from the voltage amplifier. The desired gain range of the voltage amplifier was then chosen. The carrier wave generated by the audio oscillator was adjusted to the desired frequency, either 1080 or 1200 cycles. The output of the carrier wave from the power amplifier was next adjusted to 20 units on the panel meter. The bridge of the strain gage was then balanced both resistively and capacitively so that the amplitude of the signal was at a minimum. Switch SW2 was turned to position B or C with switch SW1 remaining in position III. In this position the horizontal plates of Oscilloscope I were connected to the time base generator also shown in Fig. 7. The desired time base was chosen by adjusting switches SW3 and SW4. Times ranging from 0.01 to 0.30 seconds were used. The time base could be tested by closing switch SW6 momentarily. The trace was next positioned on the screen of the oscilloscope. The horizontal position was adjusted by means of R11 and the vertical position by means of the vertical control on the panel of the oscilloscope. With switches SW1 and SW2 in position III and position B or C, the transient pressure measuring system was ready for operation.

The camera was next mounted in front of the screen of the oscilloscope and the shutter opened. The driving gas was then charged into the

pneumatic injector from a nitrogen tank. When the gas pressure read from the Bourdon gage mounted on the pneumatic injector reached the desired value, the injection was begun by manually rotating the cocking block. A few seconds later the shutter of the camera was closed. The procedure used to measure the final pressure of the reaction products has been described previously. The electronic apparatus was then turned off, the reactor dismantled, and the parts cleaned and dried.

The procedure used to obtain a light intensity trace using Reactor I requires that all the previous adjustments be made except for the adjustments involving the voltage amplifier and the balancing of the strain gage. All photoelectric measurements of reactions in Reactor I were made with Photocircuit I. The output of Photocircuit I was connected directly to the vertical plates of the oscilloscope. The gain range of the photocircuit was selected and the "dark signal" adjusted to 20 units on the small panel meter. Having completed the time base and pulse generator adjustments, the pneumatic injector could be fired.

Experiments with Reactor II

Several combinations of measurements were made with Reactor II. Simultaneous measurements of the light intensity and the transient pressure were made. Simultaneous measurements of the injection rate and the transient pressure were also made. Some transient pressure measurements were made with no simultaneous photoelectric measurement. The experimental procedure varied only slightly for these different cases. A view of Reactor II and the electronic apparatus is shown in Fig. 30. The reactor is set up for a simultaneous measurement of the light intensity and the pressure rise.

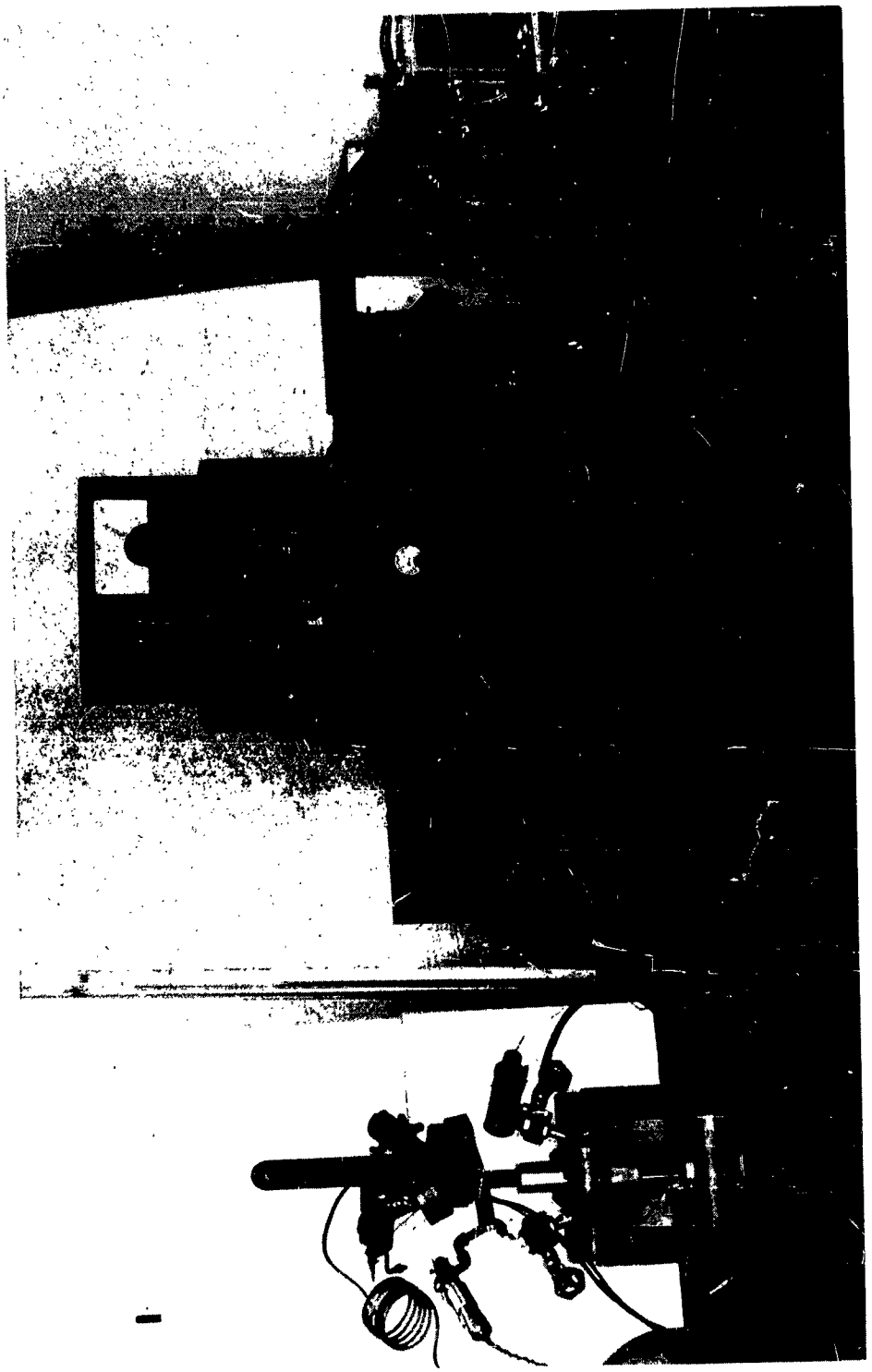

Fig. 30. Assembled Reactor II and Electronic Apparatus.

The mixing plate is first bolted to the desired cylinder block. A 0.03 inch thick Teflon sheet was used to gasket this connection along with a continuous film of Teflon. The thicker gasket is partly crushed when the pistons complete their descent. This formed a tight seal to avoid the escape of the product gases to the atmosphere. The thinner gasket prevented the reactants from leaking out of the cylinders prematurely under the influence of gravity. The baffle plate assembly was then attached to the mixing plate. The reactants were added to the top of the open cylinders by means of automatic pipets which delivered just the correct amount of material. The pistons were then prepared by rubbing either inert grease or powdered graphite into the neoprene gaskets. The pistons were next inserted into the cylinders. The air above the reactants escaped through the fine holes in the pistons. The pistons were lowered to the desired height. In some runs the amount of reactants was varied. For these runs, the pistons were lowered and the distance measured accurately with a machinist's scale; the excess reactants were removed gradually as they streamed out of the fine holes at the top of the pistons. For most of the runs, the pistons were lowered by means of a brass jig to a height that would lead to a stroke length of exactly seven-eighths inch. The amount of reactants originally added by the pipets would then just fill the cylinders. A tiny Teflon gasket was then inserted into the top of the small hole. The small piston caps were screwed into these holes. For a run in which the injection rate was to be measured, the serrated rod assembly was next placed into position. The remaining parts of the reactor were then assembled and secured.

For runs in which the light intensity was to be measured the

phototube container was attached to the window assembly at the end of one of the observation arms. The container could be fitted directly on the reactor frame and supported by the reactor when it was intended to use Photocircuit II. The container was supported separately by a ring stand and connected to the window assembly by a thin coil of sheet rubber or paper, however, when it was intended to use Photocircuit III because of the much higher sensitivity of Photocircuit III to mechanical vibrations. For runs in which the injection rate was to be measured, the phototube container was mounted as shown in Fig. 15.

The electronic adjustments that had to be made for simultaneous pressure and photoelectric measurements were as follows: The transient pressure measuring system was first adjusted by the method already described in connection with Reactor I. The output of any of the three photocircuits was connected to the vertical plates of Oscilloscope II. The output signal from the chosen photocircuit could be viewed on Oscilloscope II by turning switch SW7, shown in Fig. 7, to position E when switches SW1 and SW2 were in positions III and A, respectively. This connected the saw-tooth oscillator contained within Oscilloscope I to the horizontal plates of Oscilloscope II. The desired gain range of the photocircuit was then selected by adjusting the control on the panel of the photocircuit. Switch SW7 must then be turned to position D. With switches SW1 and SW2 in positions III and B or C, the time base was tested on Oscilloscope II by momentarily closing switch SW6. The photoelectric trace was next positioned on the screen of Oscilloscope II. The horizontal position was adjusted by means of R33 and the vertical position by means of the vertical control located on the panel of Oscilloscope II. The entire apparatus was now ready for operation.

Both cameras were then mounted in front of the oscilloscopes and the shutters opened. The driving gas was then charged into the pneumatic injector. The injector was begun by manually rotating the cocking block. After the reaction, the camera shutters were closed, the electronic apparatus turned off, and the reactor dismantled.

CHAPTER V
STUDIES OF VARIOUS REACTIONS

Studies were made of the reaction of sodium-potassium alloy with water and ethanol. These studies were designed to supplement the results obtained by McKinney. Studies were also made of several fuel-oxidant systems. The fuel-oxidant systems included:

A. Nitric acid vs. hydrazine

B. Nitric acid vs. aniline

C. Hydrogen peroxide vs. hydrazine

D. Nitric acid vs. liquid ammonia, hydrazine mixtures.

Reaction of Sodium-potassium Alloy with Water in Reactor I

Alloys of sodium and potassium are liquids at room temperature over a moderate range of composition. The alloy used for this study was obtained from the Mine Safety Appliances Co. The alloy was analyzed by the method outlined in Appendix III and found to contain 83.9% potassium by weight. The alloy reacts rapidly with both water and oxygen so that special techniques had to be used in order to load the reactor. A modification of the procedure used by McKinney to load aluminum borohydride into Reactor I was used in the present study to load the alloy into the small cylinder of Reactor I.

In this procedure, a hypodermic needle was attached to the jet of the small injection plate after the plate was attached to the cylinder. By means of a hole in the reactor above the small cylinder, it was possible to connect a long thin rod to the small piston so that it could be moved up and down within the cylinder. In this way the small piston served as the plunger of a syringe. McKinney distilled the

borohydride into a small vial that was closed by a thin rubber cap of the type used for insulin containers. The needle then was pushed through the rubber cap. The cylinder could then be filled without bringing the borohydride into contact with the atmosphere. The rubber cap method was not used, however, for the alloy. The alloy was first freed from solid material by distilling about 10 cc. into a small glass vial. The entire sample was distilled to avoid fractionation. The distillation was carried out in an all glass high vacuum apparatus using a smoky torch flame. The alloy in the vial was then covered by distilling a few cc. of dibutyl ether into the vial. The dibutyl ether was first purified by drying over some of the alloy and by bulb to bulb distillation. The vial was then removed from the vacuum apparatus and opened to the atmosphere. To load the reactor, the hypodermic needle was immersed through the ether layer and into the alloy before the plunger was raised to fill the cylinder. The vial was weighed both before and after loading the reactor. The weight loss then gave an accurate indication of whether the cylinder was filled or not. The hypodermic needle was then removed and the large cylinder filled in the usual manner.

The reaction of the alloy with excess water can be represented by Eq. 19.

(19) $$M + H_2O \longrightarrow MOH + 0.5\ H_2$$

A typical pressure vs. time trace is shown at the top of Fig. 31. The data from the trace are plotted as curve B of Fig. 32. Curve A is a plot of a run made by McKinney of the same reaction. The theoretical pressure expected from the hydrogen generated according to Eq. 19 is shown at the lower right of the figure. The pressure vs. time curves

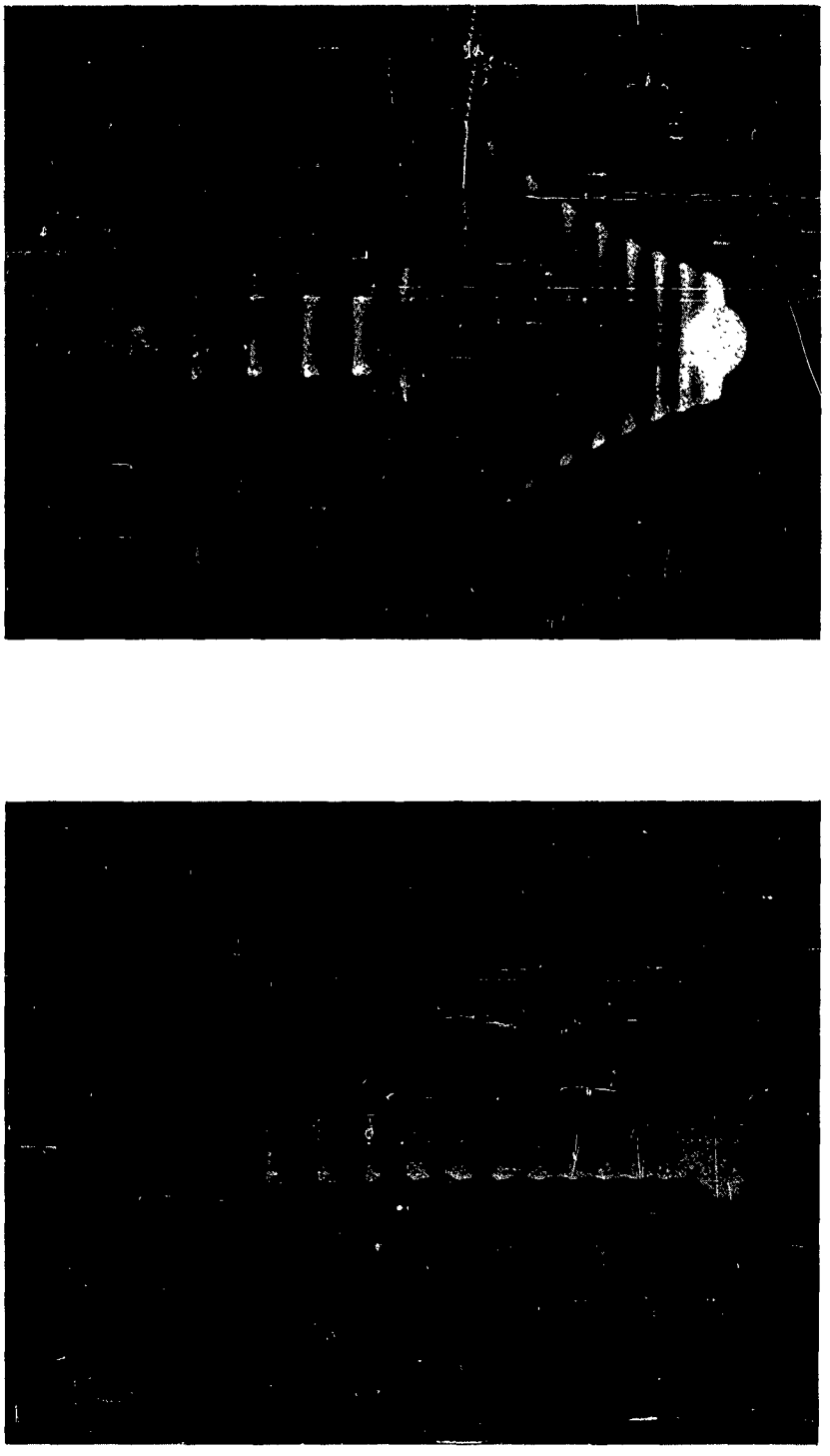

Fig. 31. Transient Pressure Traces of Alloy, Water Reaction, Run 59 and Run 60, Reactor I, Time Base: 230 msec.

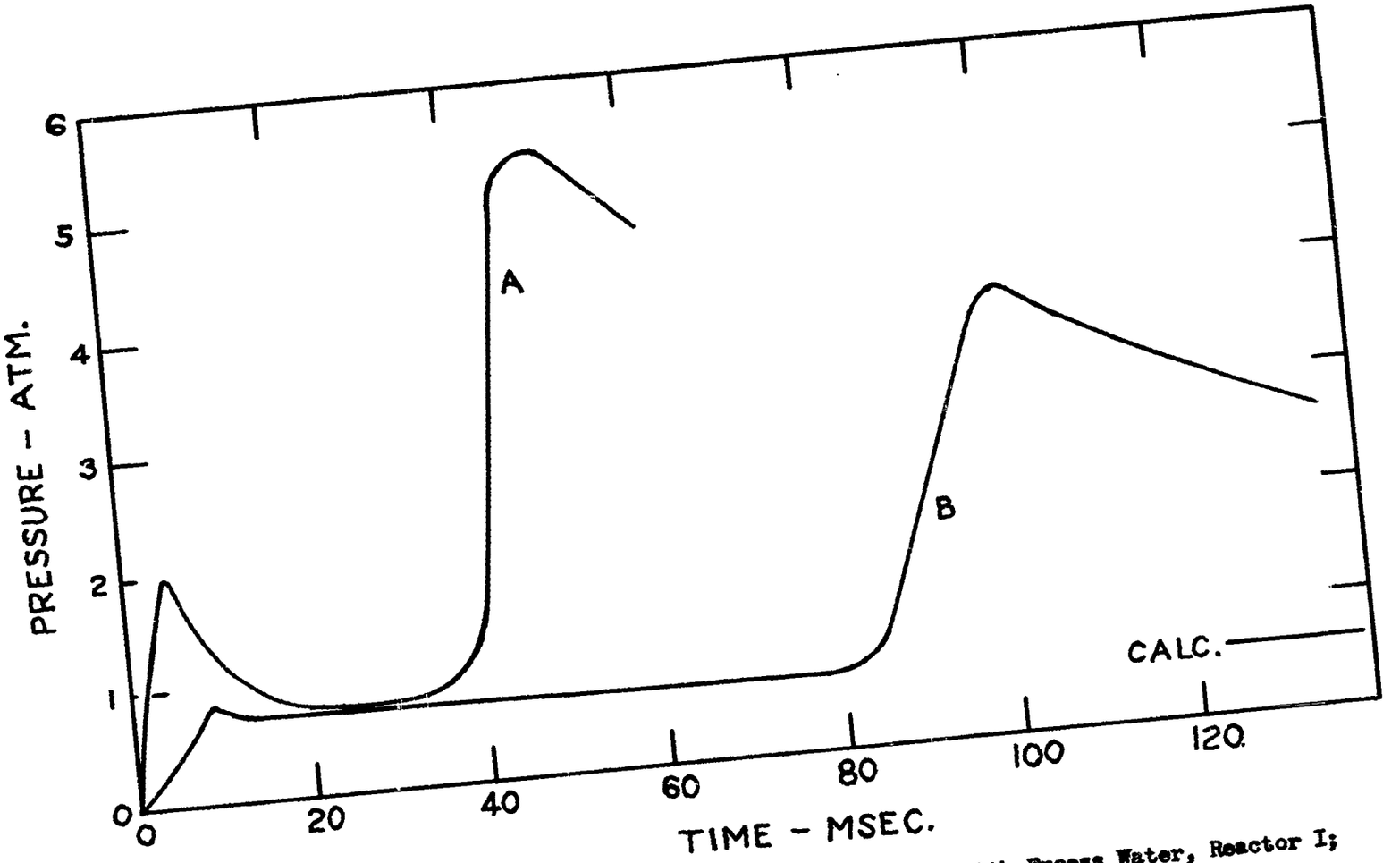

Fig. 32. Pressure Rise in Reaction of Sodium-potassium Alloy with Excess Water, Reactor I; Curve A, Run 145 (due to McKinney); Curve B, Run 59.

show two maxima, which were not entirely reproducible. In the run due to McKinney, curve A, the second pressure maximum occurred 40 msec. after mixing began, while in the run represented by curve B, the first pressure maximum was much lower and the second displaced much farther in time, occurring some 86 msec. after mixing began.

The data for the sodium-potassium alloy, water reaction are summarized in Table 20. Some of the data obtained by McKinney are included in the table. The second column of the table is the pressure of the first maximum minus the pressure corresponding to the minimum. This overswing is due to the heat of the reaction. The third column of the table gives the pressure corresponding to the minimum. This pressure is to be compared to 0.62 atm., the calculated pressure of hydrogen generated according to Eq. 19. The fourth column of the table gives the pressure corresponding to the second maximum. The second maximum will be shown to be due to an explosion occurring between the hydrogen liberated by the reaction and the air present initially in the reactor. The time between the second maximum and the beginning of injection is given in the fifth column of the table. The sixth column gives the final pressure of the reaction products measured on the 0 to 160 lb. per sq. in. Bourdon gage.

The first group of data in the table were obtained with laboratory air present in the reactor. The measured final pressures are well below the calculated hydrogen pressure of 0.62 atm. which is in agreement with the hypothesis that there was a hydrogen, oxygen explosion occurring. The window was built into Reactor I to further verify the existence of an explosion. In run 33, a very bright yellow flash was noted visually through the window. A run was made using Photocircuit I.

Table 20. Reaction of Sodium-potassium Alloy with Excess Water, Reactor I

Run	Overswing, in atm.	Minimum pressure, in atm.	Explosion pressure, in atm.	Ignition delay in msec.	Final pressure, in atm.	Footnote
33	0.11	0.70	3.40	80	vac.	a
59	0.25	0.61	3.91	86	0.07	a
36	0.43	0.65	3.57	44	-	a
155	0.44	0.57	2.52	50	-	b
152	0.53	0.79	2.96	47	-	b
154	0.75	0.79	3.40	54	-	b
145	1.44	0.73	5.52	40	-	b
52	0.10	0.61	3.32	37	0.17	c
61	0.07	0.65	3.18	40	0.10	d
60	0.31	0.48	-	-	0.48	e
54	0.31	0.48	3.47	44	0.14	f
56	0.14	0.41	2.30	22	vac.	g

[a] Laboratory air present initially.
[b] Runs made by McKinney.
[c] Reactor atmosphere contained only 5 to 10% oxygen.
[d] Water was 0.036 M in acetaldehyde.
[e] Atmosphere was 5 to 10% oxygen and water was 0.036 M in acetaldehyde.
[f] Water was 10 M in KOH.
[g] Atmosphere was 5 to 10% oxygen and water was 10 M in KOH.

The photoelectric trace is shown in Fig. 33. The light emission began about 17 msec. after mixing began.

The poor reproducibility of the height of the first maximum and the ignition delay of the explosion is probably due to the uneven descent of the two pistons in Reactor I. It is likely that the large piston started to move first. This would force water into the small cylinder containing the alloy. This early reaction heated up the unreacted alloy so that the reaction eventually took place at a higher temperature. The effective reactant ratio for the reaction occurring in the small cylinder was closer to unity than if proper mixing were obtained. This could produce excessive heating of a small amount of material and give rise to the large first maximum. The shortened ignition delay was also probably due to the high temperature created by the uneven starting of the pistons. The runs plotted in Fig. 32 show the extreme cases. Run 59, curve B, had a very small overswing and a long ignition delay while run 145, curve B, had a large overswing and a short ignition delay.

The effects of the delay in starting of the small piston on the alloy, water reaction would be more serious if the small cylinder were not full. The method used by McKinney to load the alloy into the reactor gave no indication of how much alloy actually entered the cylinder. The method used in the present study made it possible to judge how full the cylinder was. For the runs reported in Table 20, the weight loss of the sample vial varied between 0.83 and 0.90 gm. except for run 36 in which the weight loss was only 0.62 gm. Reference to the table will show that run 36 showed a relatively high overswing and a shortened ignition delay.

Several runs were made to test the effect of additives and changes

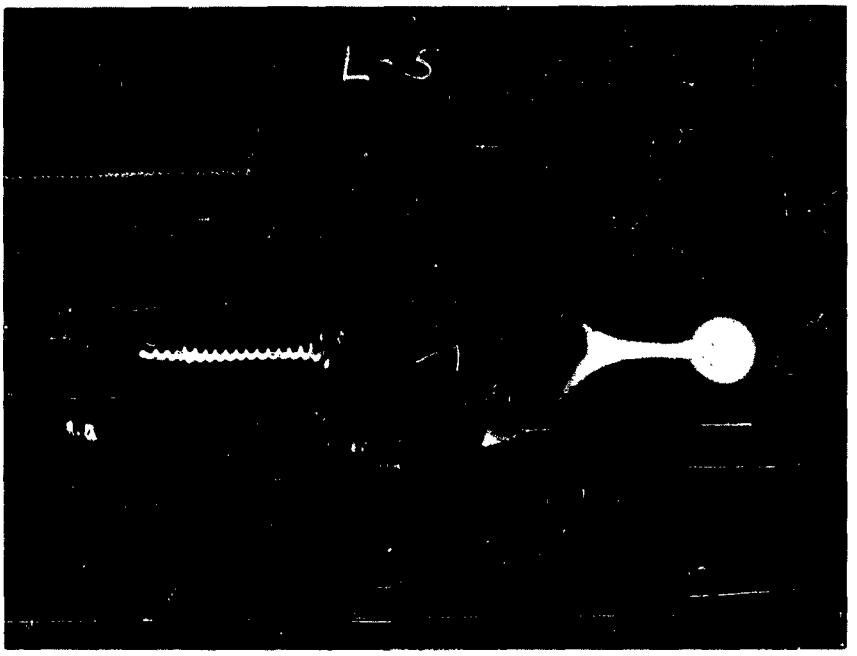

Fig. 33. Light Intensity Trace of Alloy, Water Reaction, Reactor I, Time Base: 65 msec.

of atmosphere. The reactor atmosphere was flushed with nitrogen in several runs. This was accomplished by filling a shallow glass tray in the interior of the reactor with liquid nitrogen before the reactor was completely assembled. The liquid nitrogen evaporated gradually after the reactor had been assembled. The gas was allowed to escape through a valve located on the piping leading to the strain gage. Several hours were then allowed for the reactor to reach room temperature before the injection was begun. It is not certain how much of the oxygen of the original reactor atmosphere was removed by this procedure. It was estimated that the oxygen content was reduced to a value between 5 and 10%. The data are shown in Table 20. This procedure was carried out in the case of run 52. The ignition delay was reduced to 37 msec. even though there was a low first maximum. When the water was replaced by a solution 0.036 M in acetaldehyde, the delay was found to be 40 msec. The acetaldehyde was added to remove the dissolved oxygen from the water. When the reactor was flushed and the acetaldehyde solution used, there was no ignition. The trace, run 60, is shown at the bottom of Fig. 31. It is apparent from the trace that there is no second maximum. In this case, the final pressure was closer to the expected yield of hydrogen. Two runs were made of the reaction of the alloy with an excess of 10 M KOH solution. With air present in the reactor, the ignition delay was 44 msec. When the oxygen content of the air was reduced to 5 or 10%, the ignition delay was reduced to only 22 msec.

Reaction of Sodium-potassium Alloy with Water in Reactor II

A different procedure was used to load the alloy into one of the cylinders of Reactor II. The alloy was purified in a few cases by distillation. In most cases, the alloy was freed of oxide and other

solids by filtering it through a fine glass capillary in a high vacuum apparatus. About 5 cc. of alloy were transferred from the steel container in which it was delivered from the manufacturer to the glass vacuum apparatus by means of a 5 cc. hypodermic syringe having a four inch needle. The opening in the vacuum apparatus was then sealed off. The system was evacuated and the alloy heated slightly to increase its fluidity. Nitrogen pressure was then applied to the alloy forcing it to flow through a fine glass capillary about ten inches long. The alloy discharged into a vial which could be sealed off under vacuum. The alloy showed no trace of either white oxide particles or dark solid impurities after this treatment.

The reactor was loaded by transferring the alloy from the vial to the cylinder with a medicine dropper in a dry-box. The dry-box atmosphere had to be free of both water vapor and oxygen. The dry-box was made from a large desiccator. The top of the desiccator was replaced by a one-eighth inch thick brass plate. The plate had three large holes in it. Two of these openings could be connected to rubber work gloves and the third was covered with a Plexiglass sheet. The brass plate was sealed tightly to the desiccator by three one inch wide rubber bands, tightly stretched over the connection. The reactor was partially assembled and inserted into the desiccator along with the closed alloy vial and accessory tools. The desiccator was sealed and the atmosphere flushed overnight with Matheson Co. "prepurified" nitrogen that first passed through a heated copper trap and a phosphorus pentoxide drying train. After about ten volumes of nitrogen had passed through the dry-box, the alloy could be handled with no trace of atmospheric

oxidation. The cylinder was then filled in the dry-box by the procedure described in an earlier section.

The alloy, water reaction was studied in Reactor II at a volume ratio of one to one. This corresponds to a 2.3 to 1 stoichiometric excess of water. Although the reactant ratio was fixed, the absolute amount of the two reactants could be varied from about 1.2 cc. to 0.0 cc. The reaction has been mentioned in connection with the rate of mixing studies and the study of the response of the transient pressure measuring system. Examples of the type of traces obtained are shown in Fig. 27 and Fig. 29. A pressure vs. time plot is shown in Fig. 28.

Several simultaneous measurements of the light emission and the pressure rise were made. A typical pair of traces are shown in Fig. 34. The light emission began at the same instant that injection began, i.e., the ignition delay was zero. The photoelectric trace shown in the figure (Photocircuit I) indicated that the light emission preceded the pressure rise by about one msec. This is again believed to be the time required for the first pressure pulse to travel the distance from the mixing chamber to the diaphragm of the strain gage. The operation of the photocircuit is essentially instantaneous. The light emitted by the reaction overloaded Photocircuit I so that no plot of the time distribution of the intensity could be made. The emission persisted, however, for about 20 msec.

The data obtained for the alloy, water reaction are given in Table 21. The second column of the table gives the calculated final pressure. A differing amount of reactants was used for the runs. The final pressures were calculated from Eq. 19 for the measured quantity of alloy introduced into the reactant cylinder, the volume of the reactor for the

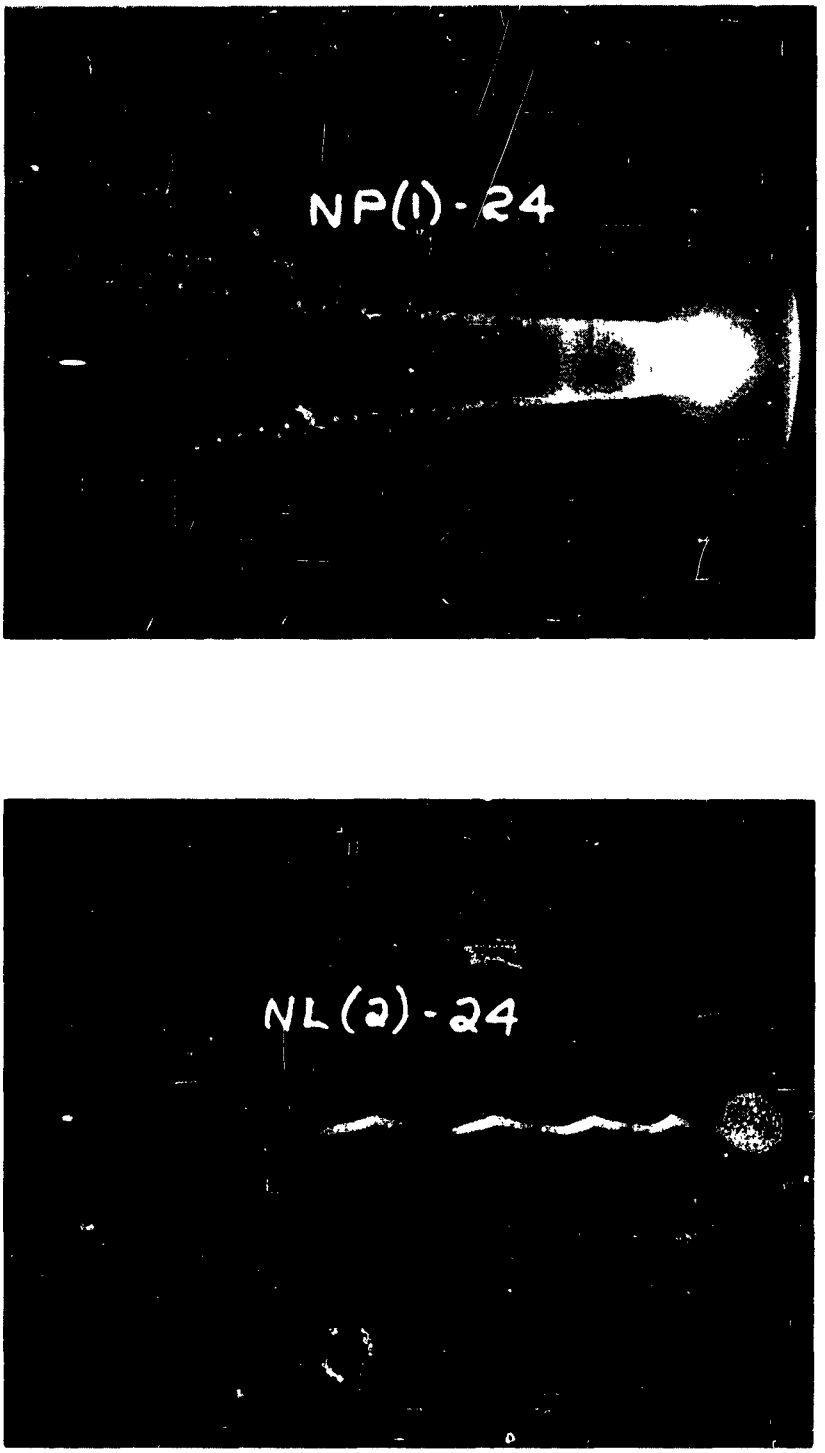

Fig. 34. Simultaneous Pressure and Light Intensity Traces of Alloy, Water Reaction, Run 24, Reactor II, Time Base: 100 msec.

Table 21. Reaction of Sodium-potassium Alloy with a 2.3 to 1 Molar Excess of Water, Reactor II

Run	Calculated final pressure, in atm.	Maximum pressure, in atm.	Observed final pressure, in atm.	Difference in calculated and observed final pressure, in atm.	Oxygen content in reactor initially, in per cent
24	1.03	8.31	-	-	21
43	0.89	3.71	0.61	0.28	21
47	0.82	6.02	0.37	0.45	21
44	0.82	6.81	0.32	0.50	21
16	0.80	6.25	0.31	0.49	21
37	0.72	6.69	0.25	0.47	21
26	0.59	3.10	0.14	0.45	21
40	0.57	4.42	0.23	0.35	21
27	0.52	3.90	0.12	0.40	21
39	0.43	2.81	0.10	0.33	21
21	0.95	5.81	-	-	1 - 2
19	0.59	3.72	0.37	0.21	1 - 2
18	0.80	3.74	0.61	0.19	0.0
17	0.61	2.59	0.37	0.24	0.0

particular run, and room temperature. The third column gives the pressure at the maximum. The fourth column gives the measured final pressure. Some of the measurements were made with the Bourdon gage; others were made by the mercury manometer method. The final column shows the calculated minus the observed value for the final pressure. The first group of data were obtained with laboratory air present in the reactor initially. The table is arranged in the order of the amount of reactants employed. The maximum pressures generally decreased as the amount of reactants were decreased with the exception of run 43 where it appears that the explosion was inhibited in some way. The difference in the calculated and observed final pressure values indicated that the explosion consumed 30 to 50% of the hydrogen yield (excluding run 43).

Several runs were made in which the reactor atmosphere was flushed with nitrogen. In two runs, 21 and 19, the reactor was flushed with tank nitrogen that was stated by the supplier to contain about 1% oxygen. Two valves were connected to Reactor II so that the atmosphere could be flushed very thoroughly. In two runs, 18 and 17, the reactor was flushed with Matheson "prepurified" nitrogen which had been first passed through a heated copper trap and through a phosphorus pentoxide drying train. The water used for these two runs was boiled and loaded into the reactor while hot. The water had several hours to reach room temperature while the reactor was being flushed. These runs showed a maximum pressure lower than those obtained with air present. The agreement between the calculated and observed final pressures was also much better. The constant discrepancy, ca. 0.21 atm., in the calculated minus observed value in the oxygen free runs is probably due to

unreacted alloy remaining in the lead tube and jet of the mixing plate.

Reaction of Sodium-potassium Alloy with Ethanol in Reactor II

The procedure for loading the alloy into Reactor II has already been described. Gold Shield Absolute Alcohol was used without further purification. The alloy was loaded in the dry-box, while the alcohol was loaded quickly in the air. The reaction was studied at a volume ratio of one to one. This corresponds to a 1.42 to 1 stoichiometric excess of the alloy over the alcohol. The reaction can be represented by Eq. 20.

(20) $$M + C_2H_5OH \longrightarrow C_2H_5OM + 0.5\ H_2$$

Three runs were made of the reaction carried out in the presence of laboratory air and three were made after the reactor had been thoroughly flushed with the highly purified nitrogen described previously.

A typical pressure vs. time plot for the reaction carried out in the presence of air is shown in Fig. 35. A powerful light flash was observed visually for these runs and hence the second maximum probably involved the hydrogen, oxygen explosion. The calculated and observed final pressures are shown at the lower right of the figure. Carbon deposits were found in the reactor after the runs suggesting the participation of alcohol in the explosion. Unreacted alloy was also found after each run. The data are summarized in Table 22. The reaction shows two pressure maxima. The pressure corresponding to the first maximum was of the correct order of magnitude to attribute to the hydrogen liberated by the reaction as expressed in Eq. 20.

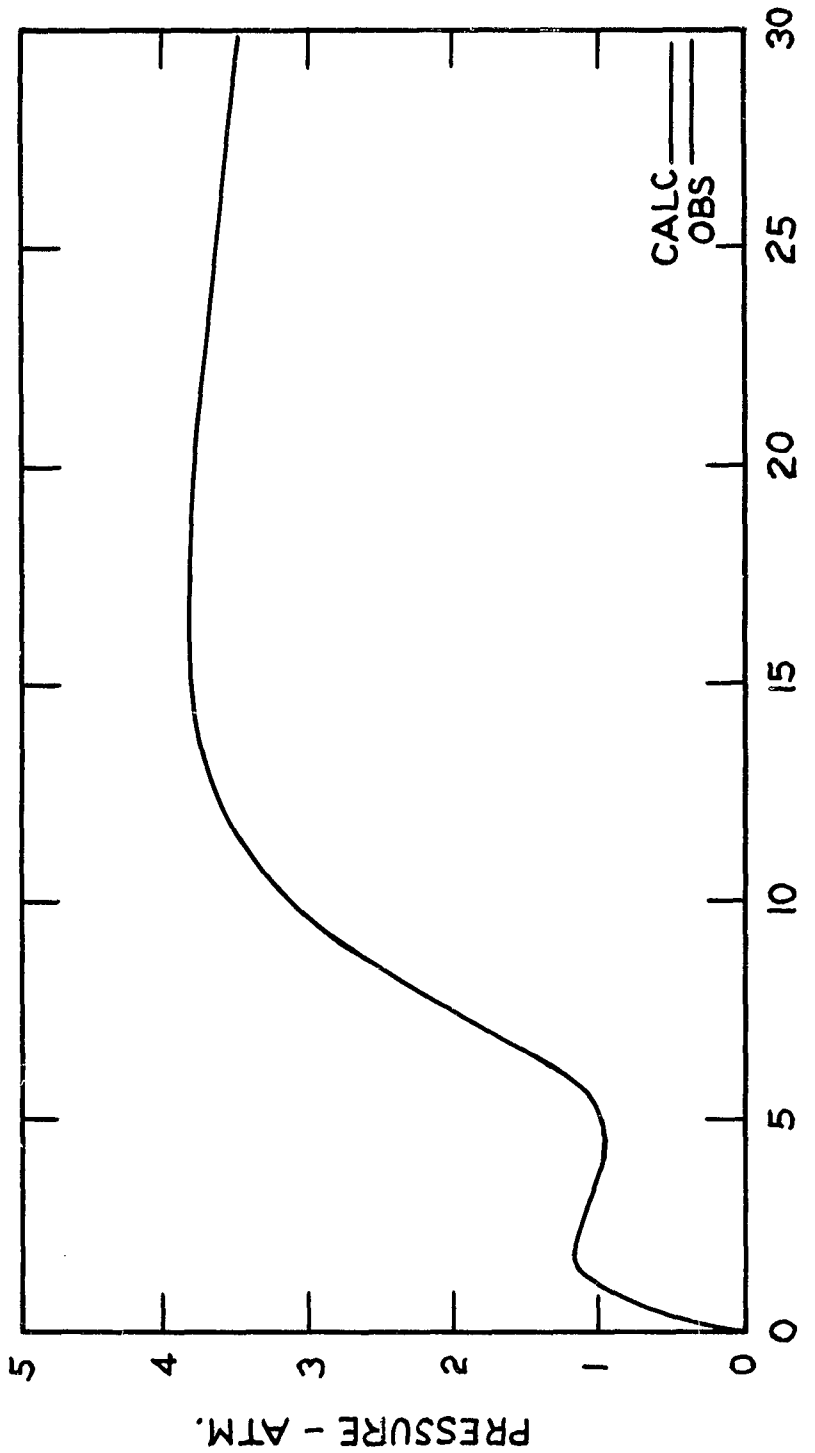

Fig. 35. Pressure Rise in Reaction of Sodium-potassium Alloy with Ethanol in the Presence of Air, Run 57, Reactor II.

Table 22. Reaction of Ethanol with a 1.42 to 1 Molar Excess of Sodium-potassium Alloy in the Presence of Air, Reactor II

Run	Calculated final pressure, in atm.	Maximum pressure, in atm.	Observed final pressure, in atm.	Ignition delay, in msec.
55	0.23	2.54	0.14	1.8
56	0.50	3.72	0.38	4.5
57	0.40	3.90	0.33	5.5

Because of the low value of this pressure and the noise associated with the traces from Reactor II, it was not possible to evaluate accurately the pressure variations occurring during the first few msec. of the reaction. The beginning of the second maximum was clearly delayed as indicated in the fifth column of Table 22. The observed final pressures were somewhat below the values calculated from the expected yield of hydrogen. The exact significance of the final pressure is most uncertain because of the fact that carbon deposits were found.

A typical pressure vs. time plot for the reaction carried out in inert atmosphere is shown in Fig. 36. The curve at the left was obtained from an oscilloscope trace in the usual way; the curve at the right was taken from readings made on the mercury manometer for a period of over an hour. The calculated final pressure is shown at the right of the figure. There is only one maximum. The pressure variations occurring during the first 30 msec. of the reaction could not be evaluated very accurately because of the effect of noise on the very low pressure values involved. The data are shown in Table 23. The reaction responsible for the slowly rising pressure occurring beyond a minute after the initiation of the reaction is not known.

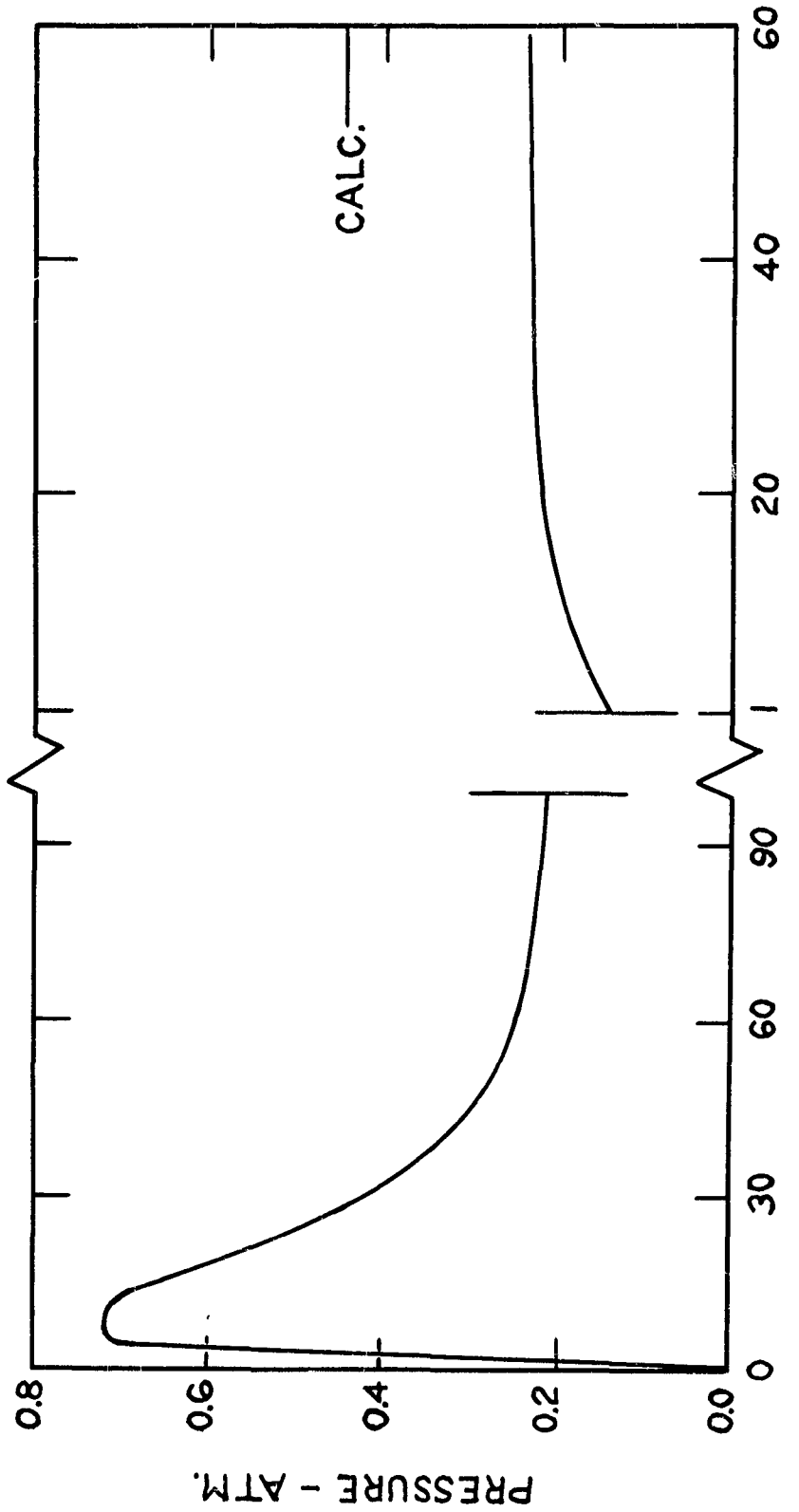

Fig. 36. Pressure Rise in Reaction of Sodium-potassium Alloy with Ethanol in the Absence of Air, Run 60, Reactor II.

Table 23. Reaction of Ethanol with a 1.42 to 1 Molar Excess of Sodium-potassium Alloy in the Absence of Air, Reactor II

Run	Calculated final pressure, in atm.	Pressure at 100 msec., in atm.	Pressure at 1 min., in atm.	Pressure at 1 hour, in atm.
58	0.409	0.16	0.13	- *
59	0.355	-	0.12	- *
60	0.445	0.22	0.14	0.23

* A slowly rising pressure was noted but not followed.

Pressure Measurements of the Hydrazine, Nitric Acid Reaction

The nitric acid used in the study was prepared by the vacuum distillation of a mixture of nitric and sulfuric acids. Approximately 100 cc. of Merck Reagent Grade Fuming Nitric Acid, about 95% HNO_3, and 100 cc. of General Chemical Co. Reagent Grade Sulfuric Acid, about 95% H_2SO_4, were mixed and placed in a 250 cc. flask contained on an all glass high vacuum apparatus. The mixture was cooled to 0°C by means of an ice bath before the apparatus was evacuated. The anhydrous nitric acid was collected in a large trap cooled by a dry ice, trichloroethylene bath. It required about 30 hours in a vacuum of 10^{-4} mm. Hg to collect 50 cc. of the anhydrous material. The material was then distilled in vacuum into a large vial and removed from the vacuum apparatus. The acid was poured quickly into a 250 cc. Erlenmeyer flask having a ground glass stopper lubricated with fluorocarbon grease. The material was stored between runs by placing the flask in a dry ice bath. The acid used for most of the runs was completely colorless. In a few runs the acid had a slight yellow color corresponding to decomposition into

nitrogen dioxide, water and oxygen. The acid was analyzed by the method outlined in Appendix III. The various batches of acid, both freshly prepared and after long periods of storage, consistently analyzed between 100.2 and 100.8% HNO_3. The nitrogen dioxide content of a badly colored batch was found to be only 0.1% by the method described in Appendix III.

The hydrazine was prepared from Matheson Co. Anhydrous Hydrazine, about 95% N_2H_4, by refluxing and vacuum fractionation from calcium or barium oxide. An equal quantity of the hydrazine and the oxide were added to the pot of an all glass vacuum distilling apparatus. The material was refluxed in a nitrogen atmosphere for several hours at a pressure of about 50 mm. Hg. The hydrazine was then fractionated, the first half being collected. The product of several such preparations were analyzed by the method outlined in Appendix III and found to be between 97.7% and 99.0% N_2H_4.

Both materials were loaded into Reactor II using the automatic pipet method described in a previous chapter. The amount of reactants used for a run were such that a stroke length of the piston system of seven-eighths inch was obtained. The resulting reactant volumes are given in Table 24 for the various reactant ratios that were studied. The corresponding weight and mole ratios are also given in the table.

The pressure generated by the reaction was found to be much higher than that obtained in the reactions of sodium-potassium alloy. Because of this, some difficulty was experienced in preventing leakage of the product gases through the piston gaskets. Difficulty also resulted from the fact that the solutions tended to back up through the gaskets during injection. This resulted in poor reproducibility of the pressure traces. At first, both gaskets on the pistons were made of neoprene and

Table 24. Amounts of Hydrazine and Nitric Acid Employed in a Run in Reactor II

Nominal reactant ratio	Volume HNO_3, in cc.	Volume N_2H_4 in cc.	Weight ratio:* nitric acid to hydrazine	Mole ratio: nitric acid to hydrazine
4 : 1	2.84	0.74	5.65	2.87
2 : 1	1.59	0.74	3.17	1.61
1.5 : 1	1.11	0.74	2.20	1.12
1 : 1	1.11	1.11	1.48	0.75
1 : 1.5	0.74	1.11	1.00	0.51
1 : 2	0.74	1.59	0.69	0.352

impregnated with an inert grease. Both hydrazine and nitric acid attacked the lower gasket resulting in severe leakage. A lower gasket made of Teflon was then tried. Teflon, however, has no elasticity and would not assume the shape of the cylinder so that although no corrosion was apparent, the single neoprene gasket did not contain the pressure adequately. The lower Teflon gasket was replaced by one made of aluminum. The aluminum did not score the stainless steel cylinder wall nor did it lose its shape readily. Again, however, the single neoprene gasket was insufficient to contain the pressure. The leakage problem was finally solved when another neoprene gasket was added to the pistons. The final arrangement consisted of one aluminum gasket located near the leading edge of the pistons and two neoprene gaskets about one-eighth inch apart located near the trailing edge of the piston. The space between the neoprene gaskets was filled with the inert grease. The pistons are shown in Fig. 5. Samples of aluminum, fluorocarbon grease, and stainless steel of the type used in the apparatus were stored under a sample of anhydrous nitric acid for several days. No corrosion or

reaction was apparent on visual inspection.

A number of runs were made during the development of the final apparatus. The result of these runs will not be reported, however, since sufficient runs were made of the reaction with the apparatus in its final form.

The reaction of nitric acid and hydrazine can be represented by Eq. 21 for the stoichiometric mixture if it is assumed that complete thermodynamic equilibrium is reached at the temperature of the flame.

$$(21) \qquad 4\ HNO_3 + 5\ N_2H_4 \longrightarrow 7\ N_2 + 12\ H_2O$$

The mole ratio corresponding to the stoichiometric mixture is then 0.80 moles nitric acid per mole hydrazine. This ratio falls in between the one to one volume ratio and the one and one-half to one ratio obtainable with Reactor II.

A typical pressure trace is shown in Fig. 37. The run was made with the one and one-half to one reactant ratio with nitric acid in excess. The pressure vs. time plot for the run is shown in Fig. 38. The pressure vs. time curves for all of the six reactant ratios showed a single pressure maximum. The time of the rise of the pressure to the maximum corresponded roughly to the time of completion of injection. The results of the pressure measurements for the reaction of one and one-half volumes of nitric acid with one volume of hydrazine are shown in Table 25. The average value of the several determinations is also shown in Table 25. The average values for all of the reactant ratios are given in Table 26.

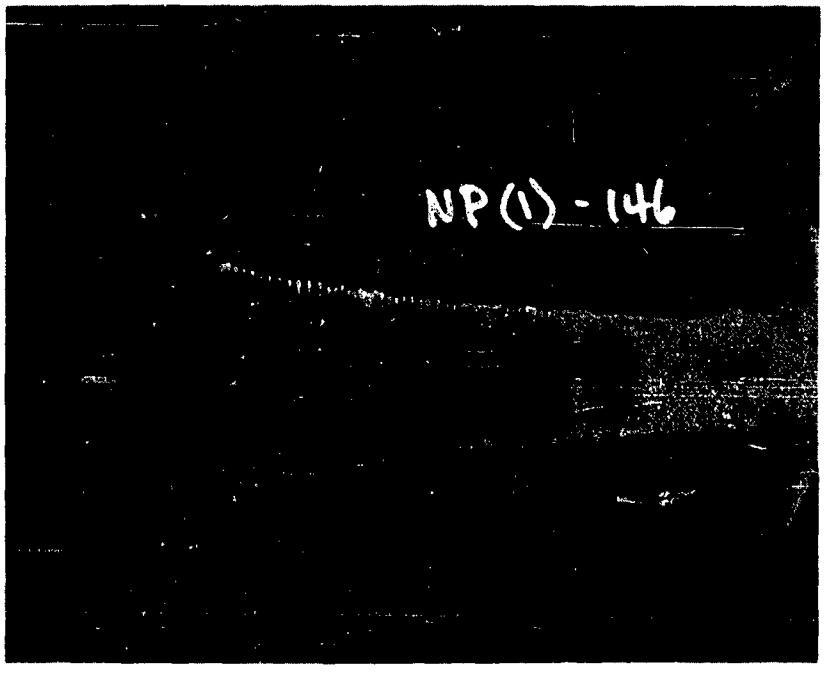

Fig. 37. Transient Pressure Trace of the Reaction of One and One-half Volumes of Nitric Acid with One Volume of Hydrazine, Run 146, Reactor II, Time Base: 100 msec.

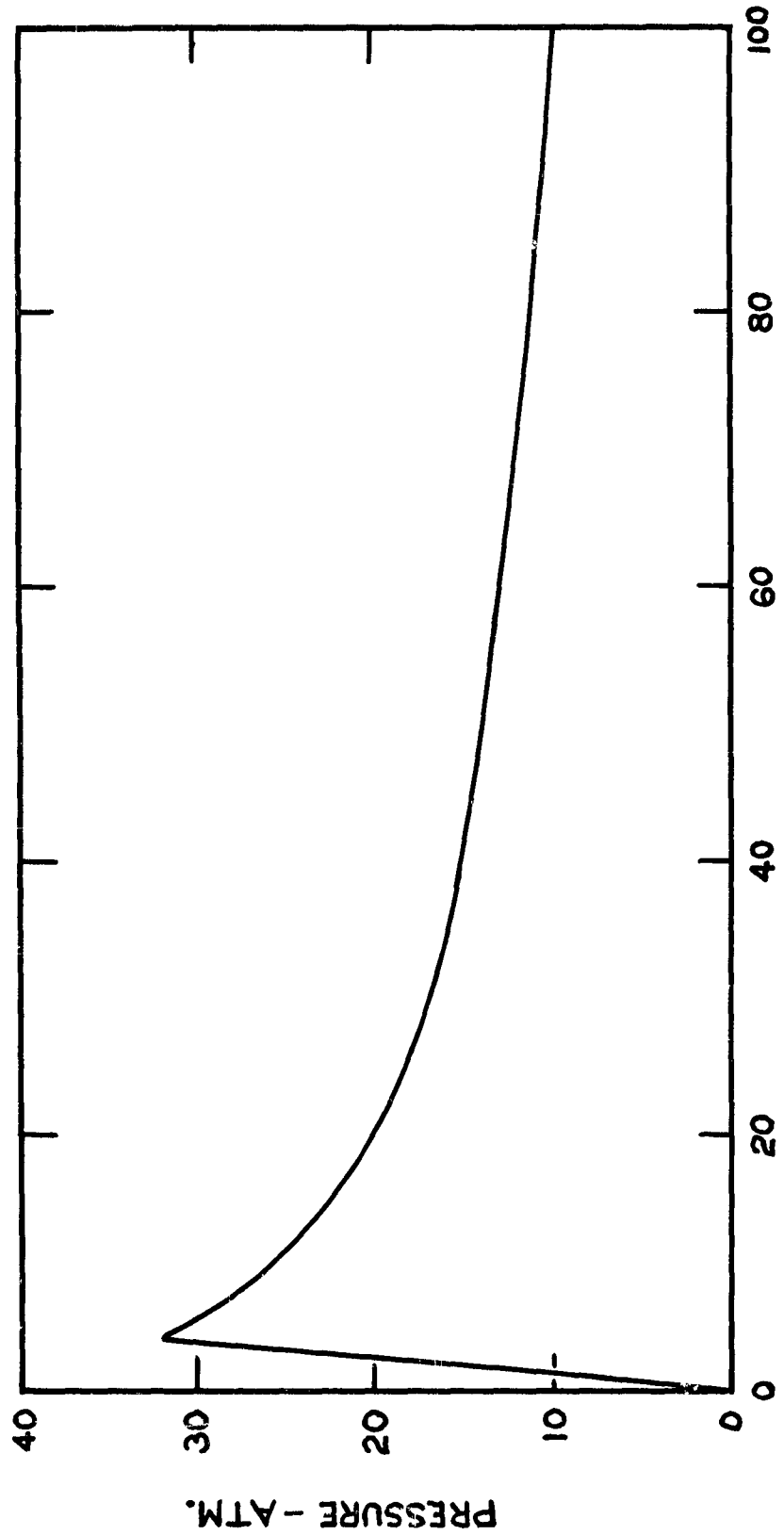

Fig. 38. Pressure Rise in Reaction of One and One-half Volumes of Nitric Acid with One Volume of Hydrazine, Run 146, Reactor II.

Table 25. Results of Pressure Measurements for the Reaction of One and One-half Volume of Nitric Acid with One Volume of Hydrazine

Run	Maximum pressure rise, in atm.	Time from the start of the pressure rise to the maximum, in msec.	Pressure, 20 msec. after the start of the pressure rise, in atm.	Final pressure, in atm.
141	32.8	4.30	20.7	-
142	31.0	4.00	19.0	1.84
146	32.0	4.00	19.6	1.79
147	30.9	3.90	19.0	1.79
Ave.	31.7	4.05	19.6	1.80

Light Emission Measurements of the Hydrazine, Nitric Acid Reaction

A number of simultaneous measurements of the transient pressure and the light emission were made for each of the six reactant ratios studied. Photocircuit II was used for all of the photoelectric measurements. The traces from a simultaneous pressure and light emission measurement are shown in Fig. 39. The results of the traces are plotted in Fig. 40. The run represented by the figure was the reaction between two volumes of hydrazine and one volume of nitric acid. The data indicated that the beginning of light emission preceded the start of the pressure rise by about 0.8 msec. The carrier wave frequency for the trace was 1080 cycles so that the relative timing between the traces has an accuracy of only about 0.5 msec. For the six reactant ratios studied, the light emission preceded the start of the pressure rise by 0.2 to 1.6 msec. Two runs made of the reaction of two volumes of nitric acid with one volume of hydrazine indicated that the pressure rise began 0.1 and 0.8 msec. before light emission began. No

Table 26. Results of Pressure Measurements for the Reaction of Hydrazine with Nitric Acid*

Nominal reactant ratio	Moles nitric acid per mole hydrazine	Time from the start of the pressure rise to the maximum, in msec.	Maximum pressure rise, in atm.	Pressure, 20 msec. after the start of the pressure rise, in atm.	Final pressure, in atm.
4 : 1	2.87	8.7	23.4	19.1	2.66
2 : 1	1.61	4.8	31.6	21.8	2.21
1.5 : 1	1.12	4.1	31.7	19.6	1.80
1 : 1	0.75	4.7	46.7	30.5	3.35
1.5 : 1	0.51	3.7	43.2	24.5	3.57
2 : 1	0.352	4.9	51.3	33.5	5.26

* Average values of several determinations.

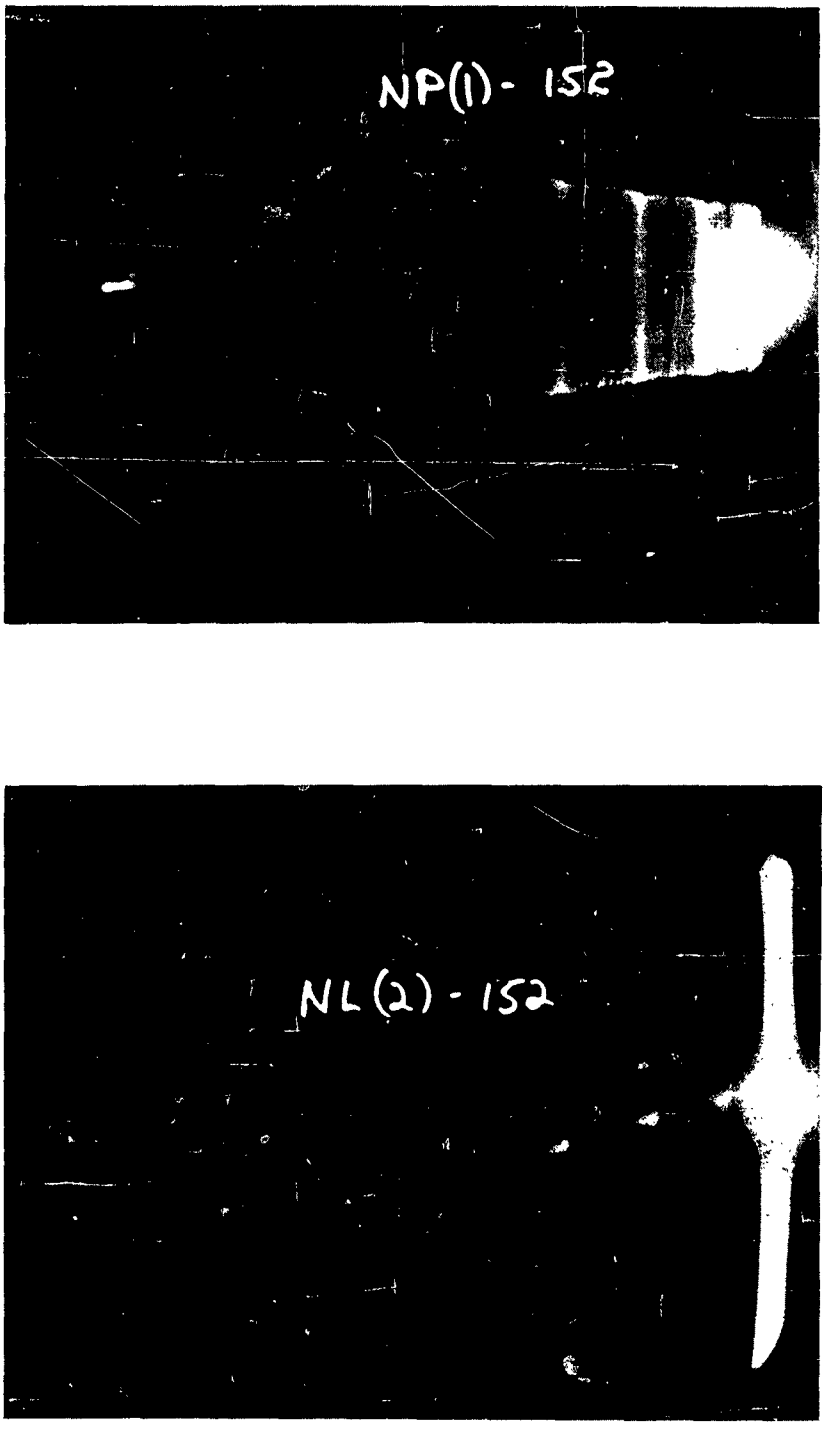

Fig. 39. Simultaneous Pressure and Light Intensity Traces of the Reaction of Two Volumes of Hydrazine with One Volume of Nitric Acid, Run 152, Reactor II, Time Base: 100 msec.

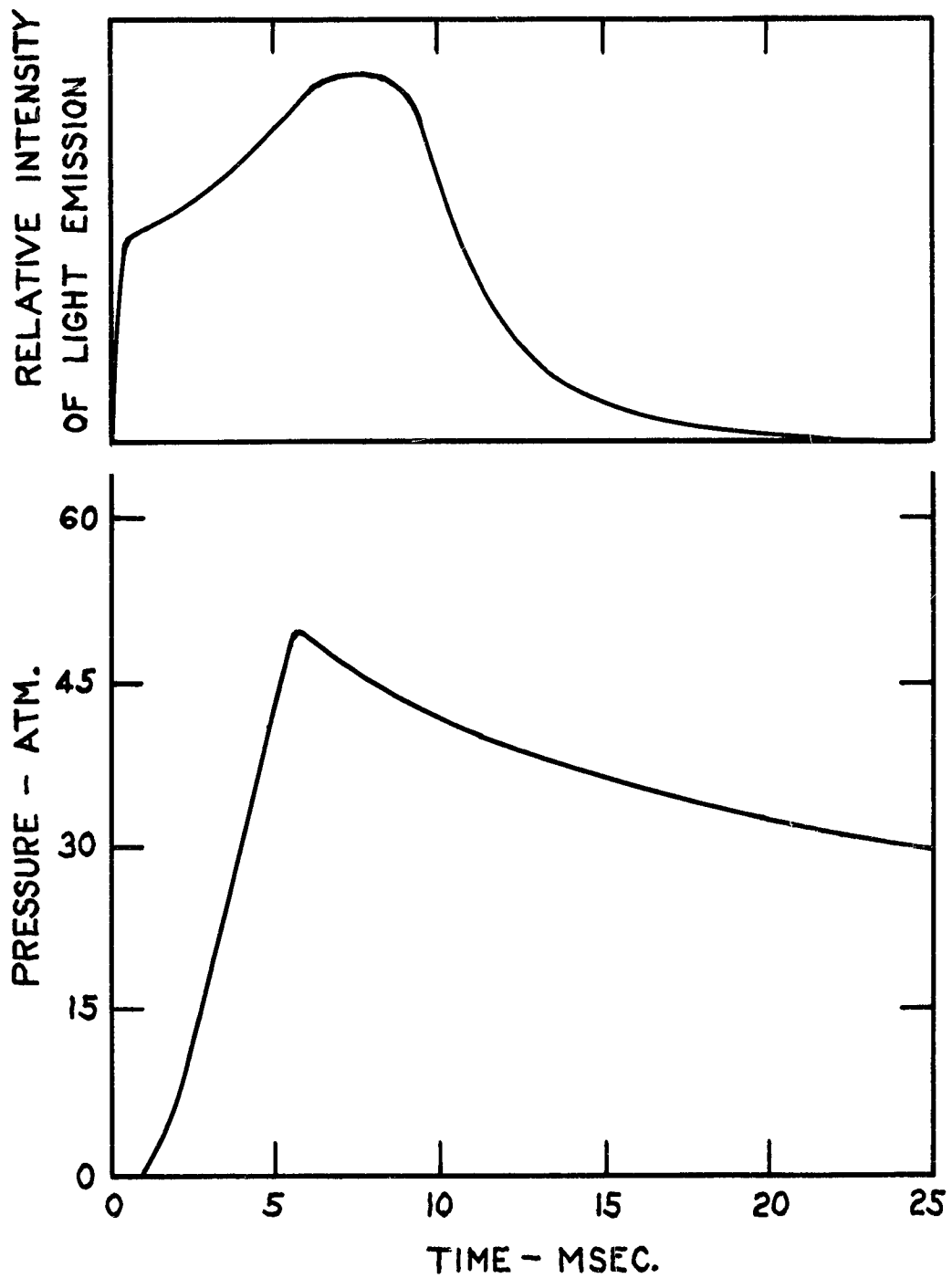

Fig. 40. Pressure Rise and Light Intensity in Reaction of Two Volumes of Hydrazine with One Volume of Nitric Acid, Run 152, Reactor II.

significance could be attached to this observation because of the estimated experimental error of 0.5 msec.

The amplitude of the photoelectric traces was not reproducible for the reasons discussed previously. The relative intensity of the light emission, however, increased as the ratio of hydrazine to nitric acid was increased. The light intensity produced by reactions in excess nitric acid was very low. Only a dull red flash was noted by visual observation. The emission persisted in some cases beyond 20 msec. for the acid rich runs. Plots of light intensity vs. time are shown in Fig. 41 for the reaction of one and one-half volumes of nitric acid with one volume of hydrazine (run 146) and for the reaction of equal volumes of the two (run 107). The light emitted by the one and one-half to one mixture persisted for only a few msec. The light emitted by the reaction in excess hydrazine persisted for a much longer time. The light emission from the three hydrazine excess reactant ratios all had a time distribution similar to that shown in Fig. 41 for the equal volume case (run 107). The light emission persisted for the hydrazine rich reactions up to 20 msec. in some cases.

Injection Rate Measurements of the Hydrazine, Nitric Acid Reaction

A number of simultaneous measurements of the transient pressure and the injection rate were made for each of the six reactant ratios studied. Photocircuit III was employed for these measurements. The traces from a typical simultaneous measurement are shown in Fig. 42. The results of the traces are plotted in Fig. 43. The plot represents a run made of the reaction of one and one-half volumes of nitric acid with one volume of hydrazine. It is apparent from the figure that the pressure rise began 2.2 msec. after the beginning of injection. The

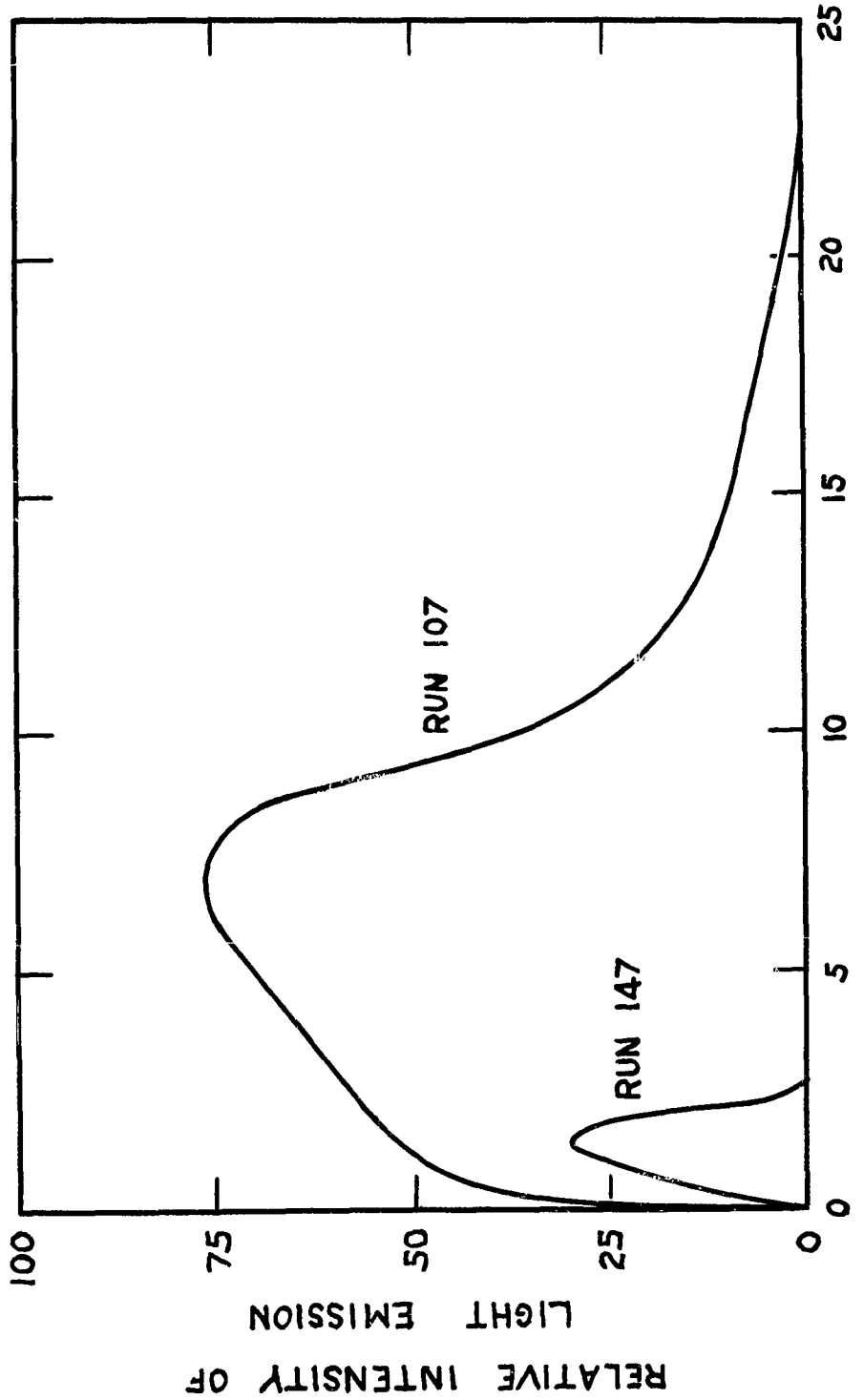

Fig. 41. Light Intensity in the Reaction of One and One-half Volumes of Nitric Acid with One Volume of Hydrazine, Run 147; and the Reaction of Equal Volumes of the Two, Run 107.

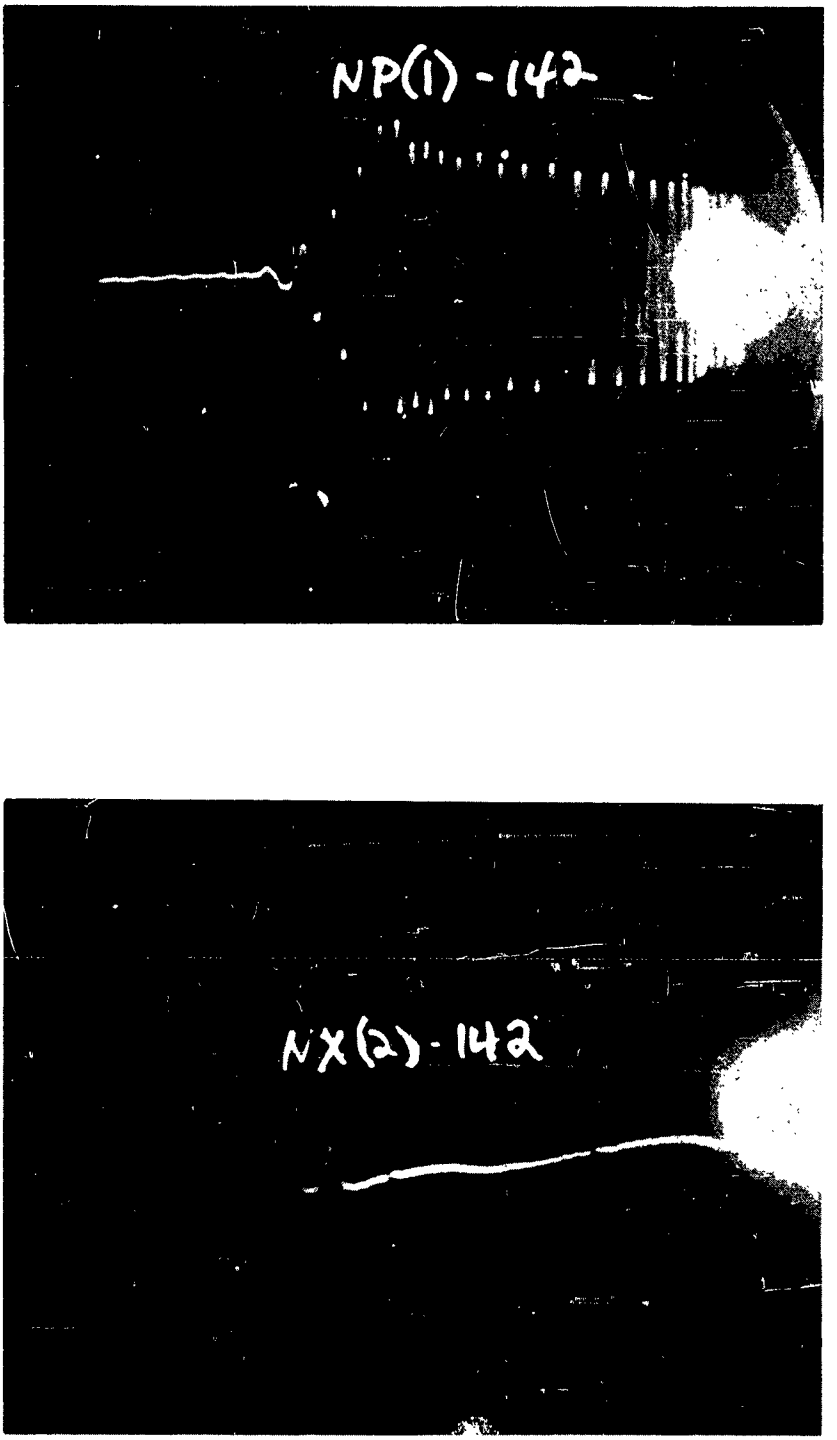

Fig. 42. Simultaneous Pressure and Injection Rate Traces of the Reaction of One and One-half Volumes of Nitric Acid with One Volune of Hydrazine, Run 142, Reactor II, Time Base: 25 msec.

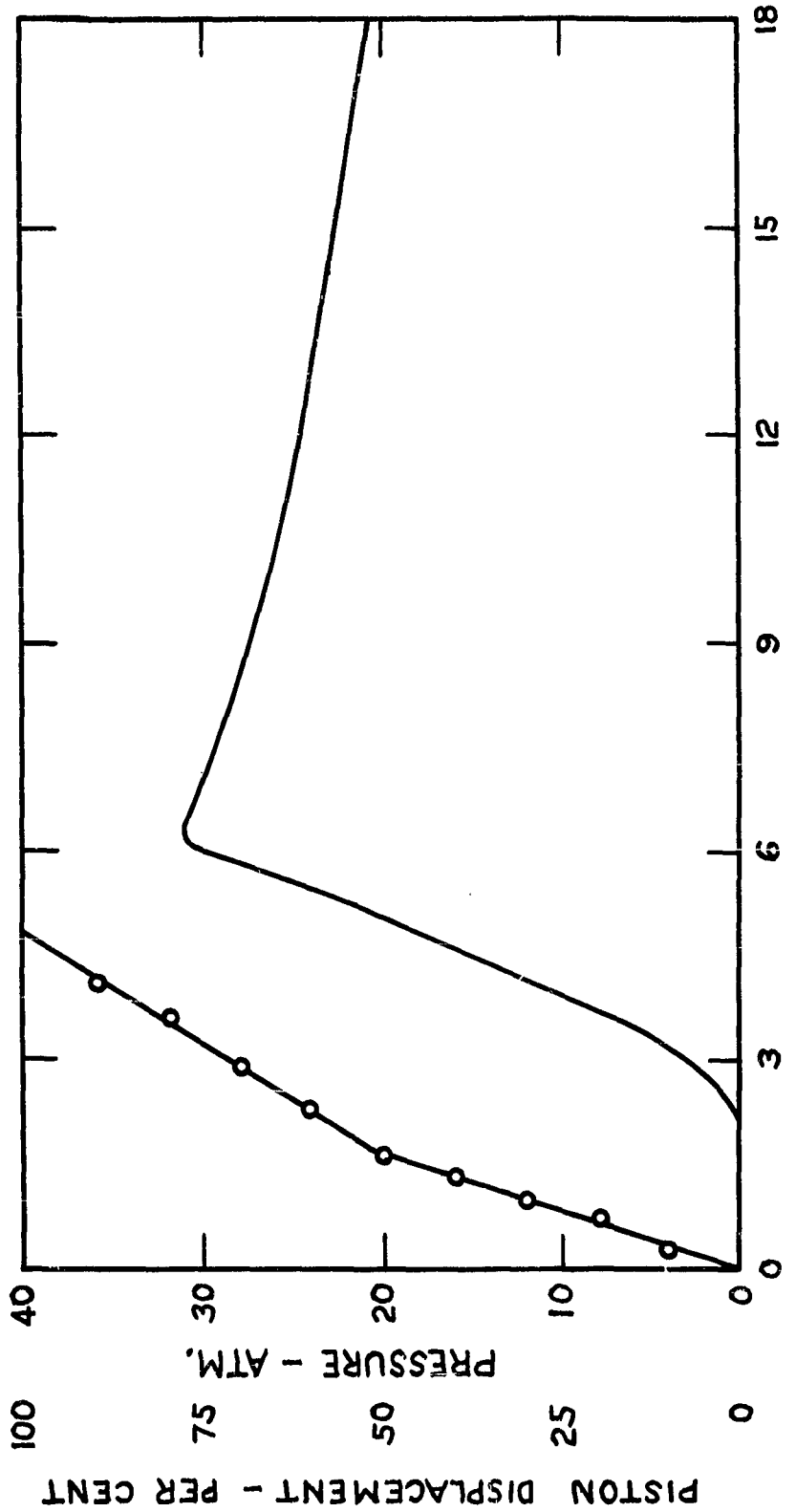

Fig. 43. Simultaneous Measurement of Injection Rate and Pressure Rise in the Reaction of One and One-half Volumes of Nitric Acid with One Volume of Hydrazine, Run 142, Reactor II.

relative timing between a pressure trace and an injection rate trace has already been estimated to be accurate to within 0.2 msec. The plot of piston position vs. time shows a definite break in the slope. This break was not observed in any of the results obtained for the injection of water. The slowing of the injection rate must have been due to the kinetic reaction of the flame on the injection system. The constancy of the injection velocity near the completion of injection suggests that a stable flame front is produced within the exit tube before injection is complete.

The time between the beginning of injection and the point of change of the injection rate was evaluated for all of the runs by graphically estimating the point of intersection of the two linear portions of the plot. The results are shown in the fourth column of Table 27. The time from the beginning of injection to the beginning of the pressure rise is reported in the fifth column of Table 27. This time varied between 1.3 and 2.2 msec. This time must be the sum of the time required for the first pressure pulse to travel from the mixing chamber to the diaphragm of the strain gage and the ignition delay referred to the pressure rise. An infinitesimal disturbance will travel through a fluid at the velocity of sound. The disturbance produced by the evolution of gases from the reaction in question probably is initiated as a shock wave and hence is propagated at a supersonic velocity. The channel connecting the strain gage to the reactor, however, has five 90° bends and various surface irregularities. A shock wave could not be propagated through such a channel without suffering numerous reflections and complex interactions with the walls of the channel. It is thus likely that the average velocity of the initial

Table 27. Results of Simultaneous Injection Rate and Transient Pressure Measurements for the Hydrazine, Nitric Acid Reaction

Run	Reactant ratio	Reactant in excess	Time to change of injection rate, in msec.	Time to start of pressure rise, in msec.	Ignition delay referred to the pressure rise, in msec.	Overall injection time, in msec.	Time from start to peak of pressure rise, in msec.
101	4 : 1	HNO_3	3.2	1.5	0.2	9.2	5.6
110	2 : 1	HNO_3	1.1	1.7	0.4	5.7	5.2
139	2 : 1	HNO_3	1.9	2.0	0.7	5.2	-
140	2 : 1	HNO_3	1.5	1.6	0.3	5.4	4.4
141	1.5 : 1	HNO_3	1.3	2.1	0.8	4.9	4.3
142	1.5 : 1	HNO_3	1.6	2.2	0.9	4.8	4.0
109	1 : 1	-	1.1	1.3	0.0	5.0	5.0
111	1 : 1	-	1.1	1.5	0.2	4.3	4.6
143	1.5 : 1	N_2H_4	2.0	1.6	0.3	4.9	4.1
144	1.5 : 1	N_2H_4	1.5	1.4	0.1	4.3	3.7
154	2 : 1	N_2H_4	1.2	1.7	0.4	6.4	5.3

disturbance is not much higher than the sonic velocity. The distance the disturbance has to travel from the exit tube of the mixing plate to the strain gage is about 1.5 feet. The velocity of sound in air at room temperature is 1120 feet per second. The time required for the pressure wave to travel this distance then could not exceed 1.3 msec.

The ignition delay referred to the beginning of the pressure rise is equal to the time to the start of the pressure rise, shown in the fifth column of the table, minus 1.3 msec. if it is assumed that the pressure wave required 1.3 msec. to reach the strain gage. The calculated ignition delay values are shown in the sixth column of the table. Values between 0.0 and 0.9 msec. were obtained. The data obtained for the time between the beginning of light emission and the beginning of the pressure rise is a direct measure of the transit time of the initial pressure wave if it is assumed that the light emission occurs simultaneously with the pressure rise. Values between 0.2 and 1.6 msec. were reported in the previous section. The calculated value of 1.3 msec. is in qualitative agreement with the observed range of values. The agreement also indicates that the pressure rise and the light emission begin simultaneously within the experimental error of the measurements.

The rate of equilibration of the pressure in the interior of the reactor with the pressure acting on the strain gage should increase rapidly during the injection. The velocity of sound in a perfect gas is directly proportional to the square root of the absolute temperature. As the reactor atmosphere becomes heated due to the heat of the reaction, the equilibration rate would increase. This would explain in part why the pressure rise seems to accelerate slightly during the

approach to the pressure peak even though the injection rate has slowed. The over-all injection time is compared to the time required for the pressure to reach the peak value in the seventh and eighth columns of Table 27. The data show that the pressure rise is completed in a somewhat shorter time than the injection time. This is also presumably due to the increased rate of pressure equilibration.

The initial injection rate corresponding to the first linear portion of the plot shown in Fig. 43 should be the rate that would be maintained if no reaction processes were involved. The initial and final injection velocities were obtained by graphical measurement of the slopes of the linear portions of the plots. The measured values are given in the sixth and seventh columns of Table 28. The injection rate is expressed as the time for the piston system to descend seven-eighths inch. The data in Table 28 show that the injection rate is decreased by a factor of approximately two because of the thrust created by the reaction process. The initial injection rate can be calculated by the method used to calculate the rate of water injection. The measured driving gas pressure given in the fourth column of Table 28 was first corrected for the pressure drop due to gas flow in the pneumatic injector using the result of the calculation reported in Appendix II. The corrected driving gas pressure was then used in conjunction with the calculations detailed in Appendix I in order to derive the calculated injection rates shown in the fifth column of the table. The calculated injection times are found to be much shorter than those observed suggesting that the reaction inhibits the injection even in the early stages of injection.

Table 28. Injection Rate Measurements for the Hydrazine, Nitric Acid Reaction

Run	Reactant ratio	Reactant in excess	Driving pressure, in lb. per sq. in.	Calculated initial injection time, in msec.	Observed initial injection time, in msec.	Observed final injection time, in msec.
101	4 : 1	HNO_3	1600	4.3	6.4	11.9
110	2 : 1	HNO_3	1600	2.1	2.7	7.5
139	2 : 1	HNO_3	1350	2.1	3.9	6.5
140	2 : 1	HNO_3	1300	2.2	3.7	6.6
141	1.5 : 1	HNO_3	1000	1.6	3.2	6.0
142	1.5 : 1	HNO_3	1000	1.6	3.3	6.0
109	1 : 1	-	1600	1.6	2.7	6.6
111	1 : 1	-	1500	1.7	2.1	6.8
144	1.5 : 1	N_2H_4	1250	1.3	3.0	5.6
143	1.5 : 1	N_2H_4	900	1.5	3.6	6.6
154	2 : 1	N_2H_4	1100	2.1	3.8	7.8

Analysis of the Products of the Hydrazine, Nitric Acid Reaction

Several methods were employed to derive information concerning the products of the reaction of hydrazine with nitric acid. The liquid products from several runs were collected by rinsing the reactor with distilled water. The resulting solution was analyzed for total acidity and for hydrazine by the methods described in Appendix III. Some of the liquid remained as droplets on various parts of the reactor and was not collected. It is estimated, however, that 80% or more of the liquid product of a run was collected by the method employed. There was no more than a trace of hydrazine found for any of the reactant ratios studied. The results of the analysis of total acidity are given in Table 29. The acid content is expressed as the percentage of the total nitric acid introduced into the reactor originally. The liquid products of several runs were allowed to evaporate to dryness. No solid products were found for any of the reactant ratios studied.

Table 29. Residual Acidity in the Liquid Products of the Hydrazine, Nitric Acid Reaction

Reactant ratio	Reactant in excess	Average acid content of liquid product, in per cent of original HNO_3	Number of determinations
4 : 1	HNO_3	25	1
2 : 1	HNO_3	17	6
1.5 : 1	HNO_3	12	4
1 : 1	-	0	3
1.5 : 1	N_2H_4	0	3
2 : 1	N_2H_4	0	3

Several runs were made in which the gaseous products were collected and sent to the Institute of Gas Technology for mass spectrometric analysis. For these runs the reactor was flushed thoroughly with tank helium before injection was begun. About two seconds after injection, the contents of the reactor were expanded into the five liter bulb system, which had previously been evacuated to a pressure of about 3 mm. Hg. The large volume was then transferred to a high vacuum apparatus. The volume containing the product gases was opened to the vacuum apparatus and a sample taken. The pressure of the sample was measured on a mercury manometer. The sample was then equilibrated with a liquid nitrogen bath by passing the gas back and forth through the cooled trap by means of a Toepler pump. The non-condensable gas in the small sample was then discarded. The condensed material was allowed to warm to room temperature. The total pressure of the condensibles could then be measured on the manometer. Since the two pressure measurements referred to the same gas volume, it was possible to evaluate the percentage of condensibles in the product gases. The condensibles were then discarded and another sample taken from the large bulb system. This sample was equilibrated with a cold trap. The non-condensible material was then expanded into a sample bulb and sent away for analysis on the mass spectrometer. The remainder of the product gases was then slowly passed through a trap cooled by liquid nitrogen so that all of the condensible products could be collected. An attempt was then made to qualitatively identify the condensible materials.

The foregoing analytical procedure was carried out on the products of the reaction of four different reactant ratios. These ratios were (1) four volumes of nitric acid to one volume of hydrazine, (2) one and

one-half volumes of nitric acid to one volume of hydrazine, (3) equal volumes of the two, and (4) two volumes of hydrazine to one volume of nitric acid. The first of these ratios is an example of an acid rich mixture. The second and third are examples of near stoichiometric mixtures. The fourth is an example of a hydrazine rich mixture. A discussion of the analysis of the products for each one of these ratios follows:

1. The reaction of four volumes of nitric acid with one volume of hydrazine: The gaseous products were crudely separated from the liquid products by the expansion of the gases into the large evacuated volume. The liquid products were allowed to remain in the reactor. The gases obtained by this manner unavoidably contained a small quantity of water vapor. The gases were then transferred to the vacuum apparatus and divided into condensible and non-condensible fractions. The gases analyzed by the mass spectrometer were only those that were not condensed by liquid nitrogen. Disregarding helium, the non-condensible gas was found to be nitrogen with only traces of hydrogen and oxygen. The condensible fraction of the product gases had the characteristic color of NO_2. The condensibles were colorless at the temperature of liquid nitrogen, however, indicating that no NO was present, since solid NO has a blue color. Any NO formed by the reaction would have been converted into NO_2 by the oxygen found in the non-condensible fraction. Any ammonia produced by the reaction would have remained in the reactor as ammonium nitrate. The only gases that could likely have been in the condensible fraction were then NO_2 and N_2O. It was not possible to separate any N_2O from the NO_2 by distillation. The sample had a pressure of 257 mm. Hg when collected in a $0^{\circ}C$ trap. The vapor

pressure of the equilibrium mixture of NO_2 and N_2O_4 at 0°C is 53 mm. Hg.[38] Any N_2O would have been entirely in the gaseous phase at this temperature so that a very rough estimate would place the total pressure of the N_2O at about 200 mm. Hg. The volume of the trap system on the high vacuum apparatus was not much greater than about 400 cc., i.e., it had approximately the same volume as the reactor, so that the total contribution of the N_2O to the final pressure of the reaction products in the reactor was probably not more than about 0.3 atm. The total final pressure for the four to one runs was shown to be 2.66 atm. in Table 26. The final result of the analysis of the reaction products is summarized in Table 30 for the four to one reactant ratio. About 10% of the original reactant moles were unaccounted for in a material balance based upon the results shown in Table 30.

Table 30. Products of the Reaction of Four Volumes of Nitric Acid with One Volume of Hydrazine

Component	Partial pressure in reactor, in atm.	Calculated millimoles	Footnote
N_2	1.17	16.1	a
O_2	0.05	0.7	a
H_2	0.01	0.1	a
N_2O	0.3	4	b
NO_2	0.3	4	b,c
N_2O_4	0.8	11	b,c
HNO_3	-	17	d
H_2O	-	64	e

[a] Calculated from mass spectrometer analysis.
[b] Condensible fraction.
[c] Based upon equilibrium constant $P^2_{NO_2}/P_{N_2O_4} = 0.136$ atm. at 25°C.
[d] Calculated from the analysis of liquid products.
[e] By difference, based upon a hydrogen balance.

2. The reaction of one and one-half volumes of nitric acid with one volume of hydrazine: The non-condensible gases were found to contain nitrogen and a small quantity of hydrogen. The condensible gases were found to comprise only 18% of the total reactor pressure excluding the original atmosphere of helium. The condensible gas had a slight yellow color indicating the presence of NO_2. The condensible material had patches of blue color at the temperature of liquid nitrogen indicating the presence of NO. The condensible material had a vapor pressure of 13 mm. Hg at -78°C. NO_2 has a vapor pressure of less than 1 mm. Hg at this temperature.[39] The pressure must have been due to NO and possibly N_2O, since they are entirely gaseous at this temperature. The composition of the non-condensible fraction was not determined further. The final result of the analysis is given in Table 31 for the one and one-half to one ratio.

Table 31. Products of the Reaction of One and One-half Volumes of Nitric Acid with One Volume of Hydrazine

Component	Partial pressure in reactor, in atm.	Calculated millimoles	Footnote
N_2	1.46	20.1	a
H_2	0.05	0.7	a
N_2O NO NO_2 N_2O_4 as NO	0.33	4.5	b
HNO_3	-	3.1	c
H_2O	-	50.2	d

[a] Calculated from mass spectrometer analysis.
[b] Condensible fraction.
[c] Calculated from analysis of liquid products.
[d] By difference, based upon a hydrogen balance.

Again, about 10% of the original reactant moles were unaccounted for in the material balance based upon the results shown in Table 31.

3. The reaction of equal volumes of nitric acid and hydrazine: The product gases appeared colorless indicating that very little if any NO_2 was formed in the reaction. Only 4% of the gases excluding the helium were condensible in liquid nitrogen. The mass spectrometer sample was passed through a dry ice trap so that some of the materials that were condensible in liquid nitrogen would be included in the mass spectrometric analysis. The mass spectrometer analysis showed nitrogen and hydrogen with traces of nitrous oxide and nitric oxide. When the entire condensible sample was collected, a slight yellow color developed indicating a very slight trace of NO_2. The blue color of the frozen material showed that NO was present. A summary of the composition of the products for the reaction of equal volumes of the two reactants is given in Table 32. Only about 3% of the original reactant moles were

Table 32. Products of the Reaction of Equal Volumes of Nitric Acid and Hydrazine

Component	Partial pressure in reactor, in atm.	Calculated millimoles	Footnote
N_2	2.82	38.8	a
H_2	0.44	6.0	a
N_2O	0.06	0.8	a
NO	0.03	0.4	a
H_2O	-	69.1	b

[a] Calculated from mass spectrometer analysis.
[b] By difference, based upon a hydrogen balance.

unaccounted for in the material balance based upon the results shown in Table 32.

4. The reaction of two volumes of hydrazine with one volume of nitric acid: The gases were completely colorless indicating the absence of NO_2. The gases were passed through a trap cooled by carbon tetrachloride slush (-23°C) before entering the mass spectrometer sample tube. It was hoped that only water vapor would be trapped out of the sample so that all of the gases could be identified by the mass spectrometer analysis. The analysis showed the presence of nitrogen, hydrogen, ammonia and traces of nitrous oxide and nitric oxide. The presence of ammonia in the gases indicated that ammonia should also be present in the liquid products. A crude calculation was made of the ammonia concentration in the aqueous phase based upon the measured concentration in the gaseous phase, the total final pressure of the run, and the absorption coefficient of ammonia. The results of the analysis for the two to one case are given in Table 33.

Table 33. Products of the Reaction of Two Volumes of Hydrazine with One Volume of Nitric Acid

Component	Partial pressure in reactor, in atm.	Calculated millimoles	Footnote
N_2	3.17	43.5	a
H_2	2.32	31.9	a
NH_3	0.36	4.9	a
NO	0.05	0.7	a
N_2O	0.01	0.1	a
H_2O	-	45.0	b
NH_3(aq)	-	9	c

[a] Calculated from mass spectrometer analysis.
[b] By difference, based upon an oxygen balance.
[c] Calculated from the absorption coefficient, $\alpha = 710$ atm.$^{-1}$

Only about 4% of the original reactant moles were unaccounted for in the material balance based upon the results shown in Table 33.

The results of the analysis for the reaction products were necessarily approximate when soluble gases such as NO_2 or NH_3 were involved. Error could have resulted from the uncertainty concerning the amount of material that was removed from the aqueous phase when the products were suddenly expanded into the large evacuated volume. Error in the analysis of the liquid products could have resulted from evaporation of the dissolved gases before the products were diluted with water. The analysis of the residual nitric acid and the analysis of the nitrogen dioxide content of the gaseous phase were complicated by the reversible reaction represented by Eq. 22:

$$(22) \qquad 2\ HNO_3 \rightleftharpoons 2\ NO_2 + 0.5\ O_2 + H_2O$$

Because of this equilibrium, the nitric acid found after a run was not necessarily unreacted material. It could have been reformed from nitrogen dioxide, water and oxygen. In the presence of a slight excess of water, the equilibrium is to the left of Eq. 22 at room temperature. This could account for the absence of oxygen in the acid rich runs.

It was uncertain how much of the reactants remained in the lead tubes and jets of the mixing plate. The volume of the lead tubes and jets was from 6 to 11% of the total volume of the reactant cylinders depending upon the reactant ratio under consideration. Some unreacted material was always found to remain in this volume after a run. It was assumed for the purposes of the material balances that the lead tubes and jets were filled with unreacted material.

Studies of the Aniline, Nitric Acid Reaction

Aniline was purified by distillation from zinc dust. The product was colorless and distilled at 182°C under a pressure of 750 mm. Hg. The refractive index of the product was measured and found to be 1.5791 at 32.5°C. The reaction of aniline with nitric acid can be represented by Eq. 23 for the stoichiometric mixture if it is assumed that the reaction reaches thermodynamic equilibrium:

$$(23) \qquad C_6H_5NH_2 + 6.2\ HNO_3 \longrightarrow 6.6\ H_2O + 3.6\ N_2 + 6\ CO_2$$

One run was made of the reaction of equal volumes of aniline and nitric acid. This corresponded to a molar ratio of 2.14 moles of acid to one mole of aniline. Only the transient pressure was measured. The pressure rise began about 2 msec. after injection began. The pressure gradually rose to about 1.5 atm. over a period of 40 msec. Large quantities of carbon and tar were found in the reactor after the run.

Two runs were made of the reaction of four volumes of acid with one volume of aniline. This corresponded to a molar ratio of 8.18 moles of acid to one mole of aniline. A simultaneous measurement of the transient pressure and the onset of light emission was made. The onset of light emission was determined using Photocircuit III. The traces are shown in Fig. 44. The transient pressure trace is shown at the top of the figure and the light intensity trace at the bottom of the figure. The point at which the light emission began could be located to within about 0.2 msec. with respect to the pressure trace. No information is provided by the measurement concerning the time at which injection began. The time from the beginning of the trace (the closing of the contacts in the pneumatic injector) to the beginning

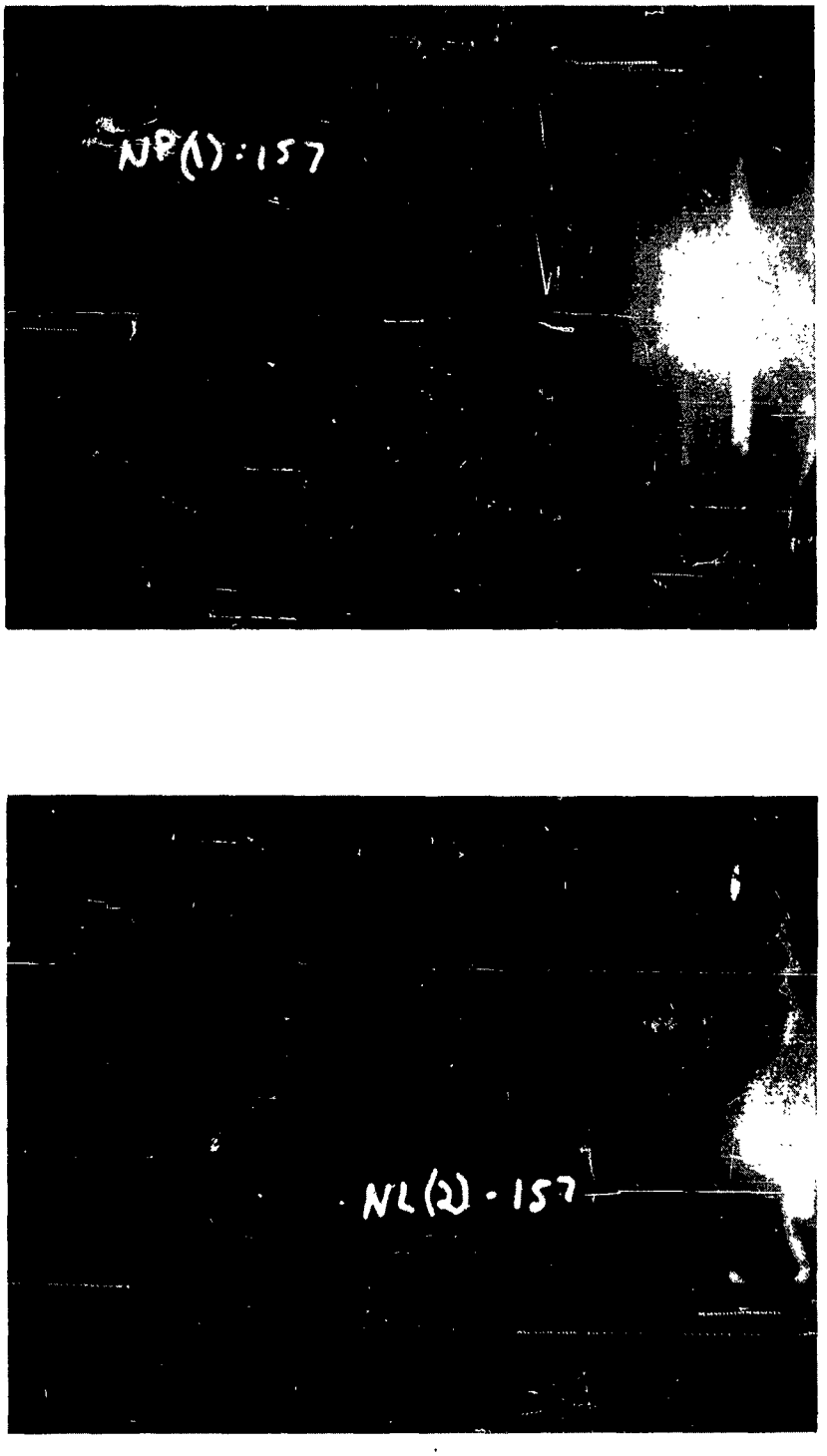

Fig. 44. Simultaneous Pressure and Light Emission Traces of the Reaction of Aniline with Nitric Acid, Run 157, Reactor II, Time Base: 25 msec.

of injection, however, was found to be between 1.0 and 1.5 msec. for the injection rate measurements made with other systems in which this time interval could be deduced. The result of the run is shown in Fig. 45. Time is plotted from the beginning of injection assuming that 1.2 msec. elapsed from the start of the trace to the beginning of injection. The moment of light emission came 2.3 msec. after injection began. The pressure rise began about 1.5 msec. later. The ignition delay was thus 2.3 msec. The further delay in the pressure rise was probably only apparent, being due to the time required for the pressure pulse to travel to the strain gage diaphragm. The maximum pressure was 42 atm. in comparison to the pressure of 1.5 atm. obtained for the one to one ratio.

Another run of the four to one ratio was made in which it was attempted to measure the injection rate. The start of injection could be clearly discerned but the remainder of the trace could not be interpreted. The beginning of the pressure rise occurred only 2.5 msec. after the beginning of injection. Allowing 1.3 msec. for the pressure pulse to reach the strain gage, the ignition delay was 1.2 msec. Damage was noted to the mixing plate after both of the four to one runs. The exit tube was widened at the outlet and had the form of a bell. The closed end of the exit tube was also bent and widened. For this reason no further studies of the aniline, nitric acid reaction were carried out. A new mixing plate was constructed to replace the damaged one.

The results of the aniline, nitric acid reaction are shown in Table 34. Large amounts of NO_2 but no carbon deposits were noted in the products resulting from the reactions reported in Table 34.

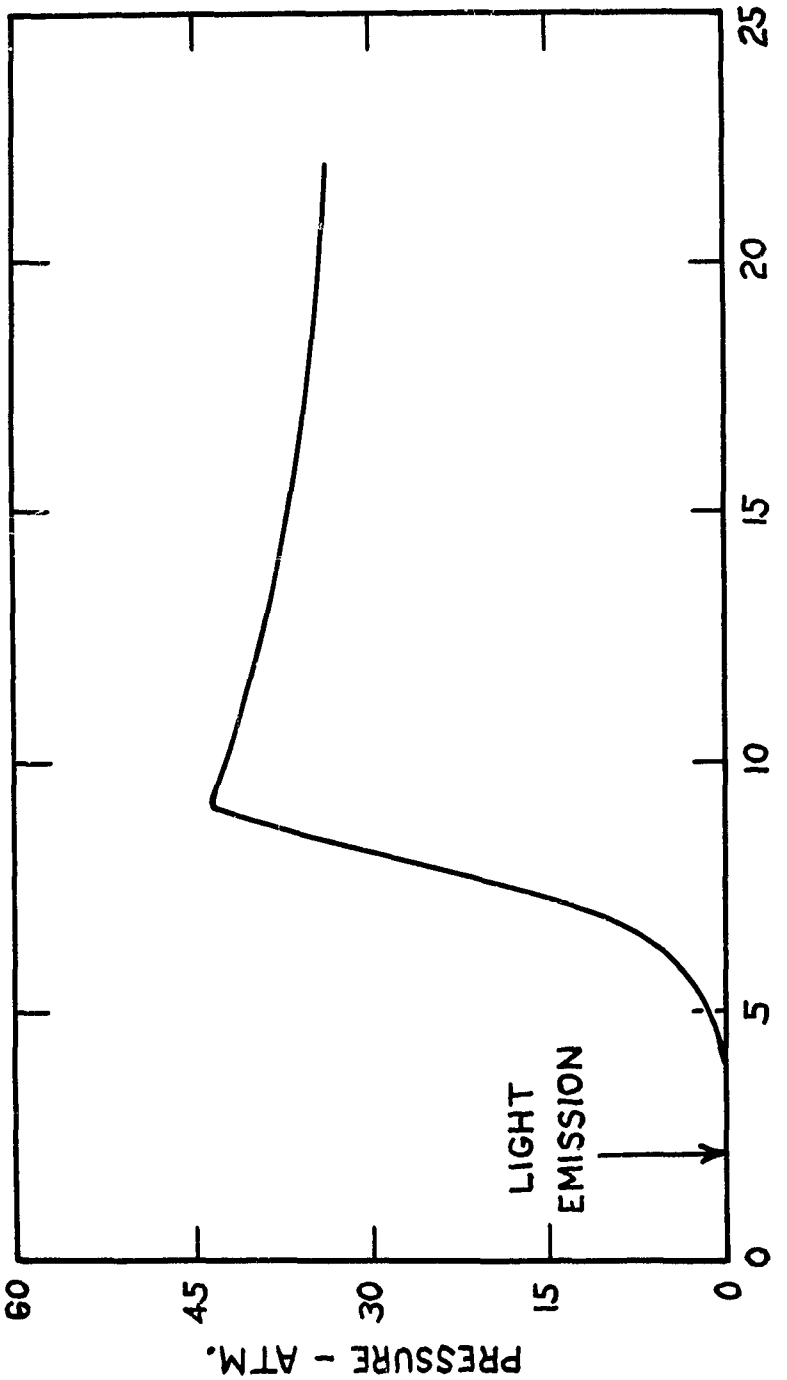

Fig. 45. Simultaneous Measurement of Pressure Rise and the Onset of Light Emission in Reaction of Aniline with Nitric Acid, Run 157, Reactor II.

Table 34. Ignition Delay in the Reaction of Four Volumes of Nitric Acid with One Volume of Aniline

Run	Ignition delay, in msec.	Maximum pressure, in atm.	Final pressure in atm.
157	2.3	42	4.31
158	1.2	35	3.24

It is likely that the damage to the apparatus resulted from the fact that the delayed ignition occurred while injection was still in progress. The flame may have flashed back along the issuing reactant stream toward the exit tube possibly reaching a detonation velocity. This could also account for the irregularities noted in the injection rate trace, since it is entirely possible that injection was interrupted or even reversed for an instant when the force of the ignition first reached the exit tube of the mixing plate.

Studies of the Hydrogen Peroxide, Hydrazine Reaction

High strength hydrogen peroxide was analyzed by the method outlined in Appendix III and found to contain 84.5% H_2O_2 by weight. The reaction can be represented by Eq. 24 for the stoichiometric mixture if it is assumed that the reaction reaches thermodynamic equilibrium:

$$N_2H_4 + 2\,H_2O_2 \longrightarrow N_2 + 4\,H_2O \qquad (24)$$

Runs were made of the reaction of equal volumes of the two reactants. This corresponded to a molar ratio of 1.15 moles of hydrogen peroxide per mole of hydrazine. Runs were also made of the reaction of two volumes of hydrogen peroxide to one volume of hydrazine. This

corresponded to a molar ratio of 2.46 moles hydrogen peroxide per mole of hydrazine.

The reaction of equal volumes of hydrogen peroxide and hydrazine showed a variable ignition delay. The data are summarized in Table 35.

Table 35. Ignition Delay Measurements of the Reaction of Equal Volumes of Hydrogen Peroxide and Hydrazine

Run	Time from the start of injection to the start of the pressure rise, in msec.	Ignition delay referred to the pressure rise, in msec.	Maximum pressure, in atm.	Final pressure, in atm.
161*	-	-	27	1.9
163	1.4	0.1	42	1.8
165	2.4	1.1	55	3.0
162	3.5	2.2	58	-

*Simultaneous measurement of the pressure rise and the onset of light emission, light emission preceded the pressure rise by 1.0 msec.

The second column of the table shows the observed time from the beginning of injection to the beginning of the pressure rise. The data were obtained from simultaneous injection rate and transient pressure measurements. It was assumed that the initial pressure pulse required 1.3 msec. to reach the diaphragm of the strain gage. The ignition delay was then equal to the time given in the second column of the table minus 1.3 msec. In the first three runs reported in the table, the ignition probably occurred while injection was still in progress. The result of the simultaneous measurement of the injection rate and the transient pressure for run 163 is shown in Fig. 46. The slope of the plot of piston position vs. time shows a sharp break indicating further that ignition did occur during the injection. The result of

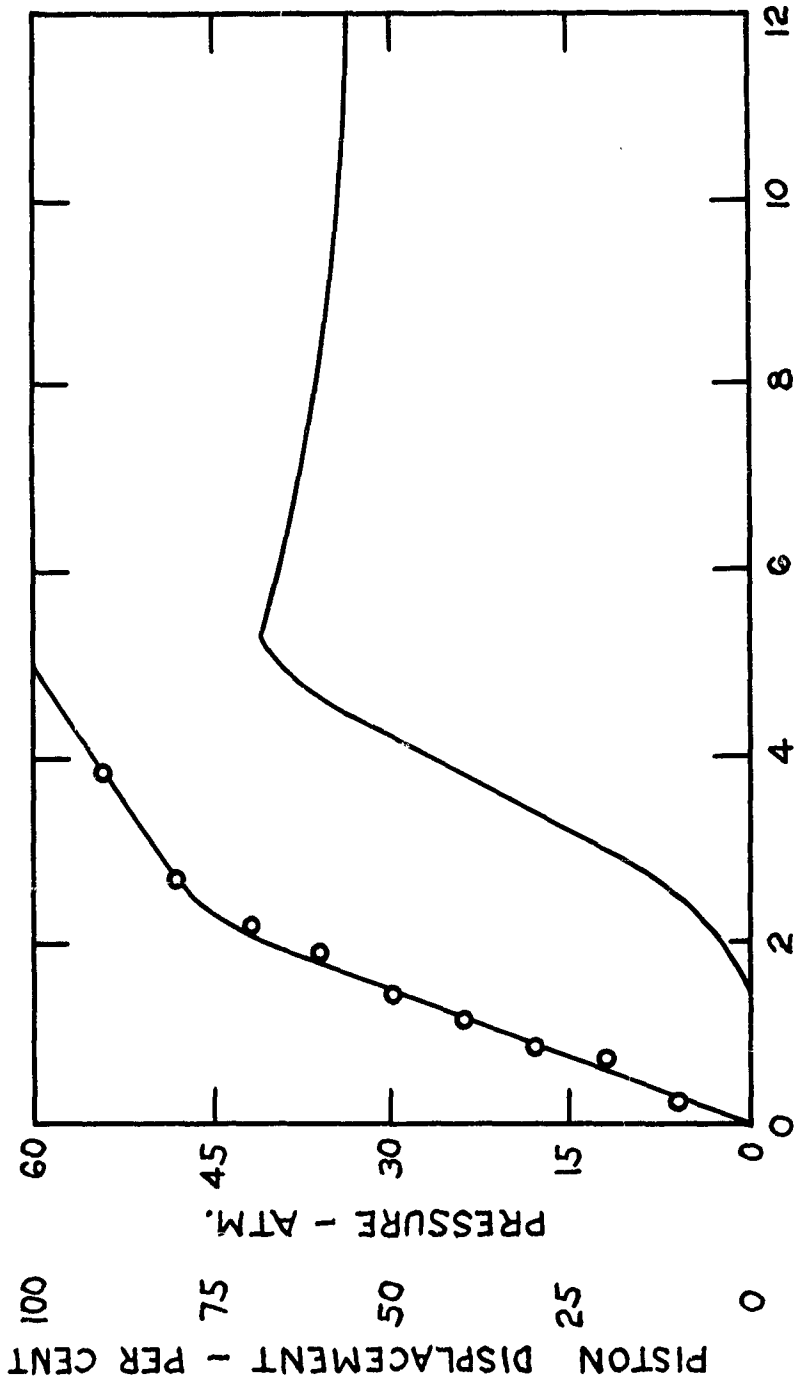

Fig. 46. Simultaneous Measurement of Injection Rate and Pressure Rise in the Reaction of Equal Volumes of Hydrogen Peroxide and Hydrazine, Run 163, Reactor II.

run 162 is shown in Fig. 47. The linear character of the injection indicated that ignition did not occur until injection was complete. The injection time for run 162 was 1.80 msec. and the driving pressure was 1600 lb. per sq. in. which is in agreement with the results obtained for the injection of water reported in Table 17.

The reaction of two volumes of hydrogen peroxide with one volume of hydrazine showed a more consistent ignition delay. The data are summarized in Table 36.

Table 36. Ignition Delay Measurements of the Reaction of Two Volumes of Hydrogen Peroxide with One Volume of Hydrazine

Run	Time from the start of injection to the start of the pressure rise, in msec.	Ignition delay referred to the pressure rise, in msec.	Maximum pressure, in atm.	Final pressure, in atm.
166	2.6	1.3	32	1.7
167	3.0	1.7	41	1.8
168*	-	-	36	1.9

*Simultaneous measurement of the pressure rise and the onset of light emission, light emission preceded the pressure rise by 0.7 msec.

The second column of the table shows the observed time from the beginning of injection to the beginning of the pressure rise. The ignition delay was again calculated on the assumption that the initial pressure pulse required 1.3 msec. to travel to the diaphragm of the strain gage. The ignition delay was found to be between 1.3 and 1.7 msec. The injection rate traces indicated that the ignition did occur during the injection.

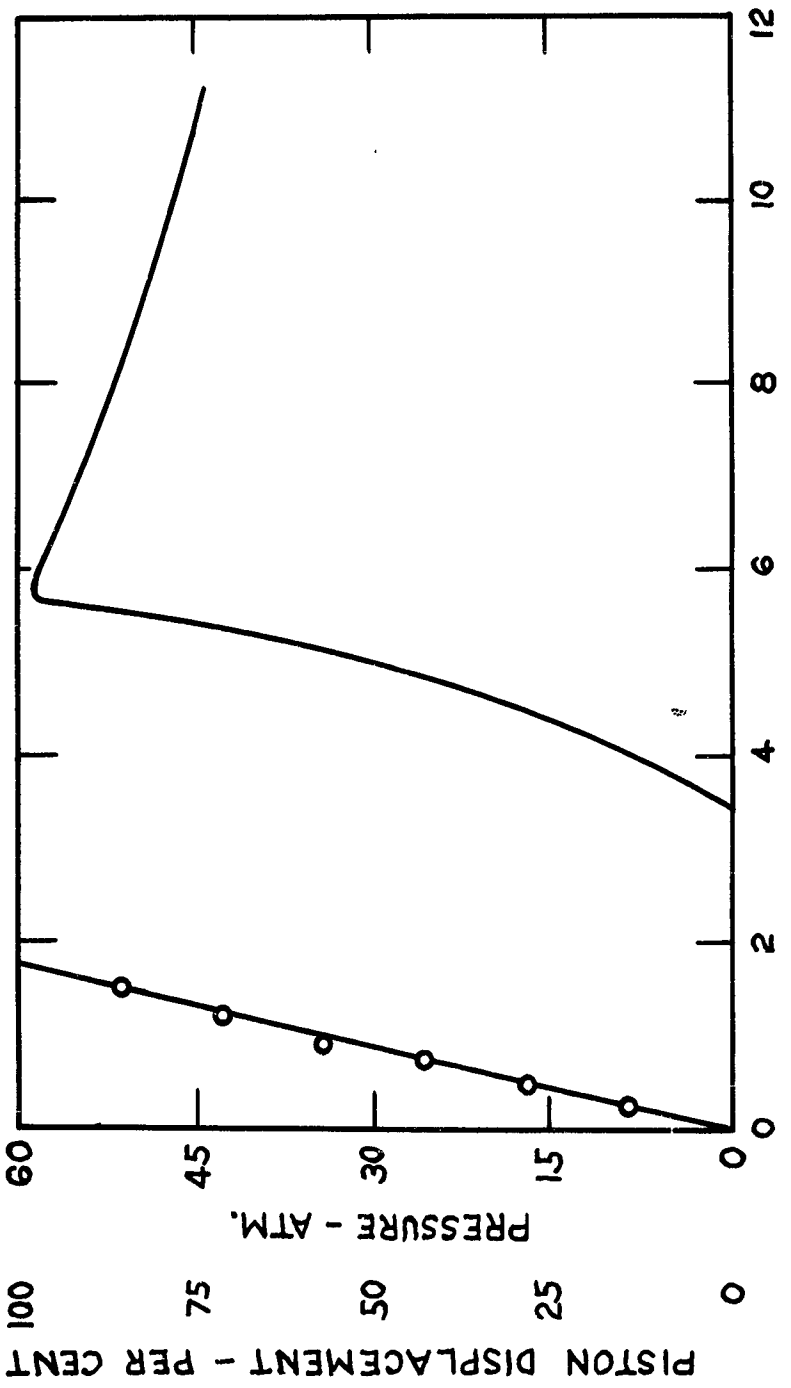

Fig. 47. Simultaneous Measurement of Injection Rate and Pressure Rise in the Reaction of Equal Volumes of Hydrogen Peroxide and Hydrazine, Run 162, Reactor II.

Studies of the Reaction Between Nitric Acid and Liquid Ammonia, Hydrazine Mixtures

The purification of nitric acid and hydrazine have already been described. The ammonia was taken from a tank of Pennsylvania Salt Co. Ankydrous Ammonia. The preparation of the liquid ammonia, hydrazine mixtures was as follows: About one gram of anhydrous hydrazine was added to a small Erlenmeyer flask which had previously been weighed. The flask was then reweighed to obtain the weight of hydrazine. The flask was quickly attached to a high vacuum apparatus by means of a ground glass joint. The hydrazine was frozen in the flask by means of a liquid nitrogen bath. The system was then evacuated. Tank ammonia was admitted at room temperature to a calibrated volume of 3.60 liters which was connected to a manometer. The amount of ammonia gas present in the calibrated volume was then calculated by means of the perfect gas law. The ammonia was allowed to condense in the flask with the hydrazine until the pressure in the large volume decreased to a sufficiently low value. A new charge of ammonia was then added to the large volume. The procedure was repeated until the desired amount of ammonia had been added to the hydrazine. The flask was removed from the vacuum apparatus, covered and stored at the temperature of dry ice.

The reactor had to be cooled before the mixture could be loaded into the reactant cylinders. The reactor was partially assembled and cooled to about -60°C by immersing it in an insulated, two liter beaker that contained a mixture of trichloroethylene and powdered dry ice. The liquid ammonia, hydrazine mixture was then transferred from the storage flask to the cylinder by means of an automatic pipet which had been cooled by immersion in liquid nitrogen. The piston was inserted into the cylinder only after it had also been cooled by

immersion in liquid nitrogen. After the nitric acid had been loaded into the other cylinder, the reactor had to be removed from the cold bath for a short time while the assembly was completed. The temperature of the reactor rose to only about -45°C during this period. The assembled reactor was then placed in the low temperature thermostatic bath and brought to the desired temperature before injection was initiated.

The runs had to be made over a rather limited temperature range. The lower limit to the temperature range was -42°C, the freezing point of anhydrous nitric acid.[40] The upper limit was -33°C, the boiling point of liquid ammonia.[38] All of the runs were made of equal volumes of the two reactants.

A run was made of the reaction of pure liquid ammonia with nitric acid. The thermocouple indicated a temperature of -47°C. At this temperature, the nitric acid should have been frozen; however, the injection appeared to have proceeded normally. Only the transient pressure was measured. The pressure showed a slight maximum of about one atmosphere. The product of the reaction was a non-volatile white solid, presumably ammonium nitrate. It thus appeared that there had been no ignition.

Two runs were made of the reaction of equal volumes of nitric acid with a mixture containing 9.0% hydrazine. Both runs were simultaneous measurements of the transient pressure and the onset of light emission using Photocircuit III. The result of one of the runs is shown in Fig. 48. Since it is not possible to determine when injection began from the traces of a simultaneous light emission and transient pressure measurement, it was again assumed that 1.2 msec. elapsed

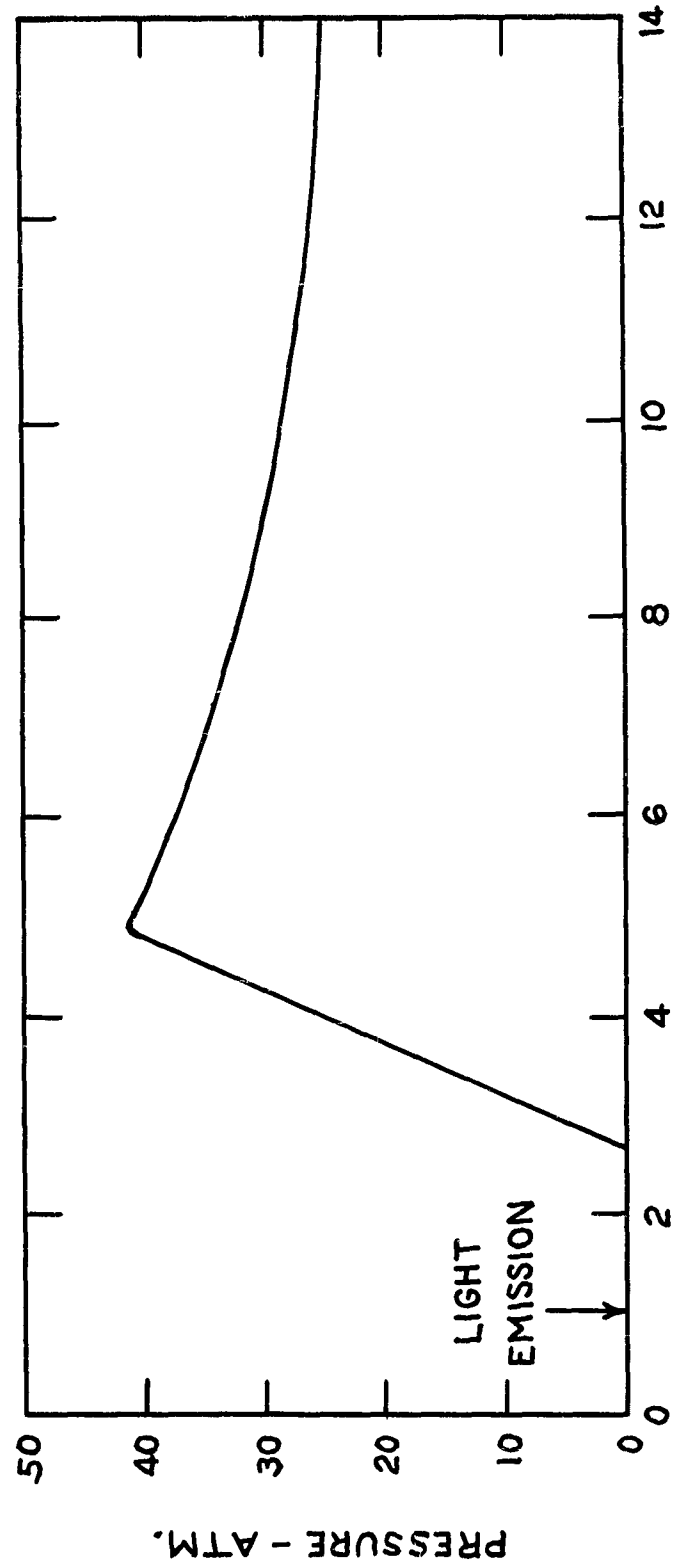

Fig. 48. Simultaneous Measurement of Pressure Rise and the Onset of Light Emission in the Reaction of Equal Volumes of Nitric Acid with a Mixture of Hydrazine and Liquid Ammonia Containing 9.0% Hydrazine, Run 174, Reactor II.

between the beginning of the time base and the start of injection. Injection rate measurements could not be made when the reactor was located in the thermostatic bath. The data for the reaction of nitric acid with the mixture containing 9.0% hydrazine are summarized in Table 37. The second column of the table shows the temperature indicated by the thermocouple located close to the reactants before injection.

Table 37. Ignition Delay Measurements of the Reaction of Equal Volumes of Nitric Acid with a Mixture of Hydrazine and Liquid Ammonia Containing 9.0% Hydrazine

Run	Temperature, in °C	Ignition delay referred to light emission, in msec.	Maximum pressure, in atm.
174	-35	1.0	41
175	-33	1.4	41

Three runs were made of the reaction of equal volumes of nitric acid and a mixture containing 2.7% hydrazine. The runs were simultaneous measurements of the transient pressure and the onset of light emission. The results are summarized in Table 38. Again it had to be assumed that injection began 1.2 msec. after the closing of the contacts in the pneumatic injector. The result of two of the runs are shown in Fig. 49. There was no light emission in runs 177 and 178. The absence of light and the very low maximum pressure indicated that no ignition occurred. It is apparent from the figure that the transient pressure for runs 176 and 177 began to follow the same course. In run 176, however, the mixture ignited giving rise to the emission of light 2.9 msec. after injection. About one msec. later the pressure began

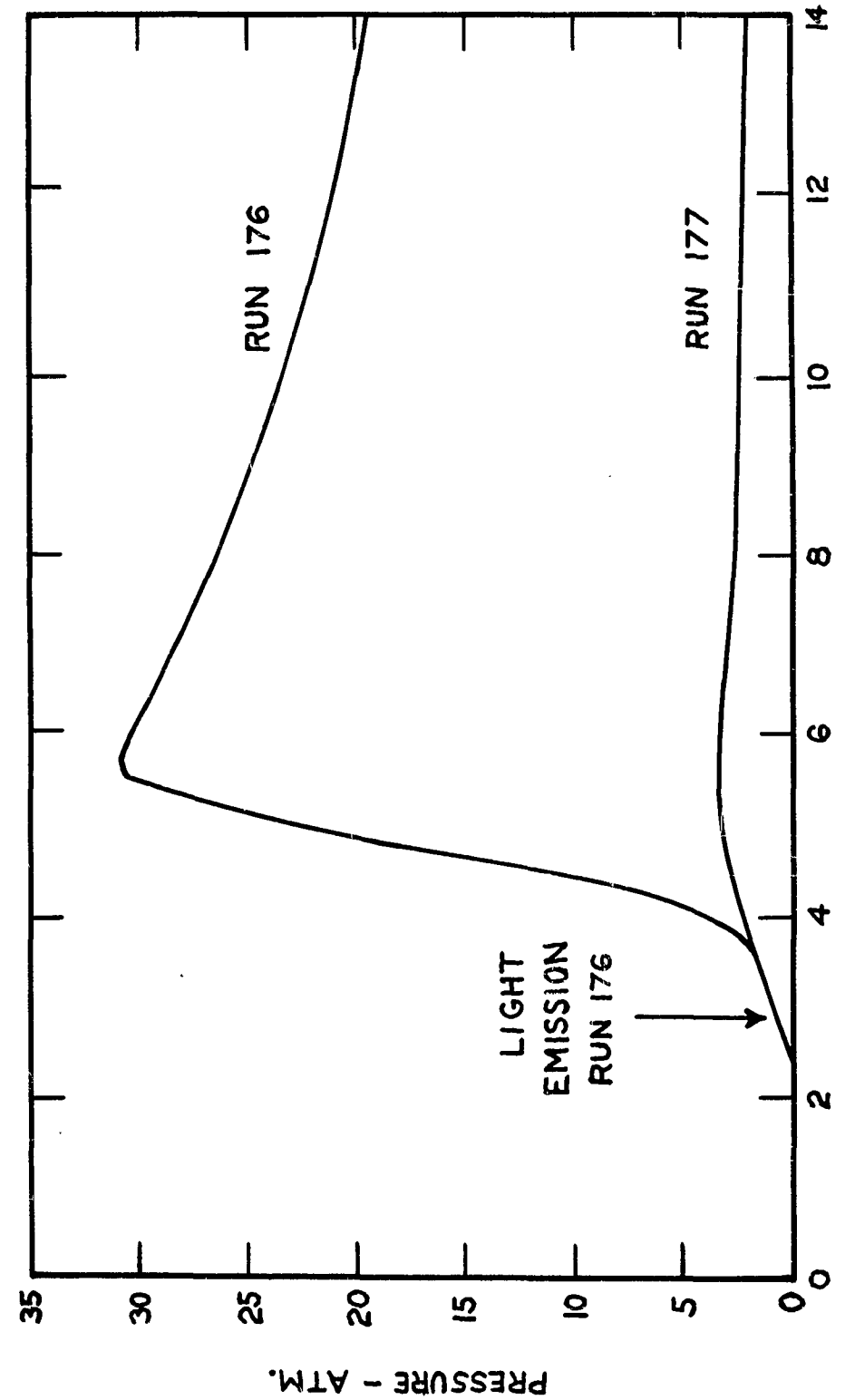

Fig. 49. Simultaneous Measurement of Pressure Rise and the Onset of Light Emission in the Reaction of Equal Volumes of Nitric Acid with a Mixture of Hydrazine and Liquid Ammonia Containing 2.7% Hydrazine, Run 176 and Run 177, Reactor II.

to rise rapidly. It is again reasonable to suppose that the light emission and the rapid pressure rise occurred simultaneously, the delay in the latter being only apparent.

Table 38. Ignition Delay Measurements of the Reaction of Equal Volumes of Nitric Acid with a Mixture of Hydrazine and Liquid Ammonia Containing 2.7% Hydrazine

Run	Temperature, in °C	Ignition delay referred to light emission, in msec.	Maximum pressure, in atm.
176	-38	2.9	31
177	-41	- *	3.5
178	-41	- *	3.5

*No ignition occurred.

CHAPTER VI
DISCUSSION

The apparatus described herein was designed to contact and mix useful quantities of two liquids in the shortest possible time. Reactor I was designed by McKinney for the purpose of studying the kinetics of rapid reactions in which a gas is formed. Reactor I contacts approximately one cc. of one reactant with a large excess of a second reactant. Reactor II was designed specifically for the purpose of studying the ignition of self-igniting fuel-oxidant systems. Reactor II contacts more nearly equal quantities of reactant solutions.

In Reactor I, the liquid reactants are forced together by the action of high pressure nitrogen gas on floating pistons. The two pistons were not mechanically coupled so that there was no way to insure that the pistons would descend together. McKinney reported that the large piston descended in 9 msec. and the small one in 5 msec. Injection measurements were made during the present research in which it was shown that the small piston completed its descent 3.5 msec. after the large piston in a particular experiment. The only reaction studied in Reactor I was the reaction of sodium-potassium alloy with excess water. The delay in descent of the small piston was shown to cause a large maximum to occur in the transient pressure sometime during the first 10 msec. of the reaction. Extreme care was required in the preparation of the piston gaskets in order to avoid a late start of the small piston. The absence of a large first maximum in some of the runs reported in Table 20 was taken as evidence for the fact that uniform piston descent had been achieved.

Reactor II was designed to avoid the difficulty due to the uneven descent of the two pistons. In Reactor II, both pistons are driven by

a single large piston which in turn is driven by high pressure nitrogen gas. This arrangement was responsible for the improved injection time obtained with Reactor II. The driving gas pressure is applied to an area of about 0.78 sq. in. The sum of the areas of the smaller pistons for the one to one injection system is only 0.15 sq. in. If an actual driving gas pressure of 2000 lb. per sq. in. were employed, the effective pressure on the reactant solutions would have been 10,000 lb. per sq. in.

Reactor II is sufficiently compact to be conveniently immersed in a thermostatic bath. Four reactant ratios were obtainable through the use of a second cylinder block, additional fittings and pistons. Several additional mixing plates were designed that allowed the mixing pattern to be varied. Only the "T" type mixing plate that was designed according to the principles established by Roughton and Chance was used, however, since it was only for this arrangement that the efficiency of mixing could be shown to be adequate.

The piston gaskets of Reactor II did not have to withstand the pressure of the driving gas. There was therefore no mechanism whereby spuriously high values of the transient or final pressure could have been obtained. Difficulty was encountered, however, in preventing leakage of the product gases from within the reactor. This difficulty was aggravated by the effect of the corrosive reactants on the neoprene piston gaskets. The difficulty was overcome when a rather close fitting aluminum gasket was used in combination with two neoprene gaskets. The aluminum prevented the bulk of the reactant solution from contacting the neoprene gaskets. The neoprene was further protected by a coating of an inert fluorocarbon grease. The neoprene

gaskets rendered the reactor pressure tight. Transient pressures up to 50 atm. and steady pressures up to 5 atm. were contained within the reactor without leakage. This is evidenced by the reproducibility of the pressure data shown in Table 25 for the hydrazine, nitric acid reaction.

Reactor II was designed to allow the routine measurement of the rate of injection. The method employed yielded the relative time corresponding to a number of positions of the piston system with respect to a stationary light beam. Studies were made of the injection of water from both cylinders of the reactor. It was found that the linear velocity of the piston descent and hence the injection rate were constant during the period of injection. This indicated that the moving parts of the reactor accelerated rapidly to the equilibrium velocity and suggested that the velocity of injection was determined entirely by the resistance to the flow of the fluids. Runs made with very tight fitting gaskets showed essentially the same injection rate as those made with loose fitting ones. It was thus feasible to use very tight fitting gaskets and thereby reduce the tendency toward leakage. In Reactor I, it was not feasible to use tight gaskets since this would have increased the tendency for the small piston to delay.

The observed injection time depended upon (1) the pressure of the driving gas applied to the pneumatic injector, (2) the reactant ratio employed, (3) the dimensions of the jets and the exit tube of the mixing plate, and (4) the stroke length employed. A stroke of seven-eighths inch was found to be most convenient and was used for most of the runs. The most rapid injection time obtained with Reactor II was 1.7 msec. for the injection of water. This run was obtained with a driving

pressure of 1900 lb. per sq. in. using the one to one reactant ratio. In all, 2.2 cc. of water were injected during this run, 1.1 cc. from each cylinder. An injection time of the order of 4.3 msec. was observed for the four to one reactant ratio; however, 3.6 cc. of water in all were injected during these runs.

The injection rate was not constant for the injection of certain fuel-oxidant mixtures. The first part of the reactants were injected at a somewhat slower rate than that noted for the injection of water. The injection rate then decreased to about one-half to one-third of its initial value. The deceleration of the injection was quite sharp, i.e., both the initial and final injection rates were reasonably constant. The change in the injection rate was thought due to the thrust created by the reaction acting on the injection system. The phenomenon was studied particularly with reference to the hydrazine, nitric acid reaction. The reactants were liquids while the products of the reaction were primarily gaseous. The conversion of liquids into gases in a flowing stream corresponds to a tremendous increase of the linear flow velocity. A change of linear flow velocity in a stream of constant mass flow rate corresponds to a change of momentum which is accompanied by a force acting in opposition to the momentum change. The force created by the reaction would be equivalent in effect to a large static pressure applied to the outlet of the exit tube. In order to slow the injection rate perceptibly, this back pressure would have to be of the same order of magnitude as the driving pressure.

The time from the beginning of injection to the change of the injection rate could not be correlated with the measured ignition delay. The ignition delay for all ratios of the hydrazine, nitric

acid reaction was found to be between 0.0 and 0.9 msec. referred to the start of the pressure rise. The time to the change of the injection rate as shown in Table 27 was found to range between 1.1 and 3.2 msec. It is likely that the reaction required this additional time after ignition to reach a steady state in the exit tube. Because of this slowing of the injection rate, the overall injection time was substantially longer than the values obtained for the water injection. Values from 4.3 msec. for the one to one reactant ratio to 9.2 msec. for the four to one reactant ratio were obtained.

The rate of injection of water was calculated by a fluid mechanical method and shown to agree to within 18% with the observed results. The rate of injection of the nitric acid, hydrazine system was also calculated. The observed initial injection rate was found to be 25 to 100% slower than those calculated. It was believed, however, that the early reaction of the two reactants may have slowed the initial injection somewhat. The calculations indicated that a pressure drop occurring in the pneumatic injector seriously affected the injection rate. The pressure acting on the driving piston may have been as low as 60% of the pressure actually applied to the pneumatic injector. This situation could have been corrected by designing an injector with a connecting duct and valve mechanism having larger inside diameters. The calculations and the observed results provide the designer of a future rapid injection system with important design information. The results also indicate that injection rates substantially faster than those reported in the present study could be obtained. The two most significant design factors in this connection are the ratio of the area of the driving piston to the areas of the small pistons and the diameters

of the ducts through which the driving gas passes. The areas of the smaller pistons, however, must be great enough to bear the large compressive stress applied to them by the driving piston.

The empirical equation developed by Chance for the expected flow rates through "T" type mixers was found to agree well with those obtained with Reactor II. The equation, however, does not take into consideration a number of important factors so that the agreement was probably fortuitous.

The time required to contact two reactants is not necessarily equal to the time necessary to mix the reactants. The mixing pattern employed in both reactors had the form of a "T". The reactants each enter one leg of the "T"; the two pass out of the mixer together through the third leg, referred to as the exit tube. Mixing begins to occur at the point of contact of the two reactants in the center of the "T". As the solution flows down the exit tube, it becomes more and more thoroughly mixed. Roughton and Millikan* have shown that the point at which solutions reach the point of 97% mixing in similar "T" type mixers moved toward the point of first contact as the flow velocity was increased. The work of Trowse* has been cited to show that the distance from the point of first contact to the point of 97% mixing was about 6 mm. for a mixer that was geometrically similar to the mixing system used in Reactor II. The linear flow velocity referred to the exit tube for the measurements made by Trowse were less than 1000 cm. per sec. The linear flow velocity referred to the exit tube for the reactions studied in Reactor II was of the order of 10,000 cm. per sec.

---

*See Table 4.

Since the exit tube of Reactor II was 8 mm. long, it was likely that 97% mixing was achieved before the reactant mixture left the exit tube of the reactor. To further insure the efficiency of mixing in Reactor II, the reacting stream was made to impinge on a baffle plate located about 25 mm. from the outlet of the exit tube.

The measurements made by Roughton and Millikan and those made by Trowse employed aqueous solutions. It is likely that mixtures such as sodium-potassium alloy and water, or hydrazine and nitric acid would not mix as readily as aqueous solutions. A direct test of the efficiency of mixing of such liquids, however, could not be devised in the present research. The best experimental evidence for the mixing obtained with both reactors lies in the results of the studies that were made of the reaction of sodium-potassium alloy with water. The pressure rise noted for this reaction reached a maximum in a time equal to that required for injection within the experimental error of the measurements.

The principal means of following the reactions under study in the reactors was the measurement of the transient pressure. The Statham Gages employed for the transient pressure measurements were stated to have a natural frequency of vibration in excess of 2000 cycles per second. The signal from the strain gages was caused to modulate the amplitude of a 1000 to 1200 cycle per second carrier wave. In effect then, a reading of the transient pressure was obtained approximately every msec. by measuring the amplitude of each wave of the resulting oscilloscope pattern. The amplitude of the oscilloscope trace was found to be accurately proportional to the pressure applied to the diaphragm of the strain gage by calibration with accurately known

static pressures. More frequent pressure readings could have been obtained by using a higher carrier wave frequency. In view of the stated natural vibration frequency of the gages, however, it is questionable whether the gages could have reproduced accurately pressure events occurring in a period of less than a msec. For the measurement of more rapid pressure variations, gages involving piezoelectric crystals are indicated. The circuitry associated with such gages is far more complex than that employed in the present study. Such gages generally do not have a linear response.

The response of a rapid pressure measuring system depends not only upon the gage employed, but also upon the geometry of the cavity in which the pressure change is produced and the connection leading to the gage. It was desired to record the pressure changes occurring in the interior of the reactors. The most direct procedure would have been to place the diaphragm of the strain gage as close as possible to the interior of the reactor. If this had been done, it was likely that liquid pellets would have struck the diaphragm during injection and given rise to random disturbances in the pressure record. Noise was observed in the pressure record even when the gage was located some distance from the reactor. The noise could not be attributed to any mechanical or electrical defect in the apparatus. It was found that the noise could be eliminated by placing obstructions in the piping leading to the strain gage. This observation indicated that the noise noted in the oscilloscope traces corresponded to actual variations of the pressure in the reactor. Similar disturbances of audio frequency were noted by Lewis and von Elbe[41] during a study of explosions of hydrogen and oxygen. They observed the disturbances only for certain

of the explosive mixtures under study. They thus concluded that the rapid pressure variations were a real manifestation of the reaction and were not instrumental in origin.

It was found that much of the noise resulting from reaction in Reactor II could be eliminated by connecting five 90° pipe elbows between the reactor and the strain gage without seriously affecting the response of the transient pressure recording system. It appeared that the noise was a function of the injection and reaction processes and of the cavity in which they occurred. In order to improve the recording speed, it would seem to be necessary to analyze the structure of the shock waves and relate them in some way to the extent of reaction. This may set an upper limit to the speed with which chemical reactions may be followed by measuring their pressure.

A second means of studying the reactions carried out in the reactors was the measurement of the intensity of the light emitted by the reactions. Three different photoelectric circuits were used for this purpose. The amplitude of the traces resulting from either Photocircuit I or Photocircuit II were a function of the light intensity. The amplitude of traces from Photocircuit I was not proportional to the light intensity. Photocircuit I was used only to show the presence and time of occurrence of the light emitted during the study of the sodium-potassium alloy reactions. The amplitude of the traces from Photocircuit II was shown to be proportional to the light intensity by a calibration procedure. The traces from Photocircuit III show precisely when the light emission from a reaction begins. They give no information regarding the intensity of the light or the time at which the emission ceases.

Several types of measurements were carried out in order to derive information regarding the reactions under study. The different types of measurements were as follows: (1) Simultaneous measurement of the transient pressure and the intensity of light emission using either Photocircuit I or Photocircuit II. A typical pair of traces using Photocircuit I is shown in Fig. 34; a typical pair of traces using Photocircuit II is shown in Fig. 39. Both the transient pressure traces and the light emission traces had an identical carrier wave frequency. Since frequencies of the order of 1000 cycles per second were used, the relative timing between the traces was no better than about 0.5 msec. (2) Simultaneous measurement of the transient pressure and the onset of light emission using Photocircuit III. A typical pair of traces are shown in Fig. 44. The photoelectric trace in this case is a single line trace. The break in the trace indicating the onset of light emission could be referred to the pressure trace so that an accuracy in the relative timing of the order of 0.2 msec. could be obtained. (3) Simultaneous measurement of transient pressure and injection rate using Photocircuit III. A typical pair of traces are shown in Fig. 42. The relative timing between the traces is probably accurate to 0.2 msec. since again the photoelectric trace was a single line.

The absolute standard of time was the frequency of the 60 cycle A C line. The line frequency was shown by McKinney to be very accurate. The pulse generator was synchronized with the A C line, so that the blanking pulses on the traces occurred at precisely known intervals. In practice, it was convenient to preset the carrier wave frequency to either 1080 cycles or 1200 cycles by comparing the carrier wave signal to the 60 cycle signal from the line. This was accomplished by

observing the Lissajous patterns on the oscilloscope. The 1080 cycle frequency shows 18 cycles for every cycle of the line voltage while the 1200 cycle frequency shows 20 cycles. The setting could be checked on the resulting trace by counting the number of cycles of the carrier wave between each blanking pulse.

The data for the ignition delay of the fuel-oxidant systems that were studied are summarized in Table 39 and Table 40. The ignition delay referred to the pressure rise is given in Table 39. The data shown in the table were obtained from simultaneous measurements of the injection rate and the transient pressure. The observed time from the beginning of injection to the beginning of the pressure rise was corrected for the time (1.3 msec.) required for the first pressure pulse to travel to the diaphragm of the strain gage. For each system, at least one simultaneous measurement of the transient pressure and light emission was made to verify the fact that the onset of light emission and the beginning of the pressure rise occurred simultaneously within the experimental error of the measurement. The total range of the observed values for the ignition delay are given in the fourth column of Table 39. Only the reaction of 1.15 moles of hydrogen peroxide with one mole of hydrazine did not show a delay reproducible to within one msec. The accuracy of the measurements was probably no better than one msec.

The data obtained for the ignition delay in the reaction of equal volumes of nitric acid with hydrazine, liquid ammonia mixtures are shown in Table 40. The ignition delay referred to light emission is given, since no injection rate measurements could be made when the reactor was located in the low temperature bath. The observed time

from the beginning of the time base (the closing of the contacts in the pneumatic injector) to the onset of light emission was corrected for the average time (1.2 msec.) between the beginning of the time base and the beginning of injection. It will be recalled that this time varied between 1.0 and 1.5 msec. for injection rate measurements of other systems. The mixture containing 2.7% hydrazine ignited only in one run. In two others, no ignition was observed.

Table 39. Results of Ignition Delay Studies of Fuel-Oxidant Systems

Fuel	Oxidant	Reactant ratio, moles oxidant per mole fuel	Ignition delay, referred to the pressure rise, in msec.
N_2H_4	HNO_3	0.352 to 2.87	0.0 - 0.9
$C_6H_5NH_2$	HNO_3	8.18	1.2 - 2.3
N_2H_4	H_2O_2	1.15	0.1 - 2.2*
N_2H_4	H_2O_2	2.46	1.3 - 1.7

* Ignition delay not reproducible.

The longest ignition delay that was observed for any of the reactions studied in the present research was 2.9 msec. These values are much lower than those observed for similar systems by other investigators. The most striking example is found for the system aniline vs. nitric acid. Gunn[23] observed a delay of 410 msec. for this system in the refined open-cup apparatus. A delay of 1.2 to 2.3 msec. was found for this system in the present study. The Kellogg Co.[22] found a delay of 5 msec. for the reaction of 96% hydrazine with 96% nitric acid in the small rocket motor. A delay of 0.0 to 0.9 msec. was observed for

the reaction of the anhydrous reactants in the present study. The Kellogg Co. also found delays ranging up to 37 msec. for the reaction of red fuming nitric acid with a mixture of ammonia and hydrazine containing 5.0% hydrazine. They observed a long delay in the reaction of white fuming nitric acid with a mixture of ammonia and hydrazine containing 2.2% hydrazine. The results obtained in the present study for the reaction of nitric acid with ammonia, hydrazine mixtures showed an ignition delay of 2.9 msec. for a mixture containing only 2.7% hydrazine. The 2.7% mixture, however, did not ignite at all in two cases.

Table 40. Results of the Ignition Delay Studies of the Reaction of Equal Volumes of Nitric Acid with Hydrazine, Liquid Ammonia Mixtures

Fuel mixture, weight per cent hydrazine	Temperature range, in °C	Ignition delay referred to light emission, in msec.
100	22 to 30	1.0
9.0	-33 to -35	1.0 - 1.4
2.7	-38 to -41	2.9*

*Result of one run, no ignition occurred in two other runs.

The short delays observed for the fuel-oxidant reactions studied in Reactor II are probably a result of two factors: (1) the mixing process did not cause a significant delay, and (2) the turbulent nature of the mixing process added impact energy to the explosive mixture. No previous investigation has been made of the phenomena of the self-ignition of fuel-oxidant systems under conditions where the efficiency and time of mixing has been so clearly demonstrated.

It is not likely, however, that the very rapid ignitions can be attributed to the improved mixing alone.

An unignited mixture of a fuel and oxidant such as hydrazine and nitric acid can be likened to a liquid explosive such as nitroglycerine. Nitroglycerine can be ignited by impact alone. Bowden, et al. have studied the ignition of nitroglycerine by impact.[42] They found that thin sheets of the material on an anvil would not ignite even under the influence of a rather strong hammer blow unless gas bubbles were present in the liquid. The authors concluded that the high temperatures produced by the adiabatic compression of the bubbles were responsible for the ignition. It was possible to estimate crudely the minimum ignition energy required to ignite the material by estimating the size of the bubbles and the compression ratio.[41] A value of 10^{-8} calories was obtained. This value is of the order of magnitude of the minimum ignition energy of gaseous mixtures found by more precise methods involving spark ignition.[41] It is thus reasonable to suppose that the impact and turbulence associated with the mixing process in Reactor II could have resulted in immediate or nearly immediate ignition.

This conclusion also results from the failure to observe a systematic increase of the ignition delay as the hydrazine concentration was decreased in the hydrazine, ammonia mixtures. The ignition delay increased to only 2.9 msec. for the mixture containing 2.7% hydrazine. The runs made of this mixture that failed to ignite indicated that the impact energy was just insufficient to ignite this mixture. Instead of observing a longer and longer delay as the hydrazine concentration or the temperature was decreased, a point was

reached where the mixture simply failed to ignite. Such behavior is more indicative of ignition by mechanical shock than it is of thermally initiated ignition showing an induction period due to the rate of a chemical reaction.

A study of the ignition delay of gaseous mixtures of hydrocarbons and oxygen was made by Jost and Teichmann[43] by a rapid compression method. They obtained a straight line when the logarithm of the ignition delay was plotted against the reciprocal of the reaction temperature. The plot was linear from delay values of a few msec. to over five seconds. The fact that the data could be represented by an Arrhenius equation indicates that the delay determining factor was due to the rate of a chemical reaction. The experimental results obtained in the present study show, nevertheless, that fuel-oxidant systems previously thought to have long ignition delays will ignite in a very short time under violent mixing conditions.

The results reported by McKinney for the reaction of sodium-potassium alloy with water in Reactor I were explained as a result of the studies made during the present research. It was found that the reaction produced hydrogen at a rate equal to the injection rate of the reactor. The first large pressure maximum was a result of local heating due to a delay in descent of the small piston. The second large maximum was the result of an explosion between the hydrogen produced by the reaction and the oxygen present initially in the reactor atmosphere. The explosion was delayed about 80 msec. with respect to the beginning of injection. The delay was decreased to about 40 msec. when the oxygen content of the reactor atmosphere was decreased to 5 or 10%. The explosion was prevented entirely when the

oxygen content of the atmosphere was reduced to 5 or 10% and when a small amount of acetaldehyde was added to the water. The acetaldehyde presumably removed the dissolved oxygen from the water.

The reaction of sodium-potassium alloy with an excess of 10 M KOH solution also produced hydrogen just as rapidly as the solutions could be mixed. The ignition delay of the hydrogen, oxygen reaction with normal air in the reactor was found to be 44 msec. When the oxygen content of the reactor atmosphere was reduced to 5 or 10%, the delay decreased to 22 msec.

The long delays obtained in Reactor I for the ignition of the hydrogen, oxygen mixture indicated that the reaction was initiated by chain carriers produced in the reaction of the alloy with water. The very low pressure overswing noted for the production of hydrogen in some of the runs shown in Table 20 indicated that the temperature did not rise high enough to cause thermal ignition of the hydrogen, oxygen reaction. It is also unlikely that the turbulence of the mixing process was responsible for the ignition since it is well known that flame will result when sodium is brought into contact with water under less violent conditions. The long delay also indicates that this mechanism was not responsible for the ignition. The actual chain carriers liberated by the initial reaction cannot be stated with certainty. A possible initiating reaction is expressed in Eq. 25:

$$(25) \qquad M + H_2O \longrightarrow MOH + H^{\cdot}$$

The hydrogen, oxygen reaction has been initiated at room temperature by introducing hydrogen atoms from a discharge tube.[44] The significance of the ignition delay is uncertain because of the uncertainty

associated with the process whereby the hydrogen produced by the alloy reaction mixed with the oxygen already in the reactor.

The data obtained for the alloy, water reaction in Reactor II indicates that there was no ignition delay for the hydrogen, oxygen explosion. The heat produced by the reaction of more nearly equal quantities of reactants may have been sufficient to cause thermal ignition of the hydrogen, oxygen reaction. The reaction of the alloy with ethanol in Reactor II also gave rise to a powerful explosion. The ignition was delayed between 1.8 and 5.5 msec. It is likely that the explosion was initiated by chain carriers produced in the reaction of the alloy with ethanol. It is possible, however, that temperatures were produced that were high enough to cause thermal ignition. The alloy, ethanol reaction carried out in the absence of oxygen showed a slow, pressure increasing reaction that was not completed for about an hour. The alloy was in excess so that the slow, pressure increasing reaction probably involved a further attack of the alloy upon the alkali ethoxide.

The analysis of the products of the reaction of hydrazine with nitric acid provides some information regarding the reactions involved. The reaction is highly exothermic. The adiabatic flame temperature for two reactant ratios are calculated in Appendix IV. The calculations are based upon the assumption that the reaction occurs adiabatically, i.e., all of the heat of reaction is used to heat up the products of the reaction. The calculation gives the equilibrium composition of the products at the calculated flame temperature as well as the equilibrium pressure that would be attained in Reactor II. The calculated results for the reaction of one and one-half volumes

of nitric acid with one volume of hydrazine (26.0 millimoles HNO_3 and 23.2 millimoles N_2H_4) are given in Table 41.

The one and one-half to one volume ratio is close to the stoichiometric ratio expressed in Eq. 21. The average maximum pressure observed in the reactor for this reactant ratio was 31.7 atm. This is to be compared to the calculated equilibrium value of 86.4 atm. The discrepancy indicates that two factors are operative that prevent the reaction from reaching an equilibrium condition: (1) the reaction is quenched through contact with metal parts of the reactor which were originally at room temperature, and (2) the products of the reaction of the material first injected into the reactor lose a large amount of heat to the reactor parts before the injection is completed. The observed products of the reaction for the one and one-half to one ratio are given in

Table 41. Equilibrium Composition of the Products of the Reaction of 26.0 millimoles HNO_3 and 23.2 millimoles N_2H_4 in a Volume of 339 cc.*

Component	Partial pressure in reactor, in atm.	Millimoles	Adiabatic flame temperature
N_2	32.93	45.81	2977°K
H_2O	40.84	56.81	
O_2	7.50	10.43	
OH	2.28	3.17	
NO	1.84	2.56	
H_2	0.64	0.89	
O	0.30	0.42	
H	0.11	0.15	
NO_2	0.01	0.01	
Total	86.44		

*One atmosphere of air was included in the calculation.

Table 31. The total quantity of the oxides of nitrogen remaining in the reactor including the residual nitric acid involved 7.6 milliatoms of N. The maximum quantity of NO to be expected from the thermodynamic calculation involved only 2.6 milliatoms N. It is thermodynamically impossible for any more NO or other nitrogen oxide to have been formed during the cooling process, since they become less stable with respect to the elements as the temperature is decreased. It was thus concluded that the reaction itself was quenched before equilibrium could be reached.

One can make a fairly accurate prediction of the expected final composition of the products at room temperature assuming that the equilibrium composition was obtained at the high temperature. The NO existing at the high temperature would be converted to NO_2 as the mixture cooled. The NO_2 would then react with some of the O_2 and H_2O to form HNO_3 according to Eq. 22. The radicals would, however, recombine to form N_2, O_2, H_2 and H_2O. The hydrogen would very likely be converted to water in the presence of the excess oxygen. This would still leave some free O_2 in the mixture, however, none was observed. Even a trace of oxygen would have been found by the mass spectrometer analysis. It appears that the quantity of NO and NO_2 formed in the reaction was sufficient to tie up all of the oxygen. The quantity of N_2 found in the reaction mixture was high enough so that it was unlikely that the N_2 came entirely from the hydrazine. The large quantity of nitrogen oxides found indicates that the nitric acid was not converted directly into nitrogen but that nitrogen oxides were formed as intermediates. The nitrogen oxides were then thermally decomposed into the elements at a slower rate.

The analysis of the products of the reaction in excess hydrazine (shown in Table 33) showed the presence of substantial quantities of ammonia. The amount of N_2 found was high enough so that the nitrogen originally contained in the hydrazine and that originally in the nitric acid must have contributed to the nitrogen found as N_2. The ammonia probably resulted from the thermal decomposition of the excess hydrazine present in the reaction mixture. Murray and Hall[18] found that the stoichiometry of hydrazine decomposition flames could be expressed by Eq. 26:

$$2\ N_2H_4 \longrightarrow N_2 + H_2 + 2\ NH_3 \qquad (26)$$

The fact that so much ammonia was found in the reaction products in the hydrazine excess case and that none was found in the acid excess runs indicates that ammonia is not an intermediate in the oxidation of hydrazine by nitric acid. The low rate of the homogeneous decomposition of ammonia has been pointed out in a previous chapter. It was shown that ammonia often persisted in high temperature reactions even though ammonia is unstable with respect to the elements at temperatures of the order of 1500°K or higher. Slight traces of NO and N_2O were also found in the reaction mixture for the hydrazine excess reaction again indicating that oxides of nitrogen are intermediates in the reduction of the acid.

The hydrogen found in the reaction of equal volumes of the reactants (Table 32) and in the reaction of two volumes of hydrazine with one volume of acid probably resulted from the thermal decomposition of the excess hydrazine and from the decomposition of some of the ammonia also formed by the decomposition of the excess hydrazine.

The adiabatic flame temperature for the reaction of four volumes of nitric acid with one volume of hydrazine was calculated since this ratio would have the lowest adiabatic flame temperature of any of the reactant ratios studied. The results are shown in Table 42.

Table 42. Equilibrium Composition of the Products of the Reaction of 23.2 millimoles Hydrazine with 66.7 millimoles of Nitric Acid in a Volume of 339 cc.

Component	Partial pressure in reactor, in atm.	Millimoles	Adiabatic flame temperature
N_2	30.13	66.98	1859°K
H_2O	35.85	79.71	
O_2	28.12	62.52	
NO	0.38	0.84	
OH	0.05	0.11	
NO_2	0.02	0.04	
Total	94.55		

The average value of the maximum pressure observed for this ratio was 23.4 atm. Again it is apparent that the reaction did not reach equilibrium. The quantity of nitrogen oxides that could be obtained by cooling a mixture of the composition shown in Table 42 would be very small. Very large quantities of NO_2 were found in the analysis of the products shown in Table 30. The quantity of nitrogen found as N_2 was somewhat less than the amount contained in the original hydrazine. It is likely that the nitrogen came entirely from the hydrazine. The nitrogen originating in the acid formed nitrogen oxides. The lower reaction temperature and the rapid quenching of the reaction was such that very little of the oxides were decomposed into the elements.

Much of the NO_2 probably resulted from the thermal decomposition of the excess nitric acid into water, oxygen and nitrogen dioxide.

If the entire quantity of reactants could have been contacted in such a way as to avoid energy transfer to the reactor parts, the calculated compositions would have been obtained. The reactions studied in the reactor were clearly stopped short of completion. The long duration of light emission observed for many of the reactant ratios indicates that reaction was not stopped the moment that the mixture contacted the reactor walls. The very low maximum pressure, however, shows that a large fraction of the energy must have been removed from the mixture during the first few msec. of reaction. The compounds such as ammonia and the nitrogen oxides that were found in the products were thus stabilized by energy loss to the reactor.

The effect of a non-reproducible ignition delay upon the maximum pressure is shown in Table 35 for the reaction of equal volumes of hydrogen peroxide and hydrazine. It was shown that in one run ignition did not occur until after injection was completed. The maximum pressure was much higher than that observed for the runs in which a shorter delay occurred. This observation shows that less energy was lost to the reactor when the reaction rate was not limited by the injection process.

CHAPTER VII
CONCLUSIONS

1. A constant volume reactor, Reactor II, was designed to rapidly contact and mix two liquid reactants in a volume ratio ranging from 4 : 1 to 1 : 1. The reactor employed a mixing pattern designed according to the principles set forth by Roughton and Chance.

2. The reactor was easily adapted to a change of the mixing pattern and could be immersed in a thermostatic bath. Satisfactory operation was obtained at temperatures as low as -40°C.

3. A photoelectric method was devised to follow the course of the injection. The injection of 2.2 cc. of water was achieved in 1.7 msec. A somewhat longer time was required for the injection of reacting fuel-oxidant systems because of the thrust created by the reaction process.

4. A fluid mechanical calculation of the injection rate was shown to agree with the observed rate of water injection. The calculation and the observed results provide information for the designer of a future rapid injection system and indicate that still more rapid rates can be obtained.

5. Reactions were studied in the reactor by following the transient pressure and the light emission. The transient pressure measuring system of McKinney was found to be very suitable. Several original photoelectric circuits were devised to follow the light emission.

6. Periodic vibrations of the transient pressure were found to occur during the early stages of the reactions under study. It was necessary to attenuate these vibrations in order to secure

interpretable records of the transient pressure. It was suggested that this phenomenon might set an upper limit to the speed with which chemical reactions may be followed by measuring their pressure.

7. The rate of mixing in the apparatus was shown to be very rapid by reference to measurements made by other investigators who employed geometrically similar mixing patterns. The hydrogen evolution in the reaction of sodium-potassium alloy with water was shown to be completed simultaneously with the completion of injection, indicating that the mixing was also completed during the injection period.

8. The two pressure maxima reported by McKinney for the reaction of sodium-potassium alloy with excess water were explained. It was shown that the first maximum was a result of local heating due to the uneven descent of the two pistons (Reactor I). The second maximum was found to be a delayed explosion of the hydrogen produced by the reaction with the oxygen present originally in the reactor atmosphere. The explosion was delayed up to 86 msec. It was likely that the explosion was initiated by chain carriers produced in the alloy, water reaction.

9. The reaction of equal quantities of sodium-potassium alloy and water was found to be completed in a time equal to the mixing time of Reactor II. Ignition was found to occur between the hydrogen produced by the reaction and the oxygen present in the reactor atmosphere without a measurable delay.

10. The reaction of equal quantities of sodium-potassium alloy with ethanol was also found to initiate the hydrogen, oxygen reaction. An ignition delay of up to 5 msec. was observed.

11. The ignition delay for certain reactant ratios of several

fuel-oxidant systems were measured and found to be less than 3 msec. in every case. The systems included:

A. Hydrazine vs. nitric acid

B. Aniline vs. nitric acid

C. Hydrazine vs. hydrogen peroxide

D. Hydrazine, liquid ammonia mixtures vs. nitric acid

The delays were significantly lower than those observed by the other investigators who employed mixing methods where the efficiency of mixing was most uncertain.

12. The very short ignition delays were attributed to (1) the rapid rate of mixing in the apparatus and (2) the impact and turbulence associated with the mixing process.

13. There was a negligible effect of the reaction temperature or of the hydrazine concentration on the ignition delay of the reaction of nitric acid with liquid ammonia, hydrazine mixtures. This result was more indicative of ignition by impact than it was of ignition controlled by the rate of a homogeneous chemical reaction.

14. The adiabatic flame temperature and the equilibrium composition of the products of the reaction of hydrazine with nitric acid were calculated. The adiabatic flame temperature for an acid rich mixture was calculated to be 1859°K; the temperature for a near stoichiometric mixture was found to be 2977°K.

15. An analysis was made of the products of the reaction of four different ratios of the hydrazine, nitric acid reaction. The products and the observed explosion pressures indicated that the reaction was quenched by energy loss to the metal parts of the reactor before equilibrium was reached. The products of the reaction indicated

that the nitric acid was first reduced to intermediate nitrogen oxides. The oxidation of the hydrazine did not appear to proceed through ammonia as an intermediate, although some ammonia was formed in the hydrazine rich mixtures presumably as a result of the thermal decomposition of the excess hydrazine.

APPENDIX I
FLUID DYNAMIC ANALYSIS OF REACTOR II

The following is an attempt to predict the injection rates obtainable with Reactor II. The formulae to be used are empirical relations found in standard engineering treatises.[34,35] The fluid mechanical system is shown schematically in Fig. 1. One of the fluids to be mixed is originally contained in the cylinder below the large piston and the other in the cylinder below the small piston. Each fluid flows from the cylinder through a lead tube into a jet and finally into the exit tube where mixing occurs. The mixed solution then flows into the interior of the reactor.

It must be assumed that the flow is steady, i.e., the equilibrium flow velocity is attained almost instantaneously and remains constant throughout injection. The flow in all ducts must be turbulent, i.e., the Reynolds number is greater than 2100. The frictional losses at each point in the flowing fluid will be estimated separately. The following is a list of symbols to be used in conjunction with Fig. 1. All pressure terms are in lb. per sq. in., all area terms are in sq. cm., all density terms are in gm. per cc., and all linear flow velocity terms are in cm. per sec.:

P = pressure of driving gas
P_1 = pressure of fluid in large cylinder
P_1^* = pressure of fluid in small cylinder
P_4 = pressure of fluid in the exit tube

A_D = area of driving gas cylinder
A_1 = area of large reactant cylinder
A_1^* = area of small reactant cylinder
A_2 = area of lead tubes

A_3 = area of jets
A_4 = area of exit tube

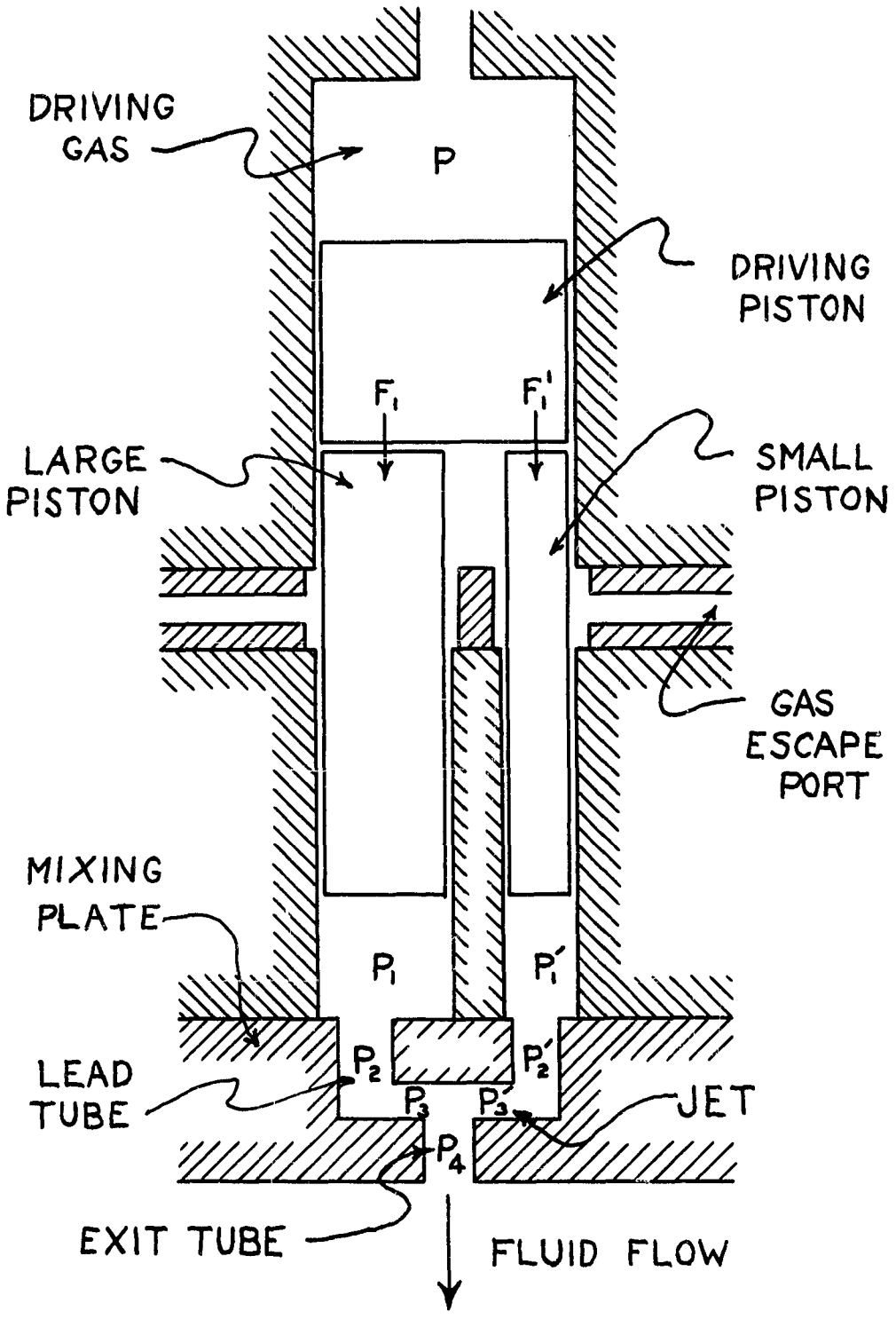

Fig. 1. Schematic Diagram of Fluid Mechanical System of Reactor II.

A_4^o = area of exit tube occupied by fluid originally contained in the large cylinder
$A_4^{o'}$ = area of exit tube occupied by fluid originally contained in the small cylinder
ρ = density of fluid originally contained in large cylinder
ρ' = density of fluid originally contained in small cylinder

u_1 = linear flow velocity of fluid in either cylinder
u_2 = linear flow velocity of fluid in lead tube
u_3 = linear flow velocity of fluid in jet
u_4 = linear flow velocity of the mixed solution in the exit tube

The force applied to the driving piston by the driving gas is the product of the pressure of the driving gas times the area of the driving piston. This force is transmitted to the two smaller pistons. If F_1 is the force transmitted to the larger of the two pistons and F_1' the force transmitted to the smaller one, then the total force is

(1) $$P A_D = F_1 + F_1'$$

If we let $r = F_1'/(F_1 + F_1')$, the pressure of the fluid in the cylinders is

(2) $$P_1 = F_1/A_1 = (1 - r)(A_D/A_1) P$$

(3) $$P_1' = F_1'/A_1 = r (A_D/A_1') P$$

The flow of the fluids originally contained in each cylinder will be treated separately. It will be assumed that each fluid occupies a separate portion of the exit tube in such a way that the linear flow velocity of the fluids are equal and equal to that of the mixed solution. If A_4 is the actual area of the exit tube and A_4^o is that portion of it occupied by the fluid originally contained in the large cylinder, then

(4) $$A_4^o = A_4 \left(\frac{A_1}{A_1 + A_1'} \right)$$

and similarly for $A_4^{o'}$ the area occupied by the fluid originally contained in the small cylinder

$$(5) \qquad A_4^{o'} = A_4 \left(\frac{A_1'}{A_1 + A_1'} \right)$$

Let us first treat the flow of the fluid from the large cylinder. This fluid is under a pressure given by Eq. 2 and is contained in a duct having an area A_1. It is flowing at a linear velocity u_1 which is necessarily equal to the rate of descent of the piston system. It has a density ρ. Eventually the fluid reaches the exit tube. Here it is under a lower pressure P_4, it has a linear velocity u_4 and it is contained in an area given by Eq. 4. Its density will be assumed to be the same as it was originally. The mechanical energy balance between these two flow cross-sections is

$$(6) \qquad \frac{u_1^2}{2} + \frac{G P_1}{\rho} = \frac{u_4^2}{2} + \frac{G P_4}{\rho} + \Sigma F$$

where $G = 68{,}947$ dynes per sq. cm. / lb. per sq. in.

ΣF = sum of losses of mechanical energy due to turbulent friction in dyne cm./gm.

Relations between the various linear flow rates result from the fact that the mass rate of flow is the same in all channels. The mass rate of flow is

$$(7) \qquad V = u_1 A_1 \rho = u_2 A_2 \rho = u_3 A_3 \rho = u_4 A_4^{o} \rho$$

Hence u_4 can be eliminated from Eq. 6 using $u_4 = u_1 A_1 / A_4^{o}$. Rearranging Eq. 6

$$(8) \qquad P_1 - P_4 = \frac{\rho u_1^2 H}{2 G} + \frac{\rho \Sigma F}{G}$$

where $H = \left(\frac{A_1}{A_4^o}\right)^2 - 1$

As the fluid flows from the cylinder into the lead tube, the flow cross-section is suddenly reduced. There is thus a frictional loss of energy. The energy loss occasioned by a sudden reduction of cross-section is given with good accuracy by

(9) $$F_{1,2} = \frac{u_2^2}{2}\left[0.50 - 0.40\left(\frac{A_2}{A_1}\right)\right] \qquad \text{for } \frac{A_2}{A_1} < 0.715$$

Eliminating $u_2 = u_1 A_1 / A_2$

(10) $$F_{1,2} = \frac{u_1^2}{2} B$$

where $$B = \left(\frac{A_1}{A_2}\right)^2 \left[0.50 - 0.40\left(\frac{A_2}{A_1}\right)\right]$$

The flow from the lead tube into the jet involves a 90° bend and a further reduction of the flow cross-section. This will be treated by calculating the losses expected for a sharp 90° bend in a duct of constant cross-section and by considering a separate reduction loss. The loss due to sudden reduction of cross-section is given by

(11) $$F_{2,3} = \frac{u_3^2}{2}\left[0.50 - 0.40\left(\frac{A_3}{A_2}\right)\right] \qquad \text{for } \frac{A_3}{A_2} < 0.715$$

Eliminating $u_3 = u_1 A_1 / A_3$

(12) $$F_{2,3} = \frac{u_1^2}{2} C$$

where $$C = \left(\frac{A_1}{A_3}\right)^2 \left[0.50 - 0.40\left(\frac{A_3}{A_2}\right)\right]$$

The losses due to the 90° bend will be treated later.

The flow from the jets into the exit tube is again accompanied by a sharp 90° bend and either a reduction or an enlargement of the flow cross-section. The loss of energy due to the sudden change of cross-section after eliminating u_3 and u_4 using Eq. 7 is

$$(13) \qquad F_{3,4} = \frac{u_1^2}{2} \; J$$

where

$$J = \left(\frac{A_1}{A_4^o}\right)^2 \left[0.50 - 0.40\left(\frac{A_4^o}{A_3}\right)\right] \qquad \frac{A_4^o}{A_3} < 0.715$$

$$J = \left(\frac{A_1}{A_4^o}\right)^2 \left[0.75\left(1 - \frac{A_4^o}{A_3}\right)\right] \qquad 0.715 < \frac{A_4^o}{A_3} < 1.00$$

$$J = \left(\frac{A_1}{A_3}\right)^2 \left(1 - \frac{A_3}{A_4^o}\right)^2 \qquad 1.00 < \frac{A_4^o}{A_3}$$

The losses occurring at bends in a pipe line are usually calculated on the assumption that an effective straight length of pipe can be substituted for the bend. The losses due to turbulent friction in a straight length of pipe can be calculated with good accuracy by

$$(14) \qquad F = 4 \frac{u_3^2}{2} \; f \; \frac{L}{D}$$

where
f is the Fanning friction factor
L is the total effective length of straight pipe
D is the diameter of the pipe

The friction factor f is a function only of the Reynolds number. It can be expressed as

$$(15) \qquad f = 0.00140 + 0.125 \, Re^{-0.32}$$

For the present case it is necessary to estimate an effective length

to allow for the two 90° bends and to evaluate the Reynolds number. The Reynolds number is given by the dimensionless ratio

$$(16) \qquad Re = \frac{D\, u\, \rho}{\mu}$$

where μ is the viscosity of the fluid.

Since the friction factor is affected only slightly by small changes in Re, it will be assumed that flow conditions in the jet represent the conditions in any flow section. This is reasonable since the principal losses occur in the 90° bends and the bends adjoin either end of the jet. The viscosities of the liquids to be considered, i.e., water, nitric acid and hydrazine, are very close to one centipoise at room temperature. This value will then be used for all calculations involving these materials. The density of nitric acid is higher than that of either water or hydrazine so that the proper values will be used.

A generally accepted value for the effective length equivalent to a sharp 90° bend is 75 diameters. The turbulent losses occurring in the actual straight sections will be estimated to be equivalent to eight diameters. Since there are two bends equivalent to a total of 150 diameters and straight sections equivalent to about 8 diameters, Eq. 14 becomes, eliminating u_3 by means of Eq. 7:

$$(17) \qquad F = \frac{u_1^2}{2}\, f\, E$$

where $$f = 0.00140 + 0.125\left(\frac{\mu}{D_3\, u_3\, \rho}\right)^{0.32}$$

$$E = 4\,(158)\left(\frac{A_1}{A_3}\right)^2$$

All of the losses can be substituted into Eq. 8

$$(18) \qquad P_1 - P_4 = \frac{\rho u_1^2}{2G} (H + B + C + J + E f)$$

A similar expression for the flow of the fluid originally contained in the small cylinder can be derived

$$(19) \qquad P_1' - P_4 = \frac{\rho' u_1^2}{2G} (H' + B' + C' + J' + E'f')$$

u_1 for both fluids is the same and is equal to the rate of descent of the piston system. P_4 is the same in both cases since both fluids pass through the same exit tube. P_1 and P_1' in Eq. 18 and Eq. 19 can be expressed in terms of the driving pressure P with the help of Eq. 2 and Eq. 3. r can then be eliminated between the two resulting equations and the final result is obtained:

$$(20) \quad \left(\frac{A_D}{A_1 + A_1'}\right) P - P_4 = \frac{u_1^2}{2G} \left[\rho\left(\frac{A_1}{A_1 + A_1'}\right) (H + B + C + J + E f) + \rho'\left(\frac{A_1'}{A_1 + A_1'}\right) (H' + B' + C' + J' + E'f')\right]$$

It should be noted that the coefficient of P in Eq. 20 is the extent of the hydraulic advantage gained in having a single large piston drive smaller ones, i.e., it would require a pressure equal to or greater than $\left[A_D/(A_1 + A_1')\right]$ P in the interior of the reactor before injection could be stopped. P_4 is the pressure in the exit tube; it must also be the pressure in the interior of the reactor since the exit tube discharges into this relatively large air space. In many of the cases to be considered this back pressure is negligible in comparison

with the first term in Eq. 20. The term on the left hand side of Eq. 20 is essentially the total pressure drop. The rate of descent of the piston system u_1 would be proportional to the square root of the pressure drop except for the slight dependence of f and f' on u_1.

For a given set of conditions, the injection rate may be calculated as follows: The terms involving only the reactor dimensions (A_D, A_1, A_1', H, H', B, B', C, C', J, J', E and E') are calculated and substituted in Eq. 20. The value of these terms depends only upon the reactant ratio under consideration. The densities of the fluids are then substituted into Eq. 20. A series of reasonable flow velocities u_1 are assumed. From these, the viscosities of the fluids and the densities of the fluids, the fraction factors f and f' are evaluated by means of Eq. 17. Using the assumed u_1 value and the corresponding friction factors, the right hand side of Eq. 20 is evaluated. Neglecting P_4, the value of P is then calculated as a function of the injection rate u_1. The injection rate is conveniently expressed as the time required for the piston system to descend seven-eighths inch, the stroke used for most of the runs. The injection time t, in msec., is related to the injection rate according to Eq. 21:

$$t = \frac{2222}{u_1} \qquad (21)$$

Calculations were made for the injection of water from both cylinders for the one to one ratio and the four to one ratio. Calculations were also made for the mixing of hydrazine and nitric acid for all reactant ratios except the four to one ratio with hydrazine in excess. The important dimensions of the injection system are given in Tables 1 and 2.

Table 1. Dimensions of Reactant Cylinders, Reactor II

Nominal volume ratio	Diameter of large cylinder, in inches	Diameter of small cylinder, in inches	A_1 Area of large cylinder, in sq. cm.	A_1' Area of small cylinder, in sq. cm.
4 : 1	0.502	0.257	1.277	0.335
2 : 1	0.376	0.257	0.716	0.335
1.5 : 1	0.314	0.257	0.498	0.335
1 : 1	0.314	0.314	0.498	0.498

Table 2. Dimensions of Injection System, Reactor II

Item	Diameter, in inches	Area, in sq. cm.	Symbol for area
Driving cylinder	1.000	5.067	A_D
Lead tube	0.152	0.117	A_2
Jets	0.098	0.049	A_3
Exit tube	0.152	0.117	A_4

The results of the calculation of the driving pressure required to obtain the assumed injection rates for the water injection are shown in Table 3. The results for the hydrazine, nitric acid injection are given in Table 4. Any desired pressure, injection rate value may be obtained by graphical interpolation from a plot of the results given in Tables 3 and 4.

Table 3. Calculated Values of the Injection Time for the Water Injection

Reactant ratio	Injection time, in msec.	Driving pressure, in lb. per sq. in.
1 : 1	1.0	2310
	1.4	1230
	1.7	855
	2.0	630
	2.3	486
	2.6	387
	2.9	316
4 : 1	2.6	2840
	3.0	2170
	3.4	1720
	3.8	1390

Table 4. Calculated Values of the Injection Time for the Nitric Acid, Hydrazine Injection

Reactant ratio	Reactant in excess	Injection time, in msec.	Driving pressure, in lb. per sq. in.
4 : 1	HNO_3	3.4	2380
		4.0	1750
		5.0	1160
		6.0	822
		7.0	617
2 : 1	HNO_3	1.5	2270
		2.6	809
		4.0	363
1.5 : 1	HNO_3	1.0	1970
		2.0	536
		3.0	251
1 : 1	-	1.0	2800
		2.0	760
		3.0	357
1.5 : 1	N_2H_4	1.0	1680
		2.0	459
		3.0	216
2 : 1	N_2H_4	1.5	1780
		2.6	636
		4.0	285

APPENDIX II
FLUID DYNAMIC ANALYSIS OF GAS FLOW IN THE PNEUMATIC INJECTOR

The following analysis is an attempt to determine the pressure drop due to nitrogen flow in the pneumatic injector during injection. The gas flow will be assumed to be steady and isothermal. A schematic diagram of the fluid mechanical system is shown in Fig. 1. During injection the flow approximates a steady Joule-Thompson expansion from a constant pressure P_3 to a lower constant pressure P_1. The gas will be assumed to be ideal.

It is shown in a paper by Beale and Docksey[37] that the Bernoulli equation for the flow from P_3 to P_2 may be expanded to include the turbulent energy loss occasioned by the sudden reduction in cross-section as the gas expands from P_3 to P_4. Their result is expressed in Eq. 1:

$$(1) \qquad P_3 - P_2 = \left[4 f \frac{L}{D} + 2 \ln \frac{P_3}{P_2} + \frac{1}{2}\left(1 + \frac{P_2}{P_3}\right)\right] \left(\frac{2 P_2}{P_3 + P_2}\right) \frac{\rho_2 v_2^2}{2 G}$$

where P_i are pressure terms in lb. per sq. in.
f is the Fanning friction factor
L is the total length of duct
D is the diameter of the duct
ρ_2 is the density of gas at the pressure P_2, in gm. per cc.
v_2 is the linear flow velocity at the point where the pressure is P_2, in cm. per sec.
G is 68,947 dynes per sq. cm./lb. per sq. in.

The density ρ_2 is related to the original density of gas in the storage reservoir according to Eq. 2:

$$(2) \qquad \rho_2 = \rho_3 \frac{P_2}{P_3}$$

We can define a quantity r as follows:

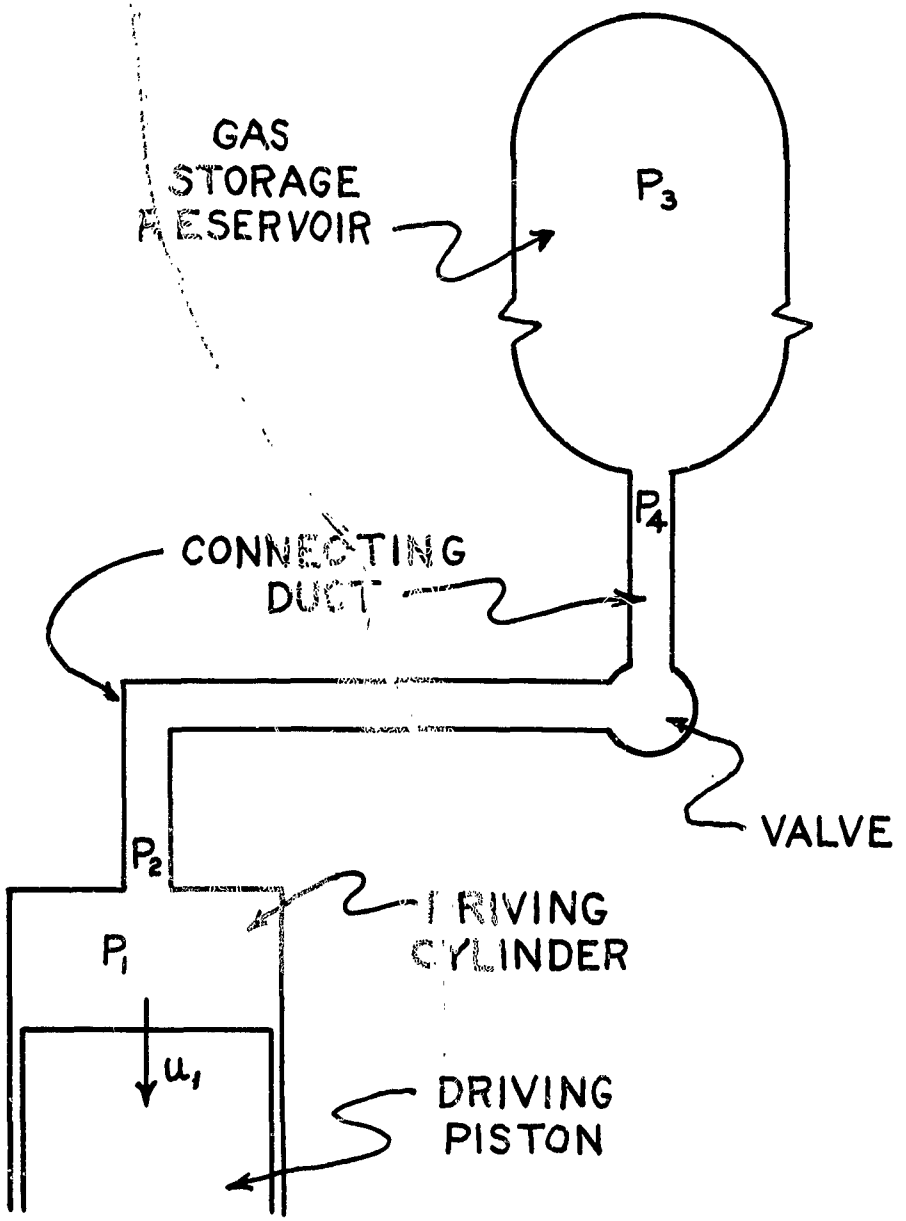

Fig. 1. Schematic Diagram of Fluid Mechanical System of the Pneumatic Injector.

$$(3) \qquad r = \frac{P_2}{P_3}$$

Substituting Eq. 2 and Eq. 3 into Eq. 1 and rearranging, Eq. 4 is obtained:

$$(4) \qquad \frac{G P_3}{\rho_3} = \left[4 f \frac{L}{D} + 2 \ln \frac{1}{r} + \frac{1}{2}(1 + r)\right] \frac{r^2}{1 - r^2} \; u_2^2$$

The left hand side of Eq. 4 can be simplified through the perfect gas law:

$$(5) \qquad \frac{G P_3}{\rho_3} = \frac{R T}{M}$$

where $R = 83.15 \times 10^6$ dynes cm.$^{-2}$, cc., mole^{-1}, $^{\circ}K^{-1}$
$T = 300^{\circ}K$
$M = 28.02$ gm. per mole

Substituting Eq. 5 into Eq. 4, Eq. 6 is obtained:

$$(6) \qquad \frac{R T}{M} = \left[4 f \frac{L}{D} + 2 \ln \frac{1}{r} + \frac{1}{2}(1 + r)\right] \frac{r^2}{1 - r^2} \; u_2^2$$

Dodge[36] points out that for high velocity flow of gases, f is substantially constant at 0.0040. There are two 90° bends in the duct connecting the gas storage reservoir and the driving cylinder. Each bend causes a frictional loss of mechanical energy equivalent to about 75 diameters of straight duct. The total length to diameter ratio is then about 150. This treatment neglects the energy losses due to flow through the actual straight lengths of duct and the losses created by certain irregularly shaped components located in the valve of the injector so that the result should be conservative. Substituting these constants into Eq. 6, we obtain Eq. 7:

$$(7) \qquad \frac{R T}{M} \frac{1}{u_2^2} = \left[2.40 + 2 \ln \frac{1}{r} + \frac{1}{2}(1 + r)\right] \frac{r^2}{1 - r^2}$$

Eq. 7 can be solved for u_2 as a function of r.

The effective pressure on the driving piston P_1 is, however, not involved in Eq. 7. It is necessary to relate the pressure P_2 to the pressure P_1. This can be done by using the expression for the enlargement loss occurring during flow from the pressure P_2 to the pressure P_1. The generalized expression for the losses occurring during a sudden enlargement of the cross-section is as follows:

$$(8) \qquad -\int_2^1 \frac{dP}{\rho} = u_1 (u_1 - u_2)$$

ρ can be eliminated by means of the perfect gas law.

$$(9) \qquad -\frac{R\,T}{M}\int_2^1 \frac{dP}{P} = u_1 (u_1 - u_2)$$

Eq. 9 can be integrated and rearranged.

$$(10) \qquad -\frac{R\,T}{M} \ln \frac{P_1}{P_2} = u_1^2 \left(1 - \frac{u_2}{u_1}\right)$$

The ratio u_2/u_1 can be evaluated because of the equality of the mass rate of flow in both the connecting duct and the driving cylinder:

$$(11) \qquad \frac{u_2}{u_1} = \frac{P_1 A_1}{P_2 A_2}$$

where A_1/A_2 is the ratio of the cross-sectional areas. The connecting duct has a diameter of 0.25 inch and the driving cylinder has a diameter of 1.00 inch. The ratio of areas is then equal to 16. We may define x as follows:

$$(12) \qquad x = \frac{P_2}{P_1}$$

Substituting Eq. 11 and Eq. 12 into Eq. 10, the desired relation is obtained:

$$(13) \qquad \frac{R\,f}{M} \ln \frac{1}{x} = u_1^2 \left(\frac{16}{x} - 1 \right)$$

A simple relation exists between u_2 and u_1. Evaluating Eq. 11, Eq. 14 is obtained:

$$(14) \qquad \frac{u_2}{u_1} = \frac{16}{x}$$

u_1 is the linear velocity of descent of the piston system. It is related to the time, in msec., required to descend seven-eighths inch by Eq. 15:

$$(15) \qquad u_1 = \frac{2222}{t}$$

The ratio of the effective driving pressure P_1 to the pressure in the gas storage reservoir P_3 is given by Eq. 16:

$$(16) \qquad \frac{P_1}{P_3} = \frac{r}{x}$$

The procedure used to calculate P_1/P_3 as a function of t, the injection time, was as follows: Various values of t were assumed; the corresponding u_1 values were then calculated from Eq. 15. The values of x corresponding to the u_1 values were then calculated by a trial and error method using Eq. 13. The corresponding values of u_2 were determined from Eq. 14. The values of r were calculated from Eq. 12 for the various values of u_2. The final values of P_1/P_3 were then determined from r and x according to Eq. 16. The results of this calculation are given in Table 1.

Table 1. Calculated Values of the Pressure Drop in the Pneumatic Injector

Injection time, in msec.	Ratio of effective driving pressure to applied pressure
1.7	0.587
2.0	0.641
2.6	0.748
3.0	0.792
4.0	0.879
5.0	0.916
6.0	0.940
8.0	0.965
10.0	0.977

APPENDIX III
ANALYTICAL PROCEDURES

The methods employed for the chemical analysis of the various reagent materials are outlined below:

Sodium-potassium Alloy

Weighing bottles were partially filled with dried dibutyl ether and weighed. Approximately 0.7 gm. of the alloy was added to the bottles by means of a medicine dropper in the drybox. The weighing bottles were then reweighed to obtain the sample weight. The contents of each bottle were poured into a dry 250 ml. Erlenmeyer flask. More ether was then added. Absolute ethanol was added dropwise until all of the alloy had been destroyed. The weighing bottles were rinsed with ethanol although no alloy appeared to be present. Water was added to bring the volume of solution up to about 100 ml. The solution was then titrated with standard 0.5 N HCl solution to the phenolphthalein end-point. From the sample weight and the volume of acid used it was possible to calculate the apparent molecular weight of the alloy. The composition could then be calculated assuming that only sodium and potassium were present.

Nitric Acid

Several different methods for sampling and analyzing fuming nitric acid are given in the reprint of a recent symposium.[45] Methods suggested in the reprint included the use of weighing burets to dispense the acid or small vials containing the acid to be broken under water. The latter methods were not used since they are of more interest in the present case where it is desired to analyze the acid actually introduced into the reactor than it was to

analyze the material in the storage flask. Acid was transferred from the storage flask to the reactor by means of automatic pipets. The method of sampling for analysis was also to transfer a sample of acid (1.5 gm.) from the storage flask to a weighed 100 ml. volumetric flask by means of the automatic pipet in such a way that no acid touched the narrow portion of the flask. The flask was then covered and reweighed. The volumetric flask was immersed in a liquid nitrogen or dry ice bath to the neck of the flask for about five minutes. The flask could then be opened and the solution diluted without fear of losing acidic vapors.

The various classifications of concentrated nitric acid solutions were defined by S. F. LaKatos in the symposium reprint.[45] The classifications were defined as follows: "White Fuming Nitric Acid refers to nitric acid of concentrations between 97.50% and 99.79% containing a maximum of oxides of nitrogen of 0.5% as nitrogen dioxide (NO_2) and a maximum of 2% of water (H_2O). Red Fuming Nitric Acid refers to nitric acid of total acidity values above 100% containing various amounts of dissolved oxides of nitrogen which vary in commercial products from 6.5% to 22% by weight. Anhydrous Nitric Acid refers to nitric acid of concentrations from 99.8% to 100.5% containing no more than 0.10% dissolved oxides of nitrogen by weight as NO_2 and no more than 0.10% water by weight."

It is necessary to use separate samples to determine the concentration of HNO_3 and that of NO_2. The procedure for determining the total acidity will be given first: To the frozen sample in the 100 ml. volumetric flask was added about 10 ml. of water and almost a stoichiometric quantity of standard 0.7 N NaOH solution. The solution in the volumetric flask was then allowed to come to room temperature.

A drop of phenolphthalein indicator solution was added. Further NaOH solution was added until the solution was just basic. The solution was then back-titrated with 0.1 N HCl. By using the much more dilute HCl solution, it was possible to locate the end-point very accurately. The analysis gives the total quantity of HNO_3 and NO_2 in the sample since the NO_2 is converted to HNO_3 when the solution is diluted with water in the presence of air.

Values of 100.2 to 100.8% HNO_3 were consistently obtained for the nitric acid prepared by distillation from sulfuric acid. The NaOH solution had been standardized against reagent grade potassium acid phthalate. It was thought possible that the phthalate was impure. The NaOH was then standardized against freshly prepared 0.7 N HCl that had been standardized by gravimetric analysis of the chloride. An identical result was obtained for the normality of the NaOH solution. The high values of the HNO_3 content were then accepted. It appeared that the method of preparation produced a small quantity of dissolved N_2O_5.

The analysis of NO_2 in the fuming nitric acid was as follows: To the frozen sample in the volumetric flask was added an excess of standard 0.1 N ceric sulfate solution. The solution was then diluted with water and back-titrated with standard 0.1 N ferrous sulfate solution to the ferroin end-point. The NO_2 was oxidized to NO_3^- according to Eq. 1:

$$(1) \qquad Ce^{++++} + NO_2 + H_2O \longrightarrow Ce^{+++} + NO_3^- + 2\,H^+$$

The ceric sulfate solution was standardized against arsenious oxide according to Eq. 2:

(2) $As_2O_3 + 5\ H_2O + 4\ Ce^{++++} \longrightarrow 2\ H_3AsO_4 + 4\ Ce^{+++} + 4\ H^+$

The quantity of NO_2 was found to be 0.11% for a badly colored sample so that the acid used in the reactor corresponded to "anhydrous nitric acid" according to the definition given above.

Hydrazine

Hydrazine was analyzed by the iodate method of Penneman and Audrieth[46] and by direct acid titration. The same sampling method was used for hydrazine. The sample (1 gm.) was transferred to a weighed 100 ml. volumetric flask by means of an automatic pipet. The flask was reweighed and immersed in a cold bath. Almost a stoichiometric quantity of standard 0.5 N HCl was then added. The neutralization reaction is shown in Eq. 3:

(3) $N_2H_4 + H^+ \longrightarrow N_2H_5^+$

After reaching room temperature, the solution was further titrated with the HCl solution to the methyl red end-point. The solution in the volumetric flask was then diluted to the mark with water. Aliquots of 10 ml. were transferred to 250 ml. Erlenmeyer flasks and diluted with 50 ml. of water. Concentrated HCl, 50 ml., was then added to the mixture. The solution was titrated with 0.1 M KIO_3 to the disappearance of the red color of wool red indicator. The reaction is expressed by Eq. 4:

(4) $N_2H_4 + IO_3^- + 2\ H^+ + Cl^- \longrightarrow ICl + N_2 + 3\ H_2O$

The direct acid titration gives the sum of the hydrazine and any ammonia that might be present. The iodate method, however, is not

affected by the presence of ammonia. The combination of the two titrations gives the concentrations of both ammonia and hydrazine. No ammonia was found in the analyses made of the anhydrous hydrazine.

Hydrogen Peroxide

The hydrogen peroxide (1 gm.) was transferred to a 100 ml. volumetric flask by means of an automatic pipet. The flask was then reweighed. The solution was diluted to the mark with water. Aliquots of 10 ml. were transferred to titration flasks. The solution was titrated with standard 0.1 N ceric sulfate solution to the ferroin end-point. The reaction is expressed in Eq. 5:

(5) $H_2O_2 + 2\ Ce^{++++} \longrightarrow 2\ Ce^{+++} + 2\ H^+ + O_2$

APPENDIX IV
CALCULATION OF ADIABATIC FLAME TEMPERATURES

The adiabatic flame temperatures for two reactant ratios of the hydrazine, nitric acid reaction were calculated. The basic heat data are expressed in Eq. 1,[47] Eq. 2,[13] Eq. 3,[48] and Eq. 4:[48]

(1) $N_2H_4(l) + O_2 \longrightarrow N_2 + 2\ H_2O(l)$ $\quad \Delta H = -148{,}635$

(2) $HNO_3(l) \longrightarrow 0.5\ N_2 + 1.5\ O_2 + 0.5\ H_2$ $\quad \Delta H = 41{,}349$

(3) $H_2O(l) \longrightarrow H_2 + 0.5\ O_2$ $\quad \Delta H = 68{,}315$

(4) $H_2O(l) \longrightarrow H_2O(g)$ $\quad \Delta H = 10{,}503$

The heats of the reactions are given in calories per mole and refer to 25°C. Eq. 5 and Eq. 6 result from obvious combinations of Eq. 1 to 4, inclusive:

(5) $HNO_3(l) + N_2H_4(l) \longrightarrow 1.5\ N_2 + 0.25\ O_2 + 2.5\ H_2O(g)$
$\Delta H = -115{,}186 \quad \Delta E = -117{,}704$

(6) $HNO_3(l) \longrightarrow 0.5\ N_2 + 1.25\ O_2 + 0.5\ H_2O$
$\Delta H = 12{,}443 \quad \Delta E = 11{,}110$

The energy change for each reaction was calculated from the reaction heats using the following relation:

(7) $\Delta H = \Delta E + \Delta n R T$

The first step in the procedure was to calculate the heat evolved by the hypothetical conversion of the liquid reactants into nitrogen, oxygen and water vapor at 25°C. It was also necessary to calculate the atomic composition of the reactants. The starting materials are given below for the two reactant ratios under consideration:

Nominal volume ratio	4 : 1	1.5 : 1
Moles hydrazine	0.02321	0.02321
Moles nitric acid	0.06665	0.02599
Moles air: nitrogen	0.01088	0.01088
oxygen	0.00289	0.00289
Reactor volume, in cc.	339	339

The heat evolved by the conversion into nitrogen, oxygen and water vapor at 25°C was calculated using Eq. 5 and Eq. 6 and is given below along with the atomic composition:

Nominal volume ratio	4 : 1	1.5 : 1
Heat, in calories	2249.3	2701.0
Gram-atoms N	0.1348	0.09417
Gram-atoms O	0.2058	0.08375
Gram-atoms H	0.1595	0.1188

The partial pressures of the assumed products at any temperature can be calculated by the simultaneous solution of Eq. 8 to Eq. 10, inclusive:

$$(8) \qquad 2\,P_{N_2} = (N)\,\frac{R\,T}{V}$$

$$(9) \qquad P_{H_2O} + 2\,P_{O_2} = (O)\,\frac{R\,T}{V}$$

$$(10) \qquad 2\,P_{H_2O} = (H)\,\frac{R\,T}{V}$$

where (N) = Gram-atoms N

(O) = Gram-atoms O

(H) = Gram-atoms H

The second step in the procedure is to calculate an approximate temperature. The number of moles of nitrogen, oxygen and water vapor were first calculated. It was then possible, using the molar energy content tables given by Lewis and von Elbe,[48] to find the temperature

reached by the three component mixture through the [illegible] available heat. This temperature for the 1.5 : 1 absorption of the [illegible]°K; for the 4 : 1 ratio the temperature was ratio was found to be 3[illegible] higher than the adiabatic flame 1870°K. This trial temperature [illegible] temperature because of the fact that the dissociation of the nitrogen, oxygen and water vapor were ignored. The dissociation reactions require energy thus decreasing the available energy to raise the temperature of the products.

The third step in the procedure was to calculate the quantity of the dissociation products. It was necessary to evaluate the partial pressures of the nitrogen, oxygen and water vapor by solving Eq. 8 to Eq. 10, inclusive, using the trial temperature given above. The partial pressure values were then substituted into the expressions given below for the dissociation equilibria:

(11) a) $H_2 + \frac{1}{2} O_2 \rightleftharpoons H_2O$ $\qquad P_{H_2} = K_a P_{H_2O} P_{O_2}^{-\frac{1}{2}}$

b) $OH + \frac{1}{2} H_2 \rightleftharpoons H_2O$ $\qquad P_{OH} = K_b P_{H_2O} P_{H_2}^{-\frac{1}{2}}$

c) $2 H \rightleftharpoons H_2$ $\qquad P_H = K_c^{\frac{1}{2}} P_{H_2}^{\frac{1}{2}}$

d) $2 O \rightleftharpoons O_2$ $\qquad P_O = K_d^{\frac{1}{2}} P_{O_2}^{\frac{1}{2}}$

e) $NO \rightleftharpoons \frac{1}{2} O_2 + \frac{1}{2} N_2$ $\qquad P_{NO} = K_e P_{O_2}^{\frac{1}{2}} P_{N_2}^{\frac{1}{2}}$

f) $NO + \frac{1}{2} O_2 \rightleftharpoons NO_2$ $\qquad P_{NO_2} = K_f^{-1} P_{NO} P_{O_2}^{\frac{1}{2}}$

g) $2 N \rightleftharpoons N_2$ $\qquad P_N = K_g^{\frac{1}{2}} P_{N_2}^{\frac{1}{2}}$

The equilibrium constants for any temperature were obtained by graphical interpolation from the data given by Lewis and von Elbe.[48] The

trial value of the partial pressure of each dissociation product [illegible] than obtained.

The fourth step of the procedure was to correct the material balance for the presence of the dissociation products. This was done using Eq. 12 to Eq. 14, inclusive:

(12) (N) $\frac{R\,T}{V} = (2\,P_{N_2}) + P_{NO} + P_{NO_2} + P_N$

(13) (O) $\frac{R\,T}{V} = (P_{H_2O} + 2\,P_{O_2}) + P_{NO} + 2\,P_{NO_2} + P_{OH} + P_O$

(14) (H) $\frac{R\,T}{V} = (2\,P_{H_2O}) + 2\,P_{H_2} + P_{OH} + P_H$

The values of the dissociation products were substituted into the equations. New values of the partial pressure of nitrogen, oxygen and water vapor were then obtained so that a correct material balance resulted.

The fifth step of the procedure was to correct the heat balance for the heat required to form the dissociation products. It was necessary to calculate the number of moles of each dissociation product. This was done using Eq. 15, the calculated partial pressures and the trial temperature:

(15) $n_i = \frac{V}{R\,T}\,P_i$

The heat required to form each dissociation product at 25°C from nitrogen, oxygen and water was calculated from Eq. 16:

(16) a) $\frac{1}{2}\,H_2O(g) \longrightarrow \frac{1}{4}\,O_2 + OH \qquad \Delta E = 38{,}811$

b) $\frac{1}{2}\,O_2 + \frac{1}{2}\,N_2 \longrightarrow NO \qquad \Delta E = 21{,}477$

c) $H_2O(g) \longrightarrow H_2 + \frac{1}{2}\,O_2 \qquad \Delta E = 57{,}502$

d) $\frac{1}{2}\,O_2 \longrightarrow O \qquad \Delta E = 58{,}737$

e) $\frac{1}{2} H_2O(g) \longrightarrow \frac{1}{4} O_2 + H \qquad \Delta E = 80{,}545$

were calculated from the tables given by Lewis and von Elbe.[48] The quantity of N and NO_2 was insufficient to affect the heat balance. The total heat required to form the dissociation products at 25°C was subtracted from the total heat given previously. The resulting heat was available for heating the total mixture from 25°C to the high temperature.

The next step in the procedure was a repetition of the second step. The adjusted temperature was found through the use of the molar energy content tables using the new composition that included the dissociation products. The resulting temperature is below the adiabatic flame temperature. The concentration of the dissociation products was evaluated at too high a temperature so that the calculated concentrations were too high. The heat required to form the dissociation products was then too high leaving too little heat to raise the temperature.

It was found most convenient to assume an intermediate temperature at this point. It was necessary also to estimate the partial pressure of oxygen, nitrogen and water vapor. The third step was then repeated. The partial pressures of the dissociation products were then evaluated at the new temperature. The fourth step, the correction of the material balance, then showed whether the correct partial pressures of the principal components had been assumed. The fifth step was then repeated correcting the original heat balance. The second step was repeated to check the assumed temperature.

For the 4 : 1 ratio, only one additional trial had to be employed to arrive at the correct temperature and composition, since

the low concentration of dissociation products did not seriously affect the heat balance. For the 1.5 : 1 ratio, it was necessary to repeat the trial and error calculation six times before accurate agreement was obtained between the assumed temperature and composition and the calculated values. The values used for the final trial are given below:

Nominal reactant ratio		4 : 1	1.5 : 1
Trial temperature, in °K		1858	2970
Trial composition, in atm.	P_{N_2}	30.13	32.85
	P_{O_2}	28.12	7.50
	P_{H_2O}	35.87	40.84

The values calculated from the trial values are as follows:

Nominal reactant ratio		4 : 1	1.5 : 1
Temperature, in °K		1859	2977
Composition, in atm.	P_{N_2}	30.13	32.93
	P_{O_2}	28.12	7.50
	P_{H_2O}	35.87	40.84
	P_{OH}	0.05	2.28
	P_{NO}	0.38	1.84
	P_{H_2}	-	0.64
	P_{O}	-	0.30
	P_{H}	-	0.11
	P_{NO_2}	0.02	0.01
Total pressure, in atm.		94.55	86.44

The agreement of the trial values with those calculated is within the accuracy of the thermodynamic data.

BIBLIOGRAPHY

1. H. Hartridge and F. J. W. Roughton, Proc. Roy. Soc. (London) A104, 376 (1923), et seq.

2. B. Chance, J. Franklin Inst. 229, 455, 613, 737 (1940).

3. C. D. McKinney, Jr., A Kinetic Study of Rapid Reactions which Evolve Gases, Ph. D. Thesis, Illinois Institute of Technology, 1950.

4. Sabanejeff, Z. anorg. Chem. 20, 21 (1899).

5. W. R. E. Hodgkinson, J. Soc. Chem. Ind. 32, 519 (1913).

6. A. G. Keenan, private communication.

7. A. S. Gordon, Third Symposium on Combustion and Flame and Explosion Phenomena, Williams and Wilkins Co., Baltimore, 1949, p. 493.

8. L. F. Audrieth and B. A. Ogg, The Chemistry of Hydrazine, John Wiley and Sons, Inc., New York, 1951, p. 123.

9. R. E. Kirk and A. W. Browne, J. Am. Chem. Soc. 50, 337 (1928).

10. M. Szwarc, J. Chem. Phys. 17, 505 (1949).

11. P. J. Askey, J. Am. Chem. Soc. 52, 970 (1930).

12. H. S. Johnston, L. Foering and R. J. Thompson, J. Phys. Chem. 57, 390 (1953).

13. W. R. Forsythe and W. F. Giauque, J. Am. Chem. Soc. 64, 48 (1942).

14. R. J. Gillespie, et al., J. Chem. Soc. 1950, 2473, et seq.

15. C. A. Bunton, et al., J. Chem. Soc. 1950, 2628, et seq.

16. W. J. Dunning and C. W. Nutt, Trans. Faraday Soc. 47, 15 (1951).

17. C. H. Bamford, Trans. Faraday Soc, 35, 1239 (1939).

18. R. C. Murray and A. R. Hall, Trans. Faraday Soc. 47, 743 (1951).

19. Tanner, Dissertation, Zurich, 1945.

20. H. G. Wolfhard and W. G. Parker, Proc. Phys. Soc. (London) A62, 722 (1949).

21. B. Lewis and G. von Elbe, Combustion, Flames and Explosions of Gases, Academic Press, Inc., New York, 1951, p. 644.

22. M. W. Kellogg Co., Preliminary Experimental Studies of Liquid Fuel Systems, Final Report, Report No. SPD 236, May 20, 1949, p. 88, et seq.

23. S. V. Gunn, J. Am. Rocket Soc., January-February, 1952, p. 33.

24. J. D. Broatch, Fuels 29, 106 (1950).

25. F. J. W. Roughton, Proc. Roy. Soc. (London) A126, 439, 470 (1930).

26. F. J. W. Roughton and G. A. Millikan, Proc. Roy. Soc. (London) A155, 258 (1936).

27. Trowse, Dissertation, Leeds, 1952.

28. F. J. W. Roughton and B. Chance, Investigations of Rates and Mechanisms of Reactions, Technique of Organic Chemistry, Volume VIII, ed. A. Weissberger, Interscience Publishers, Inc., New York, 1953, p. 669.

29. M. Kilpatrick and C. D. McKinney, Jr., J. Am. Chem. Soc. 72, 5474 (1950).

30. C. D. McKinney, Jr. and M. Kilpatrick, Rev. Sci. Insts. 22, 590 (1951).

31. C. D. McKinney, Jr. and M. Kilpatrick, An Apparatus for Measuring the Rates of Some Rapid Reactions, Technical Report No. 1, Office of Naval Research Contract N7-onr-329 III, November 1950.

32. C. C. Neas, M. W. Raymond and C. O. Ewing, M. I. T. Report No. 11, DIC 6351, November 1, 1946.

33. National Research Council, International Critical Tables, Volume III, McGraw-Hill Book Co., New York, 1928, p. 235.

34. J. H. Perry, Chemical Engineers' Handbook, 2nd. Ed., McGraw-Hill Book Co., New York, 1941, p. 800 ff.

35. W. H. Walker, W. K. Lewis, W. H. McAdams and E. R. Gilliland, Principles of Chemical Engineering, McGraw-Hill Book Co., New York, 1937, p. 74 ff.

36. B. F. Dodge, Chemical Engineering Thermodynamics, McGraw-Hill Book Co., New York, 1944, p. 351.

37. E. S. L. Beale and P. Docksey, J. Institute of Petroleum 34, 602 (1948).

38. R. T. Sanderson, Vacuum Manipulation of Volatile Compounds, John Wiley and Sons, Inc., New York, 1948, p. 117 ff.

39. D. M. Yost and H. Russell, Systematic Inorganic Chemistry, Prentice-Hall, Inc., New York, 1944, p. 28.

40. National Research Council, International Critical Tables, Volume I, McGraw-Hill Book Co., New York, 1928, p. 108.

41. B. Lewis and G. von Elbe, J. Chem. Phys. 3, 63 (1935).

42. F. P. Bowden, M. F. R. Mulcahy, R. G. Vines and A. Yoffe, Proc. Roy. Soc. (London) A188, 291 (1947).

43. W. Jost and H. Teichmann, Naturwissenschaften 27, 318 (1939).

44. E. J. Badin, J. Am. Chem. Soc. 70, 3651 (1948).

45. Research and Development Board, The Department of Defense, Symposium on Analysis of Nitric Acids, 31 December, 1951.

46. R. A. Penneman and L. F. Audrieth, Anal. Chem. 20, 1058 (1948).

47. L. F. Audrieth and B. A. Ogg, The Chemistry of Hydrazine, John Wiley and Sons, Inc., New York, 1951, p. 67.

48. B. Lewis and G. von Elbe, Combustion, Flames and Explosions of Gases, Academic Press, Inc., New York, 1951, p. 739 ff.

Copies	Addressee
1	Commanding Officer Office of Naval Research Branch Office 150 Causeway Street Boston, Massachusetts
2	Commanding Officer Office of Naval Research Branch Office 86 East Randolph Street Chicago 1, Illinois
1	Commanding Officer Office of Naval Research Branch Office 346 Broadway New York 13, New York
1	Commanding Officer Office of Naval Research Branch Office 1000 Geary Street San Francisco 9, California
1	Commanding Officer Office of Naval Research Branch Office 1030 E. Green Street Pasadena 1, California
2	Officer-in-Charge Office of Naval Research Branch Office Navy No. 100, Fleet Post Office New York, New York
6	Director Naval Research Laboratory Washington 25, D. C. Att: Technical Information Officer
2	Chief of Naval Research Office of Naval Research Washington 25, D. C. Att: Chemistry Branch
1	Office of Secretary of Defense Pentagon, Room 3D1041 Washington 25, D. C. Att: Library Branch (R and D)

Copies	Addressee
1	Dr. Ralph G. H. Siu, Research Dir. General Laboratories, QM Depot 2800 S. 20th Street Philadelphia 45, Pennsylvania
1	Dr. Warren Stubblebine, Research Dir. Chemical and Plastics Section, RDB-MPD Quartermaster General's Office Washington 25, D. C.
1	Dr. A. G. Horney Office Scientific Research USAF R and D Command, Box 1395 Baltimore, Maryland
1	Dr. A. Stuart Hunter, Tech. Dir. RDB-MPD Quartermaster General's Office Washington 25, D. C.
1	Commanding General Wright Air Development Center Wright-Patterson Air Force Base Dayton, Ohio Att: WCRRC, Dr. L. A. Wood
1	Dr. A. Weissler Department of the Army Office of the Chief of Ordnance Washington 25, D. C. Att: ORDTB-PS
1	Research and Development Group Logistics Division, General Staff Department of the Army Washington 25, D. C. Att: Dr. W. T. Read, Scient. Adv.
2	Director, Naval Research Laboratory Washington 25, D. C. Att: Chemistry Division
2	Chief of the Bureau of Ships Navy Department, Code 340 Washington 25, D. C.
2	Chief of the Bureau of Aeronautics Navy Department, Code TD-4 Washington 25, D. C.
2	Chief of the Bureau of Ordnance Navy Department, Code Rexd Washington 25, D. C.

Copies	Addressee
5	ASTIA Document Service Center Knott Building Dayton 2, Ohio
1	Dr. H. A. Zahl, Technical Dir. Signal Corps Engineering Labs. Fort Monmouth, New Jersey
1	U. S. Naval Radiological Defense Lab San Francisco 24, California Att: Technical Library
1	U. S. Naval Ordnance Test Station Inyokern, China Lake California Att: Head, Chemistry Division
1	Office of Ordnance Research 2127 Myrtle Drive Durham, North Carolina
1	Technical Command Chemical Corps Chemical Center, Maryland
1	U. S. Atomic Energy Commission Research Division Washington 25, D. C.
1	U. S. Atomic Energy Commission Chemistry Division Brookhaven National Laboratory Upton, Long Island, New York
1	U. S. Atomic Energy Commission Library Branch, Tech. Info., ORE P. O. Box E Oak Ridge, Tennessee
2	U. S. Naval Ordnance Test Station Inyokern, China Lake, California Att: Dr. D. Altman
1	Office of Technical Services Department of Commerce Washington 25, D. C.
1	Princeton University Princeton, New Jersey Att: SQUID Library
1	Applied Physics Laboratory Johns Hopkins University Silver Spring, Maryland
1	Chief of Staff, USAF Washington 25, D. C. Att: DCS/M MRD (Pentagon)
1	Office of the Chief of Ordnance Department of the Army Washington 25, D. C. Att: ORDTU (Pentagon)
1	Officer-in-Charge Ordnance R and D Division Sub-Office (Rocket) California Institute of Technology Pasadena 4, California
1	NACA, Lewis Flight Propulsion Lab Cleveland 11, Ohio Att: Dr. M. Gerstein
1	Reaction Motors, Inc. Lake Denmark Dover, New Jersey Att: Research Division
1	Aerojet Engineering Corporation Azusa, California Att: Librarian
1	Director, Naval Ordnance Laboratory White Oak Silver Spring 19, Maryland
1	Dr. W. Albert Noyes, Jr. Department of Chemistry University of Rochester Rochester 3, New York
1	Dr. Anton B. Burg Department of Chemistry University of Southern California Los Angeles 7, California
1	Dr. H. S. Johnston Department of Chemistry Stanford University Stanford, California
1	Mine Safety Appliance Company Pittsburgh, Pennsylvania Att: Dr. C. B. Jackson
1	Dr. H. I. Schlesinger Department of Chemistry University of Chicago Chicago 37, Illinois
1	Dr. Frank A. Long Department of Chemistry Cornell University Ithaca, New York
1	Dr. Leland G. Cole Jet Propulsion Lab., Chem. Section California Institute of Technology 4800 Oak Grove Drive Pasadena 3, California
1	Dr. S. C. Hight, Dir. of Research Sandia Corporation Sandia Base Albuquerque, New Mexico